# Factors influencing surface ozone variability over continental South Africa and implications for air quality and agriculture


## TL Laban

**orcid.org 0000-0002-5799-8663**


Thesis submitted in fulfilment of the requirements for the degree *Doctor of Philosophy in Science with Atmospheric Chemistry* at the North-West University

| | |
|---|---|
| Promoter: | Prof PG van Zyl |
| Co-promoter: | Prof JP Beukes |
| Assistant Promoter: | Dr AM Thompson |

Graduation October 2018

**23327278**

# ACKNOWLEDGEMENTS

“To know that we know what we know, and that we do not know, that is true knowledge.” - Henry David Thoreau (1817-62), Walden

It has been a long-held aspiration of mine to do doctoral studies, but I struggled to realise it. Many years later, life presented an opportunity, the right opportunity at the right time. It is often said that studying for a PhD is a lonely struggle to prove that you are worthy of academia, where only the fittest, strongest and luckiest survive. If that is the truth, then I was one of the luckiest, because there were so many kind and compassionate people who have supported me on this path. Their fingerprints and footprints are to be found all over the course of my journey.

Thank you to my parents, Daniel and Savi Laban, and siblings who were there in the foundational years and even today remind me that they are an extension of me. When one of us falls, we get hurt together, and when another succeeds, we share the rewards together. Our lives are intertwined and connected until the end. Thank you my dear sisters for the close bond we share, Karen Sookdew for always pointing me back to integrity and truth, Mary Laban for a brave spirit and loving heart, Jo-Ann Sayers, the youngest, but mother hen, who takes care of our brood. Thank you to my brother Keith Laban, I am proud of how far you have come and who you are today. Kay and Mark Laban, thank you for being a part of me, the memory of you can never be erased. Thank you to my extended family, wonderful grandparents, aunts, uncles, cousins, and childhood friends who have all shaped my life, because we know in Africa that it takes a village to raise a child.

I am deeply grateful to a very important person in my life, Fred Goede. This journey started because you once gave me an opportunity that brought me to this path and it continued because you stayed the distance with me. Thank you for your wonderful support and dedication along the way and for everything you have done for me. Your kindness and generosity go unsurpassed. Your words, “See this time in your life as a holiday where you get to do what you want”, helped me appreciate the privilege of full-time study and working according to my natural rhythm. You balanced what was sometimes a lonely and monotonous road with your bubbly attitude and zest for life. Hyperactivity is a blessing later in life. And now, I can help you protect your asteroid and flower.

I would like to express my most sincere gratitude to my promoters, Prof Pieter van Zyl and Prof Paul Beukes, who took turns to make substantial contributions to my progress. I am very thankful for the opportunities I received being part of their group. Thank you both for being so supportive of my research and believing and trusting in me. You taught me to stay positive and persevere in the midst of criticism and rejection. Your energy and enthusiasm and guidance and care for your students have enabled many to reach this point too. Pieter, thank you for the hard work and academic rigour you applied in order to get me to the finish line, as you understood my situation, but also my debilitating habit of tinkering too long with something. Paul, thank you for time spent on the data processing and results and applying perfectionism to the work. To Dr Berner, thanks for giving me the opportunity to learn from the sugarcane plants and connect with my ancestors.

A heartfelt thank you to the team that did the weekly maintenance at the Welgegund station for the data that was integral to this thesis; Dr Micky Josipovic, Dr Andrew Venter, Dr Kerneels Jaars and Marcell Venter. Kerneels, Marcell and Andrew, I am especially grateful for your advice, tips and hands-on help in guiding me through the final stages of the thesis writing process. Micky, thanks for sharing your office with me and lending me your monitor, you are not my boss ok (!), but somehow over time you became my boss and I let you lead me with the wisdom that comes from two continents. Petra Maritz and Lize Kok, your friendship helped me so much in my adjustment to university and transition as a student. Keitumetse Segakweng, we share a lot in common and bonded through our similar circumstances. Yolindi van Staden, Ralph Glastonbury, Jan-Stefan Swartz, Faan du Preez, Edwin Cogho, thank you for the interactions within our wider Atmospheric Chemistry Research and Chromium Technology Groups, happily conversing in English and your general helpfulness. It was a pleasure to get to know each one of you with your own special traits; your kindness and friendship made the years sweet and memorable.

Thank you to my Finnish friends, Dr Svante Henriksson and Rosa Gierens. Your support and assistance will not be forgotten.

Thank you to my colleagues at Botany, Mmbulaheni Netshimbupfe, Charné Malan, Monja Gerber, and Dr Prabhu Inbaraj; your kindness and sharing of knowledge is appreciated.

To my assistant promoter, Dr Anne Thompson, you are a true inspiration and example of a successful woman in atmospheric science. You brought your wealth of experience and expertise a little closer to me and opened my eyes to things I would not normally have seen. Thank you for your knowledge and wisdom and direction in lifting out the important and novel aspects from my maze of observations.

To Dr Nadine Borduas-Dedekind, dynamite in a small package, I really appreciate your mentoring and willingness to take on more work for my benefit.

Thank you Dr Ville Vakkari, not only for the ostrich and wine, but most importantly, for helping me improve my conceptual ideas for the manuscripts. You are highly admired as a researcher and MATLAB programmer and I am a grateful recipient of your efforts to educate others.

Thank you to Dr Santtu Mikkonen, who I have never met in person, but who still managed to be an excellent teacher to me over time and space.

Thank you to my other co-authors on my papers, for your many insights and critical comments, they significantly improved my manuscripts. I am also thankful for the efficient service received from Cecile van Zyl in language editing the thesis.

The financial assistance of the National Research Foundation, North-West University and the Atmospheric Chemistry Research Group towards this research is gratefully acknowledged and appreciated.

Thank you to my old Sasol friends and new Anglo friends; I am blessed to have crossed paths with such talented people.

Above all, my greatest thanks are to my Saviour Jesus Christ, no knowledge compares with knowing you. What a privilege and honour of my life it has been to know you. This research is a tiny glimpse into the world that is yours and that you run. You saved me through the cross and stir the best, purest, strongest parts of me to live with purpose. You are the air I breathe, that imparts life, the opposite of air pollution, and I live because you breathe life into me every day. I am proud to exalt your name in this thesis that will be viewed by many, for you are Faithful and True (Rev 19:11).

Thank you

Tracey Laban

For J.

*Two sturdy oaks I mean, which side by side,*
*Withstand the winter's storm,*
*And spite of wind and tide,*
*Grow up the meadow's pride,*
*For both are strong*

*Above they barely touch, but undermined*
*Down to their deepest source,*
*Admiring you shall find*
*Their roots are intertwined*
*Insep'rably.*

- Henry David Thoreau

# PREFACE

This thesis is submitted for examination in an article-based format, according to the academic rules of the North-West University (NWU), which make provision for the article model. All the requirements as laid out by the University regulations have been adhered to in the article-based thesis. As with a traditional format thesis, which seeks to demonstrate the contribution to knowledge in the field, the articles and supplementary chapters incorporated in this article-based PhD seek to achieve the same end.

The thesis structure follows a traditional format in terms of an introductory chapter and motivation for the study (Chapter 1), overview of relevant literature chapter (Chapter 2), methodology chapter (Chapter 3) and a concluding chapter evaluating the project and providing recommendations for further work (Chapter 7). A full bibliography is also provided. However, instead of the conventional results chapters, the three manuscripts make up Chapters 4 to 6. The manuscripts have been added into the thesis with at least one submitted to a peer-reviewed journal and the other two prepared for submission, also to peer-reviewed journals. Each manuscript has its own introduction, methodology and reference list so there might be some repetition of material in the thesis to aid the flow of the presentation, but as far as possible, the thesis has been kept concise and forms a cohesive body of work that supports the themes expressed in the introduction of the thesis. The fonts, numbering and layout of Chapters 4 to 6 (containing the manuscripts) are also not consistent with the rest of the thesis, since they were added in the formats submitted or prepared for submission as required by the respective journals.

**Rationale for submitting thesis in article format**

The choice to complete an article-based thesis was as a result of three standalone manuscripts having been prepared. The traditional format of a PhD thesis is read by fewer people than actual publications, which have a wider readership. The nature of the work made it possible to separate the findings of this research into three publishable articles; therefore it was felt that rather than writing a lengthy thesis, the emphasis should be on improving the quality of the research and pursuing the active publication of the results. Although the three articles are independent in addressing a unique research objective or question, they are connected to the themes of the research and tell a coherent story that is relevant to the study topic.

**Contextualising the articles in the overall storyline**

The topic of this PhD was associated with regional surface ozone. Three articles are presented in this thesis, with each focusing on a different aspect related to the topic. In the first article (Chapter 4), the author focused on understanding the seasonal influences and sources contributing to surface ozone variability in continental South Africa, while the second article (Chapter 5) focused on quantifying the impact of relevant atmospheric factors on surface ozone variability in continental South Africa. In the third manuscript (Chapters 6), a case study of the impacts of elevated surface ozone on sugarcane agricultural crops was performed.

The following manuscripts have been submitted or prepared for submission to a journal:

- Article 1 (Seasonal influences on surface ozone variability in continental South Africa and implications for air quality) was first submitted for consideration to *Atmospheric Chemistry and Physics*, a journal of the European Geosciences Union. The original article was published on 19 January 2018 as an *Atmospheric Chemistry and Physics Discussions* paper and can be viewed at https://www.atmos-chem-phys-discuss.net/acp-2017-1115/. At the time this thesis was prepared, a revised version of the manuscript published in ACPD was submitted to ACP and this version is presented in the thesis.
- Article 2 (Identifying the chemical and meteorological factors driving surface ozone variability over continental South Africa) was prepared for submission to *Atmospheric Environment*, an Elsevier journal. The article was formatted according to the journal requirements, i.e. Guide for Authors.
- Article 3 (Growth and physiological responses of two sugarcane varieties exposed to elevated ozone: A case study in South Africa) was prepared for submission to *South African Journal of Science*. The article was formatted according to the journal requirements, i.e. Guidelines for Authors.

Other articles, to which the author contributed as first author, which were published during the duration of this study, but not included for examination purposes, include:

- Laban, T.L., Beukes, J.P., and Van Zyl, P.G.: Measurement of surface ozone in South Africa with reference to impacts on human health (Commentary). *Clean Air Journal*, 25, No 1, 9-12, ISSN: 1017-1703, 2015.
- Laban, T.L., Beukes, J.P., Van Zyl, P.G., and Berner, J.M.: Impacts of ozone on agricultural crops in southern Africa (Commentary). *Clean Air Journal*, 25, No 1, 15-18, ISSN: 1017-1703, 2015.

For interest, both these articles can be found in Appendix B and C respectively.

# ABSTRACT

Extensive scientific research has been conducted on surface ozone ($O_3$) concentrations over several decades in North America and Europe. Through these efforts, significant information is available on the role of chemistry, meteorology and transport in the formation and local accumulation of $O_3$, as well as the adverse effects of $O_3$ on human health and vegetation in these regions. However, only a limited number of studies on surface $O_3$ measurements are available for southern Africa. The Highveld, located in the high-lying plateau in the interior of South Africa, is considered to be exposed to the highest $O_3$ concentrations. This region is the most densely populated part of South Africa, and the industrial and economic heartland of the country. High $O_3$ concentrations are observed in many urban and rural areas within the interior of South Africa, where concentrations exceed the South African National Ambient Air Quality Standard for $O_3$. Continuous, long-term measurements of surface $O_3$ concentrations are valuable indicators of possible health and environmental impacts, which can be used to inform efficient and effective regulatory standards. Within the southern African region, the only continuous, long-term record of surface $O_3$ concentrations is from the Cape Point Global Atmosphere Watch station, which is far removed from the Highveld region of South Africa and the meteorological patterns that dominate the interior of South Africa.

Together with understanding the factors affecting surface $O_3$ concentrations, more research is needed on the impacts of $O_3$ pollution on ecosystems. In terms of the effects on vegetation, although local $O_3$ concentrations in southern Africa are cumulatively above the European critical levels for crop damages, no vegetation damage has been reported. Scepticism remains that the reason that damages are not identified is due to a lack of local research attention on this topic. The impact of $O_3$ on agriculture in southern Africa is important from an economic and food security perspective.

An atmospheric measurement-based study using continuous, long-term $O_3$ measurements from four sites representing regional background and anthropogenically polluted regions in the north-eastern interior of South Africa, covering different time periods between 2006 and 2015, was conducted to explore regional and seasonal $O_3$ pollution variability over continental South Africa, as well as the most important sources contributing to $O_3$ concentrations in this region. Previous studies have suggested that the formation of surface $O_3$ over southern Africa is attributed to the combined contribution of precursors from anthropogenic and biogenic sources. The four different environments, i.e. clean savannah at Botsalano, polluted savannah at Marikana, semi-clean grassland at Welgegund, and polluted grassland at Elandsfontein showed

a similar seasonal pattern, i.e. late winter and early spring peaks, which were ascribed to increased open biomass burning endemic to this region. Back trajectory analysis was performed from which source maps were compiled at the two regional background sites, which indicated that higher $O_3$ concentrations corresponded with increased CO concentrations in air masses passing over a region in southern Africa, where a large number of open biomass fires occurred from June to September. The regional transport of CO associated with open biomass burning in southern Africa was therefore considered a significant source of surface $O_3$ in continental South Africa. The spring peak in $O_3$ in southern Africa occurs a little earlier than the spring peak in biogenic VOCs, suggesting that it is more likely biomass burning that is contributing to maximum $O_3$ than biogenic VOCs. In addition, biogenic VOC concentrations were significantly lower compared to biogenic VOC concentrations measured in other ecosystems in the world. Furthermore, to the extent that emissions of CO are proportional to those of reactive VOCs, the findings suggest that continental South Africa is VOC-limited rather than $NO_x$-limited. Therefore, the appropriate emission control strategy should be CO and VOC reduction, with the sources being mostly regional open biomass burning and household combustion, to effectively reduce peak $O_3$ in continental South Africa.

The measurement data from the four sites was also examined by multivariate statistical methods, i.e. multiple linear regression (MLR), principal component analysis (PCA) and a generalised additive model (GAM) to identify and quantify the influence of the chemical and meteorological factors driving $O_3$ variability over continental South Africa. The common finding with these statistical models was that the most important parameters explaining daily maximum $O_3$ variation in continental South Africa were relative humidity, temperature and CO concentrations, while NO levels explained $O_3$ variability to some extent. PCA indicated that these factors are not collinear after addressing multicollinearity in the data. Inter-comparison of the three statistical methods in the prediction of daily maximum $O_3$ indicated that GAM offered a slight improvement over MLR. Furthermore, all of the methods highlighted that relative humidity is one of the most important variables influencing $O_3$ levels in semi-arid South Africa, with increases in $O_3$ associated with decreases in relative humidity. Possible causes for the relationship, as suggested by literature, mainly involve loss of $O_3$ or precursor species in the atmosphere in the aqueous phase or lower relative humidity being associated with meteorological conditions not conducive to $O_3$ formation. The statistical models confirmed that regional-scale $O_3$ precursors coupled with meteorological conditions play a critical role in the daily variation of $O_3$ levels in continental South Africa.

An eight-month trial was conducted to assess the sensitivity of two sugarcane cultivars (*Saccharum* spp.) commonly farmed in South Africa to chronic exposure to elevated $O_3$ levels, as well as combined elevated $O_3$ and $CO_2$ concentrations in open-top chambers during the

growth season. As far as the candidate can assess, this was the first attempt to present quantitative exposure-response data on sugarcane under controlled conditions. Two indicators of stress could be monitored, namely plant growth and plant physiology related to photosynthetic performance. The results indicated that the growth parameters of the NCo376 cultivar showed no significant response to increased $O_3$. Although the growth of the N31 variety indicated some response to increased $O_3$, it also showed the ability to adapt to increased $O_3$ levels. Some evidence of elevated $CO_2$ countering the effects of elevated $O_3$ on growth, especially for the N31 cultivar, was observed. The physiological function (photosynthesis) of the NCo376 sugarcane variety was more susceptible to $O_3$ exposure compared to the N31 cultivar. The combined effects of elevated $O_3$ and elevated $CO_2$ improved photosynthetic efficiency and chlorophyll content relative to the $O_3$-treated plants to a certain extent, with the effects more pronounced for N31 than NCo376. It was indicated that the N31 variety is probably more tolerant towards high $O_3$ levels compared to NCo376. In general, this study indicated that the effects of $O_3$ chronic exposure were not as severe as expected in the sugarcane, while it was also indicated that these plant species are capable of evolving in order to tolerate and adapt to elevated $O_3$ levels.

Keywords: Surface ozone ($O_3$), sources, carbon monoxide (CO), $O_3$ production regime, statistical relationships, air quality, sugarcane

# LIST OF ABBREVIATIONS

| | |
|---|---|
| AOT40 | accumulated ozone exposure over a threshold of 40 ppb |
| BVOC | biogenic volatile organic compound |
| $CH_4$ | methane |
| CO | carbon monoxide |
| $CO_2$ | carbon dioxide |
| GAM | generalised additive model |
| HYSPLIT | Hybrid Single-Particle Lagrangian Integrated Trajectory |
| IPCC | Intergovernmental Panel on Climate Change |
| Jhb-Pta | Johannesburg-Pretoria |
| LT | local time |
| MLR | multiple linear regression |
| NAAQS | National Ambient Air Quality Standards |
| $NO_x$ | nitrogen oxides, namely nitric oxide (NO) and nitrogen dioxide ($NO_2$) |
| NRC | National Research Council |
| $^{\bullet}OH$ | hydroxyl radical |
| OTC | open-top chamber |
| PC | principal component |
| PCA | principal component analysis |
| PCR | principal component regression |
| $P(O_3)$ | instantaneous production rate of $O_3$ |
| PM | particulate matter |
| PM10 | particles with an aerodynamic diameter of less than or equal to 10 microns |
| PM2.5 | particles with an aerodynamic diameter of less than or equal to 2.5 microns |
| ppmv | parts per million ($10^{-6}$) |
| ppbv | parts per billion ($10^{-9}$) |

| | |
|---|---|
| pptv | parts per trillion ($10^{-12}$) |
| RMSE | root-mean-square error |
| $SO_2$ | sulphur dioxide |
| TVD | top visible dewlap |
| UNEP | United Nations Environment Programme |
| US EPA | United States Environmental Protection Agency |
| VOC | volatile organic compound |
| WHO | World Health Organization |
| WMO | World Meteorological Organization |

# TABLE OF CONTENTS

# LIST OF TABLES

## Chapter 2



## Chapter 3



## Chapter 5

# Chapter 6

# LIST OF FIGURES

## Chapter 2



## Chapter 3

# Chapter 4

# Chapter 5



# Chapter 6

# LIST OF APPENDICES

## Appendix A



## Appendix B



## Appendix C

# CHAPTER 1

## THESIS MOTIVATION, OBJECTIVES AND OVERVIEW

---

*In this chapter the importance and relevance of the research is discussed. The research gaps are highlighted and relate to limited understanding of the factors driving local $O_3$ production in continental South Africa as well as the extent of meteorological and transport influence. Gaps in knowledge also include the appropriate abatement measures required to reduce $O_3$ pollution in the region and the secondary impacts on agriculture. The specific objectives outlined in this chapter seek to address those research gaps.*

---

## 1.1 INTRODUCTION

As background concentrations of surface ozone ($O_3$) concentrations increase together with a changing emissions and meteorological environment, understanding the relationships between meteorological variability and pollutant levels is crucial in air quality research and management. Surface $O_3$ is well documented as being toxic to humans and vegetation (NRC, 2008, IPCC, 2007). However, as a secondary pollutant formed over time and distance, its atmospheric levels are often difficult to control. The difficulty is due in part to the complexity of the chemistry involving its precursor compounds, i.e. nitrogen oxides ($NO_x$), volatile organic compounds (VOCs) and carbon monoxide (CO), which have various different sources and exhibit non-linear effects on $O_3$ formation (Wang et al., 1998a). The complexity is compounded by meteorological processes, which strongly influence the rate of formation and accumulation of $O_3$ (Geddes *et al*., 2009). Also, anthropogenic emissions in the Southern Hemisphere, though less than the Northern Hemisphere (Zeng *et al.*, 2008), have a disproportionate impact on atmospheric composition and climate because they enter a relatively pristine environment and are more efficient at producing $O_3$ (Wang *et al.*, 1998b) to create a greater change in the oxidising capacity of the atmosphere (Thompson, 1992) and radiative forcing (IPCC, 2013). Therefore, understanding the factors controlling surface $O_3$ concentrations, as well as the extent to which chemical and meteorological variability influences seasonal surface $O_3$ concentrations is essential to determine their impacts on human health and vegetation, particularly on a regional scale, where this information is required to implement efficient and effective regulatory standards.

To understand the factors driving elevated $O_3$ concentrations for a region, the most common approaches are long-term observation measurements, short-term intensive research field campaigns, chemical transport modelling or an integration of these three approaches for improved results. However, it is challenging to separate the effects of individual parameters on ground-level $O_3$ concentrations. The formation process depends on the precursor sources, while dispersion processes depend on meteorological factors that affect the spatial distribution of $O_3$ concentrations. Meteorological parameters are strongly linked and interdependent, for example the dependency of atmospheric stability on temperature changes or the relationship between surface temperature and solar radiation (Gorai *et al*., 2015). Nevertheless, the need to distinguish the impacts of local emissions, meteorology and transport on surface $O_3$ concentration makes this research imperative from an atmospheric science and air quality management perspective.

Very few studies based on continuous, high time-resolution measurements of surface $O_3$ are available for southern Africa (Zunckel *et al*., 2004). However, due to the large variety of emission sources of $O_3$ precursors, as well as abundant sunshine, it is expected that the potential for elevated levels of ground-based $O_3$ is high in the region (Zunckel *et al*., 2006). The part of South Africa exposed to the highest $O_3$ concentrations is the northern and north-eastern interior parts, which accommodate approximately one-third of South Africa's population (WHO, 2016). Although some studies have attempted to address spatial $O_3$ variability (Lourens *et al*., 2011, Josipovic *et al*., 2010, Josipovic, 2009, Mokgathle, 2006, Zunckel *et al*., 2004, Jonnalagadda *et al*., 2001, Combrink *et al*., 1995), high-time resolution $O_3$ data over extended periods of time in southern Africa have not been examined. Long-term continuous measurements are very valuable to investigate interannual variation and provide estimates of long-term trends of surface $O_3$.

One study conducted in South Africa analysed the long-term measurements of $O_3$ based on passive samplers (Martins *et al*., 2007), which means that the temporal resolution was monthly averaged data only. Data averaged over a month do not allow estimation of daytime exposures. In a few cases, air quality assessments were conducted using continuous measurements, which were, however, limited to short-term duration (Laakso *et al*., 2012, Venter *et al*., 2012, Laakso *et al*., 2008). A recent study attempted to address the limitations of short-term data and low-temporal resolution data by utilising $O_3$ data covering the period from 1990 to 2007 measured at five compliance monitoring air quality stations on the South African Highveld (Balashov *et al*., 2014). The analysis demonstrated the strong sensitivity of $O_3$ to the El Niño-Southern Oscillation (ENSO) weather phenomenon, but showed little change in trends over the time period for both surface $O_3$ and $NO_x$. In addition, although routine $O_3$ monitoring is carried out in urban areas of several major municipalities, such as Johannesburg (Gauteng), Cape Town and Durban, the majority of this data

remains unpublished in peer-viewed form or is otherwise unavailable to the research community (Laakso *et al*., 2013).

An understanding of potential impacts of $O_3$ on agriculture in southern Africa is also required. While South Africa does have stringent air quality standards that aim to mitigate the impact of $O_3$ on human health, very little is known about the potential impact on agriculture in the region. International studies show a large detrimental effect of $O_3$ on agricultural productivity *(e.g.* Ghude *et al.*, 2014, Tai *et al.*, 2014). $O_3$ levels in southern Africa are in many places higher than the European critical levels determined for the protection of vegetation (Van Tienhoven *et al*., 2005). However, local species may have adapted to high $O_3$ levels, which is difficult to verify since few experimental studies on the actual vegetation impacts exist. However, even before impact studies are conducted, a reliable baseline of the current levels is needed from which to measure the adverse effects of $O_3$ exposure.

## 1.2 OBJECTIVES

The general aim of this study is to investigate the chemical and meteorological factors controlling surface $O_3$ variability in continental southern Africa and to establish the implications thereof for air quality management. A case study on the impact of elevated levels of $O_3$ on sugarcane will also be conducted to discuss the impact of surface $O_3$ on agriculture.

The specific objectives of this study include:

### 1.2.1 Determine the spatial and temporal variation of ozone at background and source locations in the north-eastern interior of South Africa

This study is based on continuous, high temporal resolution, long-term measurements collected at four representative locations in continental southern Africa. The first objective is to provide an up-to-date assessment of spatial and temporal variations of $O_3$ (and its precursors) in the north-eastern interior (continental) of South Africa, using data collected at measurement sites that represent source and background regions within the spatial domain.

### 1.2.2 Identify the probable sources and assess the contribution of individual sources to the problem of ozone pollution in South Africa

The local and regional sources contributing to surface $O_3$ in continental South Africa should be identified and their seasonality determined in order to target those sources to reduce $O_3$ levels in the region. Using back trajectories, it becomes possible to examine source-receptor relationships and the timescales of long-range and local transport, and its effect on the observed composition. It is also important to characterise the $O_3$ production regime for South Africa to implement appropriate $O_3$ control strategies.

### 1.2.3 Statistically examine the influence of chemistry and meteorology on surface ozone concentrations in continental South Africa

The chemistry governing the formation of $O_3$ depends on the concentrations of its precursors in a non-linear way (Jaffe and Ray, 2007). The complexity is compounded by the influence of meteorology and regional transport, which affect the rate of formation and local accumulation of $O_3$. Several authors use multivariate methods to relate $O_3$ concentrations to several explanatory variables that may affect and control the $O_3$ levels in a region (Awang *et al*., 2015, Dominick *et al*., 2012, Tsakiri and Zurbenko, 2011, Bloomfield *et al*., 1996). With this objective it is attempted to apply similar multivariate methods, i.e. multiple linear regression, principal component analysis and generalised additive models to the South African datasets in order to quantify the effects of precursor concentrations and meteorological conditions on surface $O_3$ concentration. Daily data summaries from four atmospheric measurement stations in continental South Africa are used to identify and quantify the chemical and meteorological drivers of $O_3$ variability at these sites.

### 1.2.4 Determine the implications of these chemical and meteorological influences on air quality management in South Africa

An understanding of the key precursors that control surface $O_3$ production can help towards establishing the $O_3$ production regime, i.e. $NO_x$- or VOC-limited, which is critical for the development of an effective $O_3$ control strategy. The sensitivity of $O_3$ formation to changes in precursor concentrations for South Africa is still a subject under investigation. Surface measurements of $NO_x$, CO (as a proxy for VOCs) and $O_3$ concentrations are analysed to evaluate the $O_3$ production regime. VOC data, which is available for one measurement site, is used to calculate the instantaneous production rate of $O_3$ as a function of $NO_x$ levels and VOC reactivity.

### 1.2.5 Investigate the impact of elevated levels of ozone on agricultural crops with a special focus on sugarcane

There is a need to understand the possible adverse effects of $O_3$ on agriculture because of the growing concern for food security and economic loss on agricultural crops, which has consequences for national economies. Here, an eight-month case study on the impact of elevated levels of $O_3$ on two local sugarcane cultivars is conducted in a controlled environment. This aim of the study is to contribute, within the wider context, to surface $O_3$ pollution impact studies on agriculture. This objective will ensure a first set of quantitative data on $O_3$ exposure-plant response for sugarcane, which is currently not available.

## 1.3 THESIS OUTLINE

In order to achieve the above-mentioned objectives, this thesis is composed of seven chapters:

- Chapter 1 provides the motivation and the major research objectives that guided this study.
- Chapter 2 presents background information on all the relevant topics to gain a broader perspective of the work in the thesis, i.e. tropospheric $O_3$ budget, sources and sinks, $O_3$ chemistry, role of meteorology and transport, air quality management, control strategies, and impacts on human health and vegetation.
- Chapter 3 describes the chosen methodology for assessment in this study, including a description of the sites used, measurement techniques, data analysis, quality control and assurance.
- Chapter 4 describes the observations of $O_3$ and other relevant gas-phase species made over a number of years in continental (north-eastern) South Africa and attempts to evaluate the $O_3$ production regime.
- Chapter 5 provides a statistical analysis of the afore-mentioned datasets and attempts to quantify the impacts of chemical and meteorological factors driving surface $O_3$ concentrations over continental South Africa.
- Chapter 6 presents the results of the case study on $O_3$ effects on sugarcane. The parameters for growth and physiological function are compared for the two cultivars.
- Finally, in Chapter 7, the findings in this thesis are evaluated by highlighting the successes and limitations of the project, as well as indicating future directions relevant to this research field.

# CHAPTER 2

## LITERATURE REVIEW

*The purpose of this chapter is to provide the necessary background on tropospheric $O_3$ that informed the research in this thesis. It describes the important processes, mainly chemistry, deposition and transport (both in the horizontal and vertical) governing the abundance of tropospheric $O_3$ as well as the impacts of $O_3$ pollution on ecosystems and implications for air quality management.*

## 2.1 INTRODUCTION TO TROPOSPHERIC OZONE

Tropospheric $O_3$ is produced *in situ* through the photochemical oxidation of volatile organic compounds (VOCs) and carbon monoxide (CO) in the presence of nitrogen oxides ($NO_x$) (Seinfeld and Pandis, 2006). A photochemical source for tropospheric $O_3$ involving precursor species was first suggested by Crutzen (1973) which also identified the key reactions involved in controlling $O_3$ in the background 'unpolluted' troposphere. As a secondary pollutant with an atmospheric lifetime of days at the surface, to weeks in the free troposphere (Finlayson-Pitts and Pitts, 1986), ground-level $O_3$ is a major air quality concern as it adversely impacts human health, natural vegetation and agricultural productivity (Van Dingenen *et al.*, 2009, The Royal Society, 2008, NRC, 1991). It is also an important greenhouse gas with an estimated globally average radiative forcing of 0.40 ± 0.20 W $m^{-2}$ (IPCC, 2013), equivalent to a quarter of the $CO_2$ forcing (Greenslade *et al.*, 2017). Tropospheric $O_3$ is the primary precursor of the hydroxyl radical ($^{\bullet}OH$), which is the main oxidant in the atmosphere responsible for the removal of many trace gases in the atmosphere (Hu *et al.*, 2017).

### 2.1.1 Stratospheric versus tropospheric ozone

$O_3$ is a natural constituent of the atmosphere, which is present in the stratosphere and troposphere (The Royal Society, 2008). Most of the earth's atmospheric $O_3$ (approximately 90%) occurs in the 'ozone layer' of the stratosphere at altitudes ranging from approximately 10 to 40 km. Although only 10% of the total atmospheric $O_3$ is found in the troposphere (Fishman *et al.*, 1990), $O_3$ is an important oxidant as all primary initiations of oxidation chains in the troposphere depend on $O_3$ (Wayne, 1991). The concentrations of $O_3$ in the troposphere are typically less than 200 ppb in

mixing ratio (molecules of $O_3$/molecules of air; 10 ppb = 2.5 x $10^{11}$ molecules $cm^{-3}$ at sea level and 298 K) compared to peak stratospheric mixing ratios of approximately 8 000 ppb. Mixing ratios of $O_3$ typically vary between 10 and 40 ppb for the remote unpolluted troposphere, with $O_3$ present at somewhat higher mixing ratios (up to 100 ppb) in the upper troposphere (Seinfeld and Pandis, 2006). At ground level, the mixing ratio of $O_3$ often exceeds 100 ppb downwind of polluted metropolitan regions and can reach over 200 ppb during high $O_3$ episodes (The Royal Society, 2008).

### 2.1.2 Global tropospheric ozone budget and lifetimes

Recent modelling studies of the global tropospheric $O_3$ budget vary in their estimates of the quantity of tropospheric $O_3$ originating from the stratosphere or from *in situ* photochemistry, but are in agreement that *in situ* production is the dominant source of $O_3$ in the troposphere, exceeding the stratospheric influx by factors of 4 to 15 (see Table 2-1). Increased photochemical production of $O_3$ is correlated with increased anthropogenic emissions of $O_3$ precursors and is responsible for the present-day tropospheric $O_3$ burden (Cooper *et al.*, 2014). Table 2-1 lists the tropospheric $O_3$ budget (sources, sinks, total burden and lifetimes) from chemistry model simulations (means and standard deviations) (Hu *et al.*, 2017 and references therein). The globally averaged lifetime of $O_3$ in the troposphere has been estimated at 22 to 24 days by the models (Hu *et al.*, 2017).

Table 2-1: Global budgets of tropospheric $O_3$ reported in literature[a] (Hu *et al.*, 2017).

| | Sources, Tg $a^{-1}$ | | Sinks, Tg $a^{-1}$ | | Burden, Tg | Lifetime, d |
|---|---|---|---|---|---|---|
| | Chemical production | Stratosphere-troposphere exchange | Chemical loss | Dry deposition | | |
| IPCC TAR[b] | 3420 ± 770 | 770 ± 400 | 3470 ± 520 | 770 ± 180 | 300 ± 30 | 24.0 ± 2.0 |
| ACCENT[c] | 4970 ± 220 | 560 ± 150 | 4570 ± 290 | 950 ± 150 | 336 ± 27 | 22.2 ± 2.2 |
| GEOS-Chem v7-02-04[d] | 4470 ± 180 | 520 ± 15 | 3940 ± 175 | 1050 ± 45 | 310 ± 10 | 22.3 ± 0.9 |
| ACCMIP[e] | 4880 ± 850 | 480 ± 100 | 4260 ± 650 | 1090 ± 260 | 337 ± 23 | 23.4 ± 2.2 |
| IPCC AR5[f] | 4620 ± 380 | 490 ± 90 | 4190 ± 380 | 960 ± 140 | 330 ± 17 | N/A |
| GEOS-Chem v10-01[g] | 4960 | 325 | 4360 | 910 | 351 | 24.2 |

[a] Model intercomparisons, with standard deviations describing the spread between models. Entries are listed chronologically.
[b] Prather *et al.* (2001)
[c] Stevenson *et al.* (2006)
[d] Wu *et al.* (2007)
[e] Young *et al.* (2013)
[f] Myhre *et al.* (2013)
[g] Hu *et al.* (2017)

Thus the average lifetime of $O_3$ in the atmosphere is <1 month, but is highly variable, dependent on factors such as season, latitude and altitude. The lifetime of $O_3$ is much shorter (2-5 days) in the boundary layer because it is more readily destroyed by surface deposition and chemical reactions (Cooper *et al.*, 2014). These global budgets do not reflect the regional variations in $O_3$, which span a wide range of sources, sinks and lifetimes of species (Monks *et al.*, 2015).

## 2.2 SOURCES AND SINKS OF TROPOSPHERIC OZONE

Many attempts have been made to better understand the sources and sinks of surface $O_3$ and their distribution. Following decades of intense study, knowledge has improved on the sources and sinks of ground-level $O_3$ in North America and Europe, but there is little information available for other parts of the globe (Hewitt, 1998). The important processes that affect regional $O_3$ are illustrated in Figure 2-1. In general, the concentration of $O_3$ at a given location is regulated by the following processes: photochemical production from local precursor (anthropogenic and biogenic) emissions, chemical destruction, losses to surface by dry deposition, atmospheric transport of $O_3$ and $O_3$ precursors from upwind locations, and stratospheric-tropospheric exchange of $O_3$-rich air (Monks *et al.*, 2015).

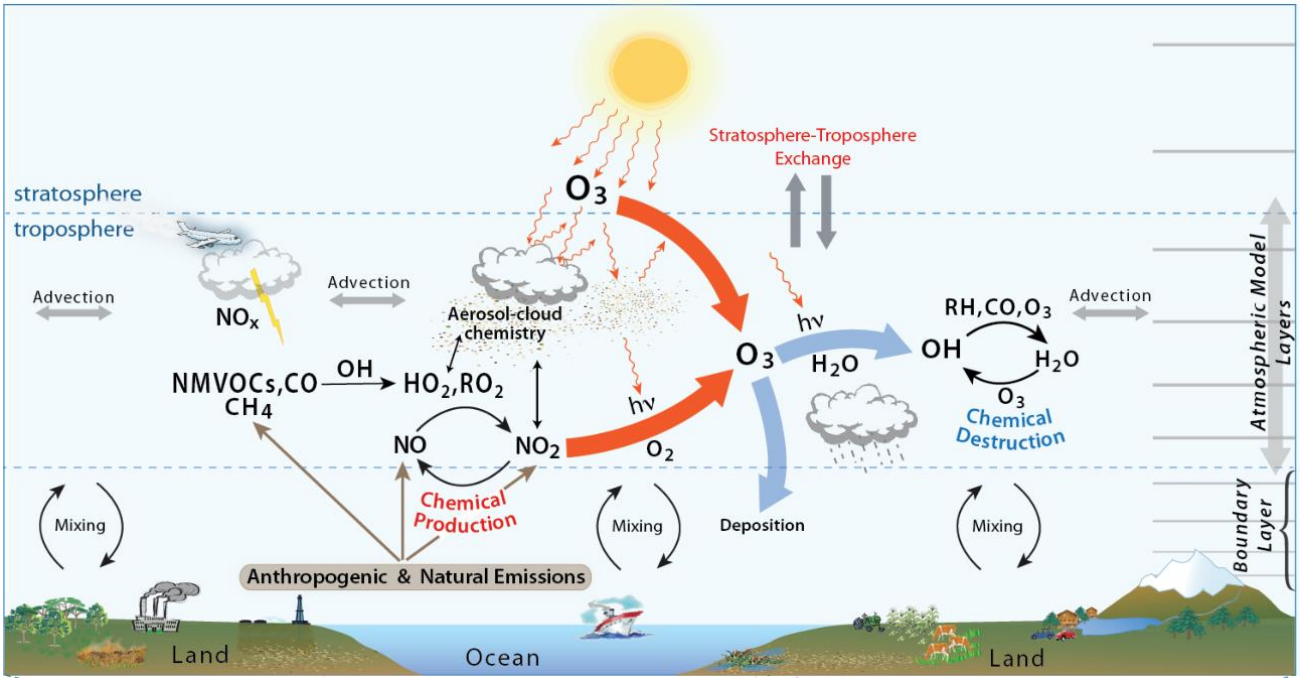


Figure 2-1: Schematic depiction of the sources and sinks of $O_3$ in the troposphere. The sources and sinks include stratosphere-to-troposphere exchange, chemical production and destruction in the troposphere and dry deposition to terrestrial and marine surfaces. $O_3$ precursor emissions are from anthropogenic and natural sources (Young *et al.*, 2018).

### 2.2.1 Chemical production of tropospheric ozone

Photolysis of $NO_2$ (reaction 2.1) in the presence of sunlight, followed by the addition of the O atom to $O_2$ (reaction 2.2), is the only known way of producing $O_3$ in the troposphere (Wayne, 1991). The body M is used to represent any third co-reactant, e.g. $N_2$, $O_2$. After the $O_3$ and nitric oxide (NO)

molecules are formed, they recombine to regenerate $NO_2$ (reaction 2.3), which will once again undergo photolysis to form $O_3$.

$$NO_2 + h\nu \rightarrow O(^3P) + NO \quad (2.1)$$

$$O_2 + O(^3P) + M \rightarrow O_3 + M \quad (2.2)$$

$$O_3 + NO \rightarrow O_2 + NO_2 \quad (2.3)$$

Due to the rapid conversion between NO and $NO_2$ during daylight, rather than attempt to treat them individually, they are combined as a group by deriving the quantity $NO_x$ (= NO + $NO_2$), which is insensitive to quick changes in UV flux (Hov, 1997). In the same way, the quantity $O_x$ (= $O_3$ + $NO_2$) proposed by Liu (1977) was defined, which is insensitive to rapid changes that convert $O_3$ to $NO_2$ and *vice versa*. In other words, the total oxidant, $O_x$, is a better measure of the true photochemical $O_3$ production than $O_3$ itself, especially in polluted environments because it excludes the effect of NO titration of $O_3$ (Pugliese *et al.*, 2014).

The fast steady state established between NO, $NO_2$ and $O_3$ (reactions 2.1, 2.2 and 2.3), is known as the null cycle, since, as soon as $O_3$ is produced, it is destroyed so the reactions result in no net change in $O_3$ (Sillman, 1999). Net production of $O_3$ occurs outside of the null cycle when an atmospheric pool of peroxy radicals ($HO_2^\bullet$ and $RO_2^\bullet$) alters the photostationary state by reacting with NO and producing new $NO_2$ (Cazorla and Brune, 2010). The main source of peroxy radicals is the reaction of the hydroxyl radical ($^\bullet$OH) with VOCs or CO (Cazorla and Brune, 2010).

$$RH + {}^\bullet OH \xrightarrow{O_2} H_2O + RO_2^\bullet \quad (2.4)$$

$$CO + {}^\bullet OH \xrightarrow{O_2} HO_2^\bullet + CO_2 \quad (2.5)$$

where RH represents VOCs (R is any organic group). The alkylperoxy ($RO_2^\bullet$) or hydroperoxy radicals ($HO_2^\bullet$) oxidises atmospheric NO:

$$RO_2^\bullet + NO \rightarrow RO^\bullet + NO_2 \quad (2.6)$$

$$HO_2^\bullet + NO \rightarrow {}^\bullet OH + NO_2 \quad (2.7)$$

reducing the sink for $O_3$ (Atkinson, 2000), since the resultant $NO_2$ leads to the production of $O_3$ through reactions 2.1 and 2.2.

Figure 2−2 (a) shows the $O_3$-$NO_x$ null chemical cycle in the absence of VOCs, while Figure 2−2 (b) shows that in the polluted troposphere, higher concentrations of primary species ($NO_x$, VOCs and

CO) are present and thus the chemical process of $O_3$ formation occurs through reaction sequences involving these primary species, which results in the conversion of NO to $NO_2$ through processes other than reaction 2.3 (Sillman, 1999).

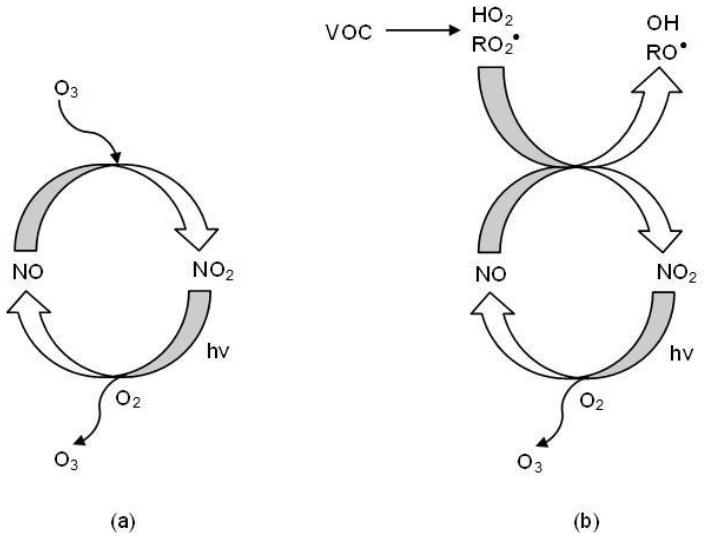


Figure 2-2: Schematic representation of the reactions involved in NO-to-$NO_2$ conversion and $O_3$ formation in (a) NO-$NO_2$-$O_3$ systems in the absence of VOCs and (b) NO-$NO_2$-$O_3$ systems in the presence of VOCs (Atkinson, 2000).

Recycling of $^{\bullet}OH$ via reaction 2.7 and further reactions of $RO^{\bullet}$ propagate the chain reactions for $O_3$ formation (Pollack *et al.*, 2012). Consequently, the rate of $O_3$ production is set by reactions 2.6 and 2.7 (Murphy *et al.*, 2007). The main fate of the resulting $RO^{\bullet}$ radical is the reaction with $O_2$:

$$RO^{\bullet} + O_2 \rightarrow R'CHO + HO_2^{\bullet} \quad (2.8)$$

to form carbonyl compounds and an $HO_2^{\bullet}$ radical (reaction 2.8) with $HO_2^{\bullet}$ reacting further with NO as shown in reaction 2.7 (Pugliese *et al.*, 2014). Therefore, in the presence of VOCs, the net reaction involving the above reactions, results in the formation of two $O_3$ molecules (Pugliese *et al.*, 2014):

$$RH + 4O_2 \rightarrow R'CHO + 2O_3 + H_2O \quad (2.9)$$

This catalytic $O_3$ production chain is terminated by the loss of $HO_x$ radicals ($HO_x^{\bullet}$ = $^{\bullet}OH$ + $RO^{\bullet}$ + $HO_2^{\bullet}$ + $RO_2^{\bullet}$), which can occur through multiple sinks for $HO_x^{\bullet}$ (Pugliese *et al.*, 2014).

Radical termination reactions that remove or convert $NO_x$, either permanently or temporary into inorganic (e.g. nitric acid) and organic nitrogen (e.g. peroxyacetylnitrate, $CH_3C(O)O_2NO_2$, often abbreviated as PAN) clearly affect the photochemical $O_3$ formation cycle in the troposphere. The

reaction between peroxy radicals and $NO_x$ forms PAN and its homologues ($RC(O)O_2NO_2$) or alkyl nitrates ($RONO_2$) as seen in reactions 2.10 and 2.11 respectively (Farmer *et al.*, 2011):

$$RC(O)O_2^{\bullet} + NO_2 \leftrightarrow RC(O)O_2NO_2 \quad (2.10)$$

$$RO_2^{\bullet} + NO + M \rightarrow RONO_2 + M \quad (2.11)$$

Reaction 2.11 is the alternative reaction path of $RO_2^{\bullet}$ with NO as opposed to reaction 2.6. While the removal of $NO_2$ by nitric acid ($HNO_3$) provides an effective sink for $NO_x$ in the planetary boundary layer, the thermally unstable PAN serves only as a temporary reservoir species for $NO_2$ (Borrell *et al.*, 1997). PAN suppresses $O_3$ formation on a local scale but enables the long-range transport of $NO_x$ at cold temperatures where its decomposition releases $NO_x$ in the remote troposphere, thereby extending $O_3$ formation (Fischer *et al.*, 2014). Conversely, alkyl nitrates are considered nearly permanent sinks for $NO_x$, terminating the catalytic cycle that leads to local $O_3$ production (Farmer *et al.*, 2011), and thus also play a role in the total $O_3$ produced.

### 2.2.2 Central role of the hydroxyl radical in the troposphere

Hydroxyl radicals dominate the daytime chemistry of the troposphere in the same manner that oxygen atoms and $O_3$ dominate the chemistry of the stratosphere (Wayne, 1991). The average lifetimes of most trace gases in the troposphere are determined by their reactivity with $^{\bullet}OH$. At night, the nitrate radical, $NO_3$, is the dominant oxidant in the troposphere (Wayne, 1991). The $^{\bullet}OH$ and $NO_3$ radicals exhibit contrasting diurnal variation in concentration, where $^{\bullet}OH$ is generated photochemically only during the day, while $NO_3$ is readily photolysed and therefore can only survive at night (Wayne, 1991).

$^{\bullet}OH$ is formed through the photolysis of $O_3$ in the presence of water vapour, which is the main source of OH radicals in the troposphere (Monks, 2005). $O_3$ is photolysed at wavelengths less than 320 nm to produce an excited $^1D$ oxygen atom that reacts with water vapour to yield OH radicals:

$$O_3 + h\nu\ (\lambda < 320\ nm) \rightarrow O(^1D) + O_2(^1\Delta_g) \quad (2.12)$$

$$O(^1D) + H_2O \rightarrow {}^{\bullet}OH + {}^{\bullet}OH \quad (2.13)$$

Other sources of OH radicals in the troposphere include photolysis of nitrous acid (HONO), the photolysis of formaldehyde ($CH_2O$) and other carbonyls in the presence of NO as well as the dark reactions of $O_3$ with alkenes (Atkinson, 2000). Reaction 2.13 is a minor fate of $O(^1D)$ compared to the quenching reaction back to ground state oxygen, $O(^3P)$ atoms:

$$O(^1D) + M \rightarrow O(^3P) + M \quad (2.14)$$

where M = $N_2$ or $O_2$

Virtually all ground state oxygen atoms will regenerate $O_3$ as observed in reaction 2.2:

$$O_2 + O(^3P) + M \rightarrow O_3 + M \quad (2.2)$$

•OH is the central player in the chemistry of $O_3$. It is part of a closely coupled system involving $HO_x$•, $NO_x$ and $O_3$ (Monks *et al.*, 2015). It reacts with all organic compounds except for chlorofluorocarbons and halons not containing H atoms (Atkinson, 2000). In the clean troposphere, roughly 70% of •OH reacts with CO and 30% with $CH_4$ to produce peroxy radicals, while in the polluted planetary boundary layer, the OH radical is responsible for the oxidation of nearly all VOCs (e.g. alkanes, alkenes and aromatic hydrocarbons with differing reactivities) (Wayne, 1991).

Since reaction with •OH is the principal scavenging mechanism for a wide variety of trace species in the atmosphere, knowledge of the tropospheric concentrations of •OH is important. Chemistry transport and box models predict •OH concentrations to be typically less than $10^6$ molecules $cm^{-3}$ or 0.04 ppt in the boundary layer (Martinez *et al.*, 2010). Direct measurement of atmospheric •OH levels is very difficult due to its very low concentration, high reactivity and subsequent short lifetime (~ 0.01-1 s), and its rapid loss rate onto surfaces of inlets (Stone *et al.*, 2012). In the past, methylchloroform ($CH_3CCl_3$) has been used to estimate the global mean •OH concentration, since its removal from the atmosphere is almost solely by reaction with •OH (Seinfeld and Pandis, 2006). The highest •OH levels are predicted in the tropics, where high humidity and intense radiation lead to a high rate of •OH production from $O_3$ photolysis to $O(^1D)$ (Martinez *et al.*, 2010). CO is the dominant sink of •OH in most of the troposphere (followed by $CH_4$), and therefore •OH levels are approximately 20% higher in the Southern Hemisphere due to higher CO levels from fossil fuel emissions in the Northern Hemisphere (Seinfeld and Pandis, 2006).

### 2.2.3 VOC-$NO_x$ ratio

VOCs and $NO_x$ compete for the •OH radical in the troposphere (Seinfeld and Pandis, 2006). At high VOC/$NO_x$ ratios (i.e. low concentrations of $NO_x$ relative to VOC concentrations), the VOC reacts preferentially with •OH to form $HO_2$• (reaction 2.4) or $RO_2$• (reaction 2.5). There is, however, insufficient $NO_x$, and therefore, instead of reacting with NO via reactions 2.6 and 2.7, peroxy radicals are lost mainly through self-reaction to form peroxides:

$$RO_2^\bullet + RO_2^\bullet \rightarrow R_2O_2 + O_2 \quad (2.15)$$

where R can be H or any organic group. Under these conditions, $O_3$ production will increase with increases in $NO_x$ and is largely unaffected by changes in VOCs (as they will just keep reacting with $^{\bullet}OH$ to form peroxy radicals that are lost through self-reaction). Conversely, at low VOC/$NO_x$ ratios (i.e. high $NO_x$ and relatively low VOCs), $NO_2$ reacts preferentially with $^{\bullet}OH$ to form nitric acid ($HNO_3$) as seen below (Stephens *et al.*, 2008):

$$^{\bullet}OH + NO_2 + M \rightarrow HNO_3 + M \quad (2.16)$$

This suppresses the OH radical, suppressing the formation of new peroxy radicals and results in less $O_3$ production. Under these conditions, an increase in VOCs (and CO) will result in an increase in the production of $HO_2^{\bullet}$+$RO_2^{\bullet}$ that leads to $O_3$ formation. Increasing $NO_x$ will not increase $O_3$ production and, in some instances, may even decrease $O_3$ production (Sillman, 1999). We can diagnose whether $O_3$ production in a region is $NO_x$- or VOC-limited by determining which of the two sinks for $HO_x$, reaction 2.15 or 2.16 is dominant. Note that VOC/$NO_x$ ratios are associated with the instantaneous production rate of $O_3$, not necessarily the ambient $O_3$ mixing ratio (Sillman, 1999).

### 2.2.4 Chemical destruction and dry deposition of tropospheric ozone

The primary sinks for tropospheric $O_3$ are chemical destruction and dry deposition to the earth's surface (Hardacre *et al.*, 2015). Photochemical destruction of $O_3$ in the presence of water vapour was discussed earlier in section 2.2.2, comprising reactions 2.12, 2.13 and 2.14, which is the primary source of $^{\bullet}OH$.

The actual rate of $O_3$ destruction by this removal path is dependent on the water vapour concentrations (reaction 2.13) (Monks, 2005), otherwise $O(^1D)$ is just quenched back to $O(^3P)$ (reaction 2.14) and reforms $O_3$ (reaction 2.2) (Seinfeld and Pandis, 2006). Furthermore, in highly polluted regions, there is direct removal of $O_3$ by reaction with NO (reaction 2.3). However, in low-$NO_x$ conditions, $O_3$ is chemically destroyed by reacting with $HO_2^{\bullet}$, leading to the further destruction of $O_3$ in a chain sequence involving formation of $^{\bullet}OH$ (Monks, 2005):

$$HO_2^{\bullet} + O_3 \rightarrow {}^{\bullet}OH + 2O_2 \quad (2.17)$$

$$^{\bullet}OH + O_3 \rightarrow HO_2^{\bullet} + O_2 \quad (2.18)$$

Dry deposition processes account for approximately 25% of the total $O_3$ removed from the troposphere (Lelieveld and Dentener, 2000). In rural areas, dry deposition to terrestrial surfaces drives the diurnal variation of $O_3$ (Simpson, 1992). The uptake of $O_3$ on the surface is governed by several factors, including shape and smoothness of the surface, wetness, the solubility of the depositing species and specific chemical or biological interactions (Holloway and Wayne, 2010). Dry

deposition of $O_3$ to vegetated surfaces occurs mainly through the leaf stomata and is controlled by stomatal conductance (Hardacre *et al.*, 2015). Due to the highly reactive nature of $O_3$ and plant leaves acting as relatively efficient sinks, $O_3$-induced damage to vegetation can occur (Felzer *et al.*, 2007).

### 2.2.5 Influence of halogens on tropospheric ozone

Halogen chemistry may provide an additional tropospheric $O_3$ sink. Interest in chemistry of reactive halogen compounds (iodine, chlorine and bromine) in the troposphere intensified after discovery of rapid $O_3$ depletion in the lowest part of the troposphere in the Artic spring, which was attributed to bromine chemistry involving Br and BrO (Barrie *et al.*, 1988). Since then, studies have indicated that halogen catalysed boundary layer $O_3$ depletion not only occurs in the Artic but also in Antartica (Kreher *et al.*, 1997, Kreher *et al.*, 1996). The following catalytic cycle explains the rapid loss in polar sunrise which is associated with high concentrations of BrO (Jacob, 2000):

$$BrO + BrO \rightarrow Br_2 + O_2 \quad (2.19)$$

$$Br_2 + h\nu \rightarrow 2Br \quad (2.20)$$

$$Br + O_3 \rightarrow BrO + O_2 \quad (2.21)$$

In the absence of $NO_x$, destruction of $O_3$ can proceed through the following cycle (Dickerson *et al.*, 1999):

$$Br + O_3 \rightarrow BrO + O_2 \quad (2.22)$$

$$BrO + HO_2 \rightarrow HOBr + O_2 \quad (2.23)$$

$$HOBr + h\nu \rightarrow OH + Br \quad (2.24)$$

Halogens other than bromine (chlorine and iodine) could also be implicated in the chemical loss of $O_3$. High concentrations of chlorine atoms (Cl) may sometimes be present in the marine boundary layer that drives a catalytic mechanism for $O_3$ loss (Jacob, 2000):

$$Cl + O_3 \rightarrow ClO + O_2 \quad (2.25)$$

$$ClO + HO_2 \rightarrow HOCl + O_2 \quad (2.26)$$

$$HOCl + h\nu \rightarrow OH + Cl \quad (2.27)$$

However the efficiency of this cycle is low because of the competing reaction (Jacob, 2000):

$$Cl + CH_4 \xrightarrow{O_2} HCl + CH_3O_2^{\bullet} \quad (2.28)$$

Reaction 2.28 provides a source of $HO_x^{\bullet}$ and can lead to $O_3$ production.

Nitryl chloride ($ClNO_2$), which is a Cl atom precursor, and acts as a reservoir for $NO_x$ has been observed at inland locations (Thornton *et al.*, 2010):

$$ClNO_2 + h\nu \rightarrow Cl + NO_2 \quad (2.29)$$

Contrary to previous studies of tropospheric halogen chemistry that focussed on coastal regions, this study found $ClNO_2$ far from the oceans, suggesting it is not just a marine or coastal problem. Chlorine atom chemistry influences levels of tropospheric $O_3$, destroying it in clean environments and enhancing its formation under polluted conditions (Baker *et al.*, 2016).

The majority of halogen-related $O_3$ destruction is attributed to role played by iodine (Carpenter *et al.*, 2013). Methyl iodide ($CH_3I$) is the dominant organic iodine compound involved in the destruction of $O_3$ as it is photolysed by radiation in the troposphere (Wayne, 1991):

$$CH_3I + h\nu \rightarrow CH_3 + I \quad (2.30)$$

$$I + O_3 \rightarrow IO + O_2 \quad (2.31)$$

$$IO + IO \rightarrow 2I + O_2 \quad (2.32)$$

The iodine (I) atoms react with $O_3$ forming iodine monoxide (IO) which undergoes a self-reaction to regenerate the I atoms.

Organic iodine compounds have been assumed to serve as the main source of oceanic iodine emissions but laboratory studies have also shown that the reaction of iodide with $O_3$ at the sea surface leads to the formation of molecular iodine ($I_2$) and hypoiodous acid (HOI) (e.g. Carpenter *et al.*, 2013):

$$H^+ + I^- + O_3 \rightarrow HOI + O_2 \quad (2.33)$$

$$H^+ + HOI + I^- \leftrightarrow I_2 + H_2O \quad (2.34)$$

Carpenter *et al.* (2013) showed that HOI is the major of the two inorganic iodine species emanating from sea surface emissions.

The sources for halogenated compounds in the troposphere appear to be mainly natural, mostly linked to methyl halides, $CH_3Cl$, $CH_3Br$ and $CH_3I$, produced in the ocean by marine photosynthetic

organisms (Wayne, 1991). Biomass burning also releases methyl halides, mainly $CH_3Br$ (Seinfeld and Pandis, 2006). Other reactive organic halogens emitted from the oceans such as bromoform ($CHBr_3$) and dibromomethane ($CH_2Br_2$) also release bromine in the troposphere that is generally observed as BrO (Leser *et al.*, 2003) and which can lead to depletion of ground level $O_3$. Limited work is available describing the impact of halogen chemistry on tropospheric $O_3$ in South Africa. The results of work by Andreae *et al.* (1996) to measure methyl halide emissions from savannah fires in southern Africa indicated that biomass burning makes a significant contribution to the atmospheric budget of $CH_3Cl$ and $CH_3Br$ but is a minor source of $CH_3I$. Tropospheric BrO was measured during a ship cruise Germany to South Africa which found typical levels of <1 to 3.6 ppt in the marine lower troposphere (Leser *et al.*, 2003).

## 2.3 OZONE PRECURSOR EMISSIONS

Biomass burning-, biogenic- (natural emissions from vegetation and soil), lightning- and anthropogenic emissions (e.g. industrial, transport and domestic burning) can be considered to be the main sources of $O_3$ precursor species in Africa (Aghedo *et al.*, 2007). Except for anthropogenic emissions, which are generally constant throughout the year, the relative importance of lightning, biomass burning or biogenic emissions on surface $O_3$ concentrations over southern Africa is highly dependent on season. The four emission source types are discussed in more detail below.

### 2.3.1 Anthropogenic

The evaluation of historical $O_3$ trends indicate that the Northern Hemisphere background $O_3$ concentration has approximately doubled compared to $O_3$ levels a century ago (Vingarzan, 2004). Changes in $O_3$ trends are linked to changes in $O_3$ precursor emissions (Hidy and Blanchard, 2015). According to model results of Fusco and Logan (2003), the increasing trend in background $O_3$ levels since 1970 can be directly attributed to the rise in surface emissions of $NO_x$ emissions from fossil fuel combustion. In contrast to $NO_x$ emissions, increases in VOC emissions from fossil fuel combustion have been more modest (Vingarzan, 2004). Although long-term reductions in VOC emissions have affected peak levels of $O_3$, i.e. $O_3$ episodes, model results indicate they have not contributed significantly to mean tropospheric $O_3$ trends (Fiore *et al.*, 2002, Lefohn *et al.*, 1998).

In the last decade, there has been some slowing down of the increasing trend in surface $O_3$ concentrations (Derwent *et al.*, 2013). Abatement measures implemented in Europe, Japan and North America have reduced $O_3$ precursor emissions leading to reductions in peak regional $O_3$ concentrations and the frequency of photochemical smog episodes at the local and regional level (The Royal Society, 2008). However, there is also evidence that background levels of $O_3$ are increasing in North America and elsewhere in the Northern Hemisphere counteracting $O_3$ reductions

achieved by domestic emission reductions (Cooper *et al.*, 2012, Vingarzan, 2004). Anthropogenic emissions of $O_3$ precursors have shifted from developed regions (i.e. Europe and North America) to developing regions (i.e. Southeast, East and South Asia), supported by appreciable increases in observed $O_3$ above these regions (Zhang *et al.*, 2016). African combustion emissions are also on the increase due to the rapid growth of African cities and the magnitude of African anthropogenic emissions is predicted to be similar to African biomass burning emissions around 2030 (Liousse *et al.*, 2014). Nigeria, South Africa and Egypt account for approximately 35%, 53% and 37% of the total African anthropogenic CO, $NO_x$ and VOC emissions respectively (Aghedo *et al.*, 2007).

Kirkman *et al.* (2000) reported that although industrial emissions in Africa are small compared to those in the Northern Hemisphere, there are expanses of concentrated emissions in southern Africa that are important on a regional scale. These regions include the Copperbelt in Zambia, associated with mining and smelting activities, Harare and the Great Dyke areas in Zimbabwe, where industries and ore smelters are concentrated, as well as the Highveld in South Africa with its high concentration of coal-fired power plants and industries (Zunckel *et al.*, 2006). In addition to the industrial sector being a significant source of emissions, the transportation sector is a growing source of urban air pollution in key African cities such as Cairo, Nairobi, Johannesburg, Cape Town and Dakar (UNEP, 2006). Vehicle emissions consist of VOCs, CO, $NO_x$ and PM (Wallington *et al.*, 2006). There is also a strong reliance on polluting fuels (e.g. coal, wood, kerosene, crop residues and animal dung) for domestic space heating and cooking throughout the region (Wichmann and Voyi, 2006), which could contribute to $O_3$ precursor emissions and thereby to $O_3$ formation (Aghedo *et al.*, 2007).

In South Africa, a large portion of the anthropogenic emissions originate in the South African Highveld, which is the industrial and economic hub of the country. This includes the Johannesburg-Pretoria megacity with a population greater than 10 million, as well as the Mpumalanga Highveld and Vaal Triangle regions (Lourens *et al.*, 2016). The latter two have been declared National Air Pollution Priority Areas by the government because of the severe air quality problems that occur in these regions (Lourens *et al.*, 2011). The air quality in the South African Highveld is directly influenced by emissions from traffic, concentrated industry and domestic burning. Industrial activities include 13 coal-fired power stations, two large petrochemical industries, as well as numerous smelters and coal mines (Jaars *et al.*, 2014). The power stations and petrochemical plants have tall smoke stacks, typically around 275-300 m, in an attempt to reduce the local impact of released pollutants. However, the removal of pollutants at higher altitudes may be a far slower process and on the regional scale may cause air pollution problems, since the pollutants can now affect more distant regions downwind (Holloway and Wayne, 2010).

Emission inventories for South Africa are still being developed and are not currently available. Preliminary estimates of national anthropogenic emissions, however, indicate that industrial, mining, transportation and biomass burning sectors are the major air emission sources in South Africa (http://www.airqualitylekgotla.co.za/assets/2017_5.2-draft-naeis-report-2015-emissions--first-results.pdf). Coal-fired power plants and industries (e.g. petrochemical coal plants) provide the large $SO_2$ and $NO_x$ emissions with additional contributions for $NO_x$ from transport and biomass burning. In general, CO is produced from three major sources, namely fossil fuel combustion, biomass burning, as well as the oxidation of methane and non-methane VOCs (Wang *et al.*, 2013). In southern Africa, biomass burning is the dominant source of CO pollution. However, in proximity of urban and industrial areas, traffic and industrial sectors provide additional contributions to CO concentrations. Regarding VOCs, the major anthropogenic sources are combustion (e.g. vehicles), fuel evaporation (e.g. petrochemical production) and chemical manufacturing (Pugliese *et al.*, 2014).

### 2.3.2 Natural

Previous strategies to reduce $O_3$ have focused on anthropogenic VOC emissions, however VOCs emitted from vegetation (known as biogenic VOC emissions) can also play a significant role in $O_3$ formation (NRC, 1991, Trainer *et al.*, 1987). It has been estimated that within the United States, emissions of biogenic VOCs during summer are equal to or even exceed the total emission of anthropogenic VOCs (Sillman, 1999). The single most important biogenic VOC for $O_3$ production is considered to be isoprene ($C_5H_8$), followed by terpenes and methanol ($CH_3OH$) (Aghedo *et al.*, 2007). Isoprene has very large global emission rates (between 500 and 750 $Tg^{-1}$) and high reactivity with $^{\bullet}OH$ (The Royal Society, 2008). In addition, isoprene emissions tend to be most intense around midday and in the afternoon during summer, which therefore occur during the time of day with the most favourable photochemical conditions and $^{\bullet}OH$ concentrations for $O_3$ formation (Wagner and Kuttler, 2014, Lee and Wang, 2006).

It is unclear whether biogenic VOCs have a similar impact in southern Africa. The regional modelling study conducted by Zunckel *et al.* (2006) showed that neither anthropogenic nor biogenic sources dominate in the formation of high $O_3$ concentrations over southern Africa, but collectively are responsible for $O_3$ production over the region. Note that the contribution by biomass burning to the formation of $O_3$ was not included in the study. Aghedo *et al.* (2007) reported that the largest contributor to surface $O_3$ pollution over Africa is biomass burning but biogenic (isoprene) emissions make a larger contribution to the global $O_3$ burden. Rural areas, particularly remote forest regions, in the Northern Hemisphere tend to be $NO_x$-limited, because $NO_x$ is relatively low and biogenic VOCs are high (Laurila *et al.*, 1999). However, Jaars *et al.* (2016) found that biogenic VOC concentrations were, in general, lower for savannah grasslands compared to other parts of the world, and

furthermore, much lower isoprene concentrations were measured compared to total aromatic concentrations at a regional background site in South Africa. Biogenic emissions likely play a more significant role in summer in the formation of $O_3$ when biomass burning emissions are small and biogenic emissions are high (Zunckel *et al.*, 2006).

Natural sources of $NO_x$ include soil, lightning and the downward transport of NO from the stratosphere (Vingarzan, 2004). During the humid summer season in continental southern Africa, the increased soil moisture enhances microbial action in the ground, causing the savannah soils to emit more NO than during the dry period of winter when soil moistures are very low and NO emissions decline (Otter *et al.*, 1999). The oxidation of biogenic $NH_3$ initiated by •OH radicals is another significant natural source of $NO_x$ (Holloway and Wayne, 2010). Natural CO production originates from the oxidation of biogenic VOCs, soil termites and vegetation, while natural $CH_4$ emissions mainly stem from wetlands (Holloway and Wayne, 2010, Finlayson-Pitts and Pitts Jr, 2000).

### 2.3.3 Biomass burning

Biomass burning is the burning of living and dead vegetation, which can be either human-initiated burning or natural lightning-induced burning (Levine, 2003). It is an important source of tropospheric $O_3$ precursors, namely $NO_x$, CO and VOCs (Crutzen and Andreae, 1990, Seiler and Crutzen, 1980), as well as greenhouse gases such as $CO_2$, $CH_4$ and nitrous oxide ($N_2O$) (Koppmann *et al.*, 2005). Most of the global biomass burning occurs in the tropical regions of South America, Southeast Asia and Africa (Levine, 2003, Hao and Liu, 1994, Crutzen and Andreae, 1990). At the continental scale, Africa is, on average, the single largest source of biomass burning emissions (dominated by savannah fires), responsible for approximately 30% of the global annual gross emissions from biomass burning (Silva *et al.*, 2003, Andreae, 1991). African biomass burning activities include savannah, forest and agricultural waste burning where “slash and burn” agricultural practices are used (Aghedo *et al.*, 2007).

African burning takes place during the dry season. The timing of the dry season varies north and south of the Equator, leading to shifts in maximum fire activity in the Northern and Southern Hemispheres (Giglio *et al.*, 2006). Consequently, African burning is characterised by two distinct burning seasons: primarily late November to early March in the Northern Hemisphere (Marenco *et al.*, 1990) and May to October for Southern Hemispheric Africa (Silva *et al.*, 2003, Scholes and Andreae, 2000). Fires typically progress in a west to east direction in the Southern Hemisphere, with peak biomass burning occurring between June and July for northern Angola, Zambia, southern Democratic Republic of Congo and Zimbabwe, while countries on the eastern coast of southern

Africa, such as Tanzania and Mozambique, experience maximum fires from September to October (Silva *et al.*, 2003, Dwyer *et al.*, 2000, Dwyer *et al.*, 1999, Barbosa *et al.*, 1999).

Although the majority of southern African fires are due to human activities, natural fires triggered by lightning strikes on dry vegetation also account for a small percentage (Ito *et al.*, 2007, Andreae, 1991). Peak fire activity and the length of the biomass burning season are coupled to the seasonal cycle of precipitation in this region (Giglio *et al.*, 2006). During the wet summer season, biomass is produced and later during the dry winter season, the dry biomass (Koppmann *et al.*, 2005, Scholes and Andreae, 2000) will induce more extensive fires and lead to a higher amount of $O_3$ precursor gases as detected during the SAFARI-92 and SAFARI 2000 field campaigns (Swap *et al.*, 2003, Thompson *et al.*, 1996). Higher fire frequencies are generally located north of 20˚S (see spatial distribution of fires in Chapter 4). Enhanced CO concentrations have been used to characterise the dispersion of biomass burning emissions over southern Africa due to its relatively long atmospheric lifetime (Mafusire *et al.*, 2016).

Domestic burning of biofuels, for space heating and cooking, also contributes to biomass burning emissions of $O_3$ precursors in southern Africa (Diab *et al.*, 2004). Incomplete combustion of wood and coal in households of developing countries is a daily practice, done mainly for economic reasons to meet the needs for cooking, lighting and space heating (Ludwig *et al.*, 2003). Household combustion within informal settlements on the South African Highveld was found to be a significant source of $NO_2$ and CO, as the morning and afternoon peaks of these species were pronounced in the cold winter months, corresponding to periods of cooking and space heating (Vakkari *et al.*, 2013, Venter *et al.*, 2012).

### 2.3.4 Lightning-induced $NO_x$ emissions

Lightning-induced $NO_x$ is the largest source of $NO_x$ in the upper troposphere, particularly in tropical regions and also in summer at the higher latitudes (Bond *et al.*, 2002). According to Schumann and Huntrieser (2007), lighting occurs mainly over land areas, with approximately 77% of all lightning occurring between $30^oS$ and $30^oN$ (Figure 2-3). Observations from space indicate that the Congo basin in central Africa is the hotspot of the world with regard to the highest flash rates, with an annual mean flash density of 80 $km^{-2}$ $yr^{-1}$, which is significant if compared, for instance, to Florida that is the hotspot in the United States with the flash densities reaching 30 $km^{-2}$ $yr^{-1}$ (Christian *et al.*, 2003). Satellite data also provided an annual mean flash density of 23 $km^{-2}$ $yr^{-1}$ for Bloemfontein, located on the South African Highveld (Christian *et al.*, 2003).

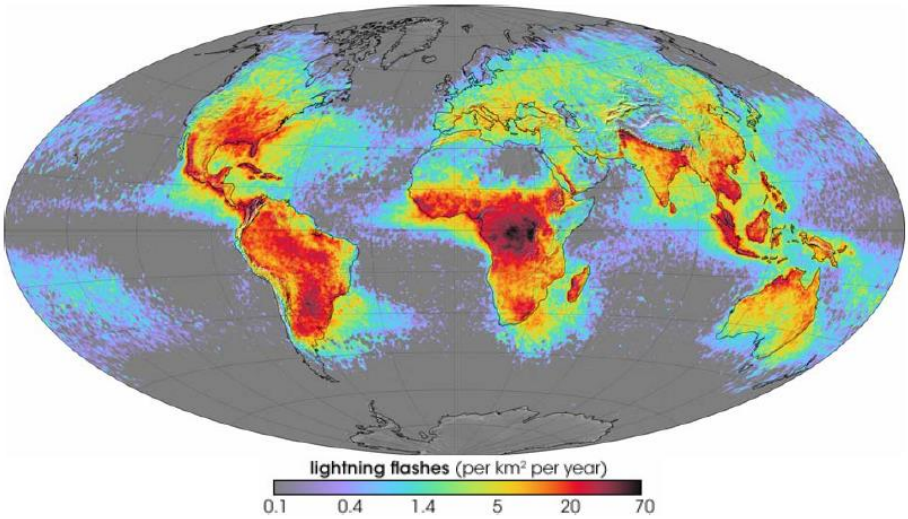


Figure 2-3: Global distribution of annually averaged lightning flash frequency density derived from data of the Lightning Imaging Sensor between 1997 and 2002, and the Optical Transient Detector between 1995 and 2000 (from NASA's Global Hydrology and Climate Center at Marshall Space Flight Center, 2006). The maximum and global mean flash density values are ~80 $km^{-2}$ $yr^{-1}$ and 2.7±0.3 $km^{-2}$ $yr^{-1}$, respectively (Schumann and Huntrieser, 2007).

A global chemistry transport model used by Marufu *et al.* (2000) showed that 27% of the tropospheric $O_3$ over Africa was caused by lightning-derived $NO_x$, although there is uncertainty in the model results because of large uncertainties associated with lightning $NO_x$ estimates used. Recent studies are trying to narrow the uncertainty of the amount of $NO_x$ produced from lightning by providing improved global estimates (e.g. Ott *et al.*, 2010, Schumann and Huntrieser, 2007, Boersma *et al.*, 2005). The global estimate of lightning $NO_x$ that is most widely used is 5±3 Tg N $yr^{-1}$ (Schumann and Huntrieser, 2007), which shows that it is several times smaller than anthropogenic and biomass burning sources, which are estimated at ~26 Tg N $yr^{-1}$ (Lamarque *et al.*, 2010). This is because lightning does not release $NO_x$ in the boundary layer, but in the middle to upper troposphere, where a large percentage of the $NO_x$ remains, which has longer lifetimes and better $O_3$ production efficiencies than in the boundary layer (Ott *et al.*, 2010). Therefore, the impacts of lightning emissions on the boundary layer are small relative to the free troposphere (Murray, 2016). Instead, it is the contribution of surface sources (biomass burning, industry and soil) that are the larger factors for $O_3$ levels in the boundary layer (Marufu *et al.*, 2000). Lightning-produced $NO_x$ over the Highveld region of South Africa was estimated to be approximately 9% of the anthropogenic $NO_x$ emissions (from coal-fired power plants) (Ojelede *et al.*, 2008).

## 2.4 ROLE OF METEOROLOGY AND TRANSPORT

The major circulation patterns governing weather patterns and controlling the tropospheric transport of atmospheric pollutants over the southern African interior are anticyclonic circulation (on its own or combined with easterly or westerly advection), as well as direct easterly or direct westerly transport patterns as indicated in Figure 2-4. However, the semi-permanent, mid-latitude anticyclone is the most prominent of these synoptic scale circulation patterns, which dominates (up to 80% of the time) in winter and is less frequent in summer (Garstang *et al.*, 1996). The subsidence caused by the anticyclonic circulation contributes to high atmospheric stability and frequent subsidence inversions, especially during wintertime over southern Africa (Tyson and Preston-Whyte, 2000). These stable layers suppress vertical mixing and allow pollutants to accumulate between the layers, while the anticyclonic vortex keeps the air masses recirculating over the subcontinent for long periods of time (Tyson *et al.*, 1996). Fine weather (clear skies, relatively cloud free) is associated with anticyclonic conditions, which are also linked to low rainfall and droughts (Tyson and Preston-Whyte, 2000).

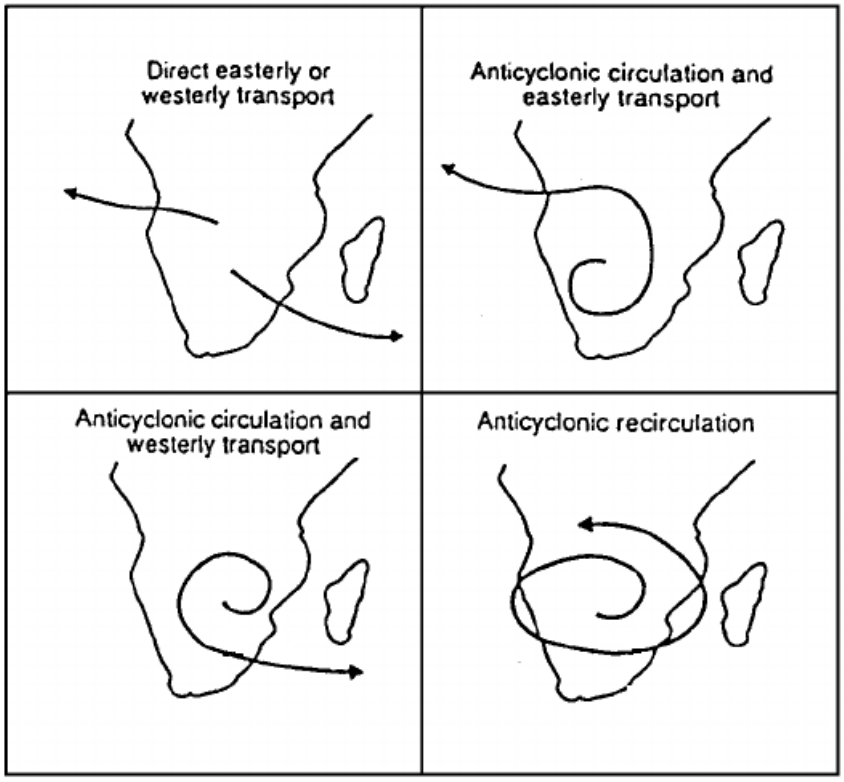


Figure 2-4: Schematic representation of major atmospheric transport patterns likely to result in easterly or westerly exiting of air masses from southern Africa or recirculation over the subcontinent (Zunckel *et al.*, 1999).

The duration and scale of these transport patterns in southern Africa depend on the season, level in the atmosphere, and the dominant circulation type (Tyson *et al.*, 1997). Anticyclonic circulation prevails in the southern and central parts, while the northern parts are more influenced by tropical easterlies. The easterly disturbances are more frequent in summer (30-50%), while the westerly wave disturbances occur regularly throughout the year (20-40%) (Garstang *et al.*, 1996). Anticyclonic activity causes recirculation over the sub-continent with an exit pathway off the sub-continent to the Atlantic Ocean at 20$^{o}$S and an exit pathway at 30$^{o}$S to the Indian Ocean (Zunckel *et al.*, 2006). The other possible transport out of the continent over south-eastern South Africa to the Indian Ocean is due to westerly disturbances during wintertime, while transport away from South Africa over northern Namibia and Angola to the Atlantic Ocean is connected mainly to easterly disturbances in summer (Garstang *et al.*, 1996).

Long-range transport is another important influence on pollutant levels and regional budgets thereof, as these species may be transported into southern Africa from distant sources, which can even be from another continent. Average $O_3$ concentrations in the free troposphere over the southern African region have been linked to long-range transport of South American biomass burning emissions that travelled towards Africa after transport into the upper troposphere by deep convection (Thompson *et al.*, 2014). Subsidence of this $O_3$-rich air from the free troposphere to the surface could increase background $O_3$ levels in the region. In addition, long-range transport of air masses from biomass burning occurring in regions north of southern Africa can also contribute significantly to concentrations of $O_3$ precursor species (Tyson *et al.*, 1997). Long-range transport of $O_3$ precursors is beyond the control of domestic regulations.

## 2.5 IMPACTS OF ELEVATED OZONE

### 2.5.1 Effects of ozone on human health

Although the health impacts of $O_3$ were not addressed in this thesis, it is an important topic that needs to be examined in future research as indicated in Chapter 7. One of the key reasons for measuring $O_3$ and investigating the underlying mechanisms involved with its formation are due to the threat that $O_3$ poses to human health. Epidemiological studies have shown that, among anthropogenic air pollutants, $O_3$ and fine particulate matter ($PM_{2.5}$) have the most significant influences on human health, including premature mortality (IPCC, 2013, NRC, 1991). Most of the impacts of $O_3$ on human health relate to the respiratory system and include reduced lung function, lung irritation and increased risk of mortality from respiratory causes (Jerrett *et al.*, 2009). However, health effects are not sufficiently understood. There is still debate on whether short-term exposure is of greater concern than longer-term exposure. The effects of repetitive high or medium exposure for

several days may be more severe than those of a single peak exposure, while the health effects associated with several days of high $O_3$ concentrations may be cumulative. However, fewer studies have reported on chronic health effects compared to acute health effects, which are well documented. Evidence of health related impacts of long-term $O_3$ exposure is derived mainly from one study (Jerrett *et al.*, 2009).

The US EPA uses health impact functions to relate changes in air pollution concentrations with health outcomes, which can be written as follows (Fann *et al.*, 2012):

$$\Delta y = y_0\left(e^{\beta \Delta x} - 1\right)Pop \qquad (2.17)$$

where:
$\Delta$y is the change in the health endpoint assessed due to a given pollutant
$y_0$ is the baseline incidence rate for the health endpoint assessed
Pop is the population affected by the change in air quality
$\Delta$x is the change in air quality
β is the effect coefficient drawn from the epidemiological study

This method was employed by Lelieveld *et al.* (2013), in which premature mortality associated with anthropogenic $PM_{2.5}$ and $O_3$ relative to unpolluted, preindustrial conditions was assessed. Therefore, $\Delta$y was the change in annual mortality due to a given pollutant (i.e. increase in mortality due to air pollution); $y_0$ was the baseline mortality rate for a given population (i.e. number of deaths in a particular year for a given population, obtained from the World Health Organization, country-level data); β is the concentration-response function derived from relative risk (RR) values in epidemiological studies; $\Delta$x is change in concentration of pollutant X (from the preindustrial level to the year 2005) and Pop is the total population with an age of ≥ 30 years exposed to the particular pollutant (Lelieveld *et al.*, 2013). Lelieveld *et al.* (2013) estimated a global respiratory mortality of 773 000/year due to $O_3$ and found that the highest premature mortality rates are found in Southeast Asia and the Western Pacific regions, where more than a dozen of the most highly polluted megacities are located. Other atmospheric modelling studies have also provided an estimate of the global burden of anthropogenic $O_3$ on premature human mortality. Anenburg *et al.* (2010) estimated 700 000 (± 300 000) deaths per year globally due to $O_3$; Lim *et al.* (2012) estimated 150 000 (50 000 to 270 000) deaths, while Silva *et al.* (2013) estimated 470 000 (95% confidence interval, 140 000 to 900 000) premature respiratory deaths associated globally with anthropogenic $O_3$. Data from a cohort study correlated with air pollution data also suggests that the risk of mortality associated with an increase in $O_3$ concentration could be significant (Jerrett *et al.*, 2009). A more

recent assessment from Lancet (Landrigan *et al.*, 2018) has attributed 300 000 (95% confidence interval, 100 000 to 400 000) deaths annually across the world to exposure to ambient $O_3$.

In many of these models, the global burden of air pollution is estimated with concentration-response functions taken from epidemiological studies conducted in the US and Europe (e.g. the American Cancer Society Cancer Prevention Study II cohort) (Lelieveld *et al.*, 2013), since there is a shortage of similar data for developing countries. However, care should be taken to apply concentration-response functions from the US and Europe to developing countries due to differences in population exposure (including pollutant concentrations, the composition of air pollutant mixtures, and activity patterns) and susceptibility (including underlying health status) that may result in large uncertainties in risk estimates (Silva *et al.*, 2013). Therefore, this highlights the critical necessity for health impact assessments using local data at a spatial resolution that is meaningful towards establishing the cost-benefit analysis of air pollution in developing countries, which include South Africa.

### 2.5.2 Effects of ozone on agriculture

The effects of $O_3$ on crops include visible injury, biomass loss (above and below the ground) and crop yield loss (Krupa *et al.*, 2001). The lesser known effects relate to physiological damage, such as reduced photosynthesis, stomatal closure, reduced leaf area index, inhibition of transpiration, reduced yield quality (e.g. nitrogen content), altered carbon allocation, and damage to reproductive ability (Wilkinson *et al.*, 2012, Felzer *et al.*, 2007). These impacts can be linked to chronic exposure to low concentrations (Felzer *et al.*, 2007) or acute exposure to high $O_3$ concentrations ($O_3$ episodes or peaks) (De Temmerman *et al.*, 2002). Chronic injury symptoms commonly manifest as bronzing, chlorosis and premature senescence, while acute injury is usually observed as flecking and stippling patches due to necrosis (Krupa *et al.*, 2001). The presence of foliar symptoms does not necessarily imply that there will be reductions in growth, yield or reproduction (Feng *et al.*, 2014).

$O_3$ affects plants by gaining access into the leaves via the stomatal pores (Wilkinson *et al.*, 2012). At the cellular level, $O_3$ is thought to give rise to the formation of reactive oxygen species (ROS), such as hydrogen peroxide ($H_2O_2$), superoxide ($O_2^-$) and $^{\bullet}OH$ radicals (Fiscus *et al.*, 2005). A rapid rise in ROS produced ('oxidative burst') in response to the $O_3$ stress induces ROS scavenging enzymes to decrease the concentrations of the damaging ROS (Long and Naidu, 2002). Although ascorbate and other scavenging systems will remove $O_3$ and ROS, the ROS that remains unscavenged causes primary damage to the leaves such as interveinal necrosis, early senescence and abscission (Wilkinson *et al.*, 2012). In terms of photosynthesis, $O_3$ has been shown to decrease photosynthetic capacity associated with a decrease in Rubisco protein (Long and Naidu, 2002).

To estimate the effects of $O_3$ on crop plants and natural vegetation, studies have been conducted in both the laboratory and in field experiments, using controlled environment greenhouse or growth chambers, open-top chambers or field plots (Felzer *et al.*, 2007). These types of experiments in which exposure to $O_3$ for an entire growth season is related to an end-of-season yield have been used to derive exposure-response relationships to establish air quality guidelines (e.g. critical levels). A large amount of scientific evidence has been accumulated over the past 30 years, in North America, Europe and more recently Asia, on the effects of elevated ambient concentrations of $O_3$ on crop yields (Wilkinson *et al.*, 2012). These exposure-response relationships have been used to assess the effects of $O_3$ globally and regionally, which show substantial impacts in terms of production and economic losses (Ghude *et al.*, 2014, Avnery *et al.*, 2011, Van Dingenen *et al.*, 2009, Holland *et al.*, 2006, Wang and Mauzerall, 2004). Global models have estimated relative yield losses to be greatest for wheat and soybean, followed by rice and maize (Avnery *et al.*, 2011, Van Dingenen *et al.*, 2009). For those regions where certain crops are a staple food source, crop yield losses due to $O_3$ damage threaten regional food security (The Royal Society, 2008). In India it was calculated that $O_3$ damage to wheat and rice resulted in yield losses sufficient to feed 94 million people living below the poverty line (Ghude *et al.*, 2014).

Several $O_3$ metrics have been devised to quantitatively describe vegetation exposure to $O_3$. The AOT40 is the preferred $O_3$ exposure index used in Europe, which is defined as the accumulated $O_3$ concentration above a threshold of 40 ppb during daylight hours over a three-month growing season (3 ppm h for agricultural crops and 5 ppm h for forests) (CLRTAP, 2014). A concentration-based approach was initially followed in Europe with the introduction of the AOT40 exposure index. However, a flux-based approach was later followed using $O_3$ uptake exposure indices (Emberson *et al.*, 2000), since the AOT40 is based on concentrations in air and does not reflect $O_3$ uptake by leaves. Therefore an uptake-based exposure index has been developed that takes into account the degree of stomatal opening over time. The Jarvis-type multiplicative stomatal conductance model is used to estimate stomatal response to different environmental variables, which, in turn, determines the $O_3$ uptake (flux) (Emberson *et al.*, 2000). This allows for the development of flux-based dose-response relationships that connect $O_3$ ambient concentration and $O_3$ uptake, which represent a more relevant exposure index for the quantification of $O_3$ effects on crops (Pleijel *et al.*, 2004).

In North America, mean exposure $O_3$ indices such as M7 and M12 (seasonal 7h and 12h mean $O_3$ concentration during daylight) were initially developed, but were later criticised for giving equal weighting to both high and low concentrations. As a result, cumulative exposure $O_3$ indices, the most frequently used being the SUM06 (sum of all hourly $O_3$ concentrations ≥ 60 ppb) and W126 (hourly concentrations weighed by a sigmoidal weighting function), were introduced to include peak and durational $O_3$ concentrations (Tong *et al.*, 2009). The US has also set a separate secondary air

quality standard for $O_3$, which is welfare-based (includes vegetation and crops). It is, however, identical to the primary health-based standards, i.e. annual fourth highest daily maximum 8-h concentration, averaged over three years should not exceed 70 ppb (Paoletti and Manning, 2007). Since damage to vegetation is cumulative, occurring over weeks to months during the growing season, there is a need for a secondary $O_3$ standard to protect vegetation compared to the short-term health standard (McCarthy and Lattanzio, 2016).

Crop species differ widely in their susceptibility to $O_3$ (Wilkinson *et al.*, 2012). A review by Mills *et al.* (2007) listed sensitivity to $O_3$ for several crops using the AOT40-concentration based function. Among the most sensitive were pulses, cotton and wheat; the moderately sensitive category included potato, rice and maize; while barley, strawberry and plum were found to be $O_3$ resistant. The sensitivity of the Phaseolus vulgaris bean cultivars to $O_3$ is well known and widely reported visible injury symptoms are observed in Europe (Feng *et al.*, 2014). Field studies with potato have demonstrated foliar injury that appeared only after the stage of maximum leaf area and increased steadily towards harvest (De Temmerman *et al.*, 2002). Comparison of rice grown in charcoal-filtered air with rice exposed to chronic elevated $O_3$ (62 ppb) revealed that many of the yield parameters were negatively affected, including photosynthesis, biomass, leaf area index, grain number and grain mass, which resulted in a 14% decrease in yield (Ainsworth, 2008). Leafy biomass crops (e.g. lettuce, spinach, chicory, cabbage) are susceptible to visible injuries, senescence and/or abscission, while root biomass crops such as potato, onion and carrot are directly vulnerable to reductions in root biomass (Wilkinson *et al.*, 2012). The effects of $O_3$ on wheat yield were studied with open-top chamber experimental data from North America, Europe and Asia (Pleijel, 2011). Using meta-analysis to summarise the 30 experiments, the average yield improvement after reducing $O_3$ in the air was 9% (Pleijel, 2011). A risk assessment was conducted for maize – a staple food in five southern African countries (Zunckel *et al.*, 2006) – in southern Africa based on the AOT40 exposure index that found values over 3 ppm h for the growing season, which suggests surface $O_3$ may pose a potential significant threat to agricultural production in southern Africa (Van Tienhoven *et al.*, 2005).

The impact of $O_3$ on crops may also be altered by other environmental factors, such as soil water content, temperature, solar radiation intensity and vapour pressure deficit (VPD), which can cause reductions in stomatal conductance and $O_3$ uptake by plants (Fiscus *et al.*, 2005, Pochanart *et al.*, 2002). Another important environmental factor is steadily increasing atmospheric $CO_2$ concentrations (IPCC, 2013). Some studies have shown that the elevated $CO_2$ affords plants with protection against $O_3$ that include reduced injuries to leaves, reduction in stomatal conductance and $O_3$ uptake into leaves, as well as increased provision of substrates for detoxification and repair processes (Fiscus *et al.*, 2005). However, other studies found that the combined effects of elevated

$O_3$ and $CO_2$ on plants provided no ameliorating effects (Rebbeck and Scherzer, 2002). Further research that follows a holistic approach is necessary to quantify the impacts of $O_3$ on crops within the context of climate change (Krupa *et al.*, 2001), which will enhance our knowledge of the integrative effects of multiple stresses and improve our ability to plan for the availability of food in future.

## 2.6 AIR QUALITY STANDARDS FOR OZONE

A summary of the air quality standards/guidelines for $O_3$ that have been adopted by various countries and regulatory agencies is found in Table 2-2 below. The most common health protection thresholds for $O_3$ are the daily maximum one-hour average and the daily maximum eight-hour moving average. Several countries and organisations have adopted the eight-hour standards (sometimes in conjunction with a one-hour standard) on the basis that eight-hour exposures have been deemed to pose a significant health risk in those areas of the world. Australia, however, has a one- and four-hour standard, since the analysis of $O_3$ episodes in major Australian urban airsheds showed that $O_3$ peaks were typically of short duration. The World Health Organization (WHO) health-based guideline for all its member states is an eight-hour standard equivalent to 100 µg/m$^3$ (or 50 ppb) for $O_3$. According to the WHO (2006), although health effects may occur below this level, there is no clear evidence of a safe concentration threshold for $O_3$, which would provide adequate protection of public health. The review and revision of air quality standards are ongoing processes as scientific knowledge improves, to ensure new information is taken into account that serves to protect human health and the environment.

Compared to the other countries, South Africa has quite a stringent eight-hour standard for $O_3$, which is similar to the EU and Canadian standards. The South African NAAQS for ground level $O_3$ is an eight-hour moving average $O_3$ concentration of 120 µg/m$^3$ (61 ppb). The eight-hour standard is attained in an area when the 99$^{th}$ percentile of the eight-hour moving average $O_3$ concentrations in a year is below 61 ppb, which is equivalent to no more than 11 exceedances per year or 1% of occasions for which exceedances of the limit value are allowed. If, in accordance with international guidelines, the local standard refers to the daily maximum concentrations of the running eight-hour mean, 11 exceedances equate to 11 days per year of permissible exceedances. Complying with the eight-hour standard is a challenge in South Africa, as a large number of exceedances of the NAAQS for $O_3$ are often reported, particularly at monitoring stations located in the Vaal Triangle and Highveld Priority Areas (http://www.saaqis.org.za).

Table 2-2: Comparison of ambient air quality standards/guidelines for selected countries and organisations.

| $O_3$ | Air Quality Standard/Guideline | | |
|---|---|---|---|
| **Averaging Period** | **Country** | **Limit Value** | **Form** |
| 1-hour | U.S.[a] | 120 ppb (240 µg/m$^3$) | Daily maximum 1-hour mean concentration. Maximum allowable exceedance of 1 day per year. |
| | China[b] | 80 ppb (160 µg/m$^3$) Grade-I | 1-hour mean concentration. |
| | | 100 ppb (200 µg/m$^3$) Grade-II | |
| | Australia[c] | 100 ppb (200 µg/m$^3$) | Daily maximum 1-hour mean concentration. Maximum allowable exceedance of 1 day a year. |
| | E.U.[d] | 90 ppb (180 µg/m$^3$) Information threshold | Daily maximum 1-hour mean concentration. |
| | | 120 ppb (240 µg/m$^3$) Alert threshold | |
| | New Zealand[e] | 75 ppb (150 µg/m$^3$) | Daily maximum 1-hour mean concentration. |
| | Japan[f] | 60 ppb (118 µg/m$^3$) | 1-hour mean concentration. The standard is for $O_x$ (photochemical oxidants) which includes $O_3$. |
| | | | |
| 4-hours | Australia[c] | 80 ppb (160 µg/m$^3$) | Daily maximum 4-hour mean concentration. Maximum allowable exceedance of 1 day a year. |
| | | | |
| 8-hours | U.K.[g] | 50 ppb (100 µg/m$^3$) | Daily maximum of a running 8-hour mean concentration. Not to be exceeded more than 10 days a year. |
| | E.U.[d] | 60 ppb (120 µg/m$^3$) | Daily maximum of a running 8-hour mean concentration. Not to be exceeded more than 25 days averaged over three years. |
| | S.A.[h] | 61 ppb (120 µg/m$^3$) | Running 8-hour mean concentration. Not to be exceeded more than 11 times a year. |
| | WHO[i] | 50 ppb (100 µg/m$^3$) | Daily maximum 8-hour mean concentration. No exceedances are allowed. |
| | U.S.[a] | 70 ppb (140 µg/m$^3$) | Annual fourth-highest daily maximum 8-hour concentration, averaged over 3 years, should not exceed the limit value. |
| | Canada[j] | 63 ppb (126 µg/m$^3$) | Annual fourth-highest daily maximum 8-hour concentration, averaged over 3 years, should not exceed the limit value. |
| | New Zealand[e] | 50 ppb (100 µg/m$^3$) | Daily maximum 8-hour mean concentration. |
| | China[b] | 50 ppb (100 µg/m$^3$) Grade-I | Daily maximum 8-hour mean concentration. |
| | | 80 ppb (160 µg/m$^3$) Grade-II | Daily maximum 8-hour mean concentration. |

[a] McCarthy and Lattanzio (2016)
[b] Zhao *et al.* (2016)
[c] From http://www.environment.gov.au/protection/air-quality/air-quality-standards
[d] From http://ec.europa.eu/environment/air/quality/standards.htm
[e] From http://www.mfe.govt.nz/publications/air/ambient-air-quality-guidelines-2002-update/2-health-based-guideline-values
[f] Wakamatsu *et al.* (2013)
[g] From https://uk-air.defra.gov.uk/air-pollution/uk-eu-limits
[h] Government Gazette Republic of South Africa (2009)
[i] WHO (2006)
[j] From https://www.ccme.ca/en/resources/air/pm_ozone.html
Note:
[1] The US EPA one-hour $O_3$ standard only applies to specific areas. As of 1997, EPA revoked the one-hour $O_3$ standard in all areas, although some areas have continued obligations under that standard ("anti-backsliding").
[2] To convert ppb to µg/m$^3$ depends on the conditions (E.U. uses 20$^o$C and 101.3 kPa whilst WHO uses 25$^o$C and 101.3 kPa); however, a simple conversion between the two units as defined here was used to compile this table: 1 ppb of $O_3$ = 2.0 µg/m$^3$. The Europeans give their guidelines/objectives in µg/m$^3$ while the North Americans specify their standards in ppb.

## 2.7 CONTROL STRATEGIES FOR OZONE

Controlling the formation of $O_3$ is not as straightforward as regulating the concentrations of its precursors, $NO_x$ and VOCs. As indicated in Chapter 1, the chemistry governing $O_3$ formation from $NO_x$ and VOCs is non-linear, while it is also influenced by local meteorology (Jaffe and Ray, 2007). In fact, the ambient $O_3$ concentration observed at a location is the combined contribution of chemistry, deposition and transport (Monks, 2000) that has occurred over several hours or a few days (Sillman, 2003). Although both $NO_x$ and VOCs contribute to the reactions that serve as the primary source of tropospheric $O_3$, a reduction of one with respect to the other can under some conditions lead to an increase in $O_3$ through decreased titration (Porter *et al.*, 2014) or have almost no effect on peak $O_3$ levels (Seinfeld and Pandis, 2006) as previously discussed. Previous studies have shown that, despite efforts to control $O_3$, many urban areas in the US are incapable of achieving the national ambient air quality standard for $O_3$ without significant reductions of both of $NO_x$ and VOC emissions (Sillman, 1999, Fiore *et al.*, 1998).

### 2.7.1 Diagnosing the ozone formation regime

The dependence of $O_3$ production on the relative ratios of VOC- and $NO_x$ concentrations (or VOC emission rates and $NO_x$ concentrations) is frequently represented by means of an $O_3$ isopleth diagram indicated in Fig. 2-5, which clearly illustrates the non-linear behaviour of $O_3$ towards concentrations of these primary pollutants (Seinfeld and Pandis, 2006). This contour plot is a useful aid to gain knowledge on the chemical regime for $O_3$ production. Two regimes can be identified with different $O_3$-$NO_x$-VOC sensitivity in Fig. 2-5. The ridge line separates the two regimes and represents a local maximum for $O_3$ versus $NO_x$ and VOC (Sillman, 1999). Above the ridge line is the 'VOC-limited' ($NO_x$-saturated) or 'VOC-sensitive' regime (low VOC/$NO_x$), where $O_3$ production is limited by the availability of VOCs. Under VOC-limited conditions, $O_3$ concentrations increase with increasing VOCs and decrease with increasing $NO_x$. Therefore, in the VOC-limited regime, VOC reductions will be most effective in reducing local $O_3$ production, and $NO_x$ controls may lead to $O_3$ increases. Below the ridge line is the '$NO_x$-limited' or '$NO_x$-sensitive' regime (high VOC/$NO_x$ ratio), where $O_3$ formation is limited by, and therefore sensitive to the availability of $NO_x$. In the $NO_x$-limited regime, $O_3$ concentrations increase with increasing $NO_x$ and are largely independent of VOCs (Sillman, 1999). Therefore, $NO_x$ reductions are most effective and VOC controls are of no benefit for decreasing $O_3$ in a $NO_x$-limited regime. Between the $NO_x$- and VOC-limited extremes, there is a transitional region where $O_3$ is nearly equally sensitive to each species, and control of both VOC and $NO_x$ might be preferred (National Research NRC, 1991).

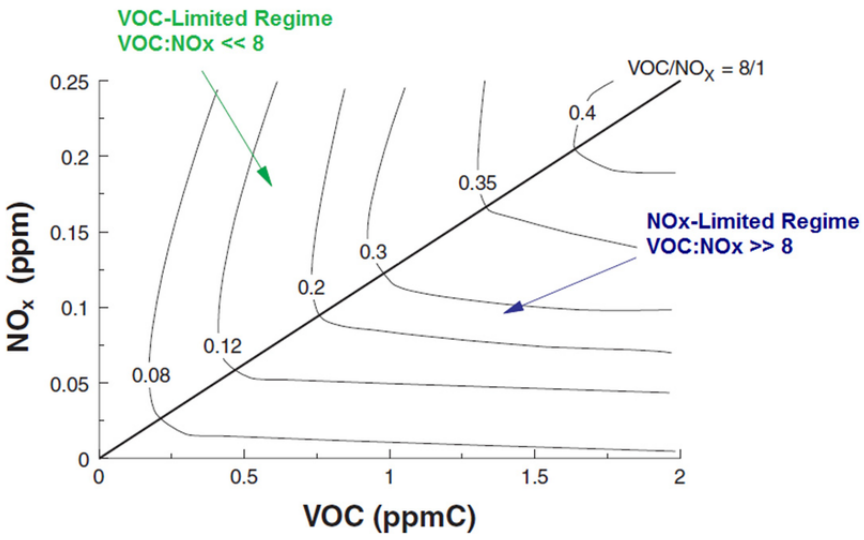


Figure 2-5: Typical $O_3$ isopleth diagram of 1-h maximum $O_3$ concentrations (ppm) calculated as a function of initial VOC and $NO_x$ concentrations (Parra and Franco, 2016).

Caution must be used when diagnosing the $O_3$ production regime as $NO_x$- or VOC-limited as $O_3$-$NO_x$-VOC sensitivity can vary for different locations and different events. $NO_x$-rich, VOC-limited air parcels always become $NO_x$-poor air parcels somewhere downwind. VOC-limited conditions often become $NO_x$-limited conditions. Although there could be times and places when VOC controls could be effective in the abatement of $O_3$, increasing $NO_x$ always eventually leads to more $O_3$ somewhere. The instantaneous production rate for $O_3$ should be calculated for all sites with measured $NO_x$ and VOC in order to get a more representative picture of the $O_3$ production regime throughout an area. Alternatively, isopleth plots should be used with other diagnostic tools, such as secondary species measurements, reactivity-weighted VOC to $NO_x$ ratios etc. to derive more information about $O_3$-$NO_x$-VOC sensitivity.

## 2.7.2 Regional control of ozone

Figure 2-6 illustrates the change in $NO_x$, $NO_2$ and $O_3$ concentrations for an air mass passing over a pollutant source region (Lövblad *et al.*, 2004). The $NO_x$ concentrations are high within a source region, which affect the photochemical production and destruction of $O_3$. Firstly, in high $NO_x$ areas, the $NO_2$ competes with VOCs for the $^{\bullet}OH$ radical to form $HNO_3$ ($NO_2 + {}^{\bullet}OH \rightarrow HNO_3 + O_2$), thereby suppressing $O_3$ production (Lövblad *et al.*, 2004). Secondly, steady NO emissions result in $O_3$ titration through the reaction with NO ($NO + O_3 \rightarrow NO_2 + O_2$). As the air mass moves away from the source region, $NO_2$ undergoes photolysis to form $O_3$, while decreasing $NO_x$ concentrations also reduce $O_3$ titration, resulting in $O_3$ levels being higher in surrounding areas downwind of the source region (Pusede and Cohen, 2012, Murphy *et al.*, 2007). This demonstrates the regional problem

associated with $O_3$. In general, $O_3$ formation in urban areas close to sources is VOC-limited (Monks *et al.*, 2015), as the rate of $O_3$ production is initially limited by the availability of VOCs. As the polluted mass is transported downwind and over rural areas, the rate of $O_3$ production is progressively limited by availability of $NO_x$ with $O_3$ formation being increasingly $NO_x$-limited (Sillman, 1999). Rural areas also tend to have $NO_x$-sensitive conditions due to the impact of biogenic VOCs (Liu *et al.*, 2018, Li *et al.*, 2011, Biesenthal *et al.*, 1998). Therefore, different control strategies would be required for different regions in order to reduce $O_3$ pollution.

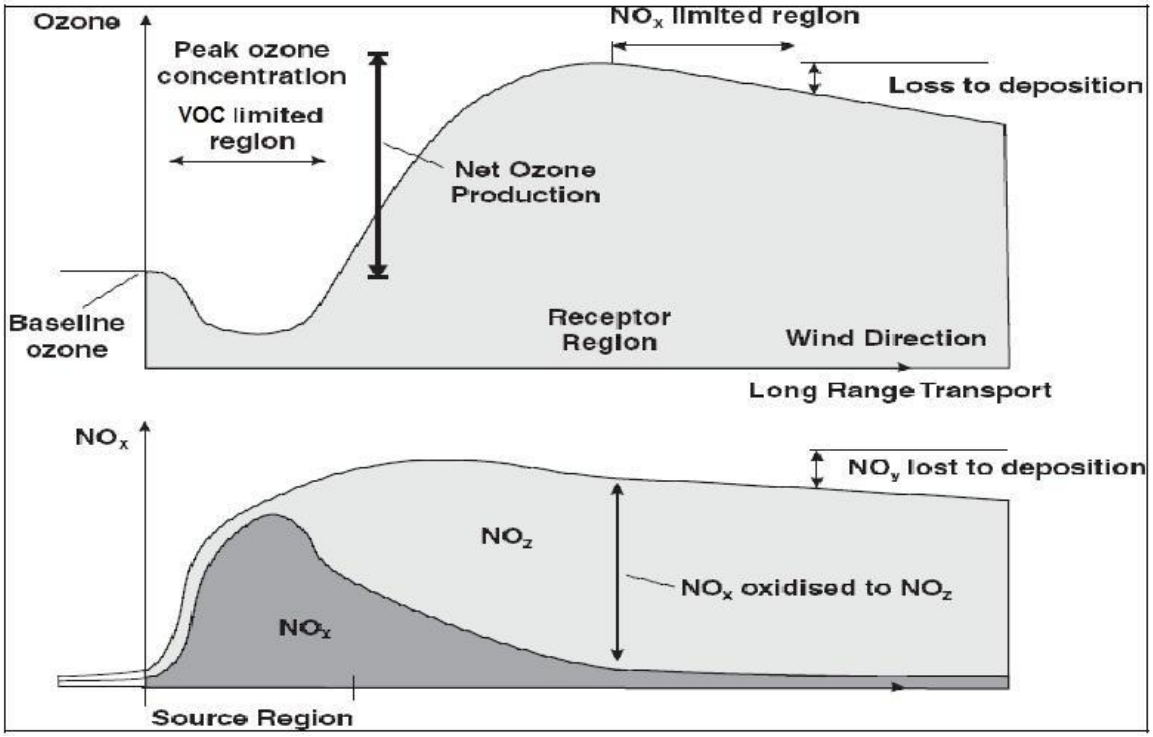


Figure 2-6: A representation of the relationship between net $O_3$ production and the amount of $NO_x$ oxidised including the VOC- and $NO_x$-limiting regions (Lövblad *et al.*, 2004).

## 2.8 CONCLUSION

In South Africa, high concentrations of both VOCs and $NO_x$ are emitted from vehicles and large industries, such as petrochemical coal plants, while coal-fired power plants are a large source of $NO_x$ emissions. These anthropogenic precursors combined with a dominant anticyclonic climatology cause exceedances of the NAAQS for $O_3$ on a regional scale (Zunckel *et al.*, 2006). Therefore, regional abatement measures rather than local abatement measures might be more effective in reducing $O_3$ over a large geographic area. Therefore, in the long term, it will be necessary to reduce both $NO_x$ and VOC emissions appreciably to gain significant reductions in regional $O_3$. In the short term, it may be necessary to identify regions as $NO_x$- or VOC-limited in order to maximise the cost effectiveness of emission reduction strategies (Laban *et al.*, 2015).

In this study, high-quality continuous ground measurement $O_3$ data obtained from four sites in the interior of South Africa was used to establish the seasonal influence on $O_3$ variability in order to determine the major sources of $O_3$ precursors, as well as the predominant $O_3$ production regime for continental South Africa. The data was also subjected to different multivariate statistical analyses in order to determine the relative significance of chemical and meteorological influences on surface $O_3$ in this region. Finally, a case study was conducted to establish the influence of increased $O_3$ on two South African sugarcane cultivars.

# CHAPTER 3

## MATERIALS AND METHODS

*In this chapter, the methodology followed to address the research objectives listed in Chapter 1 is discussed. The first part of this chapter deals with the measurement locations where the continuous air monitoring took place, describes the instrumentation utilised and indicates the appropriate data quality assurance procedures followed. Different data analysis procedures applied are also discussed. The latter part of this chapter covers the open-top chamber experiments during which air pollution impacts on sugarcane were studied.*

## 3.1 MEASUREMENT LOCATIONS FOR AIR MONITORING

Data collected at four measurement sites in the north-eastern interior of South Africa was used to examine and understand the factors affecting regional surface $O_3$ pollution (Fig. 3-1). The four inland monitoring locations represent clean/semi-clean and polluted atmospheres across South Africa. The measurement sites are all impacted by a semi-permanent anticyclonic regional atmospheric circulation system, which is dominant in the southern and central parts of southern Africa. In fact, one of the findings from two major field campaigns (SAFARI-92 and SAFARI 2000) conducted to study regional emissions in southern Africa was that locations in southern Africa, thousands of kilometres apart, are linked through the regional anticyclonic circulation feature (Swap *et al.*, 2003). Air masses associated with the anticyclonic recirculation are not representative of the clean regional background, but are aged air masses that have passed over the industrialised Highveld of South Africa (Vakkari *et al.*, 2011).

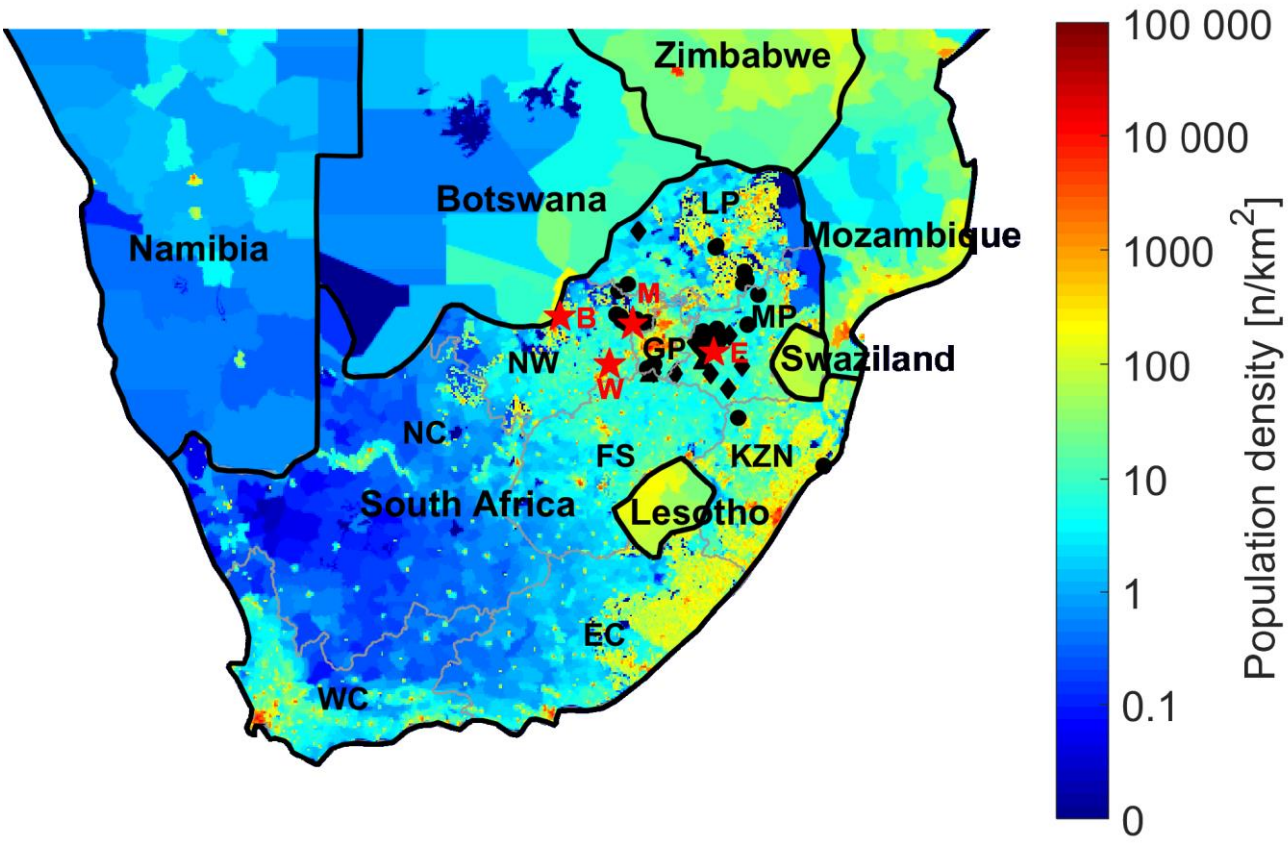


Figure 3-1: Location of the four measurement sites (W = Welgegund, B = Botsalano, M = Marikana, E = Elandsfontein) in South Africa, indicated by red stars on the map. The population density (people per km$^2$) and large anthropogenic point sources are also indicated (♦ = coal-fired power plants, ▲ = petrochemical plants, ● = metallurgical smelters). Provinces of South Africa are also indicated (WC = Western Cape, EC = Eastern Cape, NC = Northern Cape, NW = North West, FS = Free State, GP = Gauteng, MP = Mpumalanga, KZN = KwaZulu-Natal and LP = Limpopo). The figure was adapted from Venter *et al.* (2015).

### 3.1.1 Botsalano

The Botsalano measurement site (25.54$^o$ S, 25.75$^o$ E, 1420 m a.s.l.), which was situated in a game reserve in the North West Province of South Africa, is considered to be representative of regional background air. The surrounding vegetation is typical of a savannah biome, consisting of grasslands with scattered shrubs and trees (Laakso *et al.*, 2008). The area is quite sparsely populated with no local anthropogenic pollution sources (Vakkari *et al.*, 2013, Laakso *et al.*, 2008). The distance to the closest towns, Mafikeng and Zeerust, is approximately 50 km. It is in close proximity to the Botswana border (about 10 km) north of the site. The western Bushveld Igneous Complex, which is a densely populated and highly industrialised region where numerous platinum, base metal, vanadium and chromium mining/smelting industries are situated, is the largest regional

anthropogenic pollution source located approximately 150 km to the east of the reserve. Botsalano is also occasionally impacted by plumes passing over the industrialised Mpumalanga Highveld and the Johannesburg-Pretoria megacity (Vakkari *et al.*, 2011, Laakso *et al.*, 2008). In addition, the site is influenced by seasonal regional savannah wildfires during the dry period (Mafusire *et al.*, 2016, Vakkari *et al.*, 2011, Laakso *et al.*, 2008). Measurements were conducted from 20 July 2006 until 5 February 2008 (Vakkari *et al.*, 2013, Vakkari *et al.*, 2011, Laakso *et al.*, 2008).

Figure 3-2: Botsalano atmospheric research station and the surrounding area.

### 3.1.2 Marikana

The Marikana measurement site (25.70$^{o}$ S, 27.48$^{o}$ E, 1170 m a.s.l.) was located within the western Bushveld Igneous Complex. Marikana is a small mining town located approximately 30 km east of Rustenburg and approximately 100 km northwest of Johannesburg. The measurement site was located in the midst of a residential area comprising low-cost housing settlements and municipal buildings (Hirsikko *et al.*, 2012, Venter *et al.*, 2012). Anthropogenic emissions from household combustion, traffic and industry in the wider region have a strong influence on pollution at the measurement site (Venter *et al.*, 2012). Data was collected for the period 8 February 2008 to 16 May 2010, and has been used in previous studies (Vakkari *et al.*, 2013, Petäjä *et al.*, 2013, Hirsikko *et al.*, 2013, Venter *et al.*, 2012, Hirsikko *et al.*, 2012).

Figure 3-3: Marikana atmospheric research station and its surroundings.

### 3.1.3 Welgegund

The Welgegund measurement site (26.57$^{o}$ S, 26.94$^{o}$ E, 1480 m a.s.l.) is approximately 100 km west of Johannesburg and is located on a commercial arable and pastoral farm. The site is located in a grassland biome and is characterised by grazed grassveld with scattered *Vachellia erioloba* (camel thorn) trees (Jaars *et al.*, 2016). The station can be considered a regionally representative background site as it has few local anthropogenic sources. Air masses arriving at Welgegund from the west reflect a relatively clean regional background. However, the site is impacted by polluted air masses that are advected over major anthropogenic source regions in the interior of South Africa, which include the western Bushveld Igneous Complex, Johannesburg-Pretoria megacity, the Mpumalanga Highveld and the Vaal Triangle (Venter *et al.*, 2017, Jaars *et al.*, 2016, Tiitta *et al.*, 2014). In addition, Welgegund is also affected by regional savannah and grassland fires that are common in the dry season (Vakkari *et al.*, 2014). The atmospheric measurement station has been operating at Welgegund since 20 May 2010, with data measured up until 31 December 2015 utilised in this study.

Figure 3-4: Welgegund atmospheric research station (www.welgegund.org). The observations at the site include a wide range of air quality and climate change relevant parameters.

### 3.1.4 Elandsfontein

Elandsfontein (26.25$^{o}$ S, 29.42$^{o}$ E, 1750 m a.s.l.) is an ambient air quality monitoring station operated by Eskom, the national electricity supply company, primarily for legislative compliance purposes. This station was upgraded and co-managed by researchers during the EUCAARI project (Laakso *et al.*, 2012). The Elandsfontein station is situated in Mpumalanga, in the heart of the industrialised Highveld and several emission sources such as coal mines, coal-fired power-generating stations, a large petrochemical plant and major roads influence air quality at the site. The measurement site is at the top of a hill approximately 200 km east of Johannesburg and 45 km south-southeast of eMalahleni (previously known as Witbank), which is a coal mining area (Laakso *et al.*, 2012). The sources closest to Elandsfontein are the Kriel and Matla coal-fired power stations, which are located approximately 25 km west of the measurement site. Additional power stations near eMalahleni and metallurgical plants to the north also frequently impact the site (Laakso *et al.*, 2012). Being close to power plant sources implies that the Elandsfontein measurement station will be sensitive to changes in tall stack emissions. The Elandsfontein dataset covers the period 11 February 2009 until 31 December 2010 during the EUCAARI campaign (Laakso *et al.*, 2012).

Figure 3-5: Elandsfontein air quality monitoring station.

## 3.2 MEASUREMENTS

The measurements relevant to this study are discussed briefly in the following paragraphs. Detailed discussions on sampling procedures and instrumentation are presented by (Petäjä *et al.*, 2013, Venter *et al.*, 2012, Laakso *et al.*, 2008). Table 3-1 provides a summary of the key measurements conducted at the Botsalano, Marikana and Welgegund research stations, as well as the Elandsfontein routine air quality monitoring station. $O_3$ concentrations at the Welgegund, Botsalano and Marikana monitoring stations were measured using the Environment SA 41M $O_3$ analyser (Fig. 3.6 a), while a Monitor Europe ML9810B $O_3$ analyser was utilised at Elandsfontein. Both instruments operate on the principle that $O_3$ molecules strongly absorb UV radiation at a wavelength of 254 nm and the concentration is directly related to the intensity of the absorbed radiation through the Beer-Lambert law (US EPA, 1996). The $O_3$ concentration is determined from the difference between UV absorption of the gas sample and the sample with $O_3$ scrubbed air. $O_3$ concentrations are reported in ppb by volume, at a standardised temperature of 25$^{o}$C and a pressure of 101.3 kPa. CO concentrations were determined from the quantity of infrared light absorbed by CO molecules (cross flow modulated non-dispersive infrared absorption technique) with a Horiba APMA-360 analyser (Fig. 3.6 b) at Welgegund, Botsalano and Marikana, while it was not measured at Elandsfontein. Concentrations of NO and $NO_x$ (with $NO_2$ determined by subtraction) were determined through the chemiluminescence measurement principle, with a Teledyne 200AU analyser (Fig. 3.6 a) employed at Welgegund, Botsalano and Marikana, and a Thermo Electron 42i analyser at Elandsfontein. The analytical method involves the $NO_x$ analyser operating in two modes: one that measures the NO concentration by sampling ambient air directly i.e. measuring the light

intensity produced from the chemiluminescence gas phase reaction between NO and $O_3$, and one that measures the $NO_x$ concentration (sum of NO and $NO_2$) by passing the ambient air stream over a heated molybdenum catalyst (converter) heated to about 325°C that reduces $NO_2$ to NO (Dunlea *et al*., 2007). A major disadvantage of the measurement technique is that it does not measure $NO_x$ uniquely but the molybdenum catalyst additionally exhibits sensitivity to peroxyacetyl nitrates (PAN), nitric acid ($HNO_3$) and other products of the oxidation of $NO_x$ (Luke *et al.*, 2010, Dunlea *et al.*, 2007, Fehsenfeld *et al.*, 1987). The effect of this interference is that the measurement represents the upper limits of the $NO_2$ concentrations and is more nearly $NO_y$. Therefore to increase confidence in the measurements, the $NO_2$ levels determined with the Teledyne 200AU analyser were compared with a quantum cascade laser used for $NO_2$ flux measurements at Welgegund, which indicated good comparison between these two instruments.

Table 3-1: Measured parameters and instrumentation of relevance to this study at the measurement locations. The accuracy of the measurements has been indicated where available (Petäjä et al., 2013).

| **Measurement site** | **Measured quantity** | **Time resolution** | **Instrument** | **Accuracy** |
|---|---|---|---|---|
| Botsalano, Marikana and Welgegund | $O_3$ concentration (ppb) | 1 min | Environment SA 41M | 1 ppb |
| | $NO_x$ concentration (ppb) | 1 min | Teledyne 200AU | 0.1 ppb |
| | CO concentration (ppb) | 1 min | Horiba APMA-360 | 20 ppb |
| | Temperature ($^oC$) | 1 min | Rotronic MP 101A | ± 0.3$^oC$ |
| | Relative humidity (%) | 1 min | Rotronic MP 101A | |
| | Global radiation ($W/m^2$) | 1 min | LiCor LI-190SB | |
| | Wind speed (m/s) | 1 min | Vector W200P | 0.15 m/s |
| | Wind direction (degrees) | 1 min | Vector A101ML | ± 4$^o$ |
| | Precipitation (mm/hr) | 1 min | Thies 5.4103.20.041 | |
| | | | | |
| Elandsfontein | $O_3$ concentration (ppb) | 1 min | Monitor Europe ML9810B | |
| | $NO_x$ concentration (ppb) | 1 min | Thermo Electron 42i | |
| | CO concentration (ppb) | 1 min | - | |
| | Temperature ($^oC$) | 1 min | Vaisala WXT510 | |
| | Relative humidity (%) | 1 min | Vaisala WXT510 | |
| | Global radiation ($W/m^2$) | 1 min | LiCor LI-190SB | |
| | Wind speed (m/s) | 1 min | Vaisala WXT510 | |
| | Wind direction (degrees) | 1 min | Vaisala WXT510 | |
| | Precipitation (mm/hr) | 1 min | Vaisala WXT510 | |


(a) (b)

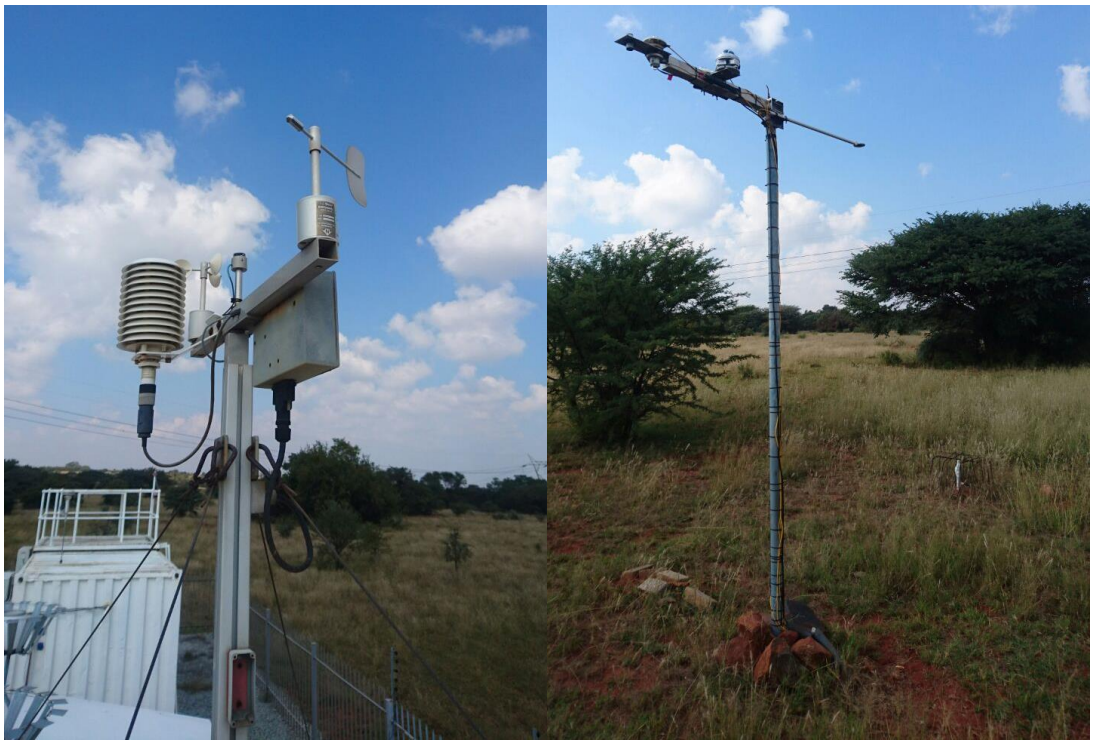

(c) (d)

Figure 3-6: Instrumentation at Welgegund atmospheric research station that is of relevance to this study, in particular (a) $NO_x$ (top) and $O_3$ (bottom) instruments, (b) CO instrument (top), (c) meteorological instruments mounted on a mast located on the roof of the station for measurements of temperature and relative humidity, wind speed and wind direction and (d) global radiation measurements from a 3 m tall mast.

Temperature and relative humidity were measured with a Rotronic MP 101A instrument (Fig. 3.6 c). The wind speed was measured by a Vector A101ML (Vector Instruments, Rhyl, UK) anemometer (Laakso *et al.*, 2013), while wind direction was measured with a Vector W200P windvane (Vector Instruments, Rhyl, UK). In terms of solar radiation, different radiation parameters were measured by upward and downward pointing sensors (Fig. 3.6 d), i.e. direct and reflected photosynthetically active radiation (Kipp & Zonen PAR lite), direct and reflected global radiation (Kipp & Zonen CMP-3) and net radiation (Kipp & Zonen NR lite). The parameter used in this study was global radiation, which is the sum of the direct solar radiation and the diffuse radiation resulting from reflected or scattered sunlight.

The gas sample inlet at these sites was approximately 1.5 m above ground-level and was mounted on the roof of the measurement station. The inlet is made of PTFE tubing (used because it is an unreactive material to prevent the absorbance of the air sample components), which is encased by a steel tube for support. A steel mesh and rain shield cover prevented insects and precipitation from entering the gas analysers (Petäjä *et al.*, 2013). The air sample also passes through a 1-2 µm Teflon filter membrane.

Remote monitoring of the data was ensured through a wireless GPRS connection. The measurement stations were visited once a week for weekly maintenance of the instruments. The gas analysers were periodically checked against calibration gases and an $O_3$ reference instrument, and adjustments made to the offset (zero) and gain (span) settings on the instruments if needed. Data quality control procedures were applied to the raw data (recorded every 1-minute and converted to 15-minute averages), which included discarding data recorded during power interruptions, electronic malfunctions, calibrations and maintenance (based on entries in an electronic diary). The remaining data were corrected based on the *in-situ* calibrations (providing zero and span values), flow checks and visual inspection. More details on the data cleaning process are presented by (Laakso *et al.*, 2008) and (Venter *et al.*, 2012).

## 3.3 DATA ANALYSIS

### 3.3.1 Air mass back trajectory analysis

Back trajectory analysis is a useful technique to determine air mass transport at receptor sites and also to trace source regions of air pollutants. The accuracy associated with this type of analysis depends on the quality of the wind data (Stohl, 1998). Although there are significant errors and large uncertainties associated with a single back trajectory (Stohl, 1998), this method is reliable for identifying particular synoptic situations in a given region with the reconstruction and analysis of a large number of atmospheric trajectories (Tang *et al.*, 2009, Stohl, 1998).

Back trajectories were calculated using the HYSPLIT 4.8 (Hybrid Single-Particle Lagrangian Integrated Trajectory model), developed by the National Oceanic and Atmospheric Administration (NOAA)'s Air Resources Laboratory (ARL) (Stein *et al.*, 2015, Draxler and Hess, 1998). The model was run with the GDAS meteorological archive produced by the US National Weather Service's National Centre for Environmental Prediction (NCEP) and archived by ARL (Air Resources Laboratory, 2017). Individual hourly four-day back trajectories for air masses arriving at a height of 100 m above ground-level were calculated for the entire measurement period at each monitoring site. Overlay back trajectory maps were generated by superimposing individual back trajectories onto the southern African map divided into a 0.5° X 0.5° grid. Colour was used to indicate the normalised percentage of trajectories passing over specific grid cells, with red and dark blue representing the highest and lowest percentages, respectively.

Overlay back trajectories were also used to compile source area maps, using the simple approach applied in other papers where concentrations of species are associated with back trajectories (Tiitta *et al.*, 2014, Vakkari *et al.*, 2013, Vakkari *et al.*, 2011). To produce these maps, each 0.5° X 0.5° grid cell was then assigned the mean concentration at the measurement site for the trajectories passing over that grid cell. A minimum of five trajectories per cell was required for the statistical reliability (Vakkari *et al.*, 2011).

### 3.3.2 Modelling instantaneous production rate of $O_3$

An opportunity was presented by the only speciated VOC dataset available and published in South Africa (Jaars *et al.*, 2016, Jaars *et al.*, 2014) to model instantaneous $O_3$ production at Welgegund. The concentration of these biogenic and anthropogenic VOCs was obtained from grab samples taken between 11:00 and 13:00 LT (i.e. local South African time, UTC+2) over the course of two extensive field campaigns conducted from February 2011 to February 2012 and from December 2013 to February 2015. During this time, six trace gases, 19 biogenic VOCs and 20 anthropogenic

VOCs, including 13 aromatic and seven aliphatic compounds were measured. The VOC reactivity was calculated from the respective rate coefficients of each VOC with OH radicals (•OH) obtained from chemical kinetic databases such as JPL, NIST and the MCM (e.g. Jaars *et al.*, 2014) to estimate $O_3$ production at 11:00 LT at Welgegund. Specifically, each VOC reactivity was then summed to obtain the total VOC reactivity for each measurement, i.e. VOC reactivity = $\sum k_{1i}[VOC]_i$.

A mathematical box model was applied to model $O_3$ production as a function of VOC reactivity and $NO_2$ concentrations. This model involves three steps, i.e. (1) the estimation of $HO_x^•$ (sum of •OH and $HO_2^•$) production, (2) the estimation of the •OH concentration, and (3) the calculation of $O_3$ production (Geddes *et al.*, 2009, Murphy *et al.*, 2006).

The production rate of $HO_x^•$ ($P(HO_x)$) depends on the photolysis rate of $O_3$ ($J_{O3}$), concentration of $O_3$ and vapour pressure of water (Jaegle *et al.*, 2001). The photolysis rate proposed for the Southern Hemisphere, i.e. $J_{O3} = 3 \times 10^{-5}$ $s^{-1}$ (Wilson, 2015), was used, from which $P(HO_x)$ was calculated as follows:

$$P(HO_X) = 2J_{O3}k_{O3}[O_3][H_2O]$$

and estimated to be $6.09 \times 10^6$ molec $cm^{-3}$ $s^{-1}$ or 0.89 ppbv $h^{-1}$ (calculated for a campaign $O_3$ average of 41 ppbv and a campaign RH average of 42 % at 11:00 LT each day) at STP. The $P(HO_x)$ at Welgegund is approximately a factor of two lower compared to other reported urban $P(HO_x)$ values (Geddes *et al.*, 2009). The factors and reactions that affect [•OH] include:

- linear dependency between •OH and $NO_x$ due to the reaction $NO + HO_2^• \rightarrow •OH + NO_2$, until •OH begins to react with elevated $NO_2$ concentrations to form $HNO_3$ ($•OH + NO_2 + M \rightarrow HNO_3 + M$);
- $P(HO_x)$ is affected by solar irradiance, temperature, $O_3$ concentrations, humidity; and
- partitioning of $HO_x^•$ between $RO_2^•$, $HO_2^•$, •OH.

[•OH] was calculated at 11:00 LT each day as follows:

$$A = k_{5eff}(\frac{VOC\ reactivity}{k_{2eff}[NO]})^2$$

$$B = k_4[NO_2] + \alpha * VOC\ reactivity$$

$$C = P(HO_x)$$

$$[•OH] = \frac{-B + \sqrt{B^2 + 24C * A}}{12 * A}$$

The instantaneous production rate of $O_3$, $P(O_3)$ could then be calculated as a function of $NO_2$ levels and VOC reactivity. A set of reactions used to derive the equations that describe the dependence of the $^{\bullet}OH$, peroxy radicals ($HO_2^{\bullet}$+ $RO_2^{\bullet}$) and $P(O_3)$ on $NO_x$ is given by Murphy *et al.* (2006), which presents the following equation to calculate $P(O_3)$:

$$P(O_3) = k_{2eff}[HO_2^{\bullet} + RO_2^{\bullet}][NO] = 2 * VOC\ Reactivity * [^{\bullet}OH]$$

where $k_2$eff is the effective rate constant of NO oxidation by peroxy radicals (chain propagation and -termination reactions in the production of $O_3$). The values of the rate constants and other parameters used as input parameters to solve the equation above can be found in Murphy *et al.* (2006) and Geddes *et al.* (2009).

## 3.4 STATISTICAL ANALYSIS

The metric used to analyse $O_3$ data depends on the purpose of the analysis, which can range from mean, median and 95$^{th}$ percentile, for a variety of time periods such as daily, monthly, seasonal and annual. In addition, respiratory symptoms have been found to be associated with the daily maximum of the eight-hour average $O_3$ concentration (Schlink *et al.*, 2006), with air quality standards and guidelines of many countries (including South Africa) designed to protect human health adopting this metric. Therefore, the relevant time scale for the assessment of variation in $O_3$ was daily summaries, considering also that the time scale of meteorological impact on $O_3$ is in the order of days (Thompson *et al.*, 2001). The raw $O_3$ data (in ppb) (15 minute averages) was converted to hourly data from which an eight-hour moving average was derived for each hour and the daily maximum of the 8-h moving average (daily max 8-h $O_3$) was computed. Daily summaries were also calculated for other variables included in the statistical analysis, i.e. $NO_2$ (in ppb), NO (in ppb), CO (in ppb), zonal (u) wind component (in m/s), meridional (v) wind component (in m/s), relative humidity (in %) solar radiation (in W/m$^2$), and the daily maximum temperature (in $^{o}$C).

The zonal (u) and meridional (v) wind components were calculated from the wind speed (in m/s) and wind direction (in degrees). Wind direction is a circular variable, so it had to be dealt with differently from the other linear variables for subsequent statistical analyses (Jammalamadaka and Lund, 2006). It first had to be converted from degrees to radians and then its u and v vectors were calculated with trigonometric functions. These u and v vectors are then multiplied by the wind speed, i.e. the vectors are weighted by the magnitude of wind speed (Grange, 2014). Finally, to convert from meteorological convention of the direction the wind is coming from to mathematical convention of direction the vector is heading to, the u and v components are multiplied by a negative sign (Grange, 2014). Only daytime measurements (11:00-17:00 local time) were used to produce the daily averages of the study variables, as the boundary layer is deep and well-mixed

during this time period and night-time chemistry and surface deposition are not an issue (Cooper *et al.*, 2012).

Pollutant concentration data is often log-transformed to satisfy parametric test assumptions (i.e. linear relationship between response and predictor variables, residuals from model fit are independent, normally distributed with a homogeneous variance) so that traditional, parametric statistics can be used. Some papers report that the performance of the regression model improves significantly if the natural logarithm transformation of the $O_3$ data is used instead of the original $O_3$ data as the response variable (Pearce *et al.*, 2011, Abdul-Wahab *et al.*, 2005, Hastie and Tibshirani, 1990), because it stabilises the variance of the $O_3$ time series (Davis *et al.*, 2011). However, in this study, the histograms of $O_3$ indicated that the data appeared to be normally distributed (and not log-normally distributed); therefore, it was deemed not necessary to log transform the original data of $O_3$.

### 3.4.1 Multiple linear regression (MLR) analysis

Multiple linear regression modelling was used to relate $O_3$ concentrations (daily max 8-h $O_3$) to meteorological and pollutant factors, as well as the relative contribution of each of these factors. The general equation for an MLR model is given by

$$Y_i = \beta_0 + \beta_1 X_{i1} + \beta_2 X_{i2} + \ldots + \beta_p X_{ip} + \varepsilon_i \quad (3.1)$$

where $Y$ is the response variable, $X_1, X_2, \ldots, X_p$ are the independent variables, $\beta_1, \beta_2, \ldots, \beta_p$ are the regression coefficients, and $\varepsilon$ is an error term or residual value associated with deviation between the observed value of $Y$ and the predicted $Y$ value from the regression equation.

Following the form of Eq. (3.1), the starting MLR model for $O_3$, incorporating variables known to have a relationship with $O_3$, can be written as:

$$daily\ max\ 8\text{-}h\ O_3 = \beta_0 + \beta_1 \cdot T + \beta_2 \cdot SR + \beta_3 \cdot RH + \beta_4 \cdot u + \beta_5 \cdot v + \beta_6 \cdot NO_2 + \beta_7 \cdot NO + \beta_8 \cdot CO + \varepsilon \quad (3.2)$$

where T is daily maximum temperature, SR is daily average global radiation, RH is daily average relative humidity, u is the zonal (east-west) wind component, v is the meridional (north-south) wind component, $NO_2$ is the daily average $NO_2$ concentration, NO is the daily average NO concentration, and CO is the daily average CO concentration.

The ordinary least squares procedure is the standard method to estimate the coefficients in the MLR equation. With this method, the regression procedure is based on finding coefficient values that minimise the sum of the squares of the residuals. A forward stepwise regression procedure was

used in which each variable was added individually to the starting model according to their statistical significance and overall increase in the explanation capability of the model. This was done to remove the least important predictor variables and to obtain the optimal combination of variables depending on the statistical indices.

The strength of relationship between each independent variable and $O_3$ was evaluated in terms of the magnitude of the t-statistic and associated p-value for statistical significance. The performance of the model was evaluated with $R^2$, adjusted $R^2$ and root mean square error (RMSE). The adjusted-$R^2$ is an $R^2$ measure that does not increase unless the new variables have additional predictive capability (unlike $R^2$ that increases when variables are added to the equation even when the new variables have no real predictive capability). The optimum MLR models considered had the largest $R^2$ and adjusted $R^2$, and smallest RMSE from a minimum number of independent variables. The main assumptions of the model are true underlying linearity, residuals are mutually independent with constant variance (homoscedasticity), and residuals are normally distributed (Ordonez *et al.*, 2005). Multicollinearity in the regression model was verified by examining the variance inflation factor (VIF) for each of the predictor variables (Otero *et al.*, 2016, Abdul-Wahab *et al.*, 2005).

A major criticism of linear regression models is that they assume linear and additive relationships between the independent variable(s) and dependent variable, while chemical and physical processes affecting $O_3$ are unlikely to be linear and additive (Thompson *et al.*, 2001). In addition, ordinary least squares fit-based MLR does not take account of measurement error in predictor variables, which may cause significant bias to the coefficients in the case of uncertain data (e.g. Pitkänen *et al.*, 2016). Another problem in the use of MLR is when the model includes multiple factors that are correlated not just to the response variable, but also to each other (i.e. multicollinearity). The presence of multicollinearity in the regression model was checked by examining the variance inflation factor (VIF) for each of the predictor variables (Otero *et al.*, 2016, Abdul-Wahab *et al.*, 2005).

### 3.4.2 Principal component analysis (PCA)

Parameters such as solar radiation, temperature and relative humidity are related properties, which could be inessential in MLR. PCA is a statistical procedure that uses an orthogonal transformation to convert a set of interrelated variables into a set of uncorrelated variables, i.e. principal components. Therefore, PCA is able to separate interrelationships (collinearity) into statistically independent basic components (Abdul-Wahab *et al.*, 2005) and determine the most important uncorrelated variables. Each principal component is a linear combination of the original predictor variables that account for the variance in the data. All the principal components are orthogonal to each other, which implies that they are uncorrelated to each other. The first principal component is

calculated such that it accounts for the highest possible variance in the dataset, followed by the concurrent components. Since the variables are measured in different units, it is necessary to standardise data before a principal component analysis is carried out, which involves scaling every variable to have a mean equal to 0 and a standard deviation equal to 1. The principal component model presents the $i^{th}$ principal component as a linear function of the p measured variables as expressed in Eq. (3.3) below:

$$Z_i = a_{i1}X_1 + a_{i2}X_2 + a_{i2}X_2 + \ldots + a_{ip}X_p \quad (3.3)$$

where *'Z'* is the principal component, *'a'* is the component loading, and *'X'* is the measured variable. The full set of principal components is as large as the original set of variables, but it is common for the sum of the variances of the first few principal components to exceed 80% of the total variance of the original data. By examining plots of these few new variables, researchers often develop a deeper understanding of the driving forces that generated the original data.

PCA was first applied to the original independent variables to transform these variables into an equal number of principal components. Only those principal components with an eigenvector greater than 1 were retained (according to the Kaiser criterion), which were then subjected to Varimax rotation to maximise the loading of a predictor variable on one component (Abdul-Wahab *et al.*, 2005). Since the eigenvectors are the correlation of the component variables with the original variables, they comprise coefficients (loadings) that indicate the relative weight of each variable in the component, which is important, since they represent the extent of the correlation between the measured variable and the principal components. Variables that load highly on a specific principal component form a related group.

PCR is a combination of PCA and MLR (Awang *et al.*, 2015), where the outputs from the PCA are used as potential predictors in order to improve the original MLR model (Awang *et al.*, 2015, Abdul-Wahab *et al.*, 2005). Either the original independent variables associated with each of the principal components with high loadings (Abdul-Wahab *et al.*, 2005) or the principal components with high loadings (Awang *et al.*, 2015) are selected to be included in the regression equation.

### 3.4.3 Generalised additive model (GAM) analysis

GAMs extend traditional linear models by allowing for an alternative distribution for the modelling of response variables that have a non-normal error distribution. In addition, GAMs do not force dependent variables to be linearly related to independent variables as in MLR, and recognise that the relationship of some explanatory variables (e.g. daily temperature) and the response variable (i.e. $O_3$ in this study) may not be linear (Gardner and Dorling, 2000). In GAMs, the response variable

depends additively on unknown smoothing functions of the individual predictors that can be (linear) parametric or non-parametric (Hastie and Tibshirani, 1990). The GAM model equation developed by Hastie and Tibshirani (1990) is given by

$$g\big(E(Y_i)\big) = \beta_0 + s_1(X_{i1}) + s_2(X_{i2}) + \ldots + s_p(X_{ip}) + \varepsilon_i \quad (3.4)$$

where $Y_i$ is the response variable, $E(Y_i)$, denotes the expected value and $g(\cdot)$ denotes the link function that links the expected value to the predictor variables $X_{i1},\ldots,X_{ip}$, $\beta_0$ is an intercept and $\varepsilon_i$ is an i.i.d. random error. For the purposes of the analysis performed in this study, the link function chosen was the identify transformation $g\big(E(Y_i)\big) = E(Y_i)$. The terms $s_1(\cdot), s_2(\cdot), \ldots, s_p(\cdot)$ are smooth functions that are estimated in a nonparametric fashion (Hastie and Tibshirani, 1990). We can estimate these smooth relationships simultaneously from the data and then predict $g(E(Y_i))$ by simply adding up these functions. The estimated smooth functions $s_k$ are the analogues of the coefficients $\beta_k$ in linear regression. In contrast to MLR, an additive regression is done by using a back-fitting procedure and thereby controlling the effects of the other predictors. GAM is able to identify covariates, $X_k$ relevant to $Y$ for a large set of potential factors (Hayn *et al.*, 2009), while it does not require any prior knowledge of the underlying relationship between $Y$ and its covariates. The latter can be obtained through separate partial residual plots, which allow visualisation of the relationships between each variable $X_k$ and the response variable, $Y$, after accounting for the effects of the other explanatory variables in the model.

Smooth parameters were automatically selected in the 'mgcv' package (Wood, 2017) in the R software environment used in this study, which is based on maximum probability methods that minimise the Akaike information criterion (AIC) score. The AIC measures the goodness-of-fit of the model in such a manner that the final model selected has the smallest AIC. The models were also evaluated with $R^2$ values and generalised cross-validation (GCV) scores (estimate of the prediction error).

## 3.5 OPEN-TOP CHAMBER TRIALS ON SUGARCANE

### 3.5.1 Experimental site

An open-top chamber (OTC) research facility situated at the North-West University, Potchefstroom, South Africa (26°40'50" S, 27°05'48" E, altitude 1348 m a.s.l.) was used to conduct the $O_3$ fumigation trials, which are indicated in Fig. 3-7. These OTCs are transparent plastic 5 $m^3$ ventilated cylinders in which plants can be enclosed and the concentrations of air pollutants controlled, while maintaining natural field meteorological conditions (Heyneke *et al.*, 2012). Since each chamber

could accommodate eight potted plants, four of each of the two sugarcane varieties investigated were placed in each chamber. In total, 64 plants were used in the study.

.

Figure 3-7: Open-top chamber facility at Potchefstroom to study air pollution and drought impacts on crops and vegetation in South Africa (Heyneke *et al.*, 2012).

## 3.5.2 Experimental design

Two commercial South African sugarcane cultivars, i.e. NCo376 and N31, were obtained from the South African Sugar Research Institute (SASRI). The N31 variety has the ability to grow rapidly and produce very high yields after an 18- to 24-month cycle, but has a relatively low sucrose content (South African Sugarcane Research Institute, 2006a). The NCo376 cultivar is a traditional South African variety with a relatively high sucrose content that produces good yields (although not as high as N31). However, the growth of the NCo376 cultivar is weaker than the N31 variety during severe water stress occurrences (South African Sugarcane Research Institute, 2006b). The growth season of sugarcane coincides with warmers months, since favourable temperatures for sugarcane growth range between 22$^{o}$C and 32$^{o}$C (Inman-Bamber and Smith, 2005).

Speedlings of the N31 and NCo376 varieties were transplanted to 30 cm pots, which were placed inside the OTCs on 9 October 2014. Four chambers served as the control chambers, which only received carbon-filtered (Purafil filter) ambient air from which $O_3$ (< 4 ppb $O_3$) and other contaminants were removed. Plants in two OTCs were exposed only to 80 ppb $O_3$, while plants in two other OTCs were exposed to a mixture of 80 ppb $O_3$ and 750 ppm $CO_2$. These concentrations

were maintained in each of the chambers during daytime (08:00-17:00) for the duration of the growth period. An $O_3$ generator (UV-20 HO, Olgear) was used to provide a continuous supply of additional $O_3$ into the ambient air stream feeding the OTCs to bring the $O_3$ concentration to the required level. The $O_3$ concentration in each chamber was controlled by means of an overflow valve, which could be adjusted to control the $O_3$ concentration within 10% of the target concentration in the chambers. The $O_3$ concentration in the OTCs was periodically verified with an $O_3$ monitor (Model 205, 2B Technologies Inc.). The 80 ppb $O_3$ exposure levels were chosen in order to relate results obtained in this study for sugarcane to $O_3$ exposure-response data available for other South African crops at this level (Berner *et al.*, 2015, Scheepers, 2011). The selection of the 750 ppm $CO_2$ level (twice ambient concentrations) was based on the two upper representative concentration pathways (RCP 6.0 and 8.5) future scenarios used in the latest IPCC assessment report (IPCC, 2013). $CO_2$ exposure commenced on 5 November 2014, while $O_3$ treatment started on 20 November 2014. The plants were grown for almost eight months and the above-ground biomass of the plants was harvested on 18 May 2015.

The soil in the pots consisted of silica sand, vermiculite and filter press in a 4:1:½ ratio, together with a 5 cm layer of gravel placed at the bottom of the pots. The pots were placed over buckets that served as water reservoirs, which were connected to a network of irrigation tubing that converges into a main water source. All pots contained four nylon suction wicks immersed in water reservoirs to draw up the water into the growth medium. Irrigation by the pot-reservoir system was carried out every morning and evening to grow the plants under well-watered conditions in order to exclude drought stress. A fertiliser solution containing macro- and micro-nutrients ideal for sugarcane growth was applied to all pots once every three weeks and dissolved by irrigation (Malan, 2017). Analysis of the soil indicated that pH, elemental concentrations, acidity and organic matter were all within acceptable limits for sugarcane (Malan, 2017). The plants were also treated with insecticide to prevent disease and insect attack (Malan, 2017).

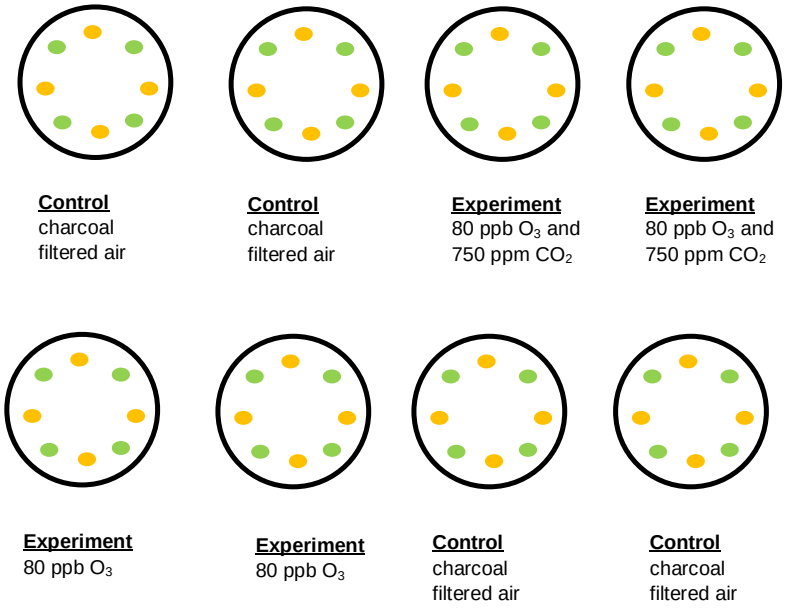


Figure 3-8: Experimental design of the open-top chamber $O_3$ fumigation trials. Note that four pots of NCo376 and four pots of N31 were placed in each OTC (eight pots per OTC) so the orange and green dots differentiate between the two cultivars and their arrangement in the chambers.

### 3.5.3 Measured parameters

The plant responses measured in this trial were growth and physiological parameters. The growth measurements, which were conducted twice a month, included the number of green and dead leaves, top visible dewlap (TVD) leaf length and width, stalk height and number of tillers. The TVD leaf blade refers to the uppermost fully expanded leaf with a clearly visible dewlap or collar (a band of membranous tissue between the leaf sheath and leaf blade) (http://edis.ifas.ufl.edu/sc076) often used in sugarcane studies. Green and dead leaves were counted starting from the base of the stalk to the TVD leaf, while the stalk height was measured from the soil surface to the TVD leaf. The number of tillers present for each plant was counted, excluding the main tiller (primary shoot or stalk).

Plant physiology effects relate to photosynthetic performance and were measured in terms of chlorophyll *a* fluorescence, stomatal conductance and chlorophyll content parameters. Chlorophyll (Chl) *a* fluorescence is used to monitor photosystem II (PSII) activity and the processes that affect it (Schansker *et al.*, 2006), which can be very useful in studying the effects of various stressors on the physiological state of plants (Stirbet, 2011). Illumination of photosynthetic samples, kept in darkness for some length of time, causes a rapid rise in fluorescence from PSII (~1 s), followed by a slow (few minutes) decline. Analysis of the fluorescence O-J-I-P transient, which describes the fluorescence changes that occur in less than 1 s, allows for the evaluation of the physiological condition of PSII

and photosynthetic electron transport chain components (Kalaji *et al.*, 2016). A portable fluorimeter Handy PEA (Plant Efficiency Analyzer, Hansatech Instrument Ltd, UK) was used to measure the chl *a* fluorescence kinetics *in situ* at a 10 µs time resolution for 1 s. Measurements were taken at night to ensure that the sample leaves have already been dark-adapted for at least one hour. The first step in the measurement process was to cover the fully expanded area of the TVD leaf blade with a small, lightweight leaf clip. A high intensity (3 500 µMol.$m^{-2}$.$s^{-1}$), short flash (1 s) was applied to the leaf, which transiently closes all PSII reaction centres, reducing the overall photochemical efficiency so that fluorescence levels rise for 1 to 2 seconds, after which the fluorescence levels typically decrease again over a time-scale of a few minutes (Maxwell and Johnson, 2000). Three replicate measurements were taken per plant. The first chl *a* fluorescence measurements were performed eight weeks after planting, where after monthly measurements were conducted.

The original fluorescence transients are double normalised between steps O (0.03 ms) and P (300 ms) of the O-J-I-P curve by using the initial ($F_0$) and maximum ($F_P$) fluorescence intensity to calculate the relative (or normalised) variable fluorescence, $V_{OP}$, between $F_0$ and $F_P$:

$$V_{\mathrm{OP}} = {(F_t - F_{0.03})}\Big/{(F_{300} - F_{0.03})}$$

where $F_t$ is the fluorescence intensity at time t after the onset of illumination; $F_{0.03}$ is the fluorescence intensity at 0.03 µs ($F_0$); and $F_{300}$ is the fluorescence intensity at 300 µs ($F_M$ or $F_P$). $V_{OP}$ values were normalised again to obtain the difference ($\Delta V_{OP} = V_{treatment} - V_{control}$) between the treated and control plant samples.

Chlorophyll content measurements commenced 17 weeks after planting, where after it was measured once a month. Three replicate measurements were made for each plant using a hand-held meter (Model CCM 300, Opti-Sciences, USA) by placing the leaf clip on the fully expanded area of the TVD leaf.

Stomatal closure by plants in response to $O_3$ stress can be a protective mechanism to prevent the damaging effects of $O_3$ uptake by the leaves. However, closing of the stomata can also limit $CO_2$ absorption, which leads to decreased photosynthetic activity (Efeoğlu *et al.*, 2009). To assess $O_3$ uptake, stomatal conductance was measured once a month using a hand-held porometer (Model AP4, Delta-T Devices, Cambridge, UK). Three measurements were taken per plant on the fully expanded area of the TVD leaf between 12:00 and 2:00 pm.

Yield-related parameters such as biomass yield and sucrose content of sugarcane at harvest were not measured in this trial, as they required specialised testing facilities.

# CHAPTER 4

# SEASONAL INFLUENCES ON SURFACE OZONE VARIABILITY IN CONTINENTAL SOUTH AFRICA AND IMPLICATIONS FOR AIR QUALITY

## 4.1 AUTHOR LIST, CONTRIBUTIONS AND CONSENT

**Tracey Leah Laban[1], Pieter Gideon van Zyl[1], Johan Paul Beukes[1], Ville Vakkari[2], Kerneels Jaars[1], Nadine Borduas-Dedekind[3], Miroslav Josipovic[1], Anne Mee Thompson[4], Markku Kulmala[5], and Lauri Laakso[2]**

1 Unit for Environmental Sciences and Management, North-West University, Potchefstroom, South Africa
2 Finnish Meteorological Institute, Helsinki, Finland
3 Department of Environmental Systems Science, ETH Zürich, Zürich, Switzerland
4 NASA/Goddard Space Flight Center, Greenbelt, Maryland, USA
5 Department of Physics, University of Helsinki, Finland

The majority of the work was done by the first author, **T.L. Laban** who was responsible for the data processing, analysis, interpretation and writing of the manuscript. Contributions of the various co-authors were as follows: P.G. van Zyl and J.P. Beukes who were the promoters of this study assisted with data interpretation and editing the text of the manuscript. M. Josipovic and K. Jaars assisted with the data collection and VOC sampling at the Welgegund measurement station. V. Vakkari and L. Laakso helped create the infrastructure at Welgegund. V. Vakkari assisted with critical revision of the manuscript and further development of the main conceptual ideas. N. Borduas-Dedekind assisted with the production of an $O_3$ isopleth plot and critical revision of the manuscript. A.M. Thompson, L. Laakso and M. Kulmala made conceptual contributions and assisted with critical revision of the manuscript.

All the co-authors on the article have been informed that the PhD will be submitted in article format and have given their consent.

## 4.2 FORMATTING AND CURRENT STATUS OF ARTICLE

A revised version of the original manuscript that was submitted to *Atmospheric Chemistry and Physics*, a European Geosciences Union journal is presented in this chapter. The journal detail can be found at http://www.atmospheric-chemistry-and-physics.net (Date of access: 25 May 2018). The article was ***received***: 1 Dec 2017, ***accepted for review***: 04 Jan 2018, ***discussion started***: 19 Jan 2018, ***revised***: 11 May 2018 (https://www.atmos-chem-phys-discuss.net/acp-2017-1115/).

# Seasonal influences on surface ozone variability in continental South Africa and implications for air quality

**Tracey Leah Laban[1], Pieter Gideon van Zyl[1]*, Johan Paul Beukes[1], Ville Vakkari[2], Kerneels Jaars[1], Nadine Borduas-Dedekind[3], Miroslav Josipovic[1], Anne Mee Thompson[4], Markku Kulmala[5], and Lauri Laakso[2]**

1 Unit for Environmental Sciences and Management, North-West University, Potchefstroom, South Africa

2 Finnish Meteorological Institute, Helsinki, Finland

3 Department of Environmental Systems Science, ETH Zürich, Zürich, Switzerland

4 NASA/Goddard Space Flight Center, Greenbelt, Maryland, USA

5 Department of Physics, University of Helsinki, Finland

*Correspondence to: P.G. van Zyl (pieter.vanzyl@nwu.ac.za)

## Abstract

Although elevated surface ozone ($O_3$) concentrations are observed in many areas within southern Africa, few studies have investigated the regional atmospheric chemistry and dominant atmospheric processes driving surface $O_3$ formation in this region. Therefore, an assessment of comprehensive continuous surface $O_3$ measurements performed at four sites in continental South Africa was conducted. The regional $O_3$ problem was evident, with $O_3$ concentrations regularly exceeding the South African air quality standard limit, while $O_3$ levels were higher compared to other background sites in the Southern Hemisphere. The temporal $O_3$ patterns observed at the four sites resembled typical trends for $O_3$ in continental South Africa, with $O_3$ concentrations peaking in late winter and early spring. Increased $O_3$ concentrations in winter were indicative of increased emissions of $O_3$ precursors from household combustion and other low-level sources, while a spring maximum observed at all the sites was attributed to increased regional biomass burning. Source area maps of $O_3$ and CO indicated significantly higher $O_3$ and CO concentrations associated with air masses passing over a region with increased seasonal open biomass burning, which indicated CO associated with open biomass burning as a major source of $O_3$ in continental South Africa. A strong correlation between $O_3$ on CO was observed, while $O_3$ levels remained relatively constant or decreased with increasing $NO_x$, which supports a

VOC-limited regime. The instantaneous production rate of $O_3$ calculated at Welgegund indicated that ~40% of $O_3$ production occurred in the VOC-limited regime. The relationship between $O_3$ and precursor species suggests that continental South Africa can be considered VOC-limited, which can be attributed to high anthropogenic emissions of $NO_x$ in the interior of South Africa. The study indicated that the most effective emission control strategy to reduce $O_3$ levels in continental South Africa should be CO and VOC reduction, mainly associated with household combustion and regional open biomass burning.

**Keywords:** ozone ($O_3$) production, $NO_x$-limited, VOC-limited, biomass burning, regional $O_3$, air quality

## 1. Introduction

High surface $O_3$ concentrations are a serious environmental concern due to their detrimental impacts on human health, crops and vegetation (National Research NRC, 1991). Photochemical smog, comprising $O_3$ as a constituent together with other atmospheric oxidants, is a major air quality concern on urban and regional scales. Emissions of $O_3$ precursors in the Southern Hemisphere, though less than the Northern Hemisphere (Zeng et al., 2008), have a disproportionate impact on atmospheric composition and climate because they enter a relatively pristine environment and are more efficient at producing $O_3$ (Wang et al., 1998) to create a greater change in the oxidising capacity of the atmosphere (Thompson, 1992) and radiative forcing (IPCC, 2013).

Tropospheric $O_3$ concentrations are regulated by three processes, i.e. chemical production/destruction, atmospheric transport, and losses to surface through dry deposition (Monks et al., 2015). The photolysis of nitrogen dioxide ($NO_2$) in the presence of sunlight is the only known way of producing $O_3$ in the troposphere (Logan, 1985). $O_3$ can recombine with nitric oxide (NO) to regenerate $NO_2$, which will again undergo photolysis to regenerate $O_3$ and NO. This continuous process is known as the $NO_x$-dependent photostationary state (PSS) and results in no net production or consumption of ozone (null cycle). However, net production of $O_3$ in the troposphere occurs outside the PSS when peroxy radicals ($HO_2$ and $RO_2$) alter the PSS by oxidising NO to produce 'new' $NO_2$ (Cazorla and Brune, 2010), resulting in net $O_3$ production. The main source of these peroxy radicals in the atmosphere is the reaction of the hydroxyl

radical ($OH^{\bullet}$) with volatile organic compounds (VOCs) or carbon monoxide (CO) (Cazorla and Brune, 2010).

$O_3$ precursor species can be emitted from natural and anthropogenic sources. Fossil fuel combustion is considered to be the main source of $NO_x$ in South Africa, which includes coal-fired power-generation, petrochemical operations, transportation and residential burning (Wells et al., 1996; Held et al., 1996; Held and Mphepya, 2000). Satellite observations indicate a well-known $NO_2$ hotspot over the South African Highveld (Lourens et al., 2012) attributed to industrial activity in the region. CO is produced from three major sources, i.e. fossil fuel combustion, biomass burning, as well as the oxidation of methane ($CH_4$) and VOCs (Novelli et al., 1992). Anthropogenic sources of VOCs are largely due to industrial and vehicular emissions (Jaars et al., 2014), while biogenic VOCs are also naturally emitted (Jaars et al., 2016). Regional biomass burning, which includes household combustion for space heating and cooking, agricultural waste burning and open biomass burning (wild fires), is a significant source of CO, $NO_x$ and VOCs (Macdonald et al., 2011; Crutzen and Andreae, 1990; Galanter et al., 2000; Simpson et al., 2011) in southern Africa. In addition, stratospheric intrusions of $O_3$-rich air to the free troposphere can also lead to elevated tropospheric $O_3$ concentrations (Yorks et al., 2009; Lin et al., 2012). $O_3$ production from natural precursor sources, the long-range transport of $O_3$ and the injections from stratospheric $O_3$ contribute to background $O_3$ levels, which is beyond the control of regulators (Lin et al., 2012).

Since $O_3$ concentrations are regulated in South Africa, $O_3$ monitoring is carried out across South Africa through a network of air quality monitoring stations established mainly by provincial governments, local municipalities and industries (http://www.saaqis.org.za). High $O_3$ concentrations are observed in many areas within the interior of South Africa, which exceed the South African standard $O_3$ limit, i.e. an eight-hour moving average of 61 ppb (e.g. Laakso et al., 2013). These exceedances can be attributed to high anthropogenic emissions of $NO_x$ and VOCs in dense urban and industrial areas (Jaars et al., 2014), regional biomass burning (Lourens et al., 2011), and $O_3$ conducive meteorological conditions (e.g. sunlight). Since $O_3$ is a secondary pollutant, high levels of $O_3$ can also be found in rural areas downwind of city centres and industrial areas. In order for South Africa to develop an effective management plan to reduce $O_3$ concentrations by controlling $NO_x$ and VOC emissions, it is important to determine whether a region is $NO_x$- or VOC-limited. However, $O_3$ production has a complex and non-linear dependence on precursor emissions (e.g. National Research NRC, 1991), which makes its

atmospheric levels difficult to control (Holloway and Wayne, 2010). Under VOC-limited conditions, $O_3$ concentrations increase with increasing VOCs, while a region is considered $NO_x$-limited when $O_3$ production increases with increasing $NO_x$ concentrations. Results from a photochemical box model study in South Africa, for instance, revealed that the Johannesburg-Pretoria megacity is within a VOC-limited regime (Lourens et al., 2016). VOC reductions would, therefore, be most effective in reducing $O_3$, while $NO_x$ controls without VOC controls may lead to $O_3$ increases. In general, it is considered that $O_3$ formations in regions close to anthropogenic sources are VOC-limited, while rural areas distant from source regions are $NO_x$-limited (Sillman, 1999).

Previous assessments of tropospheric $O_3$ over continental South Africa have focused on surface $O_3$ (Venter et al., 2012; Laakso et al., 2012; Lourens et al., 2011; Josipovic et al., 2010; Martins et al., 2007; Zunckel et al., 2004), as well as free tropospheric $O_3$ based on soundings and aircraft observations (Diab et al., 1996; Thompson, 1996; Swap et al., 2003; Diab et al., 2004). Two major field campaigns (SAFARI-92 and SAFARI 2000) were conducted to improve the understanding of the effects of regional biomass burning emissions on $O_3$ over southern Africa. These studies indicated a late winter-early spring (August and September) maximum over the region that was mainly attributed to increased regional open biomass burning during this period, while Lourens et al. (2011) also attributed higher $O_3$ concentrations in spring in the Mpumalanga Highveld to increased regional open biomass burning. A more recent study demonstrated that $NO_x$ strongly affects $O_3$ levels in the Highveld, especially in winter and spring (Balashov et al., 2014). A regional photochemical modelling study (Zunckel et al., 2006) has attempted to explain surface $O_3$ variability, which found no dominant source/s on elevated $O_3$ levels.

The aim of the current study is to provide an up-to-date assessment of the seasonal and diurnal variations in surface $O_3$ concentrations over continental South Africa, as well as to identify local and regional sources of precursors contributing to surface $O_3$. Another objective is to use available ambient data to qualitatively assess whether $O_3$ formation is $NO_x$- or VOC-limited in different environments. An understanding of the key precursors that control surface $O_3$ production is critical for the development of an effective $O_3$ control strategy.

## 2. Methodology

### 2.1 Study area and measurement stations

Continuous in-situ $O_3$ measurements obtained from four research stations in the north-eastern interior of South Africa, indicated in Fig. 1, which include Botsalano (25.54$^o$ S, 25.75$^o$ E, 1420 m a.s.l.), Marikana (25.70$^o$ S, 27.48$^o$ E, 1170 m a.s.l.), Welgegund (26.57 $^o$ S, 26.94$^o$ E, 1480 m a.s.l.) and Elandsfontein (26.25$^o$ S, 29.42$^o$ E, 1750 m a.s.l.), were analysed. This region is the largest industrial (indicated by major point sources in Fig. 1) area in South Africa, with substantial gaseous and particulate emissions from numerous industries, domestic fuel burning and vehicles (Lourens et al., 2012; Lourens et al., 2011), while the Johannesburg-Pretoria megacity is also located in this area (Fig. 1). A combination of meteorology and anthropogenic activities has amplified the pollution levels within the region. The seasons in South Africa correspond to typical austral seasons, i.e. winter from June to August, spring from September to November, summer from December to February and autumn from March to May. The climate is semi-arid with an annual average precipitation of approximately 400 to 500 mm (Klopper et al., 2006; Dyson et al., 2015), although there is considerable inter-annual variability associated with El Niño Southern Oscillation (ENSO) phenomena. Precipitation in the north-eastern interior occurs mostly during the austral summer, from October to March, whereas the region is characterised by a distinct cold and dry season from May to September, i.e. late autumn to mid-spring, during which almost no precipitation occurs. During this period, the formation of several inversion layers is present in the region, which limits the vertical dilution of air pollution, while more pronounced anticyclonic recirculation of air masses also occurs. This synoptic-scale meteorological environment leads to an accumulation of pollutants in the lower troposphere in this region, which can be transported for several days (Tyson and Preston-Whyte, 2000; Garstang et al., 1996). The SAFARI-92 and SAFARI 2000 campaigns indicated that locations in southern Africa, thousands of kilometres apart, are linked through regional anticyclonic circulation (Swap et al., 2003).

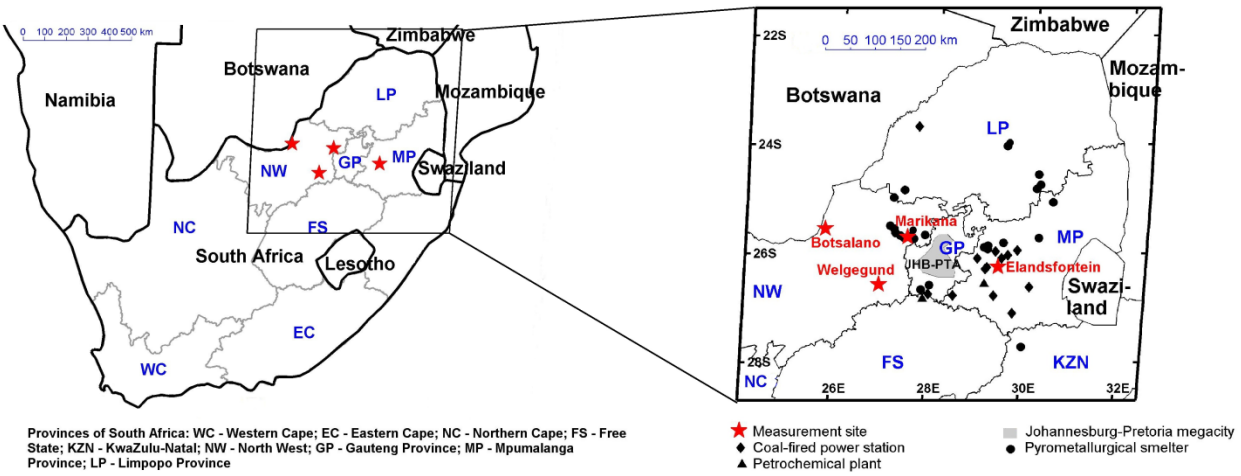


**Fig. 1.** Location of the four measurement sites in South Africa

### *2.1.1 Botsalano*

The Botsalano measurement site is situated in a game reserve in the North West Province of South Africa, which is considered to be representative of regional background air. The surrounding vegetation is typical of a savannah biome, consisting of grasslands with scattered shrubs and trees (Laakso et al., 2008). The area is quite sparsely populated and has no local anthropogenic pollution sources (Laakso et al., 2008; Vakkari et al., 2013). The western Bushveld Igneous Complex, where numerous platinum, base metal, vanadium and chromium mining/smelting industries are situated, is the largest regional anthropogenic pollution source, with the Rustenburg area located approximately 150 km to the east. Botsalano is also occasionally impacted by plumes passing over the industrialised Mpumalanga Highveld and the Johannesburg-Pretoria megacity (Laakso et al., 2008; Vakkari et al., 2011). In addition, the site is influenced by seasonal regional savannah wildfires during the dry period (Laakso et al., 2008; Vakkari et al., 2011; Mafusire et al., 2016). Measurements were conducted from 20 July 2006 until 5 February 2008 (Laakso et al., 2008; Vakkari et al., 2011; Vakkari et al., 2013).

### *2.1.2 Marikana*

The Marikana measurement site is located within the western Bushveld Igneous Complex, which is a densely populated and highly industrialised region, where mining and smelting are the predominant industrial activities. Marikana is a small mining town located approximately 30

km east of Rustenburg and approximately 100 km northwest of Johannesburg. The measurement site is located in the midst of a residential area, comprising low-cost housing settlements and municipal buildings (Hirsikko et al., 2012; Venter et al., 2012). Anthropogenic emissions from household combustion, traffic and industry in the wider region have a strong influence on the measurement site (Venter et al., 2012). Data was collected from 8 February 2008 to 16 May 2010 and has been previously used in other studies (Venter et al., 2012; Vakkari et al., 2013; Petäjä et al., 2013; Hirsikko et al., 2012; Hirsikko et al., 2013).

### *2.1.3 Welgegund*

This measurement site is approximately 100 km west of Johannesburg and is located on a commercial arable and pastoral farm. The station is surrounded by grassland savannah (Jaars et al., 2016). The station can be considered a regionally representative background site with few local anthropogenic sources. Air masses arriving at Welgegund from the west reflect a relatively clean regional background. However, the site is, similar to the Botsalano station, at times impacted by polluted air masses that are advected over major anthropogenic source regions in the interior of South Africa, which include the western Bushveld Igneous Complex, the Johannesburg-Pretoria megacity, the Mpumalanga Highveld and the Vaal Triangle (Tiitta et al., 2014; Jaars et al., 2016; Venter et al., 2017). In addition, Welgegund is also affected by regional savannah and grassland fires that are common in the dry season (Vakkari et al., 2014). The atmospheric measurement station has been operating at Welgegund since 20 May 2010, with data measured up until 31 December 2015 utilised in this study.

### *2.1.4 Elandsfontein*

Elandsfontein is an ambient air quality monitoring station operated by Eskom, the national electricity supply company, primarily for legislative compliance purposes. This station was upgraded and co-managed by researchers during the EUCAARI project (Laakso et al., 2012). The Elandsfontein station is located within the industrialised Mpumalanga Highveld at the top of a hill approximately 200 km east of Johannesburg and 45 km south-southeast of eMalahleni (previously known as Witbank), which is a coal mining area (Laakso et al., 2012). The site is influenced by several emission sources, such as coal mines, coal-fired power-generating stations, a large petrochemical plant and traffic emissions. Metallurgical smelters to the north also frequently impact the site (Laakso et al., 2012). The Elandsfontein dataset covers the

period 11 February 2009 until 31 December 2010 during the EUCAARI campaign (Laakso et al., 2012).

## 2.2 Measurements

A comprehensive dataset of continuous measurements of surface aerosols, trace gases and meteorological parameters has been acquired through these four measurement sites (Laakso et al., 2008; Vakkari et al., 2011; Venter et al., 2012; Laakso et al., 2012; Vakkari et al., 2013; Petäjä et al., 2013). In particular, ozone ($O_3$), nitric oxide (NO), nitrogen dioxide ($NO_2$) and carbon monoxide (CO), as well as meteorological parameters, such as temperature ($^oC$) and relative humidity (%) measurements were used in this study. Note that Botsalano, Marikana and Welgegund measurements were obtained with the same mobile station (first located at Botsalano, then relocated to Marikana and thereafter permanently positioned at Welgegund), while Elandsfontein measurements were conducted with a routine monitoring station. $O_3$ concentrations at Welgegund, Botsalano and Marikana research stations were measured using the Environment SA 41M $O_3$ analyser, while a Monitor Europe ML9810B $O_3$ analyser was utilised at Elandsfontein. CO concentrations were determined at Welgegund, Botsalano and Marikana with a Horiba APMA-360 analyser, while CO was not measured at Elandsfontein. $NO_x$ ($NO+NO_2$) concentrations were determined with a Teledyne 200AU $NO/NO_x$ analyser at Welgegund, Botsalano and Marikana, whereas a Thermo Electron 42i $NO_x$ analyser was used at Elandsfontein. Temperature and relative humidity were measured with a Rotronic MP 101A instrument at all the sites.

Data quality at these four measurement sites was ensured through regular visits to the sites, during which instrument maintenance and calibrations were performed. The data collected from these four stations was subjected to detailed cleaning (e.g. excluding measurements recorded during power interruptions, electronic malfunctions, calibrations and maintenance) and the verification of data quality procedures (e.g. corrections were made to data according to in-situ calibrations and flow-checks). Therefore, the datasets collected at all four measurement sites are considered to represent high quality, high resolution measurements as indicated by other papers (Laakso et al., 2008; Petäjä et al., 2013; Venter et al., 2012; 2011; Laakso et al., 2012; Vakkari et al., 2013). Detailed descriptions of the data post-processing procedures were presented by Laakso et al. (2008) and Venter et al. (2012). The data was available as 15-minute averages and all plots using local time (LT) refer to local South African time, which is UTC+2.

In order to obtain a representative spatial coverage of continental South Africa, $O_3$ data from an additional 54 ambient monitoring sites was selected. These included $O_3$ measurements from 18 routine monitoring station measurements (SAAQIS) for the period January 2012 to December 2014 (downloaded from the JOIN web interface https://join.fz-juelich.de (Schultz et al., 2017)) and 36 passive sampling sites located in the north-eastern interior of South Africa where monthly $O_3$ concentrations were determined for two years from 2006 to 2007 (Josipovic, 2009). Spatial analyses were conducted with a geographic information system mapping tool (ArcGIS software), which used ordinary kriging to interpolate the $O_3$ concentrations measured at the 58 sites in order to build the spatial distribution. The interpolation method involved making an 80/20% split of the data (80% for model development, 20% for evaluation), where 20% were used to calculate the root mean square error (RMSE = 0.2804331). Optimal model parameters were selected using an iterative process and evaluated on the basis of the best performance statistics obtained (reported in the ArcGIS kriging output), with particular emphasis on minimising the RMSE. The extent of area was 23.00154974 (top), -29.03070026 (bottom), 25.74238974 (left) and 32.85246366 (right).

### 2.3 Air mass history

Individual hourly four-day back trajectories for air masses arriving at an arrival height of 100 m above ground-level were calculated for the entire measurement period at each monitoring site, using HYSPLIT 4.8 (Hybrid Single-Particle Lagrangian Integrated Trajectory model) (Stein et al., 2015; Draxler and Hess, 1998). The model was run with the GDAS meteorological archive produced by the US National Weather Service's National Centre for Environmental Prediction (NCEP) and archived by ARL (Air Resources Laboratory, 2017). Overlay back trajectory maps were generated by superimposing individual back trajectories onto a southern African map divided into 0.5° X 0.5°grid cells. In addition, source maps were compiled by assigning each grid cell with a mean measured $O_3$ and CO concentration associated with trajectories passing over that cell, similar to previous methods (Vakkari et al., 2011; Vakkari et al., 2013; Tiitta et al., 2014). A minimum of ten trajectories per cell were required for the statistical reliability.

## 2.4 Modelling instantaneous production rate of $O_3$

The only speciated VOC dataset available and published in South Africa exists for Welgegund (Jaars et al., 2016; Jaars et al., 2014), which could be used to model instantaneous $O_3$ production at this site. The concentration of these biogenic and anthropogenic VOCs was obtained from grab samples taken between 11:00 and 13:00 LT over the course of two extensive field campaigns conducted from February 2011 to February 2012 and from December 2013 to February 2015. During this time, six trace gases, 19 biogenic VOCs and 20 anthropogenic VOCs, including 13 aromatic and seven aliphatic compounds were measured. The VOC reactivity was calculated from the respective rate coefficients of each VOC with $^{\bullet}OH$ radicals obtained from chemical kinetic databases such as JPL, NIST and the MCM (e.g. Jaars et al., 2014) to estimate ozone production at 11:00 LT at Welgegund. Specifically, each VOC reactivity was then summed to obtain the total VOC reactivity for each measurement, i.e. VOC reactivity = $\sum k_{1i}[VOC]_i$. The major contributors to VOC reactivity are depicted in Fig. A1 and include, in approximate order of contribution, *o*-xylene, CO, styrene, *p*,*m*-xylene, toluene, ethylbenzene limonene, isoprene, $\alpha$-pinene, $\beta$-pinene and hexane. Of note, key compounds such as methane are not included, which could contribute to VOC reactivity, and therefore this VOC reactivity can only be a lower estimate. However, if a global ambient concentration of 1.85 ppm and a rate of oxidation by $^{\bullet}OH$ radicals of $6.68 \times 10^{-15}$ $cm^3$ $molec^{-1}$ $s^{-1}$ are assumed (Srinivasan et al., 2005), a VOC reactivity of 0.3 $s^{-1}$ would be obtained and would therefore account for a small increase in the VOC reactivity calculated in Fig. A1 and Fig. 10.

A mathematical box-model was applied to model $O_3$ production as a function of VOC reactivity and $NO_2$ concentrations. This model involves three steps, i.e. (1) the estimation of $HO_x$ (sum of $^{\bullet}OH$ and $HO_2^{\bullet}$ radicals) production, (2) the estimation of the $^{\bullet}OH$ radical concentration, and (3) the calculation for $O_3$ production (Murphy et al., 2006; Geddes et al., 2009). The VOC concentrations are the limiting factor in the ability to model $O_3$ production at Welgegund, since only data for the 11:00 to 13:00 LT grab samples was available (Fig. A1). Therefore, the model approach does not coincide with peak $O_3$ typically observed around 14:00 to 15:00 LT, and therefore likely represents a lower estimate.

The production rate of $HO_x$ ($P(HO_x)$) depends on the photolysis rate of $O_3$ ($J_{O3}$), concentration of $O_3$ and vapour pressure of water (Jaegle et al., 2001). The photolysis rate proposed for the

Southern Hemisphere, i.e. $J_{O3} = 3 \times 10^{-5}$ $s^{-1}$ (Wilson, 2015), was used, from which $P(HO_x)$ was calculated as follows:

$$P(HO_X) = 2J_{O3}k_{O3}[O_3][H_2O]$$

and estimated to be $6.09 \times 10^6$ molec $cm^{-3}$ $s^{-1}$ or 0.89 ppbv $h^{-1}$ (calculated for a campaign $O_3$ average of 41 ppbv and a campaign RH average of 42 % at 11:00 LT each day) at STP. The $P(HO_x)$ at Welgegund is approximately a factor of two lower compared to other reported urban $P(HO_x)$ values (Geddes et al., 2009). The factors and reactions that affect [•OH] include:

- linear dependency between •OH and $NO_x$ due to the reaction $NO + HO_2 \rightarrow$ •OH + $NO_2$, until •OH begins to react with elevated $NO_2$ concentrations to form $HNO_3$ ($OH + NO_2 + M \rightarrow HNO_3 + M$);
- $P(HO_x)$ is affected by solar irradiance, temperature, $O_3$ concentrations, humidity; and
- partitioning of $HO_x$ between $RO_2$, $HO_2$, OH.

[•OH] was calculated at 11:00 LT each day as follows:

$$A = k_{5eff}(\frac{VOC\ reactivity}{k_{2eff}[NO]})^2$$

$$B = k_4[NO_2] + \alpha * VOC\ reactivity$$

$$C = P(HO_x)$$

$$[OH] = \frac{-B + \sqrt{B^2 + 24C * A}}{12 * A}$$

The instantaneous production rate of $O_3$, $P(O_3)$ could then be calculated as a function of $NO_2$ levels and VOC reactivity. A set of reactions used to derive the equations that describe the dependence of the •OH, peroxy radicals ($HO_2$•+$RO_2$•) and $P(O_3)$ on $NO_x$ is given by Murphy et al. (2006), which presents the following equation to calculate $P(O_3)$:

$$P(O_3) = k_{2eff}[HO_2 + RO_2][NO] = 2 * VOC\ Reactivity * [OH]$$

where $k_2$eff is the effective rate constant of NO oxidation by peroxy radicals (chain propagation and -termination reactions in the production of $O_3$). The values of the rate constants and other parameters used as input parameters to solve the equation above can be found in Murphy et al. (2006) and Geddes et al. (2009).

## 3. Results and discussion

### 3.1 Temporal variation of $O_3$

In Fig. 2, the monthly and diurnal variations for $O_3$ concentrations measured at the four sites in this study are presented (time series plotted in Fig. A2). Although there is some variability between the sites, monthly $O_3$ concentrations show a well-defined seasonal variation at all four sites, with maximum concentrations occurring in late winter and spring (August to November), which is expected for the South African interior as indicated above and previously reported (Zunckel et al., 2004; Diab et al., 2004; Combrink et al., 1995). In Fig., A3 monthly averages of meteorological parameters and total monthly rainfall for Welgegund are presented to indicate typical seasonal meteorological patterns for continental South Africa. These $O_3$ peaks in continental South Africa generally point to two major contributors of $O_3$ precursors, i.e. open biomass burning (wild fires) (Fishman and Larsen, 1987; Vakkari et al., 2014), and increased low-level anthropogenic emissions, e.g. increased household combustion for space heating and cooking (Oltmans et al., 2013; Lourens et al., 2011). In addition to the seasonal patterns of $O_3$ precursor species, during the dry winter months, synoptic scale recirculation is more predominant and inversion layers are more pronounced, while precipitation is minimal (e.g. Tyson and Preston-Whyte, 2000). These changes in meteorology result in the build-up of precursor species that reach a maximum in August/September when photochemical activity starts to increase. The diurnal concentration profiles of $O_3$ at the four locations follow the typical photochemical cycle, i.e. increasing during daytime in response to maximum photochemical production and decreasing during the night-time due to titration with NO. $O_3$ levels peaked from midday to afternoon, with a maximum at approximately 15:00 (LT, UTC+2). From Fig. 2, it is also evident that night-time titration of $O_3$ at Marikana is more pronounced as indicated by the largest difference between daytime and night-time $O_3$ concentrations in comparison to the other sites, especially compared to Elandsfontein where night-time concentrations of $O_3$ remain relatively high in winter.

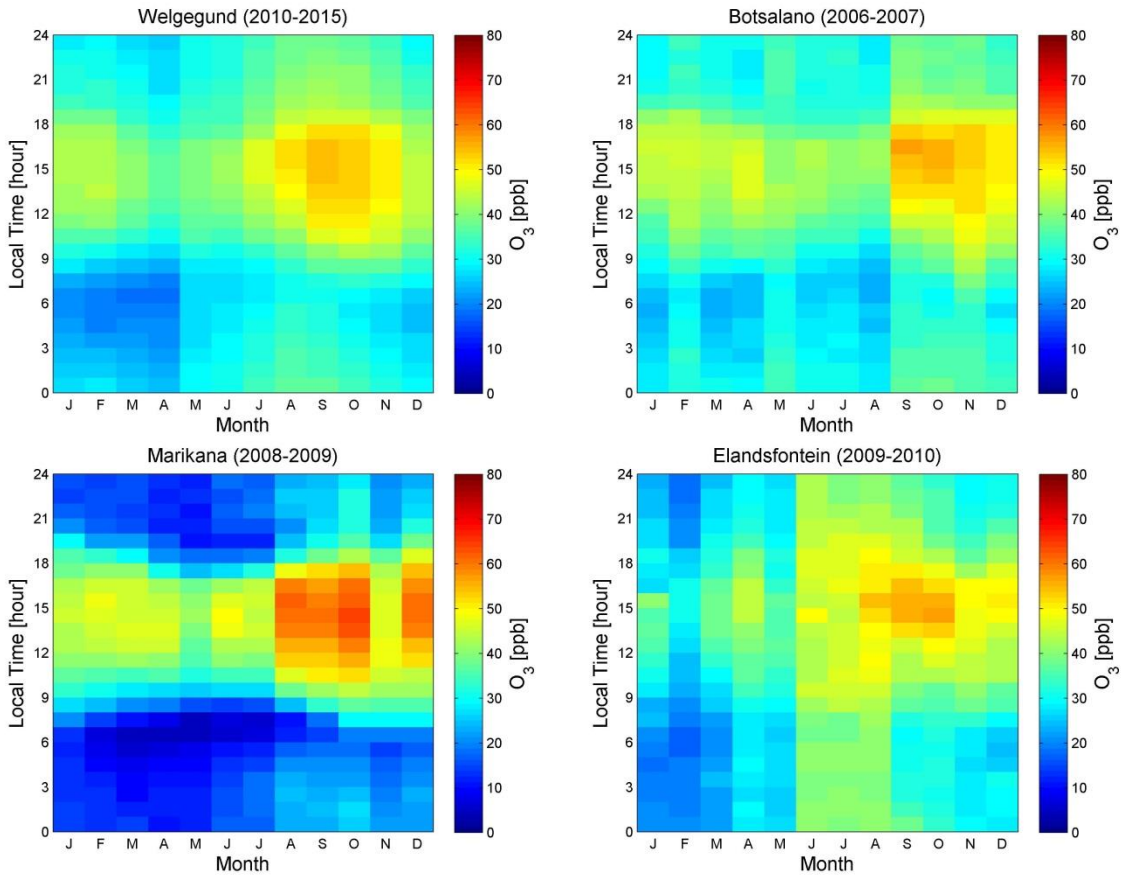


**Fig. 2.** Seasonal and diurnal variation of median $O_3$ concentrations at Welgegund, Botsalano, Marikana and Elandsfontein. The $O_3$ measurement periods varied among sites, which combined spanned a period from July 2006 to December 2015.

### 3.2 Spatial distribution of $O_3$ in continental South Africa

Fig. 3 depicts the spatial pattern of mean surface $O_3$ concentrations over continental South Africa during springtime (S-O-N), when $O_3$ is usually at a maximum as indicated above. Also presented in Fig. 3, are 96-hour overlay back trajectory maps for the four main study sites over the corresponding springtime periods. The mean $O_3$ concentration over continental South Africa ranged from 20 ppb to 60 ppb during spring. From Fig. 3, it can be seen that $O_3$ concentrations at the industrial sites Marikana and Elandsfontein were higher than $O_3$ levels at Botsalano and Welgegund. As mentioned previously, Elandsfontein is located within the industrialised Mpumalanga Highveld with numerous large point sources of $O_3$ precursor species. It is also

evident from Fig. 3 that rural measurement sites downwind from Elandsfontein, such as Amersfoort, Harrismith and Glückstadt had significantly higher $O_3$ concentrations, which can be attributed to the formation of $O_3$ during the transport of precursor species from source regions. Lourens et al. (2011) indicated that higher $O_3$ concentrations were associated with sites positioned in more rural areas in the Mpumalanga Highveld. Venter et al. (2012) attributed high $O_3$ concentrations at Marikana, which exceeded South African standard limits on a number of occasions, to the influence of local household combustion for cooking and space heating, as well as to regional air masses with high $O_3$ precursor concentrations. Higher $O_3$ concentrations were also measured in the north-western parts of Gauteng, at sites situated within close proximity to the Johannesburg-Pretoria megacity, while the rural Vaalwater site in the north also has significantly higher $O_3$ levels. From Fig. 3, it is evident that $O_3$ can be considered a regional problem with $O_3$ concentrations being relatively high across continental South Africa during spring. Fig. 3 also clearly indicates that the four research sites where surface $O_3$ was assessed in this study are representative of continental South Africa.

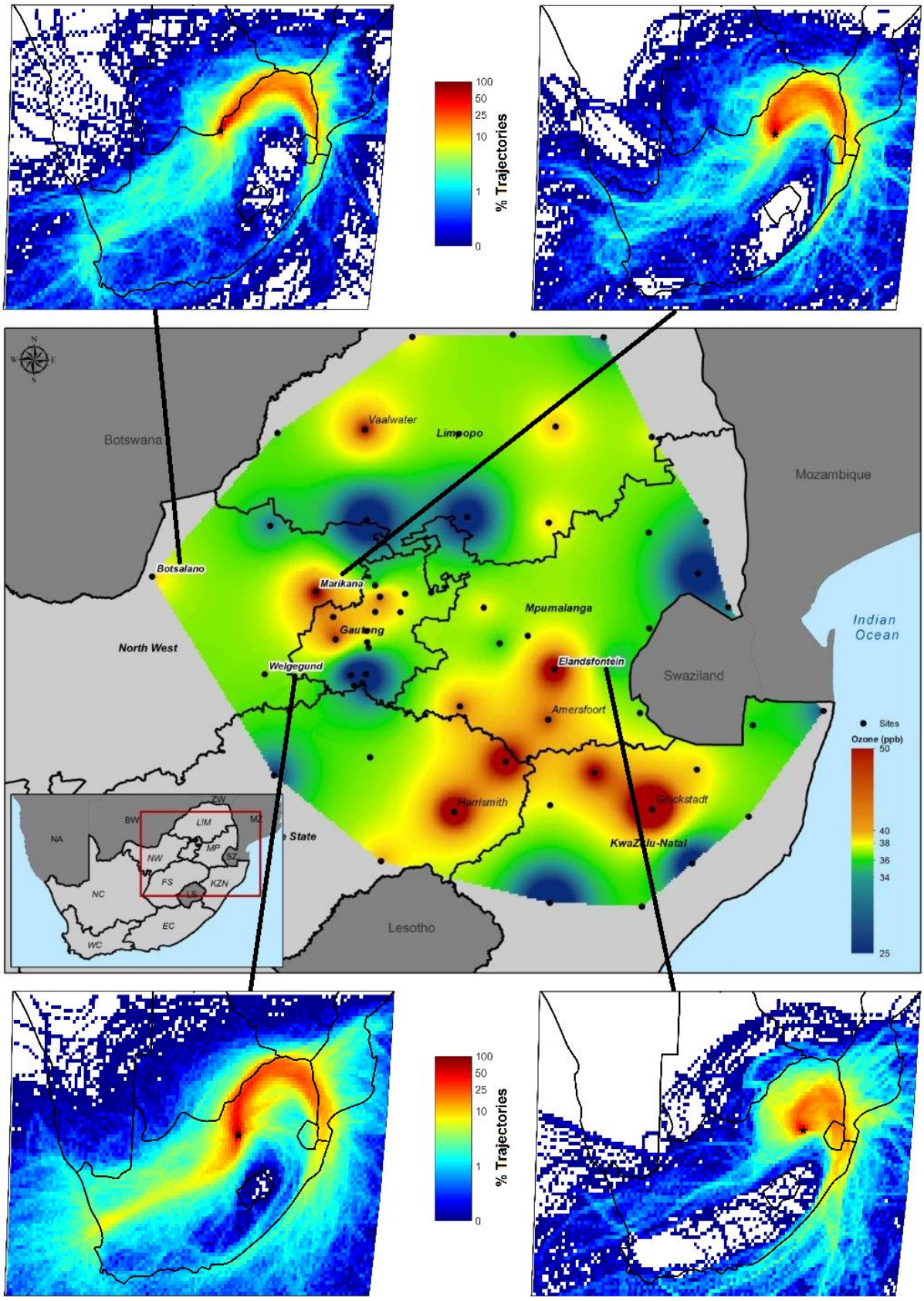
100
50
25
10
1
0
% Trajectories
Botswana
Mozambique
Vaalwater
Limpopo
Botsalano
Marikana
Mpumalanga
Gauteng
North West
Welgegund
Elandsfontein
Swaziland
Amersfoort
Indian Ocean
Sites
Ozone (ppb)
50
40
38
36
34
25
Harrismith
Glückstadt
KwaZulu-Natal
Lesotho
NA
BW
ZW
LIM
MZ
NW
MP
SZ
FS
KZN
NC
LS
EC
WC
State
100
50
25
10
1
0
% Trajectories

**Fig. 3.** The main (central) map indicating spatial distribution of mean surface $O_3$ levels during springtime over the north-eastern interior of southern Africa ranging between 23.00 $^{o}$ S and 29.03 $^{o}$ S, and 25.74 $^{o}$ E and 32.85 $^{o}$ E. The data for all sites was averaged for years when the ENSO cycle was not present (by examining SST anomalies in the Niño 3.4 region). Black dots indicate the sampling sites. The smaller maps (top and bottom) indicate 96-hour overlay back trajectory maps for the four main study sites, over the corresponding springtime periods.

### 3.3 Comparison with international sites

In an effort to contextualise the $O_3$ levels measured in this study, the monthly $O_3$ concentrations measured at Welgegund were compared to monthly $O_3$ levels measured at monitoring sites in other parts of the world (downloaded from the JOIN web interface https://join.fz-juelich.de (Schultz et al., 2017)) as indicated in Fig. 4. Welgegund was used in the comparison since it had the most extensive data record, while the measurement time period considered was from May 2010 to December 2014. The seasonal $O_3$ cycles observed at other sites in the Southern Hemisphere are comparable to the seasonal cycle at Welgegund, with slight variations in the time of year when $O_3$ peaks as indicated in Fig. 4. Cape Grim, Australia; GoAmazon T3 Manancapuru, Brazil; Ushuaia, Argentina; and El Tololo, Chile are regional background GAW (Global Atmosphere Watch) stations with $O_3$ levels lower than the South African sites. However, the $O_3$ concentrations at El Tololo, Chile are comparable to Welgegund. Oakdale, Australia and Mutdapliiy, Australia are semi-rural and rural locations, which are influenced by urban and industrial pollution sources, which also had lower $O_3$ concentrations compared to Welgegund.

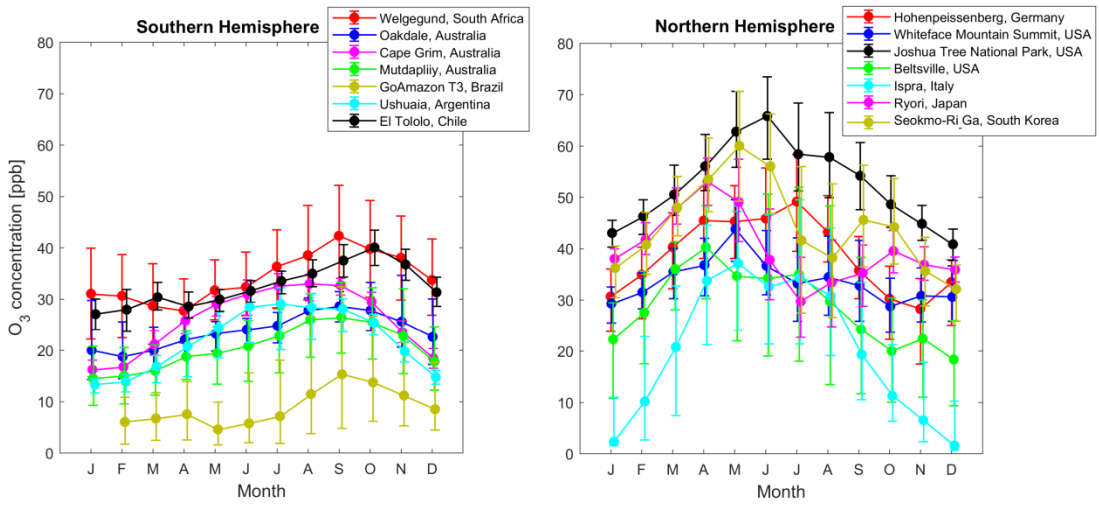


**Fig. 4.** Seasonal cycle of $O_3$ at rural sites in other parts of the world. The dots indicate monthly median (50$^{th}$ percentile) and the upper and lower limits the 25$^{th}$ and 75$^{th}$ percentile, respectively for monthly $O_3$ concentrations. The data is averaged from May 2010 to December 2014, except in a few instances where 2014 data was not available.

The Northern Hemispheric $O_3$ peak over mid-latitude regions is similar to seasonal patterns in the Southern Hemisphere where a springtime $O_3$ maximum is observed (i.e. Whiteface Mountain Summit, Beltsville, Ispra, Ryori and Seokmo-Ri Ga). However, there are other sites in the Northern Hemisphere where a summer maximum is more evident (Vingarzan, 2004), i.e. Joshua Tree and Hohenpeissenberg. The discernible difference between the hemispheres is that the spring maximum in the Southern Hemisphere refers to maximum $O_3$ concentrations in late winter and early spring, while in the Northern Hemisphere, it refers to a late spring and early summer $O_3$ maximum (Cooper et al., 2014). The spring maximum in the Northern Hemisphere is associated with stratospheric intrusions (Zhang et al., 2014; Parrish et al., 2013), while the summer maximum is associated with photochemical $O_3$ production from anthropogenic emissions of $O_3$ precursors being at its highest (Logan, 1985; Chevalier et al., 2007). Maximum $O_3$ concentrations at background sites in the United States and Europe are similar to values at Welgegund in spring with the exception of Joshua Tree National Park in the United States, which had significantly higher $O_3$ levels. This is most likely due its high elevation and deep boundary layer (~4 km asl) during spring and summer allowing free tropospheric $O_3$ to be more effectively mixed down to the surface (Cooper et al., 2014). Maximum $O_3$ levels at the two sites in East Asia (Ryori and Seokmo-Ri Ga) were also generally higher than at Welgegund, especially at Seokmo-Ri Ga.

## 3.4 Sources contributing to surface $O_3$ in continental South Africa

As indicated above (section 3.1), the $O_3$ peaks in continental South Africa usually reflect increased concentrations of precursor species from anthropogenic sources during winter, as well as the occurrence of regional open biomass burning in late winter and early spring. In addition, stratospheric $O_3$ intrusions during spring (Lefohn et al., 2014) could also partially contribute to increased surface $O_3$ levels.

### 3.4.1 Anthropogenic and open biomass burning emissions

A comparison of the $O_3$ seasonal cycles at background and polluted locations is useful for source attribution. From Fig. 3, it is evident that daytime $O_3$ levels peaked at Elandsfontein, Marikana and Welgegund during late winter and spring (August to October), while $O_3$ levels at Botsalano peaked later in the year during spring (September to November). This suggests that Elandsfontein, Marikana and Welgegund were influenced by increased levels of $O_3$ precursors from anthropogenic and open biomass burning emissions (i.e. $NO_x$ and CO indicated in Fig. A4 and Fig. A5, respectively – time series plotted in Fig. A7 and A8), while $O_3$ levels at Botsalano were predominantly influenced by regional open biomass burning (Fig. A5). Although Welgegund and Botsalano are both background sites, Botsalano is more removed from anthropogenic source regions than Welgegund is (section 2.1.3), which is therefore not directly influenced by the increased concentrations of $O_3$ precursor species associated with anthropogenic emissions during winter. Daytime $O_3$ concentrations were the highest at Marikana throughout most of the year, which indicates the influence of local and regional sources of $O_3$ precursors at this site (Venter et al., 2012). In addition, a larger difference between $O_3$ concentrations in summer and winter/spring is observed at Marikana compared to Welgegund and Botsalano, which can be attributed to local anthropogenic emissions (mainly household combustion) of $O_3$ precursors at Marikana.

$O_3$ concentrations at Elandsfontein were lower compared to the other three sites throughout the year, with the exception of the winter months (June to August). The major point sources at Elandsfontein include $NO_x$ emissions from coal-fired power stations and are characterised by high-stack emissions, which are emitted above the low-level night-time inversion layers. During day time, downwards mixing of these emitted species occurs, which results in daytime peaks of $NO_x$ (as indicated in Fig. A5 and by Collett et al., 2010) and subsequent $O_3$ titration. In contrast,

Venter et al. (2012) indicated that, at Marikana, low-level emissions associated with household combustion for space heating and cooking were a significant source of $O_3$ precursor species, i.e. $NO_x$ and CO. The diurnal pattern of $NO_x$ and CO (Fig. A4 and Fig. A5, respectively) at Marikana was characterised by bimodal peaks during the morning and evening, which resulted in increased $O_3$ concentrations during daytime and night-time titration of $O_3$, especially during winter. Therefore, the observed differences in night-time titration at Marikana and Elandsfontein can be attributed to different sources of $O_3$ precursors, i.e. mainly low-level emissions (household combustion) at Marikana (Venter et al., 2012) compared to predominantly high-stack emissions at Elandsfontein (Collette et al., 2010). The higher $O_3$ concentrations at Elandsfontein during winter are most likely attributed to the regional increase in $O_3$ precursors.

The spring maximum $O_3$ concentrations can be attributed to increases in widespread regional biomass burning in this region during this period (Vakkari et al., 2014; Lourens et al., 2011). Biomass burning has strong seasonality in southern Africa, extending from June to September (Galanter et al., 2000), and is an important source of $O_3$ and its precursors during the dry season. In an effort to elucidate the influence of regional biomass burning on $O_3$ concentrations in continental South Africa, source area maps of $O_3$ were compiled by relating $O_3$ concentrations measured with air mass history, which are presented in Fig. 5 (a). Source area maps were only generated for the background sites Welgegund and Botsalano, since local sources at the industrial sites Elandsfontein and Marikana would obscure the influence of regional biomass burning. In addition, maps of spatial distribution of fires during 2007, 2010 and 2015 were compiled with the MODIS collection 5 burnt area product (Roy et al., 2008; Roy et al., 2005; Roy et al., 2002), which are presented in Fig. 6.

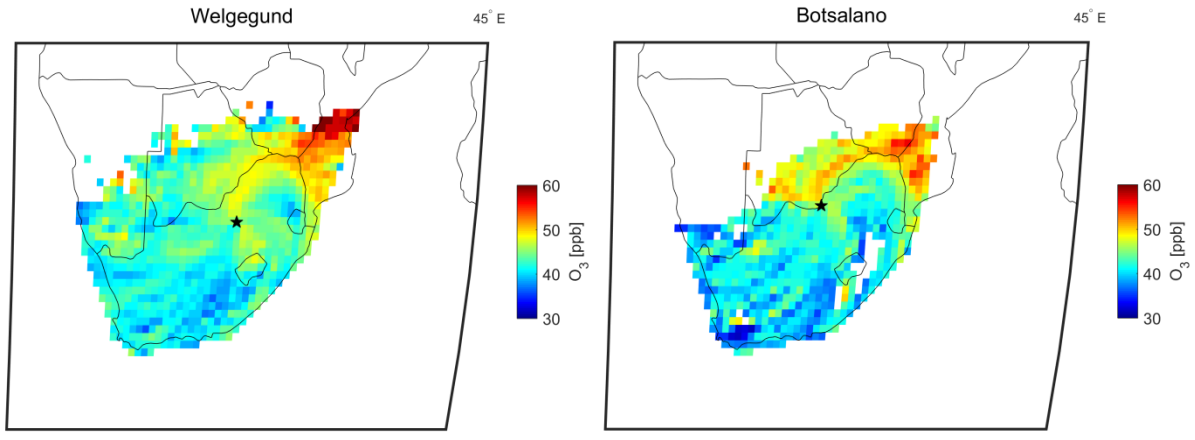


**(a)**

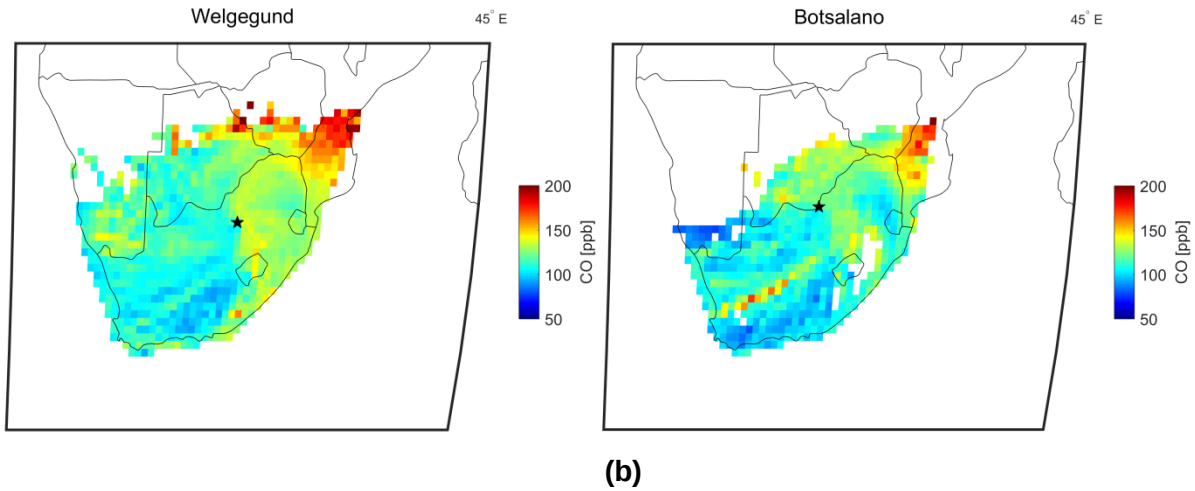


**(b)**

**Fig. 5.** Source area maps of (a) $O_3$ concentrations and (b) CO concentrations for the background sites Welgegund and Botsalano. The black star represents the measurement site and the colour of each pixel represents the mean concentration of the respective gas species. At least ten observations per pixel are required.

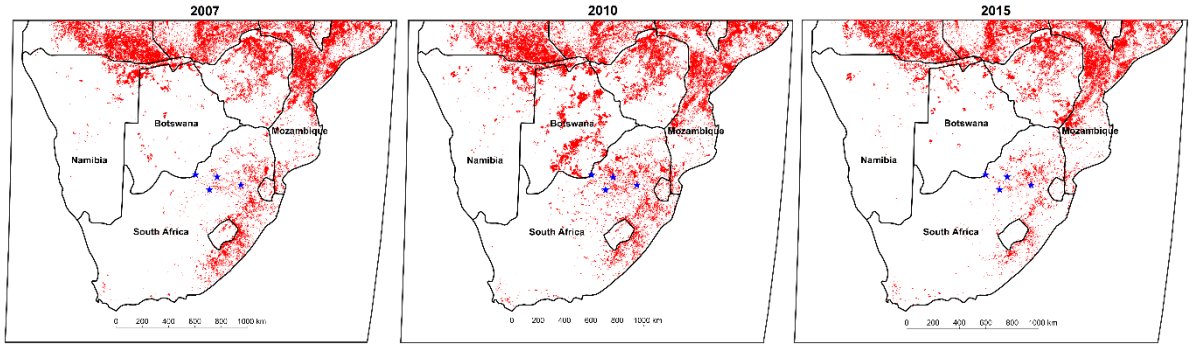


**Fig. 6.** Spatial distribution of fires in 2007, 2010 and 2015 from MODIS burnt area product. Blue stars indicate (from left to right) Botsalano, Welgegund, Marikana and Elandsfontein.

The highest $O_3$ concentrations measured at Welgegund and Marikana were associated with air masses passing over a sector north to north-east of these sites, i.e. southern and central Mozambique, southern Zimbabwe and south-eastern Botswana. $O_3$ concentrations associated with air masses passing over central and southern Mozambique were particularly high. In addition to $O_3$ source maps, CO source maps were also compiled for Welgegund and Botsalano, as indicated in Fig. 5 (b). It is evident that the CO source maps indicated a similar pattern than that observed for $O_3$ with the highest CO concentrations corresponding with the

same regions where $O_3$ levels are the highest. From the fire maps in Fig. 6, it can be observed that a large number of fires occur in the sector, associated with higher $O_3$ and CO concentrations, with the fire map indicating, especially, a high fire frequency occurring in central Mozambique. During 2007, more fires occurred in Botswana compared to the other two years, which is also reflected in the higher $O_3$ levels measured at Botsalano during that year for air masses passing over this region. Open biomass burning is known to emit more CO than $NO_x$, while CO also has a relatively long atmospheric lifetime (1 to 2 months, Kanakidou and Crutzen, 1999) compared to $NO_x$ (6 to 24 hours, Beirle et al., 2003) and VOCs (few hours to a few weeks, Kanakidou and Crutzen, 1999) emitted from open biomass burning. Enhanced CO concentrations have been used previously to characterise the dispersion of biomass burning emissions over southern Africa (Mafusire et al., 2016). Therefore, the regional transport of CO and VOCs (and $NO_x$ to a lesser extent) associated with biomass burning occurring from June to September in southern Africa can be considered an important source of surface $O_3$ in continental South Africa (Fig. A5).

### 3.4.2 Stratospheric $O_3$

Elevated levels of tropospheric $O_3$ may also be caused by stratospheric intrusion of $O_3$-rich air (Zhang et al., 2014; Parrish et al., 2013; Lin et al., 2012), especially on certain days during late winter and spring when $O_3$ is the highest on the South African Highveld (Thompson et al., 2014). However, the importance of the stratospheric source over continental South Africa has not yet been specifically addressed. The assessment of meteorological fields and air quality data at high-elevation sites is required to determine the downward transport of stratospheric $O_3$. Alternatively, stratospheric $O_3$ intrusions can be estimated through concurrent in-situ measurements of ground-level $O_3$, CO and humidity, since stratospheric intrusions of $O_3$ into the troposphere are characterised by elevated levels of $O_3$, high potential vorticity, low levels of CO and low water vapour (Stauffer et al., 2017; Thompson et al., 2015; Thompson et al., 2014). Thompson et al. (2015) defined low CO as 80 to 110 ppbv, while low relative humidity (RH) is considered <15 %. In Fig. 7, the 95$^{th}$ percentile $O_3$ levels (indicative of "high $O_3$") corresponding to low daily average CO concentrations (< 100 ppb) are presented together with the daily average RH. Only daytime data from 07:00 to 18:00 (LT) was considered in order to exclude the influence of night-time titration. From Fig. 7, it is evident that very few days complied with the criteria indicative of stratospheric $O_3$ intrusion, i.e. high $O_3$, low CO and low RH, which indicates a very small influence of stratospheric intrusion on surface $O_3$ levels. However, it must be noted

that the attempt in this study to relate surface $O_3$ to stratospheric intrusions is a simplified qualitative assessment and more quantitative detection methods should be applied to understand the influence of stratospheric intrusions on surface $O_3$ for this region.

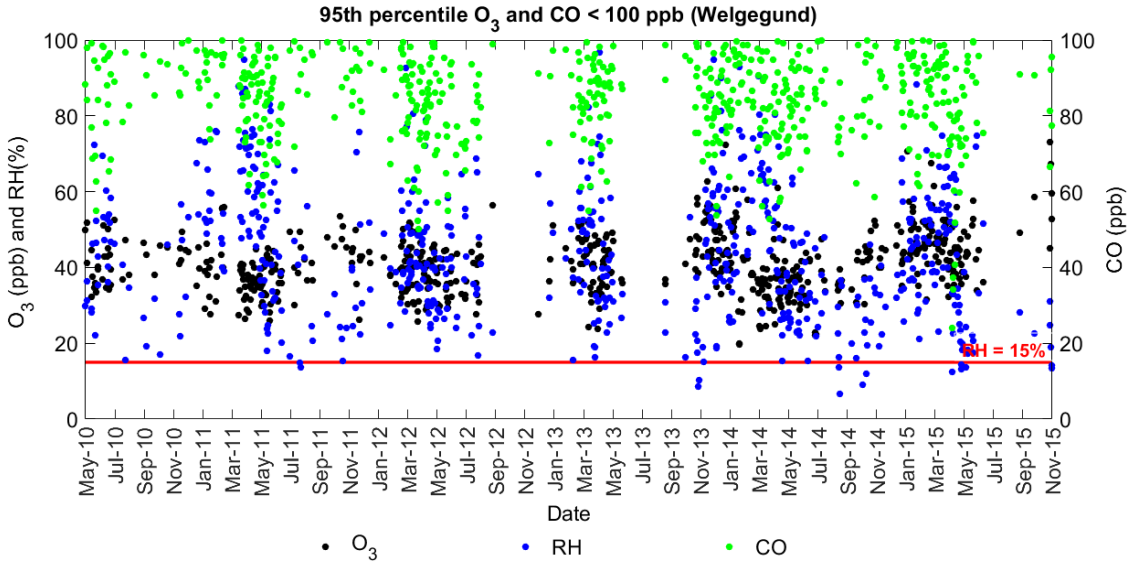


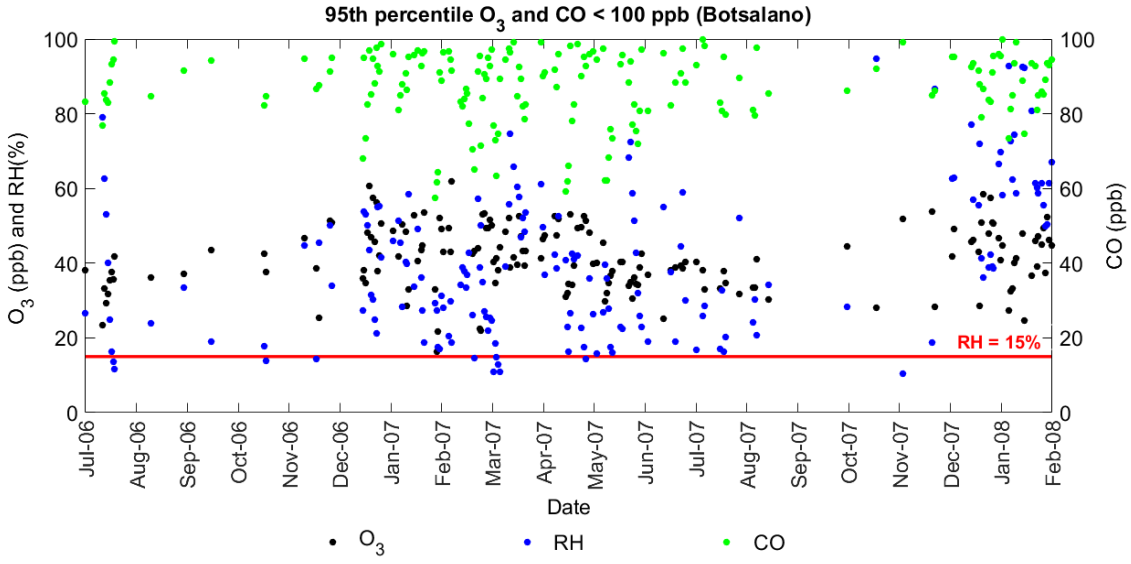


**Fig. 7.** Simultaneous measurements of $O_3$ (daily 95$^{th}$ percentile), CO (daily average ppb) and RH (daily average) from 07:00 to 18:00 LT at Welgegund, Botsalano and Marikana.

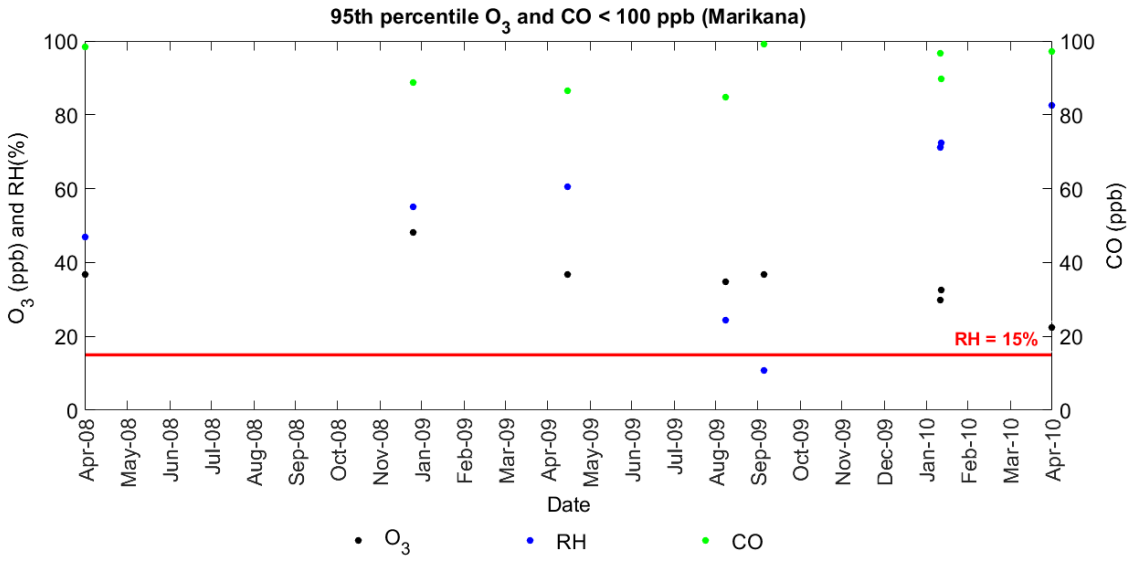


**Fig. 7.** Continued.

## 3.5 Insights into the $O_3$ production regime

The relationship between $O_3$, $NO_x$ and CO was used as an indicator to infer the $O_3$ production regime at Welgegund, Botsalano and Marikana (no CO measurements were conducted at Elandsfontein as indicated above), since no continuous VOC measurements were conducted at each of these sites. However, as indicated in Section 2.4, a two-year VOC dataset was available for Welgegund (Jaars et al., 2016; Jaars et al., 2014), which was used to calculate the instantaneous production rate of $O_3$ as a function of $NO_2$ levels and VOC reactivity (Geddes et al., 2009; Murphy et al., 2006).

### 3.5.1 The relationship between $NO_x$, CO and $O_3$

In Fig. 8, the correlations between $O_3$, $NO_x$ and CO concentrations at Welgegund, Botsalano and Marikana are presented, which clearly indicate higher $O_3$ concentrations associated with increased CO levels, while $O_3$ levels remain relatively constant (or decrease) with increasing $NO_x$. The highest $O_3$ concentrations occur for $NO_x$ levels below 10 ppb, since the equilibrium between photochemical production of $O_3$ and chemical removal of $O_3$ shifts towards the former, i.e. greater $O_3$ formation. In general, there seems to exist a marginal negative correlation between $O_3$ and $NO_x$ (Fig. A6) at all four sites, which is a reflection of the photochemical

production of $O_3$ from $NO_2$ and the destruction of $O_3$ through $NO_x$ titration. These correlations between $NO_x$, CO and $O_3$ indicate that $O_3$ production in continental South Africa is limited by CO (and VOC) concentrations, i.e. VOC-limited.

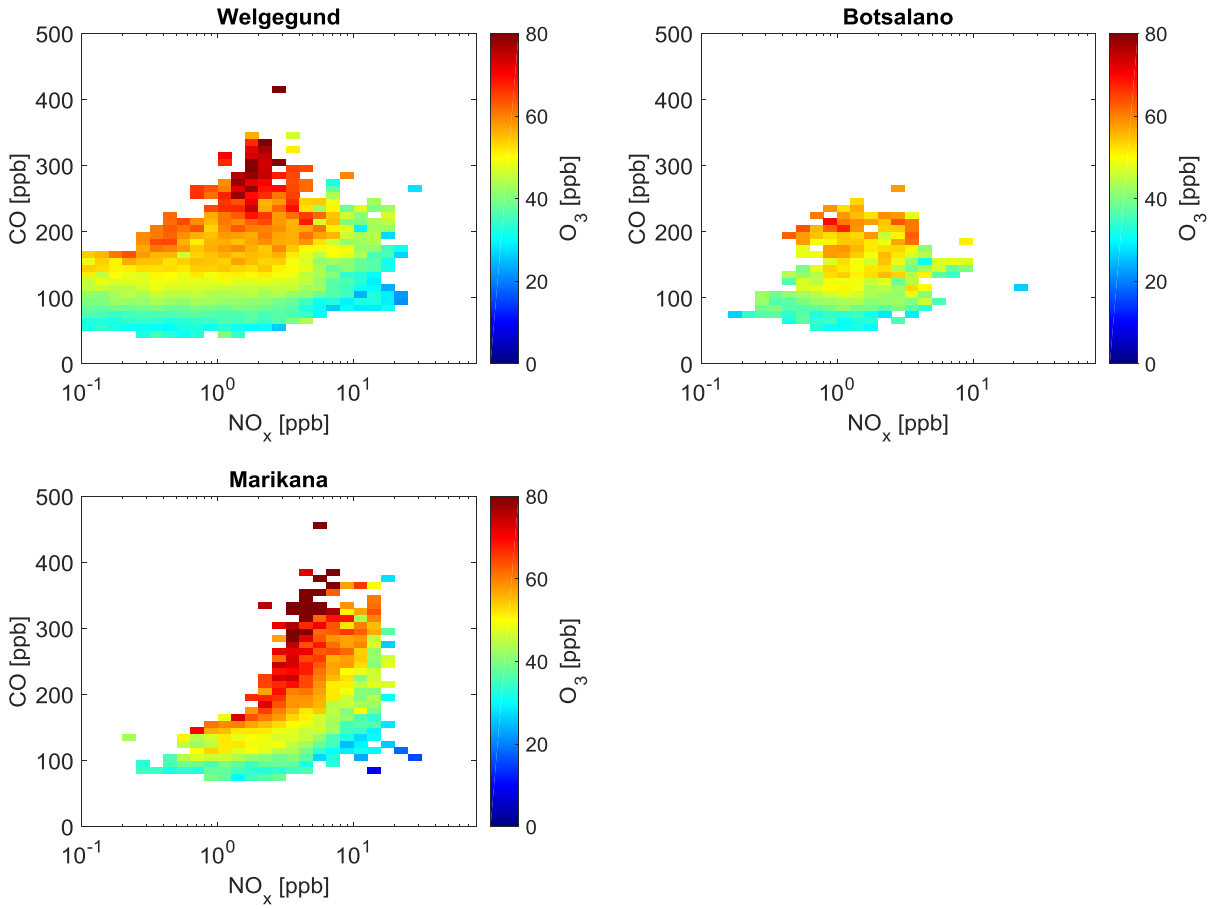


**Fig. 8.** Mean $O_3$ concentration averaged for $NO_x$ and CO bins. Measurements were only taken from 11:00 to 17:00 LT when photochemical production of $O_3$ is at a maximum.

This finding shows a strong correlation between $O_3$ and CO and suggests that high $O_3$ can be attributed to the oxidation of CO in the air masses, i.e. as long as there is a sufficient amount of $NO_x$ present in a region, CO serves to produce $O_3$. Although $NO_x$ and VOCs are usually considered as the main precursors in ground-level $O_3$ formation, CO acts together with $NO_x$ and VOCs in the presence of sunlight to drive photochemical $O_3$ formation. According to Fig. 8, reducing CO emissions should result in a reduction in surface $O_3$ and it is assumed that this response is analogous to that of VOCs. It is, however, not that simple, since the ambient $NO_x$ and VOCs concentrations are directly related to the instantaneous rate of production of $O_3$ and not necessarily to the ambient $O_3$ concentration at a location, which is the result of chemistry,

deposition and transport that have occurred over several hours or a few days (Sillman, 1999). Notwithstanding the various factors contributing to increased surface $O_3$ levels, the correlation between ambient CO and $O_3$ is especially relevant given the low reactivity of CO with respect to $^{\bullet}OH$ radicals compared to most VOCs, which implies that the oxidation of CO probably takes place over a timescale of several days. It seems that the role of CO is of major importance in tropospheric chemistry in this region, where sufficient $NO_x$ is present across continental South Africa and biogenic VOCs are relatively less abundant (Jaars et al., 2016), to fuel the $O_3$ formation process.

### 3.5.2 Seasonal change in $O_3$-precursors relationship

Seasonal changes in the relationship between $O_3$ and precursor species can be indicative of different sources of precursor species during different times of the year. In Fig. 9, the correlations between $O_3$ levels with $NO_x$ and CO are presented for the different seasons, which indicate seasonal changes in the dependence of elevated $O_3$ concentrations on these precursors. The very high CO concentrations relative to $NO_x$, i.e. high CO to $NO_x$ ratios, are associated with the highest $O_3$ concentrations, which are most pronounced (highest $CO/NO_x$ ratios) during winter and spring. This indicates that the winter and spring $O_3$ maximum is primarily driven by increased peroxy radical production from CO and VOCs. The seasonal maximum in $O_3$ concentration coincides with the maximum CO concentration at the background sites, while the $O_3$ peak occurs just after June/July when CO peaked at the polluted site Marikana (Fig. A5). This observed seasonality in $O_3$ production signifies the importance of precursor species emissions from open biomass burning during winter and spring in this region, while household combustion for space heating and cooking is also an important source of $O_3$ precursors, as previously discussed. The strong diurnal CO concentration patterns observed during winter at Marikana (Fig. A5) substantiate the influence of household combustion on CO levels as indicated by Venter et al. (2012).

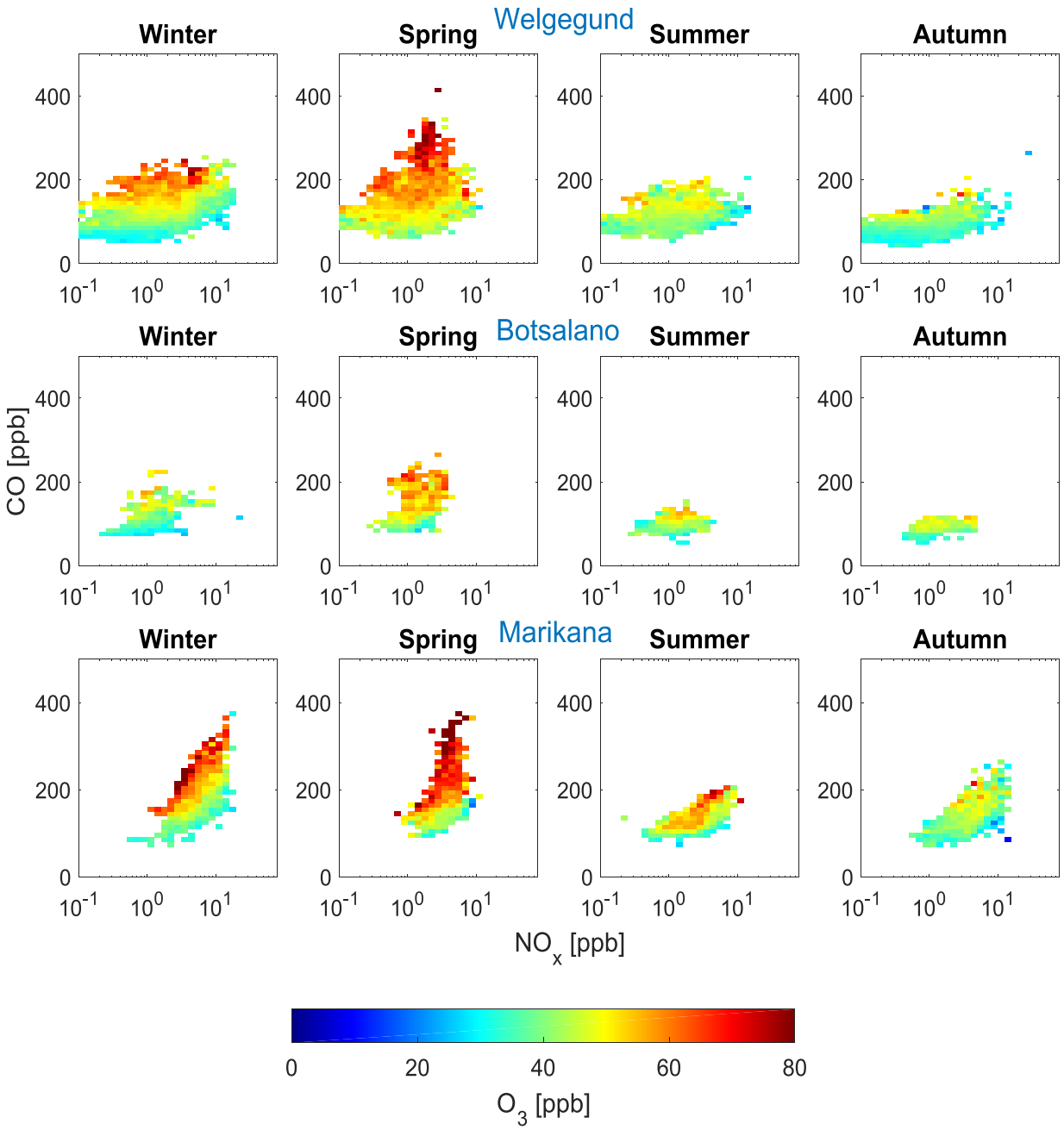


**Fig. 9.** Seasonal plots of the relationship between $O_3$, $NO_x$ and CO at Welgegund, Botsalano and Marikana.

### 3.5.3 $O_3$ production rate

In Fig. 10, $P(O_3)$ as a function of VOC reactivity calculated from the available VOC dataset for Welgegund (Section 2.4) and $NO_2$ concentrations is presented. $O_3$ production at Welgegund during two field campaigns, specifically at 11:00 LT, was found to range between 0 and 10 ppbv

$h^{-1}$. The average $P(O_3)$ over the 2011 to 2012 and the 2014 to 2015 campaigns combined were 3.0 ± 1.9 ppbv $h^{-1}$ and 3.2 ± 3.0 ppbv $h^{-1}$, respectively. The dashed black line in Fig. 10, called the ridge line, separates the $NO_x$- and VOC-limited regimes. To the left of the ridge line is the $NO_x$-limited regime, when $O_3$ production increases with increasing $NO_x$ concentrations. The VOC-limited regime is to the right of the ridge line, when $O_3$ production decreases with increasing $NO_x$. According to the $O_3$ production plot presented, approximately 40% of the data is found in the VOC-limited regime area, which would support the regional $O_3$ analysis conducted for continental South Africa in this study. However, the $O_3$ production plot for Welgegund transitions between $NO_x$- and VOC-limited regimes, with Welgegund being in a $NO_x$-limited production regime the majority of the time, especially when $NO_x$ concentrations are very low (<1 ppb). As indicated in section 2.4, limitations to this analysis include limited VOC speciation data, as well as a single time-of-day grab sample. The $O_3$ production rates can therefore only be inferred at 11:00 am LT despite $O_3$ concentrations peaking during the afternoon at Welgegund. Therefore, clean background air $O_3$ production is most-likely $NO_x$-limited (Tiitta et al., 2014), while large parts of the regional background of continental South Africa can be considered VOC-limited.

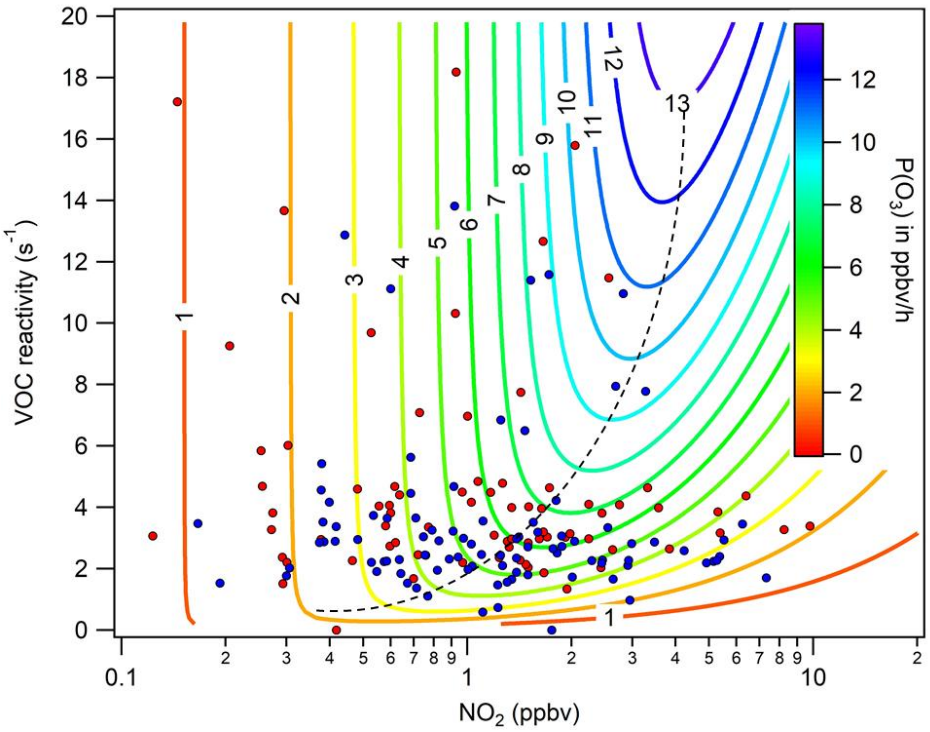


**Fig. 10.** Contour plot of instantaneous $O_3$ production ($P(O_3)$) at Welgegund using daytime (11:00 LT) grab sample measurements of VOCs and $NO_2$. The blue dots represent the first campaign (2011-2012), and the red dots indicate the second campaign (2014-2015).

## 3.6 Implications for air quality management

### 3.6.1 Ozone exceedances

The South African National Ambient Air Quality Standard (NAAQS) for $O_3$ is an eight-hour moving average limit of 61 ppbv with 11 exceedances allowed annually (Government Gazette Republic of South Africa, 2009). Fig. 11 shows the average number of days per month when this $O_3$ standard limit was exceeded at the four measurement sites. It is evident that the daily eight-hour-$O_3$-maximum concentrations regularly exceeded the NAAQS threshold for $O_3$ and the number of exceedances annually allowed at all the sites, including the most remote of the four sites, Botsalano. At the polluted locations of Marikana and Elandsfontein, the $O_3$ exceedances peak early on in the dry season (June onwards), while at the background locations of Welgegund and Botsalano, the highest numbers of exceedances occur later in the dry season (August to November). These relatively high numbers of $O_3$ exceedances at all the sites (background and industrial) highlight the regional $O_3$ problem in South Africa, with background sites being impacted by the regional transport of $O_3$ precursors from anthropogenic and biomass burning source regions.

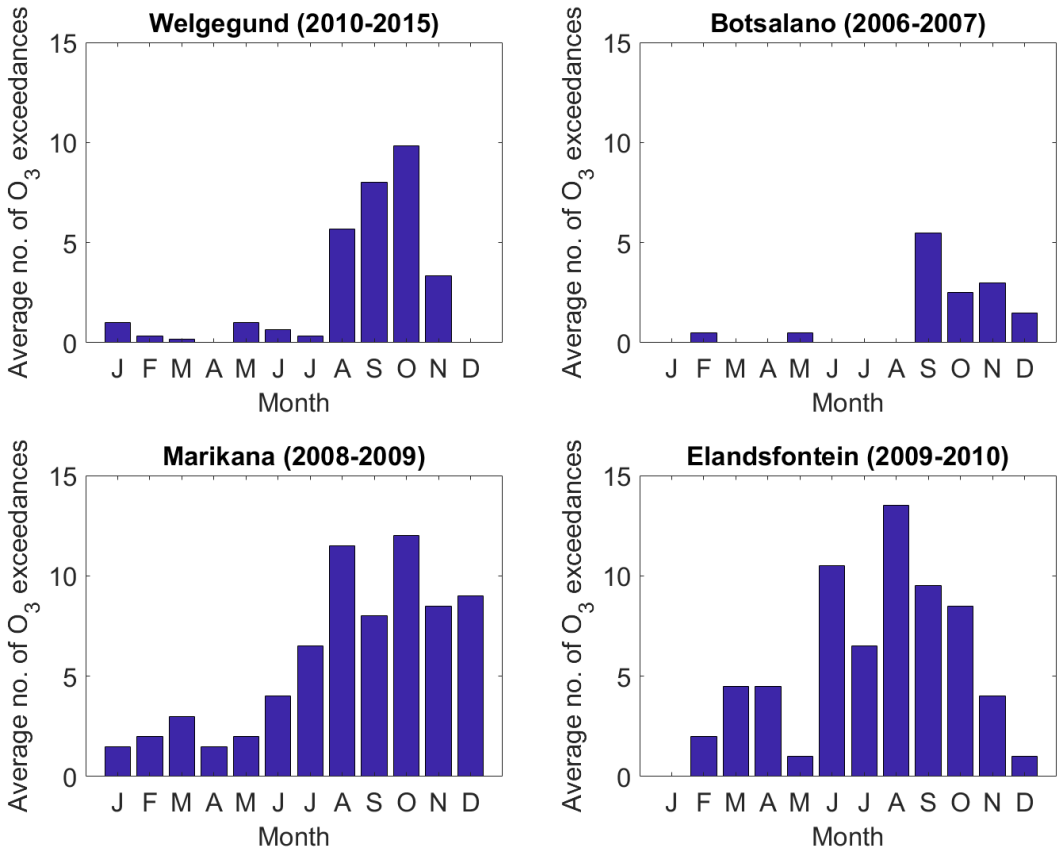


**Fig. 11.** Monthly number of exceedances of the daily 8-h-$O_3$-max (i.e. highest value of all available 8-hour moving averages in that day) above 61 ppbv at Welgegund, Botsalano, Marikana and Elandsfontein.

### 3.6.2 $O_3$ control strategies

As indicated above (sections 3.4 and 3.5), $O_3$ formation in the regions where Welgegund, Botsalano and Marikana are located can be considered VOC-limited, while the highly industrialised region with high $NO_x$ emissions where Elandsfontein is located could also be considered VOC-limited. Rural remote regions are generally considered to be $NO_x$-limited due to the availability of $NO_x$ and the impact of BVOCs (Sillman, 1999). However, Jaars et al. (2016) indicated that BVOC concentrations at a savannah grassland were at least an order of magnitude lower compared to other regions in the world. Therefore, very low BVOC concentrations, together with high anthropogenic emissions of $NO_x$ in the interior of South Africa, result in VOC-limited conditions at background sites in continental South Africa.

It is evident that reducing CO- and VOC concentrations associated with anthropogenic emissions, e.g. household combustion, vehicular emissions and industries, would be the most efficient control strategy to reduce peak $O_3$ concentrations in the interior of South Africa. It is also imperative to consider the seasonal variation in the CO and VOC source strength in managing $O_3$ pollution in continental southern Africa. This study also revealed the significant contribution of biomass burning to $O_3$ precursors in this region, which should also be considered when implementing $O_3$ control strategies. However, since open biomass burning in southern Africa is of anthropogenic and natural origin, while $O_3$ concentrations in continental South Africa are also influenced by transboundary transport of $O_3$ precursors from open biomass burning occurring in other countries in southern Africa (as indicated above), it is more difficult to control. Nevertheless, open biomass burning caused by anthropogenic practices (e.g. crop residue, pasture maintenance fires, opening burning of garbage) can be addressed.

## 4. Conclusions

A spatial distribution map of $O_3$ levels in the interior of South Africa indicated the regional $O_3$ problem in continental South Africa, which was signified by the regular exceedance of the South African air quality standard limit. The seasonal and diurnal $O_3$ patterns observed at the four sites in this study resembled typical trends for $O_3$ in continental South Africa, with $O_3$ concentrations peaking in late winter and early spring (cf. Zunckel et al., 2004), while daytime $O_3$ corresponded to increased photochemical production. The seasonal $O_3$ trends observed in continental southern Africa could mainly be attributed to the seasonal changes in emissions of $O_3$ precursor species and local meteorological conditions. Increased $O_3$ concentrations in winter at Welgegund, Marikana and Elandsfontein reflected increased household combustion for space heating and the trapping of low-level pollutants near the surface. A spring maximum observed at all the sites was attributed to increased regional open biomass burning. Significantly higher $O_3$ concentrations, which corresponded with increased CO concentrations, were associated with air masses passing over a region in southern Africa, where a large number of open biomass fires occurred from June to September. Therefore, the regional transport of CO associated with open biomass burning in southern Africa was considered a significant source of surface $O_3$ in continental South Africa. A very small contribution from the stratospheric intrusion of $O_3$-rich air to surface $O_3$ levels at the four sites was indicated.

The relationship between $O_3$, $NO_x$ and CO at Welgegund, Botsalano and Marikana indicated a strong correlation between $O_3$ and CO, while $O_3$ levels remained relatively constant (or decreased) with increasing $NO_x$. Although $NO_x$ and VOCs are usually considered to be the main precursors in ground-level $O_3$ formation, CO can also drive photochemical $O_3$ formation. The seasonal changes in the relationship between $O_3$ and precursors species also reflected the higher CO emissions associated with increased household combustion in winter, and open biomass burning in late winter and spring. The calculation of the $P(O_3)$ from a two-year VOC dataset at Welgegund indicated that at least 40% of $O_3$ production occurred in the VOC-limited regime. These results indicated that large parts in continental South Africa can be considered VOC-limited, which can be attributed to high anthropogenic emissions of $NO_x$ in this region. It is, however, recommended that future studies should investigate more detailed relationships between $NO_x$, CO, VOCs and $O_3$ through photochemical modelling analysis, while concurrent measurement of atmospheric VOCs and $^{\bullet}OH$ would also contribute to the better understanding of surface $O_3$ in this region.

In this paper, some new aspects on $O_3$ in continental South Africa have been indicated, which must be taken into consideration when $O_3$ mitigation strategies are deployed. Emissions of $O_3$ precursor species associated with the concentrated location of industries in this area could be regulated, while CO and VOC emissions associated with household combustion and regional open biomass burning should also be targeted. However, emissions of $O_3$ precursor species related to factors such as household combustion associated with poor socio-economic circumstances and long-range transport provide a bigger challenge for regulators.

**Acknowledgements**

The financial assistance of the National Research Foundation (NRF) towards this research is hereby acknowledged. Opinions expressed and conclusions arrived at are those of the authors and are not necessarily to be attributed to the NRF. We thank the Tropospheric Ozone Assessment Report (TOAR) initiative for providing the surface ozone data used in this publication. The authors are also grateful to Eskom for supplying the Elandsfontein data. Thanks are also due to Dirk Cilliers from the NWU for the GIS assistance. V Vakkari is a beneficiary of an AXA Research Fund postdoctoral grant. This work was partly funded by the Academy of Finland Centre of Excellence program (grant no. 272041).

## 5. References


Air Resources Laboratory: Gridded Meteorological Data Archives, available at: https://www.ready.noaa.gov/archives.php, 2017.

Balashov, N. V., Thompson, A. M., Piketh, S. J., and Langerman, K. E.: Surface ozone variability and trends over the South African Highveld from 1990 to 2007, Journal of Geophysical Research: Atmospheres, 119, 4323-4342, doi:10.1002/2013JD020555, 2014.

Beirle, S., Platt, U., Wenig, M., and Wagner, T.: Weekly cycle of NO 2 by GOME measurements: A signature of anthropogenic sources, Atmospheric Chemistry and Physics, 3, 2225-2232, 2003.

Cazorla, M., and Brune, W. H.: Measurement of Ozone Production Sensor, Atmospheric Measurement Techniques, 3, 545-555, doi:10.5194/amt-3-545-2010, 2010.

Chevalier, A., Gheusi, F., Delmas, R., Ordóñez, C., Sarrat, C., Zbinden, R., Thouret, V., Athier, G., and Cousin, J. M.: Influence of altitude on ozone levels and variability in the lower troposphere: a ground-based study for western Europe over the period 2001-2004, Atmos. Chem. Phys., 7, 4311-4326, doi:10.5194/acp-7-4311-2007, 2007.

Collett, K. S., Piketh, S. J., and Ross, K. E.: An assessment of the atmospheric nitrogen budget on the South African Highveld, South African Journal of Science, doi:10.4102/sajs.v106i5/6.220, 2010.

Combrink, J., Diab, R., Sokolic, F., and Brunke, E.: Relationship between surface, free tropospheric and total column ozone in two contrasting areas in South Africa, Atmospheric Environment, 29, 685-691, 1995.

Cooper, O. R., Parrish, D., Ziemke, J., Balashov, N., Cupeiro, M., Galbally, I., Gilge, S., Horowitz, L., Jensen, N., and Lamarque, J.-F.: Global distribution and trends of tropospheric ozone: An observation-based review, Elem Sci Anth, 2, 2014.

Crutzen, P. J., and Andreae, M. O.: Biomass Burning in the Tropics: Impact on Atmospheric Chemistry and Biogeochemical Cycles, Science, 250, 1669-1678, doi:10.1126/science.250.4988.1669, 1990.

Diab, R., Thompson, A., Mari, K., Ramsay, L., and Coetzee, G.: Tropospheric ozone climatology over Irene, South Africa, from 1990 to 1994 and 1998 to 2002, Journal of Geophysical Research: Atmospheres, 109, 2004.

Diab, R. D., Thompson, A. M., Zunckel, M., Coetzee, G. J. R., Combrink, J., Bodeker, G. E., Fishman, J., Sokolic, F., McNamara, D. P., Archer, C. B., and Nganga, D.: Vertical ozone distribution over southern Africa and adjacent oceans during SAFARI-92, Journal of Geophysical Research: Atmospheres, 101, 23823-23833, doi:10.1029/96JD01267, 1996.

Draxler, R. R., and Hess, G. D.: An overview of the HYSPLIT_4 modeling system of trajectories, dispersion, and deposition, Australian Meteorological Magazine, 47, 295-308, 1998.

Dyson, L. L., Van Heerden, J., and Sumner, P. D.: A baseline climatology of sounding-derived parameters associated with heavy rainfall over Gauteng, South Africa, International Journal of Climatology, 35, 114-127, 2015.

Fishman, J., and Larsen, J. C.: Distribution of total ozone and stratospheric ozone in the tropics: Implications for the distribution of tropospheric ozone, Journal of Geophysical Research: Atmospheres, 92, 6627-6634, doi:10.1029/JD092iD06p06627, 1987.

Galanter, M., Levy, H., and Carmichael, G. R.: Impacts of biomass burning on tropospheric CO, $NO_x$, and $O_3$, Journal of Geophysical Research: Atmospheres, 105, 6633-6653, 2000.

Garstang, M., Tyson, P. D., Swap, R., Edwards, M., Kållberg, P., and Lindesay, J. A.: Horizontal and vertical transport of air over southern Africa, Journal of Geophysical Research: Atmospheres, 101, 23721-23736, doi:10.1029/95JD00844, 1996.

Geddes, J. A., Murphy, J. G., and Wang, D. K.: Long term changes in nitrogen oxides and volatile organic compounds in Toronto and the challenges facing local ozone control, Atmospheric Environment, 43, 3407-3415, doi:https://doi.org/10.1016/j.atmosenv.2009.03.053, 2009.

Held, G., Scheifinger, H., Snyman, G., Tosen, G., and Zunckel, M.: The climatology and meteorology of the Highveld, Air pollution and its impacts on the South African Highveld. Johannesburg: Environmental Scientific Association, 60-71, 1996.

Held, G., and Mphepya, J.: Wet and dry deposition in South Africa, Proceedings, XI Congresso Brasiliero de Meteorologia (CDROM), SBMET, Rio de Janeiro, 2000, 16-20,

Hirsikko, A., Vakkari, V., Tiitta, P., Manninen, H. E., Gagné, S., Laakso, H., Kulmala, M., Mirme, A., Mirme, S., Mabaso, D., Beukes, J. P., and Laakso, L.: Characterisation of sub-micron particle number

concentrations and formation events in the western Bushveld Igneous Complex, South Africa, Atmospheric Chemistry and Physics, 12, 3951-3967, doi:10.5194/acp-12-3951-2012, 2012.

Hirsikko, A., Vakkari, V., Tiitta, P., Hatakka, J., Kerminen, V. M., Sundström, A. M., Beukes, J. P., Manninen, H. E., Kulmala, M., and Laakso, L.: Multiple daytime nucleation events in semi-clean savannah and industrial environments in South Africa: analysis based on observations, Atmospheric Chemistry and Physics, 13, 5523-5532, doi:10.5194/acp-13-5523-2013, 2013.

Holloway, A. M., and Wayne, R. P.: Atmospheric chemistry, Royal Society of Chemistry, Cambridge, xiii, 271 p. pp., 2010.

IPCC: Climate change 2013: The physical science basis: contribution of Working Group I to the Fifth Assessment Report of the Intergovernmental Panel on Climate Change, edited by: Stocker, T. F., Qin, D., Plattner, G.-K., Tignor, M., Allen, S. K., Boschung, J., Nauels, A., Xia, Y., Bex, B., and Midgley, B., Cambridge University Press, 2013.

Jaars, K., Beukes, J. P., van Zyl, P. G., Venter, A. D., Josipovic, M., Pienaar, J. J., Vakkari, V., Aaltonen, H., Laakso, H., Kulmala, M., Tiitta, P., Guenther, A., Hellén, H., Laakso, L., and Hakola, H.: Ambient aromatic hydrocarbon measurements at Welgegund, South Africa, Atmospheric Chemistry and Physics, 14, 7075-7089, doi:10.5194/acp-14-7075-2014, 2014.

Jaars, K., van Zyl, P. G., Beukes, J. P., Hellén, H., Vakkari, V., Josipovic, M., Venter, A. D., Räsänen, M., Knoetze, L., Cilliers, D. P., Siebert, S. J., Kulmala, M., Rinne, J., Guenther, A., Laakso, L., and Hakola, H.: Measurements of biogenic volatile organic compounds at a grazed savannah grassland agricultural landscape in South Africa, Atmospheric Chemistry and Physics, 16, 15665-15688, doi:10.5194/acp-16-15665-2016, 2016.

Josipovic, M.: Acidic deposition emanating from the South African Highveld - a critical levels and critical loads assessment (Ph.D. thesis), University of Johannesburg, 2009.

Josipovic, M., Annegarn, H. J., Kneen, M. A., Pienaar, J. J., and Piketh, S. J.: Concentrations, distributions and critical level exceedance assessment of $SO_2$, $NO_2$ and $O_3$ in South Africa, Environmental monitoring and assessment, 171, 181-196, doi:10.1007/s10661-009-1270-5, 2010.

Kanakidou, M., and Crutzen, P. J.: The photochemical source of carbon monoxide: Importance, uncertainties and feedbacks, Chemosphere-Global Change Science, 1, 91-109, 1999.

Klopper, E., Vogel, C. H., and Landman, W. A.: Seasonal climate forecasts–potential agricultural-risk management tools?, Climatic Change, 76, 73-90, 2006.

Laakso, L., Laakso, H., Aalto, P. P., Keronen, P., Petäjä, T., Nieminen, T., Pohja, T., Siivola, E., Kulmala, M., Kgabi, N., Molefe, M., Mabaso, D., Phalatse, D., Pienaar, K., and Kerminen, V. M.: Basic characteristics of atmospheric particles, trace gases and meteorology in a relatively clean Southern African Savannah environment, Atmospheric Chemistry and Physics, 8, 4823-4839, doi:10.5194/acp-8-4823-2008, 2008.

Laakso, L., Vakkari, V., Virkkula, A., Laakso, H., Backman, J., Kulmala, M., Beukes, J. P., van Zyl, P. G., Tiitta, P., Josipovic, M., Pienaar, J. J., Chiloane, K., Gilardoni, S., Vignati, E., Wiedensohler, A., Tuch, T., Birmili, W., Piketh, S., Collett, K., Fourie, G. D., Komppula, M., Lihavainen, H., de Leeuw, G., and Kerminen, V. M.: South African EUCAARI measurements: seasonal variation of trace gases and aerosol optical properties, Atmospheric Chemistry and Physics, 12, 1847-1864, doi:10.5194/acp-12-1847-2012, 2012.

Laakso, L., Beukes, J. P., Van Zyl, P. G., Pienaar, J. J., Josipovic, M., Venter, A. D., Jaars, K., Vakkari, V., Labuschagne, C., Chiloane, K., and Tuovinen, J.-P.: Ozone concentrations and their potential impacts on vegetation in southern Africa, in: Climate change, air pollution and global challenges understanding and perspectives from forest research, edited by: Matyssek, R., Clarke, N., Cudlin, P., Mikkelsen, T. N., Tuovinen, J.-P., Wieser, G., and Paoletti, E., Elsevier, 1 online resource (647 pages), 2013.

Lefohn, A. S., Emery, C., Shadwick, D., Wernli, H., Jung, J., and Oltmans, S. J.: Estimates of background surface ozone concentrations in the United States based on model-derived source apportionment, Atmospheric Environment, 84, 275-288, doi:https://doi.org/10.1016/j.atmosenv.2013.11.033, 2014.

Lin, M., Fiore, A. M., Cooper, O. R., Horowitz, L. W., Langford, A. O., Levy, H., Johnson, B. J., Naik, V., Oltmans, S. J., and Senff, C. J.: Springtime high surface ozone events over the western United States: Quantifying the role of stratospheric intrusions, Journal of Geophysical Research: Atmospheres, 117, D00V22, doi:10.1029/2012JD018151, 2012.

Logan, J. A.: Tropospheric ozone: Seasonal behavior, trends, and anthropogenic influence, Journal of Geophysical Research: Atmospheres, 90, 10463-10482, doi:10.1029/JD090iD06p10463, 1985.

Lourens, A. S., Beukes, J. P., Van Zyl, P. G., Fourie, G. D., Burger, J. W., Pienaar, J. J., Read, C. E., and Jordaan, J. H.: Spatial and temporal assessment of gaseous pollutants in the Highveld of South Africa, South African Journal of Science, 107, 1-8, 2011.

Lourens, A. S. M., Butler, T. M., Beukes, J. P., Van Zyl, P. G., Beirle, S., Wagner, T. K., Heue, K.-P., Pienaar, J. J., Fourie, G. D., and Lawrence, M. G.: Re-evaluating the $NO_2$ hotspot over the South African Highveld, doi:10.4102/sajs.v108i11/12.1146, 2012.

Lourens, A. S. M., Butler, T. M., Beukes, J. P., Van Zyl, P. G., Fourie, G. D., and Lawrence, M. G.: Investigating atmospheric photochemistry in the Johannesburg-Pretoria megacity using a box model, South African Journal of Science, 112, 1-11, doi:http://dx.doi.org/10.17159/sajs.2016/2015-0169, 2016.

Macdonald, A. M., Anlauf, K. G., Leaitch, W. R., Chan, E., and Tarasick, D. W.: Interannual variability of ozone and carbon monoxide at the Whistler high elevation site: 2002–2006, Atmos. Chem. Phys., 11, 11431-11446, doi:10.5194/acp-11-11431-2011, 2011.

Mafusire, G., Annegarn, H. J., Vakkari, V., Beukes, J. P., Josipovic, M., Van Zyl, P. G., and Laakso, L.: Submicrometer aerosols and excess CO as tracers for biomass burning air mass transport over southern Africa, Journal of Geophysical Research: Atmospheres, 121, 10262-10282, doi:10.1002/2015JD023965, 2016.

Martins, J. J., Dhammapala, R. S., Lachmann, G., Galy-Lacaux, C., and Pienaar, J. J.: Long-term measurements of sulphur dioxide, nitrogen dioxide, ammonia, nitric acid and ozone in southern Africa using passive samplers, South African Journal of Science, 103, 336-342, http://www.scielo.org.za/scielo.php?script=sci_arttext&pid=S0038-23532007000400018&nrm=iso, 2007.

Monks, P. S., Archibald, A. T., Colette, A., Cooper, O., Coyle, M., Derwent, R., Fowler, D., Granier, C., Law, K. S., Mills, G. E., Stevenson, D. S., Tarasova, O., Thouret, V., von Schneidemesser, E., Sommariva, R., Wild, O., and Williams, M. L.: Tropospheric ozone and its precursors from the urban to the global scale from air quality to short-lived climate forcer, Atmospheric Chemistry and Physics, 15, 8889-8973, doi:10.5194/acp-15-8889-2015, 2015.

Murphy, J. G., Day, D. A., Cleary, P. A., Wooldridge, P. J., Millet, D. B., Goldstein, A. H., and Cohen, R. C.: The weekend effect within and downwind of Sacramento: Part 2. Observational evidence for chemical and dynamical contributions, Atmospheric Chemistry and Physics Discussions, 2006, 11971-12019, doi:10.5194/acpd-6-11971-2006, 2006.

Novelli, P. C., Steele, L. P., and Tans, P. P.: Mixing ratios of carbon monoxide in the troposphere, Journal of Geophysical Research: Atmospheres, 97, 20731-20750, 1992.

NRC: Rethinking the Ozone Problem in Urban and Regional Air Pollution, The National Academies Press, Washington, DC, 524 pp., 1991.

Oltmans, S. J., Lefohn, A. S., Shadwick, D., Harris, J. M., Scheel, H. E., Galbally, I., Tarasick, D. W., Johnson, B. J., Brunke, E. G., Claude, H., Zeng, G., Nichol, S., Schmidlin, F., Davies, J., Cuevas, E., Redondas, A., Naoe, H., Nakano, T., and Kawasato, T.: Recent tropospheric ozone changes – A pattern dominated by slow or no growth, Atmospheric Environment, 67, 331-351, doi:https://doi.org/10.1016/j.atmosenv.2012.10.057, 2013.

Parrish, D. D., Law, K. S., Staehelin, J., Derwent, R., Cooper, O. R., Tanimoto, H., Volz-Thomas, A., Gilge, S., Scheel, H. E., Steinbacher, M., and Chan, E.: Lower tropospheric ozone at northern midlatitudes: Changing seasonal cycle, Geophysical Research Letters, 40, 1631-1636, doi:10.1002/grl.50303, 2013.

Petäjä, T., Vakkari, V., Pohja, T., Nieminen, T., Laakso, H., Aalto, P. P., Keronen, P., Siivola, E., Kerminen, V.-M., Kulmala, M., and Laakso, L.: Transportable aerosol characterization trailer with trace gas chemistry: design, instruments and verification, Aerosol and Air Quality Research, 13, No. 2, 421-435, doi:10.4209/aaqr.2012.08.0207, 2013.

Roy, D., Lewis, P., and Justice, C.: Burned area mapping using multi-temporal moderate spatial resolution data—A bi-directional reflectance model-based expectation approach, Remote Sensing of Environment, 83, 263-286, 2002.

Roy, D., Frost, P., Justice, C., Landmann, T., Le Roux, J., Gumbo, K., Makungwa, S., Dunham, K., Du Toit, R., and Mhwandagara, K.: The Southern Africa Fire Network (SAFNet) regional burned-area product-validation protocol, International Journal of Remote Sensing, 26, 4265-4292, 2005.

Roy, D. P., Boschetti, L., Justice, C. O., and Ju, J.: The collection 5 MODIS burned area product—Global evaluation by comparison with the MODIS active fire product, Remote Sensing of Environment, 112, 3690-3707, 2008.

Schultz, M. G., Schröder, S., Lyapina, O., Cooper, O., Galbally, I., Petropavlovskikh, I., von Schneidemesser, E., Tanimoto, H., Elshorbany, Y., and Naja, M.: Tropospheric Ozone Assessment Report: Database and metrics data of global surface ozone observations, Elem Sci Anth, 5, doi:http://doi.org/10.1525/elementa.244, 2017.

Sillman, S.: The relation between ozone, $NO_x$ and hydrocarbons in urban and polluted rural environments, Atmospheric Environment, 33, 1821-1845, doi:http://dx.doi.org/10.1016/S1352-2310(98)00345-8, 1999.

Simpson, I. J., Akagi, S., Barletta, B., Blake, N., Choi, Y., Diskin, G., Fried, A., Fuelberg, H., Meinardi, S., and Rowland, F.: Boreal forest fire emissions in fresh Canadian smoke plumes: C1-C10 volatile organic compounds (VOCs), $CO_2$, CO, $NO_2$, NO, HCN and $CH_3CN$, Atmospheric Chemistry and Physics, 11, 6445-6463, 2011.

Stauffer, R. M., Thompson, A. M., Oltmans, S. J., and Johnson, B. J.: Tropospheric ozonesonde profiles at long-term US monitoring sites: 2. Links between Trinidad Head, CA, profile clusters and inland surface ozone measurements, Journal of Geophysical Research: Atmospheres, 122, 1261-1280, 2017.

Stein, A. F., Draxler, R. R., Rolph, G. D., Stunder, B. J. B., Cohen, M. D., and Ngan, F.: NOAA's HYSPLIT atmospheric transport and dispersion modeling system, Bulletin of the American Meteorological Society, 96, 2059-2077, doi:10.1175/bams-d-14-00110.1, 2015.

Swap, R. J., Annegarn, H. J., Suttles, J. T., King, M. D., Platnick, S., Privette, J. L., and Scholes, R. J.: Africa burning: A thematic analysis of the Southern African Regional Science Initiative (SAFARI 2000), Journal of Geophysical Research: Atmospheres, 108, doi:10.1029/2003JD003747, 2003.

Thompson, A. M.: The oxidizing capacity of the Earth's atmosphere: Probable past and future changes, Science, 256, 1157-1165, 1992.

Thompson, A. M.: Biomass burning and the atmosphere—accomplishments and research opportunities, Atmospheric Environment, 30, i-ii, doi:https://doi.org/10.1016/S1352-2310(96)90021-7, 1996.

Thompson, A. M., Balashov, N. V., Witte, J. C., Coetzee, J. G. R., Thouret, V., and Posny, F.: Tropospheric ozone increases over the southern Africa region: bellwether for rapid growth in Southern Hemisphere pollution?, Atmospheric Chemistry and Physics, 14, 9855-9869, doi:10.5194/acp-14-9855-2014, 2014.

Thompson, A. M., Stauffer, R. M., Miller, S. K., Martins, D. K., Joseph, E., Weinheimer, A. J., and Diskin, G. S.: Ozone profiles in the Baltimore-Washington region (2006–2011): satellite comparisons and DISCOVER-AQ observations, Journal of Atmospheric Chemistry, 72, 393-422, 2015.

Tiitta, P., Vakkari, V., Croteau, P., Beukes, J. P., van Zyl, P. G., Josipovic, M., Venter, A. D., Jaars, K., Pienaar, J. J., Ng, N. L., Canagaratna, M. R., Jayne, J. T., Kerminen, V. M., Kokkola, H., Kulmala, M., Laaksonen, A., Worsnop, D. R., and Laakso, L.: Chemical composition, main sources and temporal variability of $PM_1$ aerosols in southern African grassland, Atmospheric Chemistry and Physics, 14, 1909-1927, doi:10.5194/acp-14-1909-2014, 2014.

Tyson, P. D., and Preston-Whyte, R. A.: The weather and climate of southern Africa, 2nd ed., xii, 396 pages pp., 2000.

Vakkari, V., Laakso, H., Kulmala, M., Laaksonen, A., Mabaso, D., Molefe, M., Kgabi, N., and Laakso, L.: New particle formation events in semi-clean South African savannah, Atmospheric Chemistry and Physics, 11, 3333-3346, doi:10.5194/acp-11-3333-2011, 2011.

Vakkari, V., Beukes, J. P., Laakso, H., Mabaso, D., Pienaar, J. J., Kulmala, M., and Laakso, L.: Long-term observations of aerosol size distributions in semi-clean and polluted savannah in South Africa, Atmospheric Chemistry and Physics, 13, 1751-1770, doi:10.5194/acp-13-1751-2013, 2013.

Vakkari, V., Kerminen, V.-M., Beukes, J. P., Tiitta, P., van Zyl, P. G., Josipovic, M., Venter, A. D., Jaars, K., Worsnop, D. R., Kulmala, M., and Laakso, L.: Rapid changes in biomass burning aerosols by atmospheric oxidation, Geophysical Research Letters, 41, 2644-2651, doi:10.1002/2014GL059396, 2014.

Venter, A. D., Vakkari, V., Beukes, J. P., Van Zyl, P. G., Laakso, H., Mabaso, D., Tiitta, P., Josipovic, M., Kulmala, M., Pienaar, J. J., and Laakso, L.: An air quality assessment in the industrialised western Bushveld Igneous Complex, South Africa, South African Journal of Science, doi:10.4102/sajs.v108i9/10.1059, 2012.

Venter, A. D., van Zyl, P. G., Beukes, J. P., Josipovic, M., Hendriks, J., Vakkari, V., and Laakso, L.: Atmospheric trace metals measured at a regional background site (Welgegund) in South Africa, Atmospheric Chemistry and Physics, 17, 4251-4263, doi:10.5194/acp-17-4251-2017, 2017.

Vingarzan, R.: A review of surface ozone background levels and trends, Atmospheric Environment, 38, 3431-3442, doi:https://doi.org/10.1016/j.atmosenv.2004.03.030, 2004.

Wang, Y., Logan, J. A., and Jacob, D. J.: Global simulation of tropospheric $O_3$-$NO_x$-hydrocarbon chemistry: 2. Model evaluation and global ozone budget, Journal of Geophysical Research: Atmospheres, 103, 10727-10755, doi:doi:10.1029/98JD00157, 1998.

Wells, R., Lloyd, S., and Turner, C.: National air pollution source inventory, Air pollution and its impacts on the South African Highveld. Johannesburg: Environmental Scientific Association, 3-9, 1996.

Yorks, J. E., Thompson, A. M., Joseph, E., and Miller, S. K.: The variability of free tropospheric ozone over Beltsville, Maryland (39N, 77W) in the summers 2004–2007, Atmospheric Environment, 43, 1827-1838, 2009.

Zeng, G., Pyle, J., and Young, P.: Impact of climate change on tropospheric ozone and its global budgets, Atmospheric Chemistry and Physics, 8, 369-387, 2008.

Zhang, L., Jacob, D. J., Yue, X., Downey, N. V., Wood, D. A., and Blewitt, D.: Sources contributing to background surface ozone in the US Intermountain West, Atmos. Chem. Phys., 14, 5295-5309, doi:10.5194/acp-14-5295-2014, 2014.

Zunckel, M., Venjonoka, K., Pienaar, J. J., Brunke, E. G., Pretorius, O., Koosialee, A., Raghunandan, A., and van Tienhoven, A. M.: Surface ozone over southern Africa: synthesis of monitoring results during the Cross Border Air Pollution Impact Assessment project, Atmospheric Environment, 38, 6139-6147, doi:https://doi.org/10.1016/j.atmosenv.2004.07.029, 2004.

Zunckel, M., Koosailee, A., Yarwood, G., Maure, G., Venjonoka, K., van Tienhoven, A. M., and Otter, L.: Modelled surface ozone over southern Africa during the Cross Border Air Pollution Impact Assessment project, Environmental Modelling & Software, 21, 911-924, doi:https://doi.org/10.1016/j.envsoft.2005.04.004, 2006.

## Appendix A

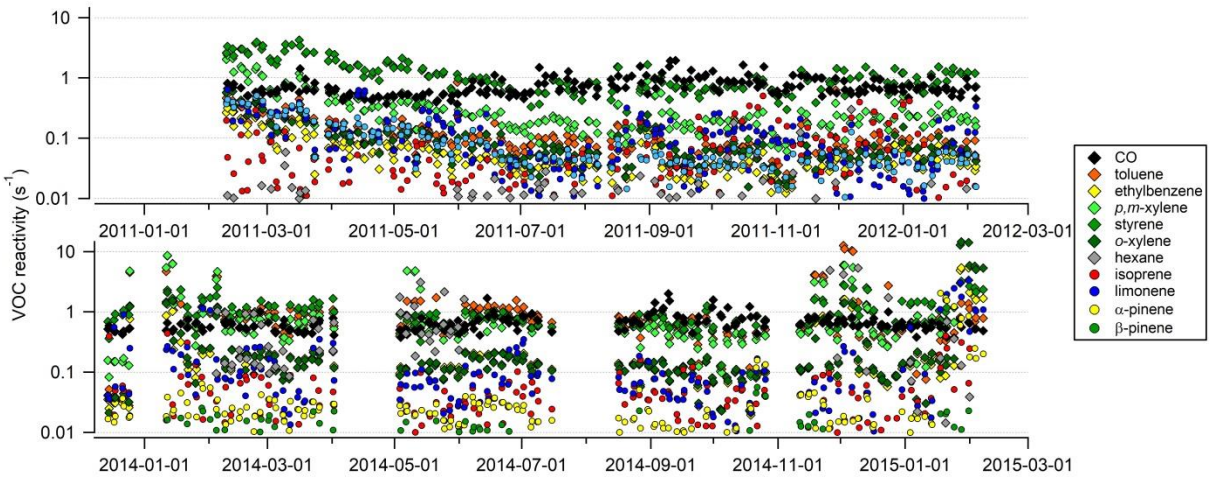


**Fig. A1.** Individual VOC reactivity time series. In the calculation of instantaneous $O_3$ production ($P(O_3)$), CO was treated as a VOC.

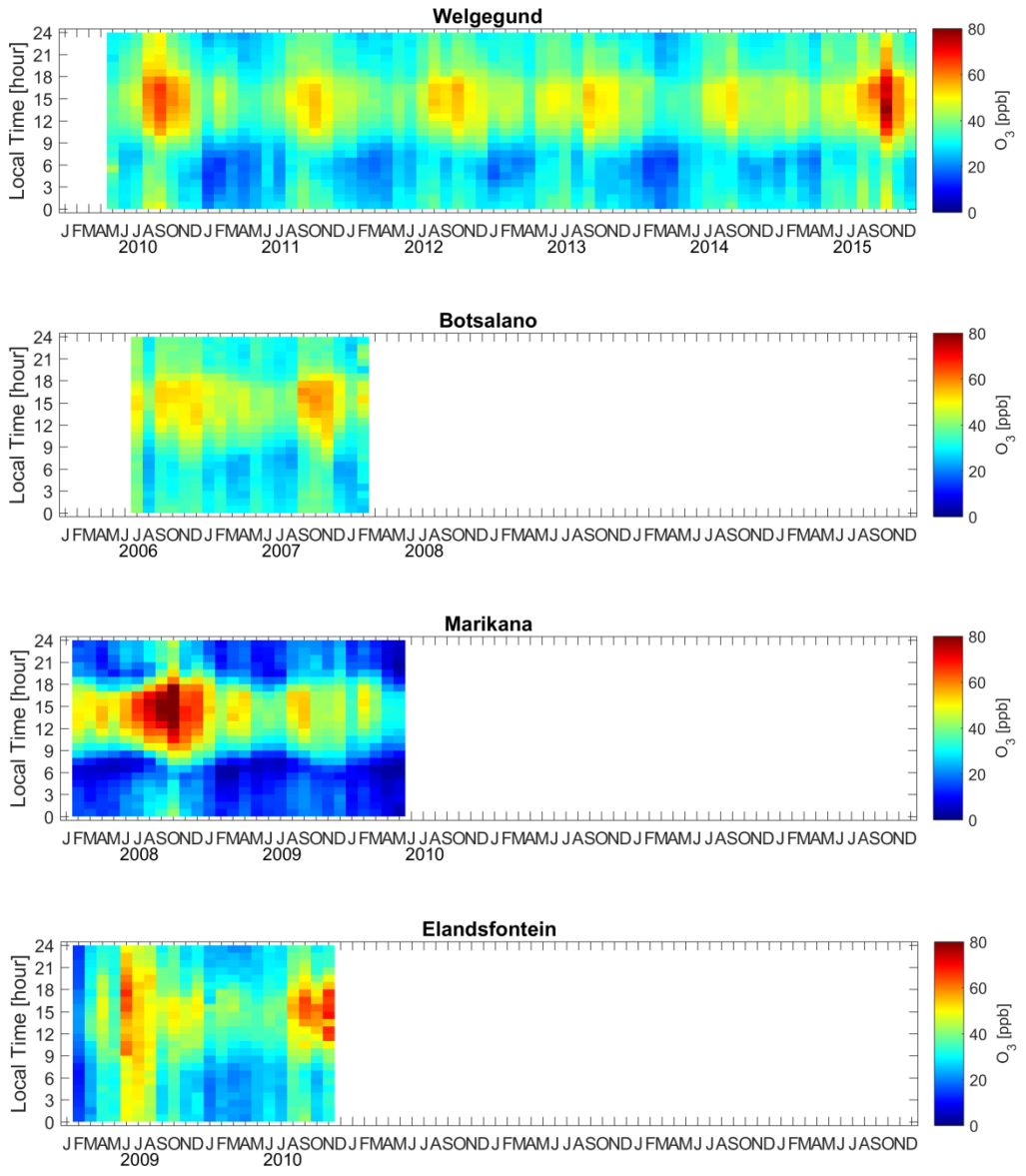


**Fig. A2.** Time series of monthly median $O_3$ concentrations for each hour of the day at the four sites.

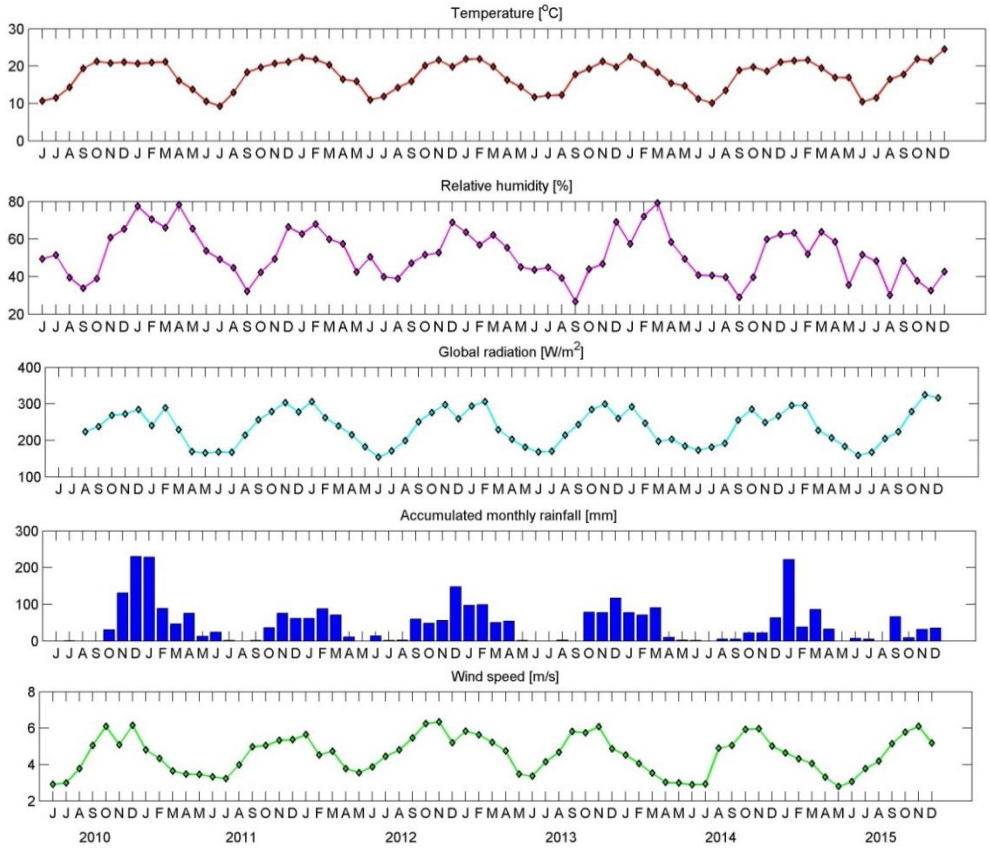


**Fig. A3.** Monthly averages of meteorological parameters at Welgegund to show typical seasonal patterns in continental South Africa. In the case of rainfall, the total monthly rainfall values are shown.

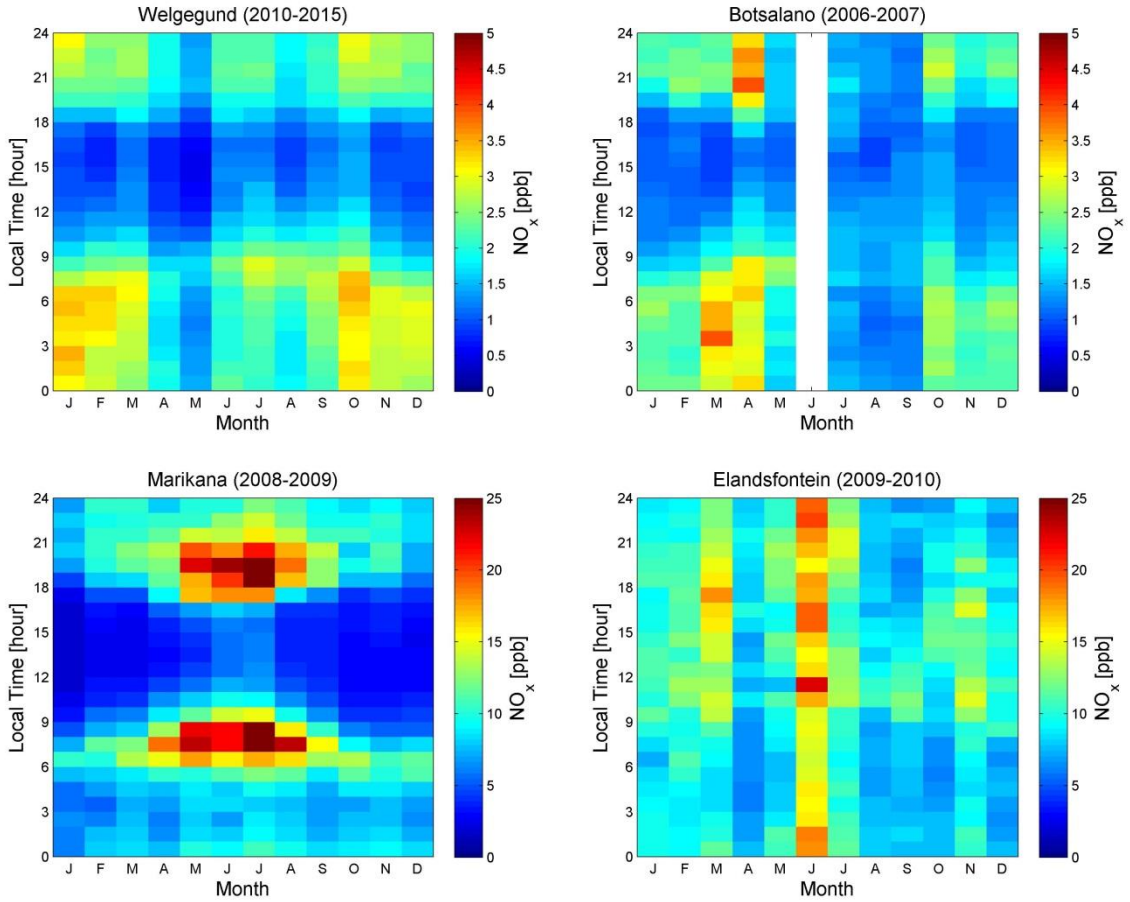


**Fig. A4.** Seasonal and diurnal variation of $NO_x$ at Welgegund, Botsalano, Marikana and Elandsfontein (median values of $NO_x$ concentration were used).

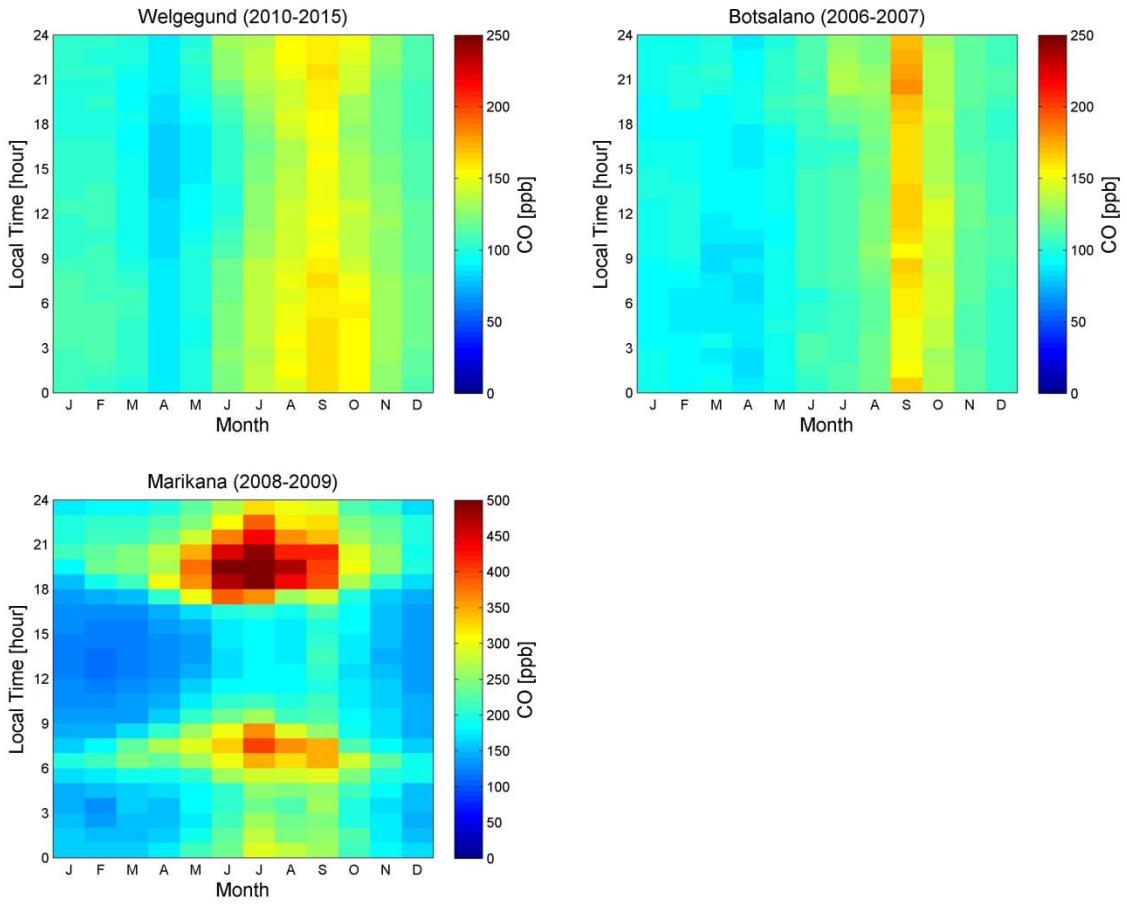


**Fig. A5.** Seasonal and diurnal variation of CO at Welgegund, Botsalano and Marikana (median values of CO concentration were used). Note that CO was not measured at Elandsfontein.

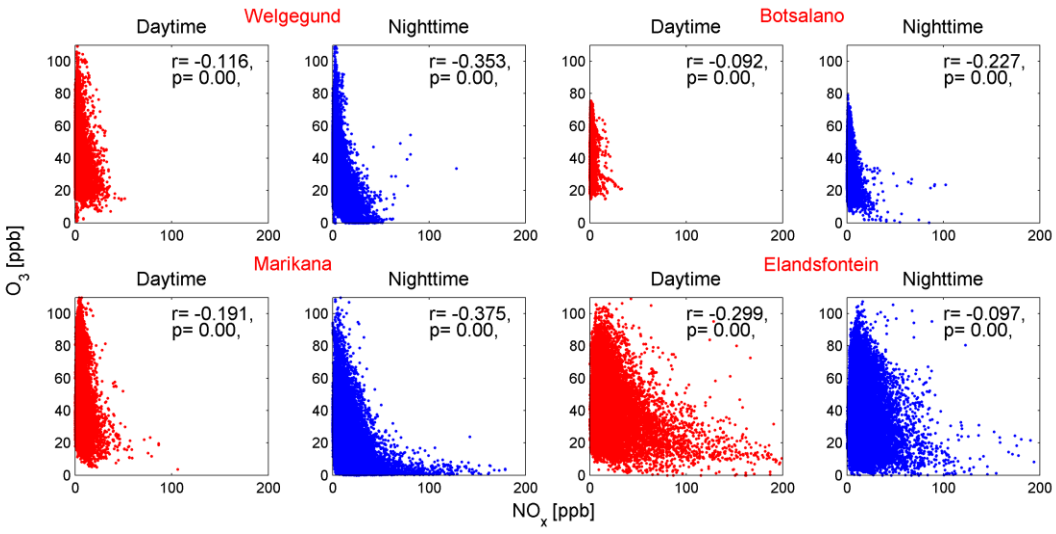


**Fig. A6.** Scatter plots of $O_3$ vs. $NO_x$ for daytime (9:00 a.m. to 4:52 p.m.), and night-time (5:00 p.m. to 8:52 a.m.) at Welgegund, Botsalano and Marikana and Elandsfontein. The correlation coefficient (r) has a significance level of $p < 10^{-10}$, which means that r is statistically significant ($p < 0.01$).

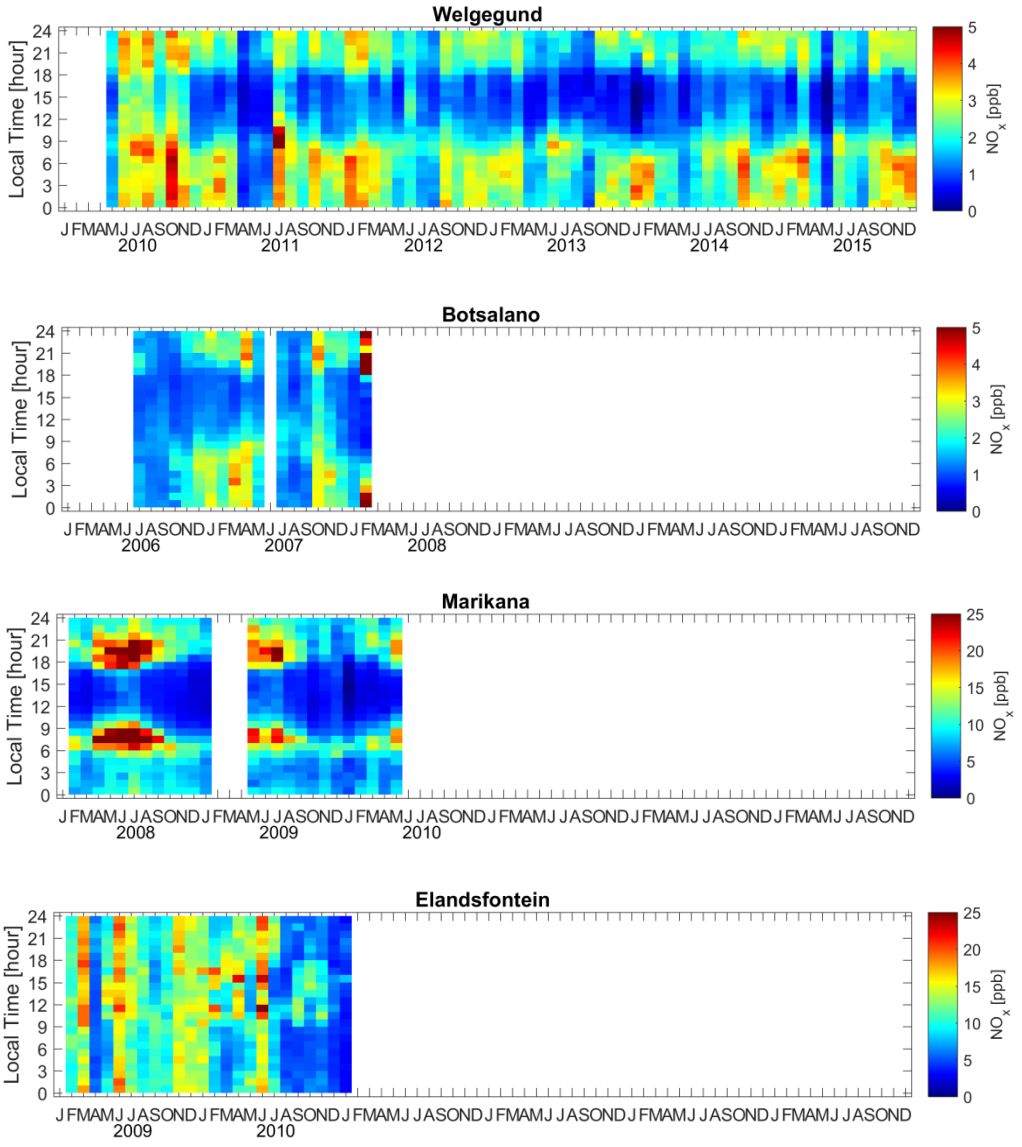


**Fig. A7.** Time series of monthly median $NO_x$ concentrations for each hour of the day at the four sites.

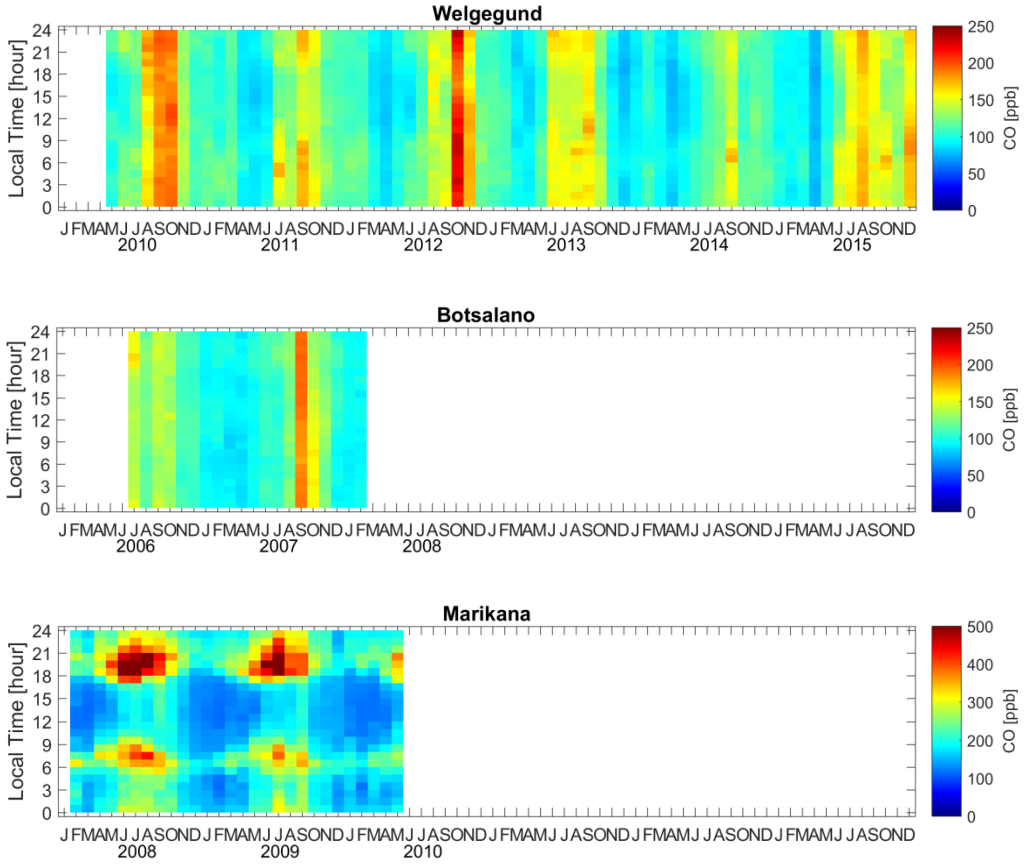


**Fig. A8.** Time series of monthly median CO concentrations for each hour of the day at the four sites.

# CHAPTER 5

# STATISTICAL ANALYSIS OF FACTORS DRIVING SURFACE OZONE VARIABILITY OVER CONTINENTAL SOUTH AFRICA

## 5.1 AUTHOR LIST, CONTRIBUTIONS AND CONSENT

**Tracey Leah Laban[1], Pieter Gideon van Zyl[1], Johan Paul Beukes[1], Santtu Mikkonen[2], Leonard Santana[3], Miroslav Josipovic[1], Ville Vakkari[4], Anne M. Thompson[5], Markku Kulmala[6], and Lauri Laakso[4]**

[1]Unit for Environmental Sciences and Management, North-West University, Potchefstroom, South Africa

[2]Department of Applied Physics, University of Eastern Finland, Kuopio, Finland

[3]School of Mathematical and Statistical Sciences, North-West University, Potchefstroom Campus, South Africa

[4]Finnish Meteorological Institute, Helsinki, Finland

[5]NASA/Goddard Space Flight Center, Greenbelt, Maryland, USA

[6]Department of Physics, University of Helsinki, Finland

The majority of the work was done by the first author, **T.L. Laban** who was responsible for the data processing, analysis, interpretation and writing of the manuscript. Contributions of the various co-authors were as follows: P.G. van Zyl and J.P. Beukes who were the promoters of this study assisted with data interpretation and editing the text of the manuscript. S. Mikkonen and L. Santana provided important feedback on the statistical methods employed and assisted with critical revision of the manuscript. M. Josipovic assisted with the data collection at the Welgegund measurement station. V. Vakkari and L. Laakso helped create the infrastructure at Welgegund. A.M. Thompson and M. Kulmala made conceptual contributions to the study.

All the co-authors on the article have been informed that the PhD will be submitted in article format and have given their consent.

## 5.2 FORMATTING AND CURRENT STATUS OF ARTICLE

The article was formatted in accordance with the journal specifications to which it will be submitted, i.e. *Atmospheric Environment*. The article is presented in the style, format and length required by the journal. The author's guide that was followed in preparation of the article was available at https://www.elsevier.com/journals/atmospheric-environment/1352-2310/guide-for-authors (Date of access: 25 May 2018). At the time when this PhD was submitted for examination, this article had not yet been submitted for review, but the intention is to submit it soon thereafter.

# Statistical analysis of factors driving surface ozone variability over continental South Africa

**Tracey Leah Laban[1], Pieter Gideon van Zyl[1*], Johan Paul Beukes[1], Santtu Mikkonen[2], Leonard Santana[3], Miroslav Josipovic[1], Ville Vakkari[4], Anne M. Thompson[5], Markku Kulmala[6], and Lauri Laakso[4]**

1 Unit for Environmental Sciences and Management, North-West University, Potchefstroom Campus, South Africa

2 Department of Applied Physics, University of Eastern Finland, Kuopio, Finland

3 School of Mathematical and Statistical Sciences, North-West University, Potchefstroom Campus, South Africa

4 Finnish Meteorological Institute, Helsinki, Finland

5 NASA/Goddard Space Flight Center, Greenbelt, Maryland, USA

6 Department of Physics, University of Helsinki, Finland

*Correspondence to: P.G. van Zyl (pieter.vanzyl@nwu.ac.za)

## Abstract

Statistical relationships between surface ozone ($O_3$) concentration, precursor species and meteorological conditions in continental South Africa were examined in this paper. Data obtained from four measurement stations in north-eastern South Africa were statistically analysed. Three multivariate statistical methods were applied in the investigation, i.e. multiple linear regression (MLR) to study linear dependencies, principal component analysis (PCA) to remove multicollinearity among independent variables, and generalised additive model (GAM) analysis to investigate non-linear relationships between $O_3$ and factors possibly influencing $O_3$ levels. MLR models indicated that meteorology and precursor species concentrations are able to explain ~50% of the variability in daily maximum $O_3$ levels. MLR analysis revealed that atmospheric carbon monoxide (CO) was the strongest factor affecting the daily $O_3$ variability, followed by temperature and/or relative humidity. In summer, daily $O_3$ variances were mostly associated with relative humidity, while winter $O_3$ levels were mostly linked to temperature. PCA indicated that CO, temperature and relative humidity were not strongly collinear. GAM also identified CO, temperature and relative humidity as the strongest factors affecting the daily

variation of $O_3$. Partial residual plots found that temperature, radiation and nitrogen oxides most likely have a non-linear relationship with $O_3$, while the relationship with relative humidity and CO is probably linear. An inter-comparison between $O_3$ levels modelled with the three statistical models compared to measured $O_3$ concentrations showed that the GAM model ($R^2$ values of 70-85%) offered a slight improvement over the MLR model. All three models were sensitive to the inclusion of the previous day's $O_3$ concentration as a variable. These findings emphasise the critical role of regional-scale $O_3$ precursors coupled with meteorological conditions in daily variances of $O_3$ levels in continental South Africa.

*Keywords:* tropospheric ozone ($O_3$), multiple linear regression, principal component analysis, generalised additive models, Welgegund

## 1. Introduction

High surface $O_3$ concentrations are a concern because of its detrimental impacts on human health and ecosystem functioning (NRC, 2008; IPCC, 2007). $O_3$ is a major respiratory irritant and exposure to high concentrations of $O_3$ has been linked to short-term mortality (Bell et al., 2004). The potential for $O_3$ damage to plants is, especially, a concern when agricultural yields are reduced, which threatens the food security and economies of countries that rely strongly on agricultural production. Additionally, surface $O_3$ acts as a 'greenhouse gas' due to its effects on radiative forcing (Ordonez et al., 2005), while tropospheric $O_3$ can also affect new particle formation in the atmosphere (e.g. Mikkonen et al., 2011). $O_3$ in the troposphere is produced by the photochemical oxidation of nitrogen oxides ($NO_x$ = NO + $NO_2$) in the presence of carbon monoxide (CO) and volatile organic compounds (VOCs) (Seinfeld and Pandis, 2006). However, high $O_3$ levels are not only a result of chemistry associated with precursor emissions, but are also related to meteorological conditions conducive to the formation, transport and removal of air pollutants (Melkonyan and Kuttler, 2012). Local meteorological parameters, such as temperature, relative humidity, sunlight, and wind speed and -direction play a significant role in $O_3$ variability (Ooka et al., 2011; Tsakiri and Zurbenko, 2011). These multiple factors influencing surface $O_3$ levels have confounded the effect of individual parameters on ground-level $O_3$, thereby making it challenging to separate the impacts of local emissions, meteorology and transport on surface $O_3$ concentrations (Gorai et al., 2015).

Statistical models relating ambient $O_3$ concentrations to meteorological variables have been developed for the purpose of the prediction of $O_3$ concentrations, the estimation of long-term $O_3$ trends, as well as explaining the underlying chemical and meteorological processes affecting $O_3$ concentrations (Thompson et al., 2001). Some of these statistical methods were critically reviewed by Thompson et al. (2001), which included regression-based methods (Ooka et al., 2011; Abdul-Wahab et al., 2005; Fiore et al., 1998), time-series filtering (Tsakiri and Zurbenko, 2011; Milanchus et al., 1998; Rao and Zurbenko, 1994), multivariate statistical techniques such as cluster analysis and principal component analysis (PCA) (Awang et al., 2015; Melkonyan and Kuttler, 2012; Dominick et al., 2012; Abdul-Wahab et al., 2005), as well as neural networks (Gardner and Dorling, 2000; Guardani et al., 2003; Gardner and Dorling, 1998; Comrie, 1997). The most widely used statistical technique to relate $O_3$ concentrations to influencing factors is linear regression, because of its user-friendliness and straightforward interpretability (Cardelino et al., 2001; Comrie, 1997). However, the relationship between $O_3$ levels and certain meteorological effects is typically non-linear, while some explanatory variables are collinear. Collinearity between predictor variables does not necessarily influence the output of the statistical model, but can be problematic if the purpose is to explain the influence of specific variables on the mean response (Neter et al., 1996).

Although non-linear regression models for $O_3$ forecasting have been developed (Thompson et al., 2001; Bloomfield et al., (1996); Lin and Cobourn, (2007), these models are difficult to interpret and explain in summarised form to the public (Pearce et al., 2011; Thompson et al., 2001). Neural network models are capable of dealing with non-linear associations and interactions between predictor variables. However, these models result in ‘black-box’ models that are also not easy to interpret or justify (Chaloulakou et al., 2003). Generalised additive models (GAM), which are an extension of linear regression, are also able to handle non-linear associations between atmospheric parameters by smoothing each of the simultaneous input variables using spline smoothing or weighted averaging (Hastie and Tibshirani, 1990). Melkonyan and Kuttler (2012) suggested that PCA is the most appropriate method to identify multivariate relationships between pollutants and meteorological factors. However, the interpretation of PCA results can also be difficult, particularly for relating trends to the original input variables contained within each principal component (Zou et al., 2006).

Southern Africa is the largest industrialised region in Africa, where high $O_3$ levels may be expected due to the high rate of precursor emissions from anthropogenic sources, coupled with

the abundance of sunlight throughout the year (Zunckel et al., 2006). In addition, this region is also influenced by large-scale open biomass burning, which is considered to be a significant source of $O_3$ precursor species. Laban et al. (2018) indicated that CO emissions associated with biomass burning (household combustion and open biomass burning) contributed significantly to high $O_3$ levels, while it was also indicated that large parts of the regional background in South Africa can be considered VOC-limited. The seasonal variation of $O_3$ in southern Africa is fairly well known, with concentrations tending to peak during late winter and spring months (Zunckel et al., 2004; Diab et al., 2004; Combrink et al., 1995). Although the temporal and spatial variability is generally attributed to meteorological conditions and/or precursor emissions, the response of $O_3$ with respect to changing emission levels and meteorological fluctuations is not well understood for this region (Laban et al., 2018). Therefore, the aim of this study was to utilise statistical models to distinguish the complex effects of meteorological parameters and precursor emissions influencing $O_3$ chemistry and concentrations in continental South Africa, as well as to quantify the strength of association of $O_3$ with these factors in order to better understand the underlying mechanisms responsible for the changes in surface $O_3$ levels in this region.

## 2. Material and methods

### 2.1 Description of the study area

Data from continuous *in-situ* measurements conducted at four measurement sites (indicated in Table 1) in the north-eastern interior of South Africa were obtained for statistical analysis. This region is the largest industrial area in South Africa, with substantial emissions of atmospheric pollutants from anthropogenic activities, e.g. industries, domestic fuel burning and vehicles (Lourens et al., 2012; Lourens et al., 2011). A combination of meteorology and anthropogenic activities has amplified pollution levels within the region. These four measurement stations represent high quality data and comprehensive measurements conducted at these sites have been utilised in several papers (Venter et al., 2017; Jaars et al., 2016; Jaars et al., 2014; Tiitta et al., 2014; Vakkari et al., 2013; Hirsikko et al., 2013; Laakso et al., 2012; Hirsikko et al., 2012; Venter et al., 2012; Vakkari et al., 2011; Laakso et al., 2008). Detailed descriptions of the locations of these measurement stations and their surroundings are provided in Laban et al. (2018).

**Table 1.** Measurement stations from which meteorological- and air pollutant data utilised for statistical analysis were obtained

| Measurement site | Latitude Longitude (decimal degrees) | Elevation (m) a.s.l. | Measurement period | Site description |
|---|---|---|---|---|
| Welgegund | 26.57° S 26.94° E | 1480 | May 2010-Dec 2015 | Rural, background |
| Botsalano | 25.54° S 25.75° E | 1420 | Jul 2006-Jan 2008 | Rural, background |
| Marikana | 25.70° S 27.48° E | 1170 | Feb 2008-Apr 2010 | Rural, residential, industrial |
| Elandsfontein | 26.25° S 29.42° E | 1750 | Feb 2009-Jan 2011 | Rural, industrial |

## 2.2 Data treatment

Respiratory symptoms have been found to be associated with the daily maximum of the eight-hour average $O_3$ concentration (Schlink et al., 2006). Therefore, the South African National Ambient Air Quality Standards and other international standards, designed to protect human health, are based on this metric. Consequently, the daily maximum 8-h moving average $O_3$ concentrations (daily max 8-h $O_3$) were utilised in the statistical analysis (dependent variable). The choice of input (independent) variables for the models was based on literature (Awang et al., 2015; Camalier et al., 2007; Ordonez et al., 2005; Abdul-Wahab et al., 2005; Dueñas et al., 2002), as well as exploratory analysis and a general understanding of $O_3$-related processes. Daytime (11:00-17:00 local time) daily average concentrations were calculated for $NO_2$, NO and CO, while daily mean values for zonal (u) wind component, meridional (v) wind component, relative humidity and solar radiation were determined. Daily maximum temperatures were included in models. Only daytime measurements were used in the statistical models, since the boundary layer is deep and well mixed during this period, as well as to exclude night-time chemistry (Cooper et al., 2012). Other variables such as soil moisture and precipitation, as well as $SO_2$- and $H_2S$ levels were also explored, but were found to have only a minor influence on daily max 8-h $O_3$. Since the $O_3$ data utilised in this study were normally distributed, it was not necessary to log-transform the original data to satisfy parametric test assumptions.

Exploratory descriptive statistics (calculation of mean, median, minimum, maximum and standard deviation) were employed prior to the statistical analyses in order to gain a general

understanding of meteorological $O_3$, $NO_x$ and CO variations at the measurement locations. Correlation coefficients were also calculated as a measure of the linear relationship between $O_3$ and each variable.

## 2.3 Statistical methods

Three different statistical methods, namely MLR, PCA and GAM were used to statistically evaluate the datasets. A separate model was built for each measurement site and used to investigate the influence of meteorological and precursor species (indicated in section 2.2.) variability on daily max 8-h $O_3$ at each site. The statistical calculations were performed using MATLAB version R2013a or R software environment (R Development Core Team, 2009).

### 2.3.1 Multiple linear regression (MLR)

Multiple linear regression modelling was used to relate $O_3$ concentrations (daily max 8-h $O_3$) to meteorological and pollutant factors, as well as the relative contribution of each of these factors. The general equation for an MLR model is given by

$$Y_i = \beta_0 + \beta_1 X_{i1} + \beta_2 X_{i2} + \ldots + \beta_p X_{ip} + \varepsilon_i \quad (1)$$

where $Y$ is the response variable, $X_1, X_2, \ldots, X_p$ are the independent variables, $\beta_1, \beta_2, \ldots, \beta_p$ are the regression coefficients, and $\varepsilon$ is an error term or residual value associated with deviation between the observed value of $Y$ and the predicted $Y$ value from the regression equation. The ordinary least squares procedure is the standard method to estimate the coefficients in the MLR equation. With this method, the regression procedure is based on finding coefficient values that minimise the sum of the squares of the residuals. A forward stepwise regression procedure was used in which each variable was added individually to the starting model according to their statistical significance and overall increase in the explanation capability of the model. This was done to remove the least important predictor variables and to obtain the optimal combination of variables depending on the statistical indices.

The strength of relationship between each independent variable and $O_3$ was evaluated in terms of the magnitude of the t-statistic and associated p-value for statistical significance. The performance of the model was evaluated with $R^2$, adjusted $R^2$ and root mean square error

(RMSE). The adjusted-$R^2$ is an $R^2$ measure that does not increase unless the new variables have additional predictive capability (unlike $R^2$ that increases when variables are added to the equation even when the new variables have no real predictive capability). The optimum MLR models considered had the largest $R^2$ and adjusted $R^2$, and smallest RMSE from a minimum number of independent variables. The main assumptions of the model are true underlying linearity, residuals are mutually independent with constant variance (homoscedasticity), and residuals are normally distributed (Ordonez et al., 2005). Multicollinearity in the regression model was verified by examining the variance inflation factor (VIF) for each of the predictor variables (Otero et al., 2016; Abdul-Wahab et al., 2005).

### 2.3.2 Principal component analysis (PCA) and -regression (PCR)

Parameters such as solar radiation, temperature and relative humidity are related properties, which could be inessential in MLR. PCA is a statistical procedure that uses an orthogonal transformation to convert a set of interrelated variables into a set of uncorrelated variables, i.e. principal components. Therefore, PCA is able to separate interrelationships (collinearity) into statistically independent basic components (Abdul-Wahab et al., 2005) and determine the most important uncorrelated variables. Each principal component is a linear combination of the original predictor variables that account for the variance in the data. All the principal components are orthogonal to each other, which implies that they are uncorrelated to each other. The first principal component is calculated such that it accounts for the highest possible variance in the dataset, followed by the concurrent components. Since the variables are measured in different units, it is necessary to standardise data before a principal component analysis is carried out, which involves scaling every variable to have a mean equal to 0 and a standard deviation equal to 1. The principal component model presents the $i^{th}$ principal component as a linear function of the p measured variables as expressed in Eq. (2) below:

$$Z_i = a_{i1}X_1 + a_{i2}X_2 + a_{i2}X_2 + \ldots + a_{ip}X_p \quad (2)$$

where *'Z'* is the principal component, *'a'* is the component loading, and *'X'* is the measured variable. The full set of principal components is as large as the original set of variables, but it is common for the sum of the variances of the first few principal components to exceed 80% of the total variance of the original data. By examining plots of these few new variables, researchers often develop a deeper understanding of the driving forces that generated the original data.

PCA was first applied to the original independent variables to transform these variables into an equal number of principal components. Only those principal components with an eigenvector greater than 1 were retained (according to the Kaiser criterion), which were then subjected to Varimax rotation to maximise the loading of a predictor variable on one component (Abdul-Wahab et al., 2005). Since the eigenvectors are the correlation of the component variables with the original variables, they comprise coefficients (loadings) that indicate the relative weight of each variable in the component, which is important, since they represent the extent of the correlation between the measured variable and the principal components. Variables that load highly on a specific principal component form a related group.

PCR is a combination of PCA and MLR (Awang et al., 2015), where the outputs from the PCA are used as potential predictors in order to improve the original MLR model (Awang et al., 2015; Abdul-Wahab et al., 2005). Either the original independent variables associated with each of the principal components with high loadings (Abdul-Wahab et al., 2005) or the principal components with high loadings (Awang et al., 2015) are selected to be included in the regression equation.

### 2.3.3 Generalised additive models (GAMs)

GAMs extend traditional linear models by allowing for an alternative distribution for the modelling of response variables that have a non-normal error distribution. In addition, GAMs do not force dependent variables to be linearly related to independent variables as in MLR, and recognise that the relationship of some explanatory variables (e.g. daily temperature) and the response variable (i.e. ozone in this study) may not be linear (Gardner and Dorling, 2000). In GAMs, the response variable depends additively on unknown smoothing functions of the individual predictors that can be (linear) parametric or non-parametric (Hastie and Tibshirani, 1990). The GAM model equation developed by Hastie and Tibshirani (1990) is given by

$$g\big(E(Y_i)\big) = \beta_0 + s_1(X_{i1}) + s_2(X_{i2}) + \ldots + s_p(X_{ip}) + \varepsilon_i \quad (3)$$

where $Y_i$ is the response variable, $E(Y_i)$ denotes the expected value and $g(\cdot)$ denotes the link function that links the expected value to the predictor variables $X_{i1}, \ldots, X_{ip}$, $\beta_0$ is an intercept and $\varepsilon_i$ is an i.i.d. random error. For the purposes of the analysis performed in this study, the link

function chosen was the identify transformation $g\big(E(Y_i)\big) = E(Y_i)$. The terms $s_1(\cdot), s_2(\cdot), \ldots, s_p(\cdot)$ are smooth functions that are estimated in a nonparametric fashion (Hastie and Tibshirani, 1990). We can estimate these smooth relationships simultaneously from the data and then predict $g(E(Y_i))$ by simply adding up these functions. The estimated smooth functions $s_k$ are the analogues of the coefficients $\beta_k$ in linear regression. In contrast to MLR, an additive regression is done by using a back-fitting procedure and thereby controlling the effects of the other predictors. GAM is able to identify covariates, $X_k$ relevant to $Y$ for a large set of potential factors (Hayn et al., 2009), while it does not require any prior knowledge on the underlying relationship between $Y$ and its covariates. The latter can be obtained through separate partial residual plots, which allow visualisation of the relationships between each variable $X_k$ and the response variable, $Y$, after accounting for the effects of the other explanatory variables in the model.

Smooth parameters were automatically selected in the 'mgcv' package (Wood, 2017) in the R software environment used in this study, which is based on maximum probability methods that minimise the Akaike information criterion (AIC) score. The AIC measures the goodness-of-fit of the model in such a manner that the final model selected has the smallest AIC. The models were also evaluated with $R^2$ values and generalised cross-validation (GCV) scores (estimate of the prediction error).

## 3. Results and discussion

### 3.1 Exploratory analysis

#### 3.1.1 Descriptive statistics

As indicated in section 2.2, descriptive statistics were performed prior to the statistical analyses in order to gain a general understanding of meteorological, $O_3$, $NO_x$ and CO variations at the measurement locations, which are presented in Table 2. It is evident that Elandsfontein and Marikana are the more polluted sites, as indicated by higher $NO_2$, NO and CO median values, whereas Botsalano had the lowest median values for $NO_2$, NO and CO. Note that $O_3$ concentrations are similar at all sites, even though Botsalano and Welgegund are considered regional background sites. The regional problem associated with $O_3$ in southern Africa was indicated by Laban et al. (2018). The large standard deviations of $NO_2$ and NO concentrations can be attributed to occasional high pollution events.

**Table 2.** Descriptive statistics of the daily summaries of the key variables used in the study

| | Time scale | Statistics | Welgegund | Botsalano | Marikana | Elandsfontein |
|---|---|---|---|---|---|---|
| $[O_3]$ | Daily 8-h max | Mean | 47 | 47 | 50 | 48 |
| ppb | | Median | 46 | 48 | 48 | 47 |
| | | Min | 8 | 21 | 14 | 11 |
| | | Max | 114 | 73 | 113 | 102 |
| | | Std Dev | 11 | 9 | 16 | 16 |
| $[NO_2]$ | Daily average | Mean | 2.0 | 1.5 | 5.7 | 13.2 |
| ppb | | Median | 1.4 | 1.3 | 4.8 | 10.8 |
| | | Min | -0.4 | 0.2 | 0.0 | 0.2 |
| | | Max | 21.2 | 11.4 | 20.9 | 68.3 |
| | | Std Dev | 1.9 | 1.0 | 3.3 | 9.7 |
| [NO] | Daily average | Mean | 0.4 | 0.3 | 2.8 | 4.5 |
| ppb | | Median | 0.2 | 0.2 | 1.6 | 2.6 |
| | | Min | -0.4 | -0.1 | -0.3 | 0.1 |
| | | Max | 6.9 | 5.3 | 52.8 | 42.5 |
| | | Std Dev | 0.7 | 0.4 | 3.8 | 5.4 |
| [CO] | Daily average | Mean | 126 | 118 | 197 | |
| ppb | | Median | 116 | 109 | 181 | |
| | | Min | 23 | 57 | 85 | |
| | | Max | 412 | 308 | 591 | |
| | | Std Dev | 45 | 35 | 68 | |
| Solar Radiation | Daily average | Mean | 508 | 508 | 462 | 522 |
| $W/m^2$ | | Median | 490 | 504 | 458 | 541 |
| | | Min | 14 | 31 | 24 | 3 |
| | | Max | 871 | 835 | 884 | 1005 |
| | | Std Dev | 154 | 137 | 146 | 156 |
| Temperature | Daily maximum | Mean | 24 | 25 | 26 | 21 |
| $^oC$ | | Median | 25 | 26 | 27 | 21 |
| | | Min | 5 | 8 | 10 | 6 |
| | | Max | 38 | 36 | 37 | 30 |
| | | Std Dev | 5 | 5 | 5 | 4 |
| Relative Humidity | Daily average | Mean | 42 | 40 | 49 | 52 |
| % | | Median | 40 | 38 | 48 | 53 |
| | | Min | 6 | 7 | 10 | 9 |
| | | Max | 100 | 95 | 100 | 96 |
| | | Std Dev | 18 | 19 | 18 | 18 |
| Zonal (u) wind | Daily average | Mean | 0.7 | -2.8 | 0.5 | 0.4 |
| component | | Median | 1.1 | -3.3 | 0.5 | 0.9 |
| (m/s) | | Min | -13.1 | -13.4 | -6.9 | -9.1 |
| | | Max | 12.9 | 10.0 | 8.0 | 8.7 |
| | | Std Dev | 3.6 | 3.9 | 2.4 | 3.2 |

| | Time scale | Statistics | Welgegund | Botsalano | Marikana | Elandsfontein |
|---|---|---|---|---|---|---|
| Meridional (v) wind component (m/s) | Daily average | Mean | -0.8 | -0.6 | -0.3 | -0.8 |
| | | Median | -0.8 | -0.6 | -0.2 | -0.7 |
| | | Min | -10.4 | -7.4 | -5.7 | -10.0 |
| | | Max | 10.9 | 6.3 | 5.9 | 5.2 |
| | | Std Dev | 2.7 | 1.9 | 1.4 | 2.4 |

### 3.1.2 Calculation of correlation coefficients

In Table 3, Pearson correlation coefficients (r) relating $O_3$ concentration with individual atmospheric parameters at the four measurement locations are presented. It is evident that $O_3$ has a positive correlation with temperature and global radiation, while it is negatively correlated with relative humidity. A relatively strong positive correlation with CO was observed, with $NO_2$ and NO correlations with $O_3$ almost negligible due to the time scale. The correlations with u and v wind components are also weak, as given by their low correlation coefficients. Exploratory Pearson correlations indicate that variability in $O_3$ levels is in general associated (positively or negatively) with CO ($r(O_3,CO)$ = 0.3 to 0.6), relative humidity ($r(O_3, RH)$ = -0.2 to -0.5) and temperature ($r(O_3, T)$ = 0.2 to 0.5). The significance of CO on $O_3$ levels at these sites was indicated by Laban et al. (2018). The relative significance of CO, relative humidity and temperature highlighted with these correlations is further explored in subsequent sections through more advanced statistical methods, as indicated in section 2.3.

**Table 3.** Pearson correlation coefficient (r) for the different variables with their associated p-values (P) for data from the four sites

| | | Daily 8-h max $O_3$ (ppb) | | | |
|---|---|---|---|---|---|
| | | **Welgegund** | **Botsalano** | **Marikana** | **Elandsfontein** |
| Daily average $NO_2$ (ppb) | **r** | 0.113 | 0.061 | 0.128 | -0.096 |
| | **P** | 0.000 | 0.197 | 0.001 | 0.018 |
| Daily average NO (ppb) | **r** | -0.077 | -0.141 | -0.026 | -0.211 |
| | **P** | 0.001 | 0.003 | 0.508 | 0.000 |
| Daily average CO (ppb) | **r** | 0.554 | 0.543 | 0.330 | |
| | **P** | 0.000 | 0.000 | 0.000 | |
| Daily average radiation ($W/m^2$) | **r** | 0.204 | 0.324 | 0.290 | 0.237 |
| | **P** | 0.000 | 0.000 | 0.000 | 0.000 |
| Daily maximum temp ($^oC$) | **r** | 0.374 | 0.518 | 0.434 | 0.207 |
| | **P** | 0.000 | 0.000 | 0.000 | 0.000 |
| Daily average relative humidity (%) | **r** | -0.428 | -0.242 | -0.486 | -0.451 |
| | **P** | 0.000 | 0.000 | 0.000 | 0.000 |
| Zonal (u) wind component (m/s) | **r** | -0.002 | -0.094 | 0.074 | 0.079 |
| | **P** | 0.921 | 0.033 | 0.042 | 0.052 |
| Meridional (v) wind component (m/s) | **r** | -0.167 | -0.253 | -0.083 | -0.070 |
| | **P** | 0.000 | 0.000 | 0.023 | 0.085 |

## 3.2 Multiple linear regression analysis

A summary of the contributions of independent variables to variation of the dependent variable (daily max 8-h $O_3$) included in the optimum MLR models obtained for each of the measurement sites is presented in Table 4. VIF values ranging between 1.00 and 2.00 for all the independent variables indicated moderate collinearity, which did not contribute to unstable parameter estimates or the necessity to remove any independent variables from the models. Regression analysis explained approximately 50% of the variability ($R^2 \approx 0.5$) of daily max 8-h $O_3$ concentrations at Welgegund, Botsalano and Marikana, with lower $R^2$ (0.261) at Elandsfontein attributed to CO not measured at this site and not included in the MLR.

From Table 4, it is evident that CO, T and RH make the most significant contributions to the variance in daily max 8-h $O_3$ at all the sites as indicated by the magnitude of the t-statistics. Notable contributions are also made by NO levels at Welgegund and Elandsfontein. A positive regression coefficient associated with temperature is expected due to the photochemical production of $O_3$. In addition, evaporative emissions of anthropogenic VOCs increase at high temperatures (Ordonez et al., 2005), which could favour $O_3$ formation. Relative humidity had a negative regression coefficient and a significant t-statistic at three of the sites, which indicate that low relative humidity is associated with high daily max 8-h $O_3$. This influence of relative humidity on $O_3$ variances suggests that atmospheric wet conditions can affect $O_3$ production and loss, which will be explored later in this paper. Surprisingly, the contribution of relative humidity to $O_3$ variation was similar to that of temperature at Welgegund, while it had the most significant contribution at Elandsfontein (in the absence of any CO measurements). CO levels have the highest contribution to variations in daily max 8-h $O_3$ at Welgegund and Botsalano, i.e. the two regional background sites, while it had the second highest contribution at the industrialised Marikana site. Laban et al. (2018) indicated that CO emissions associated with regional open biomass burning, as well as household combustion for space heating and cooking, contributed significantly to $O_3$ levels in the interior of southern Africa. Negative regression coefficients associated with NO at Welgegund and Elandsfontein can be attributed to $O_3$ titration in the presence of high NO levels.

**Table 4.** Summary of the optimum MLR models for each site showing the individual variable contributions to daily max 8-h $O_3$

| **WELGEGUND** | **Constant** | **T ($^oC$)** | **RH (%)** | **u (m/s)** | **v (m/s)** | **NO (ppb)** | **CO (ppb)** |
|---|---|---|---|---|---|---|---|
| Regression coefficient (β) | 29.31 | 0.41 | -0.17 | -0.28 | 0.11 | -2.99 | 0.12 |
| Standard error | 1.17 | 0.03 | 0.01 | 0.06 | 0.06 | 0.27 | 0.00 |
| t-statistic | 25.10 | 11.71 | -16.44 | -5.00 | 1.74 | -11.23 | 29.87 |
| P-value | 4.61E-119 | 1.45E-30 | 1.41E-56 | 6.20E-07 | 0.082156854 | 2.60E-28 | 5.85E-159 |
| **$R^2$=0.529** | **Adjusted $R^2$=0.528** | | **RMSE=6.75** | | **F-statistic=330** | | |
| **BOTSALANO** | **Constant** | **T ($^oC$)** | **Rad ($W/m^2$)** | **CO (ppb)** | | | |
| Regression coefficient (β) | 8.03 | 0.69 | 0.01 | 0.14 | | | |
| Standard error | 1.72 | 0.08 | 0.00 | 0.01 | | | |
| t-statistic | 4.67 | 8.65 | 2.91 | 16.17 | | | |
| P-value | 3.86E-06 | 7.34E-17 | 0.003734848 | 2.03E-47 | | | |
| **$R^2$=0.531** | **Adjusted $R^2$=0.528** | | **RMSE=6.41** | | **F-statistic=184** | | |
| **MARIKANA** | **Constant** | **T ($^oC$)** | **RH (%)** | **u (m/s)** | **NO (ppb)** | **CO (ppb)** | |
| Regression coefficient (β) | 8.92 | 1.45 | -0.25 | -0.83 | -0.57 | 0.09 | |
| Standard error | 4.98 | 0.12 | 0.03 | 0.23 | 0.15 | 0.01 | |
| t-statistic | 1.79 | 12.58 | -7.53 | -3.68 | -3.87 | 10.46 | |
| P-value | 7.35E-02 | 1.66E-32 | 1.73E-13 | 2.58E-04 | 0.000121169 | 1.07E-23 | |
| **$R^2$=0.454** | **Adjusted $R^2$=0.449** | | **RMSE=12.46** | | **F-statistic=104** | | |
| **ELANDSFONTEIN** | **Constant** | **RH (%)** | **v (m/s)** | **NO (ppb)** | | | |
| Regression coefficient (β) | 71.25 | -0.39 | -0.64 | -0.67 | | | |
| Standard error | 1.73 | 0.03 | 0.23 | 0.10 | | | |
| t-statistic | 41.16 | -12.90 | -2.79 | -6.54 | | | |
| P-value | 4.20E-176 | 9.66E-34 | 5.47E-03 | 1.29E-10 | | | |
| **$R^2$=0.261** | **Adjusted $R^2$=0.257** | | **RMSE=13.56** | | **F-statistic=70** | | |

where T is daily maximum temperature, Rad is daily average global radiation, RH is daily average relative humidity, u is the zonal (east-west) wind component, v is the meridional (north-south) wind component, $NO_2$ is the daily average $NO_2$ concentration, NO is the daily average NO concentration and CO is the daily average CO concentration.

Since $O_3$ has strong seasonal variation, MLR analysis was also performed for each season: winter (JJA), spring (SON), summer (DJF) and autumn (MAM) in order to evaluate the major factors driving $O_3$ variability during different seasons. Maximum $O_3$ concentrations generally occur in late winter and spring (August-November) for continental southern Africa (Zunckel et al., 2004; Diab et al., 2004; Combrink et al., 1995). In Table 5, the independent variables with the most significant contributions (i.e. highest t-statistic values in the optimum model) to $O_3$ variability for different seasons are presented for each site.

**Table 5.** Most important explanatory variables for daily max 8-h $O_3$ for each season (ranked in decreasing order of importance as given by the magnitude of their t-statistic)

| | **Summer** | **Autumn** | **Winter** | **Spring** |
|---|---|---|---|---|
| **WELGEGUND** | NO<br>$NO_2$<br>RH<br>CO<br>Rad | CO<br>RH<br>NO<br>T | CO<br>NO<br>T<br>u | CO<br>NO<br>T<br>v<br>RH |
| **BOTSALANO** | CO<br>RH | CO<br>T | CO<br>T<br>RH | CO<br>NO<br>Rad<br>T |
| **MARIKANA** | RH<br>$NO_2$<br>NO<br>v | $NO_2$<br>NO<br>RH<br>T<br>u<br>v | T<br>CO | CO<br>T |
| **ELANDSFONTEIN** | T | T<br>NO<br>RH | NO<br>$NO_2$<br>T | T<br>$NO_2$<br>Rad |

CO makes the highest contribution to the variance in daily max 8-h $O_3$ during all the seasons at Botsalano, during autumn, winter and spring at Welgegund, as well as during spring (second highest in winter) at Marikana, which signifies the influence of CO levels on $O_3$ concentrations in continental South Africa. The seasonal pattern of CO is also reflected in the seasonal variations of contributing factors to $O_3$ variability as indicated by a less important influence of CO levels on the variance in $O_3$ during summer at Welgegund and Marikana. Increased CO emissions in this region are associated with increased household combustion and open biomass burning during

winter and spring (Laban et al., 2018). This is also indicated by increased contributions of NO and $NO_2$ to $O_3$ variances at Welgegund and Marikana during summer, i.e. increased $O_3$ titration/formation mainly associated with NO and $NO_2$ levels. CO has the highest influence on variation $O_3$ throughout the year at Botsalano, which can be ascribed to the site being more removed from source regions compared to Welgegund. The important influence of relative humidity $O_3$ levels is also apparent, as indicated by increases in its contribution to $O_3$ variances during months coinciding with the wet season, i.e. mid-October to mid-May (mostly summer and autumn). The wet season is also characterised by lower concentrations of air pollutants (and $O_3$ precursors) due to wet deposition. Daily maximum temperature remains an important contributor to variance in daily max 8-h $O_3$, except during summer at Welgegund, Botsalano and Marikana. This can be attributed to relatively constant higher temperatures occurring during summer, with $O_3$ variability associated with other influencing factors, e.g. relative humidity. In the absence of CO measurements at Elandsfontein, daily maximum temperature contributes most significantly to $O_3$ variability at Elandsfontein on a seasonal scale, which can be attributed to the influence of temperature on the vertical mixing of tall stack emissions of power plants (Ordonez et al., 2005). The highest contribution of NO on $O_3$ variance at Elandsfontein in winter can be attributed to more pronounced inversion layers, as well as increased household combustion for space heating and cooking.

### 3.3 Principal component analysis (PCA)

PCA revealed four principal components (factors) with eigenvalues greater than 1 at each of the sites, which explained approximately 80% of the variation in the data. These factors (labelled PC1, PC2, PC3 and PC4) were subjected to Varimax rotation, which are presented with their respective loadings, eigenvalues and variances in Table 6. Factor loadings $\geq$ 0.5 (or close to 0.5) were considered significant, i.e. strongly correlated within each principal component.

**Table 6.** Factor loadings after PCA Varimax rotation at the four measurement sites. Loadings ≥ 0.5 (or close to 0.5) are indicated in bold

| **Welgegund** | **Rotated principal component loadings** | | | |
|---|---|---|---|---|
| | **PC1** | **PC2** | **PC3** | **PC4** |
| T ($^{o}$C) | -0.060 | **0.640** | -0.215 | -0.012 |
| Rad (W/m$^2$) | 0.060 | **0.728** | 0.166 | -0.031 |
| RH (%) | -0.132 | -0.076 | -0.035 | **0.755** |
| u (m/s) | -0.274 | -0.028 | 0.020 | **-0.549** |
| v (m/s) | 0.145 | -0.089 | **0.802** | -0.157 |
| $NO_2$ (ppb) | **0.637** | -0.093 | -0.052 | -0.020 |
| NO (ppb) | **0.545** | 0.167 | 0.188 | 0.179 |
| CO (ppb) | 0.420 | -0.101 | **-0.493** | -0.266 |
| | | | | |
| **Eigenvalue (variance)** | 2.260 | 1.620 | 1.230 | 1.379 |
| **Variance (%)** | 34.825 | 24.967 | 18.961 | 21.247 |
| **Cumulative variance (%)** | 34.825 | 59.792 | 78.753 | 100.000 |
| **Botsalano** | **Rotated principal component loadings** | | | |
| | **PC1** | **PC2** | **PC3** | **PC4** |
| T ($^{o}$C) | **-0.646** | -0.049 | -0.001 | 0.068 |
| Rad (W/m$^2$) | **-0.673** | -0.003 | 0.039 | -0.136 |
| RH (%) | 0.270 | **-0.540** | 0.066 | -0.404 |
| u (m/s) | 0.049 | **0.667** | -0.070 | -0.012 |
| v (m/s) | 0.177 | **0.506** | 0.185 | -0.300 |
| $NO_2$ (ppb) | 0.045 | -0.042 | **0.668** | 0.211 |
| NO (ppb) | -0.084 | 0.029 | **0.710** | -0.157 |
| CO (ppb) | 0.115 | -0.052 | 0.070 | **0.809** |
| | | | | |
| **Eigenvalue (variance)** | 1.701 | 1.746 | 1.802 | 1.328 |
| **Variance (%)** | 25.861 | 26.552 | 27.404 | 20.184 |
| **Cumulative variance (%)** | 25.861 | 52.412 | 79.816 | 100.000 |

5

**Table 6.** Continued

| **Marikana** | **Rotated principal component loadings** | | | |
|---|---|---|---|---|
| | **PC1** | **PC2** | **PC3** | **PC4** |
| T ($^{o}$C) | -0.110 | **-0.602** | -0.108 | 0.016 |
| Rad (W/m$^2$) | -0.089 | **-0.625** | 0.021 | -0.105 |
| RH (%) | -0.376 | 0.484 | -0.177 | -0.181 |
| u (m/s) | -0.039 | 0.037 | -0.020 | **0.973** |
| v (m/s) | -0.034 | 0.032 | **0.967** | -0.020 |
| $NO_2$ (ppb) | **0.563** | 0.096 | -0.001 | -0.063 |
| NO (ppb) | 0.439 | 0.034 | 0.070 | 0.057 |
| CO (ppb) | **0.571** | -0.011 | -0.130 | -0.048 |
| | | | | |
| **Eigenvalue (variance)** | 2.510 | 2.194 | 0.996 | 1.031 |
| **Variance (%)** | 37.288 | 32.600 | 14.791 | 15.322 |
| **Cumulative variance (%)** | 37.288 | 69.888 | 84.678 | 100.000 |
| **Elandsfontein** | **Rotated principal component loadings** | | | |
| | **PC1** | **PC2** | **PC3** | **PC4** |
| T ($^{o}$C) | **0.762** | 0.006 | -0.108 | 0.154 |
| Rad (W/m$^2$) | **0.616** | 0.004 | 0.103 | -0.236 |
| RH (%) | -0.083 | 0.034 | -0.067 | **0.802** |
| u (m/s) | -0.137 | 0.109 | **-0.580** | -0.439 |
| v (m/s) | -0.084 | 0.073 | **0.798** | -0.203 |
| $NO_2$ (ppb) | -0.049 | **0.651** | -0.001 | -0.130 |
| NO (ppb) | 0.066 | **0.747** | 0.011 | 0.161 |
| | | | | |
| **Eigenvalue (variance)** | 1.556 | 1.676 | 1.313 | 1.287 |
| **Variance (%)** | 26.674 | 28.738 | 22.517 | 22.072 |
| **Cumulative variance (%)** | 26.674 | 55.411 | 77.928 | 100.000 |

Similar factor loadings were determined for each of the four principal components identified for each site, i.e. a factor with high loadings of T and Rad, a factor with high loadings of NO and $NO_2$, a factor with a high loading of CO and a factor with a high loading of RH. At Elandsfontein, one factor was highly loaded with the wind direction vectors. Therefore, PCA indicated that the predominant factors identified by MLR driving variances in daily max 8-h $O_3$, i.e. CO, T and RH (as well as NO levels in certain instances) are not inter-correlated. Collinearity is expected between T and radiation, as well as NO and $NO_2$ as revealed by PCA. In addition, PC1 at Marikana with high loadings of CO and $NO_2$ (and NO) is indicative of the influence of household combustion at this site, as indicated by Venter et al. (2012). Furthermore, the correlation between $NO_2$, NO and CO at Welgegund in PC1 also reflects the influence of similar sources of

these species at Welgegund and signifies that Welgegund lies in a region between a $NO_x$- and VOC-limited $O_3$ production regime, as indicated by Laban et al. (2018). CO is also strongly correlated to meridional wind vector in PC3 at the regional background site Welgegund, which can be attributed the regional transport of CO emissions. Welgegund is influenced by the major source regions in the interior of South Africa and a relatively clean background sector to the west (Tiitta et al., 2014; Jaars et al., 2014). In addition, Welgegund is also impacted on by regional biomass burning, contributing to increased CO emissions (Vakkari et al., 2013). In contrast to Welgegund, CO at Botsalano is not correlated to NO and $NO_2$ and is the only major loading in PC4 at this site.

### 3.4 Generalised additive model (GAM) analysis

Given the complex and non-linear chemistry of $O_3$ (NRC, 1991), the datasets were also statistically analysed with GAM. A summary of the optimum (highest $R^2$ and lowest AIC) GAM models is shown in Table 7. According to the F-statistics of the optimum models obtained with GAM, RH and CO make the highest contributions to variances in $O_3$ concentrations at all four sites, with T and NO also contributing to $O_3$ variances. These results correspond to the most significant independent variables contributing to variance in $O_3$ levels indicated by MLR.

**Table 7.** Summary of the optimum GAM for each site showing the individual variable contributions to daily max 8-h $O_3$. This was done with the function gamm in R, which takes into account autocorrelation in the $O_3$ data

| | | | | | |
|---|---|---|---|---|---|
| | **GAMM (Welgegund)** | | | | |
| | Family: Gaussian | | | | |
| | Link function: identity | | | | |
| | Formula: | | | | |
| | daily max 8-h $O_3$ ~ s(T) + s(RH) + s(u) + s($NO_2$) + s(NO) + s(CO) | | | | |
| | Parametric coefficients: | | | | |
| | term | Estimate | Std. Error | t value | Pr(> I t I ) |
| | (Intercept) | 45.59 | 0.40 | 114.00 | <2e-16 |
| | Approximate significance of smooth terms: | | | | |
| | term | edf | Ref.df | F | p-value |
| 1 | s(T) | 2.78 | 2.78 | 4.29 | 4.10E-03 |
| 2 | s(RH) | 1.00 | 1.00 | 100.93 | < 2e-16 |
| 3 | s(u) | 2.07 | 2.07 | 3.18 | 3.47E-02 |
| 4 | s($NO_2$) | 4.86 | 4.86 | 9.83 | 5.26E-09 |
| 5 | s(NO) | 3.87 | 3.87 | 24.84 | < 2e-16 |
| 6 | s(CO) | 5.53 | 5.53 | 36.18 | < 2e-16 |
| | R-sq. (adj) = 0.487 | AIC = 10756 | | n = 1767 | |
| | **GAMM (Botsalano)** | | | | |
| | Family: Gaussian | | | | |
| | Link function: identity | | | | |
| | Formula: | | | | |
| | daily max 8-h $O_3$ ~ s(T) + s(RH) + s(CO) | | | | |
| | Parametric coefficients: | | | | |
| | term | Estimate | Std. Error | t value | Pr(> I t I ) |
| | (Intercept) | 46.6921 | 0.60 | 77.38 | <2e-16 |
| | Approximate significance of smooth terms: | | | | |
| | term | edf | Ref.df | F | p-value |
| 1 | s(T) | 2.57 | 2.57 | 11.24 | 1.96E-06 |
| 2 | s(RH) | 1.00 | 1.00 | 22.14 | 3.28E-06 |
| 3 | s(CO) | 4.09 | 4.09 | 46.74 | < 2e-16 |
| | R-sq. (adj) = 0.522 | AIC = 3013 | | n = 492 | |

**Table 7.** Continued

| | | | | | |
|---|---|---|---|---|---|
| | **GAMM (Marikana)** | | | | |
| | Family: Gaussian | | | | |
| | Link function: identity | | | | |
| | Formula: | | | | |
| | daily max 8-h $O_3$ ~ s(T) + s(RH) + s($NO_2$) + s(NO) + s(CO) | | | | |
| | Parametric coefficients: | | | | |
| | term | Estimate | Std. Error | t value | Pr(> \| t \| ) |
| | (Intercept) | 51.36 | 1.91 | 26.89 | <2e-16 |
| | Approximate significance of smooth terms: | | | | |
| | term | edf | Ref.df | F | p-value |
| 1 | s(T) | 1 | 1.00 | 9.47 | 2.18E-03 |
| 2 | s(RH) | 1 | 1.00 | 19.228 | 1.36E-05 |
| 3 | s($NO_2$) | 3.194 | 3.19 | 3.16 | 2.23E-02 |
| 4 | s(NO) | 6.452 | 6.45 | 12.06 | 1.64E-13 |
| 5 | s(CO) | 1 | 1.00 | 52.93 | 9.85E-13 |
| | R-sq. (adj) = 0.352 | AIC = 4327 | | n = 630 | |
| | **GAMM (Elandsfontein)** | | | | |
| | Family: Gaussian | | | | |
| | Link function: identity | | | | |
| | Formula: | | | | |
| | daily max 8-h $O_3$ ~ s(T) + s(RH) + s(u) + s(NO) | | | | |
| | Parametric coefficients: | | | | |
| | term | Estimate | Std. Error | t value | Pr(> \| t \| ) |
| | (Intercept) | 48.444 | 1.47 | 32.94 | <2e-16 |
| | Approximate significance of smooth terms: | | | | |
| | term | edf | Ref.df | F | p-value |
| 1 | s(T) | 2.10 | 2.10 | 8.686 | 1.68E-04 |
| 2 | s(RH) | 1.00 | 1.00 | 10.033 | 1.62E-03 |
| 3 | s(u) | 4.15 | 4.15 | 3.323 | 1.60E-02 |
| 4 | s(NO) | 1.00 | 1.00 | 28.852 | 1.11E-07 |
| | R-sq. (adj) = 0.180 | AIC = 4449 | | n = 598 | |

To diagnose the nature of the relationships between $O_3$ and each of the independent variables, partial residual plots were examined (Fig. 1). The partial residual plot of each independent variable, $X_k$, versus the smooth function, $s(X_k)$, shows the relationship between $X_k$ and $Y$, given that the other independent variables are also included in the model. These residual plots indicate that, in the temperature range 20 to 35°C, the relationship between daily max 8-h $O_3$ and T is positive and linear at Welgegund, Botsalano and Elandsfontein, while a change in slope is evident at lower temperatures. At Marikana, however, T is linearly and positively correlated for the entire T range. At all four sites, the change in $O_3$ with a change in relative humidity is linear and negatively correlated over the entire humidity range. For CO, the partial residual plot identified a positive linear relationship (although there is a small change in slope around 150-200 ppb for Welgegund and Botsalano) across the concentration range for Marikana. For NO and $NO_2$, there is sometimes a more complex (non-linear) fit in their partial residual response, suggesting other effects confounding with NO and $NO_2$.

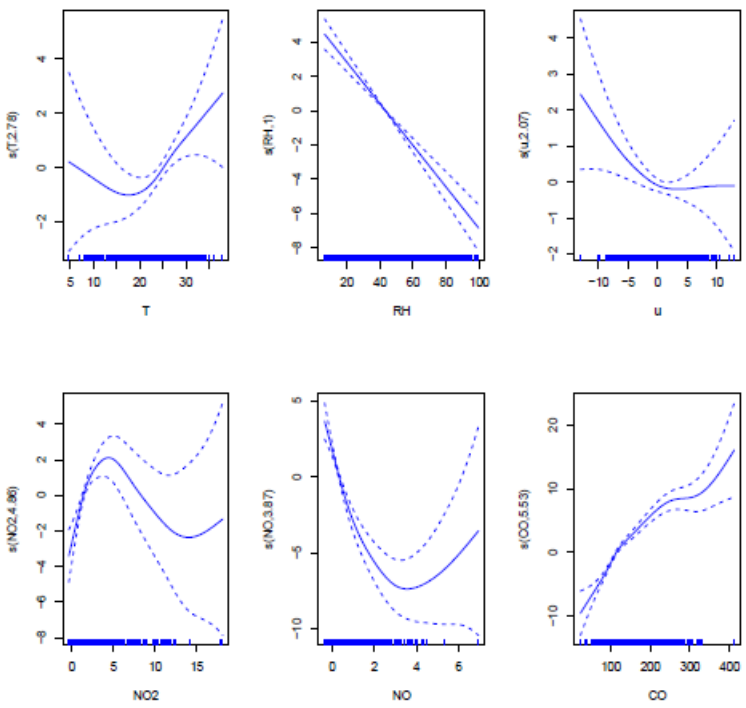


**(a) Welgegund**

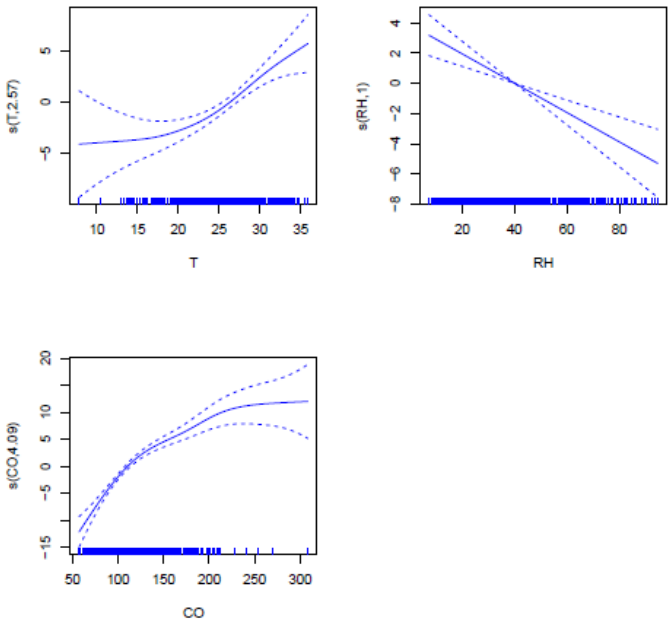


**(b) Botsalano**

5

**Fig. 1.** Partial residual plots of independent variables contained in the optimum solution from the GAM for $O_3$. The solid line in each plot is the estimate of the spline smooth function bounded by 95% confidence limits (i.e. ±2 standard errors of the estimate). The tick marks along the horizontal axis represent the density of data points of each explanatory variable (rug plot).

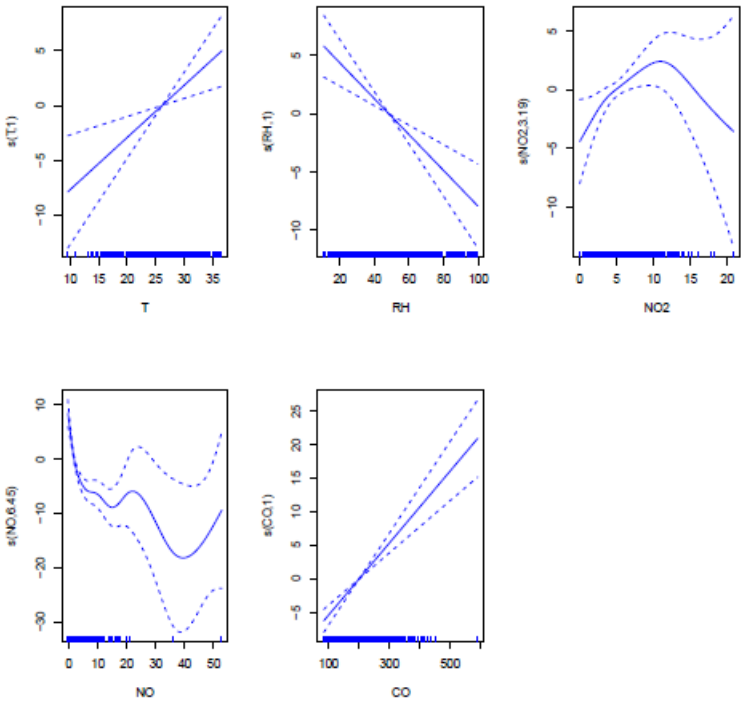


**(c) Marikana**

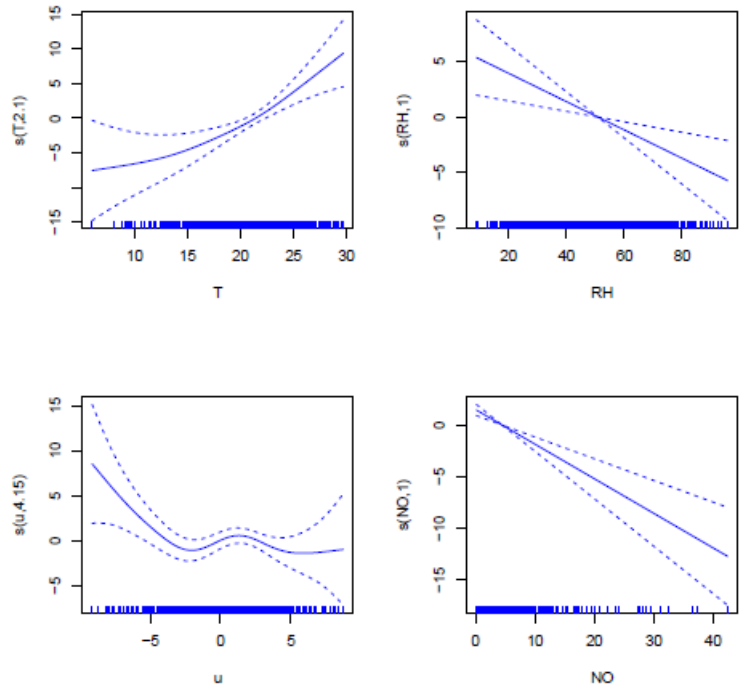


**(d) Elandsfontein**

5

**Fig. 1.** Continued

### 3.5 Comparison of statistical models

In order to relate the statistical models utilised in this study, the differences between $O_3$ concentrations calculated with each model and measured $O_3$ levels (expressed as $R^2$ and RMSE) were compared and presented in Table 8. The factors obtained with PCA were also included in an MLR model to perform PCR, as indicated in section 2.3.2, which are presented in Table 8. Previous-day daily max 8-h $O_3$ was also included as an independent variable in the evaluation of these models in order to deal with the autocorrelation (persistence) in the data and to increase model performance (Comrie, 1997), since it could also contribute to daily max 8-h $O_3$ (Otero et al., 2016). Previous-day daily max 8-h $O_3$ was not included in sections 3.2 to 3.4 where the influence of different independent variables on variances of $O_3$ was evaluated, since it could suppress the influence of other independent variables (Achen, 2001). The complete statistics from each of the models are presented in Tables A1, A2 and A3 of the appendix. It is evident from Table 8 that inclusion of the previous-day daily max 8-h $O_3$ increases the performance of the MLR and GAM models, as reflected by the relative contribution to total explained variance (i.e. $R^2$ significantly increases). The results show that the $O_3$ concentrations calculated with non-parametric GAM compared slightly better to measured $O_3$ concentrations than $O_3$ levels calculated with MLR and PCR, as indicated by the highest $R^2$- and smallest RMSE values for GAM. However, less complicated MLR models are also suitable to evaluate contributions of factors to variances in $O_3$ levels. In addition, the inclusion of only previous-day daily max 8-h $O_3$, T, RH and CO in these statistical models explained approximately 70% of the variance in daily max 8-h $O_3$, which implies that these are the main factors influencing variations in $O_3$ concentrations in continental South Africa.

**Table 8.** Comparison of statistical models in predicting daily max 8-h $O_3$ at the four measurement sites

| Measurement site | Method | Model | $R^2$ | RMSE |
|---|---|---|---|---|
| **WELGEGUND** | MLR | daily max 8-h $O_3$ = 9.10 + 0.59*$O_3$-1 + 0.28*T − 0.10*RH − 0.21*u + 0.08*v − 1.44*NO + 0.07*CO | 0.77 | 4.75 |
| | PCR | daily max 8-h $O_3$ = -0.13 − 0.42*PC1 + 5.96*PC2 + 0.86*PC3 − 0.71*PC4 | 0.62 | 6.00 |
| | GAM | daily max 8-h $O_3$ = 45.59 + s($O_3$-1) + s(T) + s(RH) + s(u) + s(v) + s($NO_2$) + s(NO) + s(CO) | 0.79 | 4.47 |
| **BOTSALANO** | MLR | daily max 8-h $O_3$ = -0.31 + 0.48*$O_3$-1 + 0.45*T + 0.005*Rad + 0.09*CO | 0.70 | 5.14 |
| | PCR | daily max 8-h $O_3$ = -0.25 − 4.88*PC1 – 0.09*PC2 + 0.07*PC3 − 2.18*PC4 | 0.64 | 5.63 |
| | GAM | daily max 8-h $O_3$ = 46.75 + s($O_3$-1) + s(T) + s(Rad) + s(u) + s(v) + s(CO) | 0.73 | 4.69 |
| **MARIKANA** | MLR | daily max 8-h $O_3$ = -18.19 + 0.73*$O_3$-1 + 0.48*T + 0.01*Rad + 0.70*v − 0.24*NO + 0.07*CO | 0.83 | 6.93 |
| | PCR | daily max 8-h $O_3$ = 0.01 + 4.15*PC1 - 3.73*PC2 + 1.01*PC3 − 9.93*PC4 | 0.77 | 8.04 |
| | GAM | daily max 8-h $O_3$ = 51.09 + s($O_3$-1) + s(T) + s(Rad) + s(u) + s($NO_2$) + s(NO) + s(CO) | 0.85 | 6.40 |
| **ELANDSFONTEIN** | MLR | daily max 8-h $O_3$ = 18.45 + 0.68*$O_3$-1 + 0.32*T − 0.19*RH − 0.29*v + 0.15*$NO_2$ − 0.49*NO | 0.67 | 9.03 |
| | PCR | daily max 8-h $O_3$ = −0.31 − 0.38*PC1 −2.31*PC2 − 1.44*PC3 + 10.36*PC4 | 0.61 | 9.88 |
| | GAM | daily max 8-h $O_3$ = 48.81 + s($O_3$-1) + s(T) + s(RH) + s(u) + s($NO_2$) + s(NO) | 0.69 | 8.64 |

## 3.6 Insights into major factors driving $O_3$ variances

As indicated above, CO, RH and T were identified by all three statistical models as the major factors driving variances in $O_3$ levels in southern Africa. In many empirical and modelling

studies, temperature is generally considered the most strongly correlated with $O_3$ concentrations (Camalier et al., 2007; Dawson et al., 2007; Lin and Cobourn, 2007; Cobourn, 2007; Baertsch-Ritter et al., 2004; Hubbard and Cobourn, 1998; Ryan, 1995; Jacob et al., 1993), which therefore has been used as a reasonable proxy to account for the combined influence of meteorological and chemical factors on $O_3$ concentrations (Rasmussen et al., 2012; Tsakiri and Zurbenko, 2011; Jacob et al., 1993). High temperatures are usually associated with high solar radiation that contributes to increased photochemical reaction rates, as well as other meteorological conditions favouring $O_3$ production, such as high pressure, stagnation of air masses and reduced cloud cover (Jacob et al., 1993; NRC, 1991). Jaars et al. (2014) also indicated that increased ambient VOC concentrations at Welgegund were associated with higher temperatures resulting from higher evaporation rates, which could also contribute to the increased $O_3$ formation potential of VOCs. The positive correlation between $O_3$ and temperature is also largely driven by the chemical equilibrium between $NO_x$ and peroxyacetylnitrate (PAN), which serves as a reservoir for $NO_x$ (Jacob et al., 1993). The enhanced decomposition of PAN at high temperatures to regenerate stored $NO_x$ results in local $O_3$ production being maximised (Sillman, 1999; Sillman and Samson, 1995; Jacob et al., 1993).

Some studies have indicated the significance of relative humidity to surface $O_3$ concentrations (Davis et al., 2011; Camalier et al., 2007). In the eastern United States, for instance, a north-south divide in terms of meteorological parameters controlling $O_3$ levels has been discussed in various studies (Tawfik and Steiner, 2013; Rasmussen et al., 2012; Davis et al., 2011; Camalier et al., 2007; Zheng et al., 2007), with temperature most strongly correlated with $O_3$ at high latitude and strongly negatively correlated with relative humidity at lower latitude. This strong negative relationship between $O_3$ and relative humidity is not widely understood, with several authors presenting possible explanations:

- The $O_3$-relative humidity correlation is closely related to the $O_3$-temperature correlation, where temperature is the actual cause of $O_3$ variability, simultaneously affecting relative humidity and $O_3$ concentration (Bloomer et al., 2009; Camalier et al., 2007);
- High relative humidity can be associated with increased cloud cover and reduced UV radiation, which limits the photochemical production of $O_3$ to occur (Porter et al., 2015; Davis et al., 2011; Camalier et al., 2007);
- High relative humidity is associated with wet deposition (precipitation), which does not affect $O_3$ directly, but leads to the removal of soluble species such as $HNO_3$ and $H_2O_2$

and consequently the availability of $NO_x$ and OH (Wild, 2007). Furthermore, increased relative humidity increases the stomatal conductance of plants (Kavassalis and Murphy;(2017)) and therefore also the dry deposition of surface $O_3$;

- Increased concentrations of atmospheric water vapour provide a chemical sink for $O_3$ through the reaction with water after photolysis, instead of the quenching reaction where $O_3$ is regenerated;
- Higher relative humidity can lead to more liquid water on aerosol particles, causing increased loss of gas phase $NO_x$ via the heterogeneous reaction of dinitrogen pentoxide ($N_2O_5$) on particulates (Bertram and Thornton, 2009). Jia and Xu (2014) also showed that increased relative humidity can greatly reduce $O_3$ through the transfer of $NO_2$- and $ONO_2$-containing species (reactive nitrogen species) to the particulate phase;
- Increased surface $O_3$ concentrations associated with stratospheric intrusions are associated with low water vapour (Stauffer et al., 2017; Thompson et al., 2015; Thompson et al., 2014);
- $O_3$-relative humidity correlation can also result from a shift in the soil-moisture atmosphere coupling regime (evapotranspiration-limiting regimes), reflecting the simultaneous impact of soil moisture deficit on near-surface humidity, temperature and radiation (Tawfik and Steiner, 2013).

All these afore-mentioned explanations could contribute to the significant (negative) correlation between $O_3$ variances and relative humidity observed for southern Africa. However, the relative role of temperature and relative humidity in driving $O_3$ variability is not yet fully disentangled due to their interdependency with the order of their significance possibly related to short-term dependencies, i.e. weather- and precursor emissions fluctuations. The significance of the influence of temperature and relative humidity on surface $O_3$ is also indicated by substantial higher $O_3$ concentrations measured during spring in 2015 at Welgegund. Dry and warm conditions were associated with the El Niño weather cycle, which persisted into the first half of 2016 with the 2015/2016 rain season being one of the warmest and driest in approximately 35 years.

The influence of CO on tropospheric $O_3$ formations is well known. CO and VOCs are the main sources of peroxy radicals that alter the photostationary state of $O_3$ production. Laban et al. (2018) indicated the important influence of CO on surface $O_3$ levels in southern Africa. CO emissions were attributed to household combustion for space heating and regional open

biomass burning. Source maps indicated that $O_3$ and CO had similar regional sources with the highest concentrations of these species corresponding with the regions where a large number of wild fire events occurred. Furthermore, it was also indicated by Laban et al. (2018) that increased surface $O_3$ levels correlated with higher CO concentrations at Welgegund, Botsalano and Marikana, while it was implied that regional background regions in southern Africa could be considered VOC limited.

## 4. Conclusions

The study provided some insights into major factors driving surface $O_3$ variability by utilising three statistical models. Three multivariate statistical models, MLR, PCA and GAM, were utilised to determine the influence of meteorological conditions and precursor species on $O_3$ variability in continental southern Africa. Temperature, global radiation, relative humidity, wind speed and -direction, as well as NO, $NO_2$ and CO concentrations measured at Welgegund, Botsalano, Marikana and Elandsfontein were included as input parameters in these models. MLR indicated that CO, temperature and relative humidity made the largest contribution in explaining variances in daily max 8-h $O_3$ at all the sites, while NO levels contributed to $O_3$ variability at Welgegund and Elandsfontein. PCA revealed meaningful factors, i.e. temperature and radiation, CO, relative humidity, and NO and $NO_2$, which indicated that these parameters in different principal components are not strongly collinear and contributed independently to variances calculated with MLR. The nonlinear GAM also indicated that CO, temperature and relative humidity were the most important parameters influencing variances in $O_3$ levels. Partial residual plots also indicated that temperature, radiation and $NO_x$ most likely have a non-linear relationship with daily max 8-h $O_3$, while the relationship with relative humidity and CO is probably linear. Comparison of the measured $O_3$ concentrations with $O_3$ levels calculated with MLR and GAM indicated that $O_3$ levels calculated with both these models compared well to measured $O_3$ values if previous-day maximum $O_3$ concentration was also included in the model, with GAM performing slightly better. MLR was also conducted with principal components identified with PCA as input parameters, which had a weaker comparison to measured $O_3$ concentrations.

The influence of temperature on $O_3$ variability is expected, while Laban et al. (2018) indicated the significance of CO emissions associated with biomass burning on surface $O_3$ levels in southern Africa. The significant effect of relative humidity on $O_3$ variability, i.e. lower $O_3$ associated with increased relative humidity was unexpected, which can be attributed to a

number of factors mainly involving loss of $O_3$ or precursor species in the atmosphere in the aqueous phase or lower relative humidity being associated with meteorological conditions not conducive to $O_3$ formation. Relative humidity was the strongest meteorological predictor at two of the four continental sites studied. Therefore, the influence of relative humidity should not be underestimated in atmospheric $O_3$ formation and prediction models.

In conjunction with local meteorological parameters and pollutant concentration variables utilised in this study, other synoptic-scale meteorological contributions to surface $O_3$ should also be investigated, e.g. large-scale atmospheric circulation over this region. In addition, it is also important that volatile organic compounds (VOCs), which are important precursors of surface $O_3$, are included in statistical models. No continuous long-term VOC measurements were conducted at any of the sites. Jaars et al. (2014) and Jaars et al. (2016) did, however, report on aromatic VOCs and biogenic VOCs collected with grab samples (two-hour daily samples) during a two-year sampling campaign at Welgegund. This data was not from a statistical perspective considered sufficient to be included in the statistical models utilised in this study. However, Jaars et al. (2014) and Jaars et al. (2016) did indicate that VOC concentrations measured at Welgegund were relatively low, with BVOCs being an order of magnitude lower compared to aromatic VOCs measured at Welgegund, as well as being significantly lower compared to BVOC concentrations measured in other ecosystems in the world. Photochemical box models can also be used to investigate the main reactions that participate in $O_3$ formation. A greater scientific understanding of the factors influencing surface $O_3$ concentrations in South Africa will allow regional air quality models to be improved for the prediction of surface $O_3$ concentrations and exceedances of the ambient air quality standards. It could be a step towards developing operational $O_3$ forecast models for cities and towns in South Africa.

**Acknowledgements**

This work is based on the research supported in part by the National Research Foundation of South Africa (grant numbers 97006 and 111287). Opinions expressed and conclusions arrived at are those of the authors and are not necessarily to be attributed to the NRF. The authors are also grateful to Eskom for supplying the Elandsfontein data. V Vakkari is a beneficiary of an AXA Research Fund postdoctoral grant. This work was partly funded by the Academy of Finland Centre of Excellence program (grant no. 272041, 307331).

## 5. References


Abdul-Wahab, S. A., Bakheit, C. S., and Al-Alawi, S. M.: Principal component and multiple regression analysis in modelling of ground-level ozone and factors affecting its concentrations, Environmental Modelling & Software, 20, 1263-1271, 2005.

Achen, C. H.: Why Lagged Dependent Variables Can Suppress the Explanatory Power of Other Independent Variables, Ann Arbor, 1001, 48106-41248, 2001.

Awang, N. R., Ramli, N. A., Yahaya, A. S., and Elbayoumi, M.: Multivariate methods to predict ground level ozone during daytime, nighttime, and critical conversion time in urban areas, Atmospheric Pollution Research, 6, 726-734, 2015.

Baertsch-Ritter, N., Keller, J., Dommen, J., and Prevot, A.: Effects of various meteorological conditions and spatial emission resolutions on the ozone concentration and ROG/$NO_x$ limitation in the Milan area (I), Atmospheric Chemistry and Physics, 4, 423-438, 2004.

Bell, M. L., McDermott, A., Zeger, S. L., Samet, J. M., and Dominici, F.: Ozone and short-term mortality in 95 US urban communities, 1987-2000, Jama, 292, 2372-2378, 2004.

Bertram, T., and Thornton, J.: Toward a general parameterization of $N_2O_5$ reactivity on aqueous particles: the competing effects of particle liquid water, nitrate and chloride, Atmospheric Chemistry and Physics, 9, 8351-8363, 2009.

Bloomer, B. J., Stehr, J. W., Piety, C. A., Salawitch, R. J., and Dickerson, R. R.: Observed relationships of ozone air pollution with temperature and emissions, Geophysical Research Letters, 36, 2009.

Bloomfield, P., Royle, J. A., Steinberg, L. J., and Yang, Q.: Accounting for meteorological effects in measuring urban ozone levels and trends, Atmospheric Environment, 30, 3067-3077, doi:http://dx.doi.org/10.1016/1352-2310(95)00347-9, 1996.

Camalier, L., Cox, W., and Dolwick, P.: The effects of meteorology on ozone in urban areas and their use in assessing ozone trends, Atmospheric Environment, 41, 7127-7137, 2007.

Cardelino, C., Chang, M., John, J. S., Murphey, B., Cordle, J., Ballagas, R., Patterson, L., Powell, K., Stogner, J., and Zimmer-Dauphinee, S.: Ozone predictions in Atlanta, Georgia: Analysis of the 1999 ozone season, Journal of the Air & Waste Management Association, 51, 1227-1236, 2001.

Chaloulakou, A., Saisana, M., and Spyrellis, N.: Comparative assessment of neural networks and regression models for forecasting summertime ozone in Athens, Science of the Total Environment, 313, 1-13, 2003.

Cobourn, W. G.: Accuracy and reliability of an automated air quality forecast system for ozone in seven Kentucky metropolitan areas, Atmospheric Environment, 41, 5863-5875, 2007.

Combrink, J., Diab, R., Sokolic, F., and Brunke, E.: Relationship between surface, free tropospheric and total column ozone in two contrasting areas in South Africa, Atmospheric Environment, 29, 685-691, 1995.

Comrie, A. C.: Comparing neural networks and regression models for ozone forecasting, J. Air Waste Manage. Assoc., 47, 653-663, 1997.

Cooper, O. R., Gao, R. S., Tarasick, D., Leblanc, T., and Sweeney, C.: Long-term ozone trends at rural ozone monitoring sites across the United States, 1990–2010, Journal of Geophysical Research: Atmospheres, 117, 2012.

Davis, J., Cox, W., Reff, A., and Dolwick, P.: A comparison of CMAQ-based and observation-based statistical models relating ozone to meteorological parameters, Atmospheric Environment, 45, 3481-3487, 2011.

Dawson, J. P., Adams, P. J., and Pandis, S. N.: Sensitivity of ozone to summertime climate in the eastern USA: A modeling case study, Atmospheric Environment, 41, 1494-1511, 2007.

Diab, R., Thompson, A., Mari, K., Ramsay, L., and Coetzee, G.: Tropospheric ozone climatology over Irene, South Africa, from 1990 to 1994 and 1998 to 2002, Journal of Geophysical Research: Atmospheres, 109, 2004.

Dominick, D., Juahir, H., Latif, M. T., Zain, S. M., and Aris, A. Z.: Spatial assessment of air quality patterns in Malaysia using multivariate analysis, Atmospheric Environment, 60, 172-181, 2012.

Dueñas, C., Fernández, M. C., Cañete, S., Carretero, J., and Liger, E.: Assessment of ozone variations and meteorological effects in an urban area in the Mediterranean Coast, Science of The Total Environment, 299, 97-113, doi:http://dx.doi.org/10.1016/S0048-9697(02)00251-6, 2002.

Fiore, A. M., Jacob, D. J., Logan, J. A., and Yin, J. H.: Long-term trends in ground level ozone over the contiguous United States, 1980–1995, Journal of Geophysical Research: Atmospheres, 103, 1471-1480, 1998.

Gardner, M., and Dorling, S.: Meteorologically adjusted trends in UK daily maximum surface ozone concentrations, Atmospheric Environment, 34, 171-176, 2000.

Gardner, M. W., and Dorling, S.: Artificial neural networks (the multilayer perceptron)—a review of applications in the atmospheric sciences, Atmospheric Environment, 32, 2627-2636, 1998.

Gorai, A., Tuluri, F., Tchounwou, P., and Ambinakudige, S.: Influence of local meteorology and $NO_2$ conditions on ground-level ozone concentrations in the eastern part of Texas, USA, Air Quality, Atmosphere and Health, 8, 81-96, 2015.

Guardani, R., Aguiar, J. L., Nascimento, C. A., Lacava, C. I., and Yanagi, Y.: Ground-level ozone mapping in large urban areas using multivariate statistical analysis: Application to the Sao Paulo Metropolitan area, Journal of the Air & Waste Management Association, 53, 553-559, 2003.

Hastie, T., and Tibshirani, R.: Generalized additive models, Wiley Online Library, 1990.

Hayn, M., Beirle, S., Hamprecht, F. A., Platt, U., Menze, B. H., and Wagner, T.: Analysing spatio-temporal patterns of the global $NO_2$-distribution retrieved from GOME satellite observations using a generalized additive model, Atmospheric Chemistry and Physics, 9, 6459-6477, 2009.

Hirsikko, A., Vakkari, V., Tiitta, P., Manninen, H. E., Gagné, S., Laakso, H., Kulmala, M., Mirme, A., Mirme, S., Mabaso, D., Beukes, J. P., and Laakso, L.: Characterisation of sub-micron particle number concentrations and formation events in the western Bushveld Igneous Complex, South Africa, Atmospheric Chemistry and Physics, 12, 3951-3967, doi:10.5194/acp-12-3951-2012, 2012.

Hirsikko, A., Vakkari, V., Tiitta, P., Hatakka, J., Kerminen, V. M., Sundström, A. M., Beukes, J. P., Manninen, H. E., Kulmala, M., and Laakso, L.: Multiple daytime nucleation events in semi-clean savannah and industrial environments in South Africa: analysis based on observations, Atmospheric Chemistry and Physics, 13, 5523-5532, doi:10.5194/acp-13-5523-2013, 2013.

Hubbard, M. C., and Cobourn, W. G.: Development of a regression model to forecast ground-level ozone concentration in Louisville, KY, Atmospheric Environment, 32, 2637-2647, 1998.

IPCC: Climate change 2007: The physical science basis: contribution of Working Group I to the Fourth Assessment Report of the Intergovernmental Panel on Climate Change, edited by: Solomon, S., Qin, D., Manning, M., Chen, Z., Marquis, M., Averyt, K. B., Tignor, M., and Miller, H. L., Cambridge University Press, Cambridge ; New York, viii, 996 p. pp., 2007.

Jaars, K., Beukes, J. P., van Zyl, P. G., Venter, A. D., Josipovic, M., Pienaar, J. J., Vakkari, V., Aaltonen, H., Laakso, H., Kulmala, M., Tiitta, P., Guenther, A., Hellén, H., Laakso, L., and Hakola, H.: Ambient aromatic hydrocarbon measurements at Welgegund, South Africa, Atmospheric Chemistry and Physics, 14, 7075-7089, doi:10.5194/acp-14-7075-2014, 2014.

Jaars, K., van Zyl, P. G., Beukes, J. P., Hellén, H., Vakkari, V., Josipovic, M., Venter, A. D., Räsänen, M., Knoetze, L., Cilliers, D. P., Siebert, S. J., Kulmala, M., Rinne, J., Guenther, A., Laakso, L., and Hakola, H.: Measurements of biogenic volatile organic compounds at a grazed savannah grassland agricultural landscape in South Africa, Atmospheric Chemistry and Physics, 16, 15665-15688, doi:10.5194/acp-16-15665-2016, 2016.

Jacob, D. J., Logan, J. A., Gardner, G. M., Yevich, R. M., Spivakovsky, C. M., Wofsy, S. C., Sillman, S., and Prather, M. J.: Factors regulating ozone over the United States and its export to the global atmosphere, Journal of Geophysical Research: Atmospheres, 98, 14817-14826, 1993.

Kavassalis, S. C., and Murphy, J. G.: Understanding ozone-meteorology correlations: A role for dry deposition, Geophysical Research Letters, 44, 2922-2931, 2017.

Laakso, L., Laakso, H., Aalto, P. P., Keronen, P., Petäjä, T., Nieminen, T., Pohja, T., Siivola, E., Kulmala, M., Kgabi, N., Molefe, M., Mabaso, D., Phalatse, D., Pienaar, K., and Kerminen, V. M.: Basic characteristics of atmospheric particles, trace gases and meteorology in a relatively clean Southern African Savannah environment, Atmospheric Chemistry and Physics, 8, 4823-4839, doi:10.5194/acp-8-4823-2008, 2008.

Laakso, L., Vakkari, V., Virkkula, A., Laakso, H., Backman, J., Kulmala, M., Beukes, J. P., van Zyl, P. G., Tiitta, P., Josipovic, M., Pienaar, J. J., Chiloane, K., Gilardoni, S., Vignati, E., Wiedensohler, A., Tuch, T., Birmili, W., Piketh, S., Collett, K., Fourie, G. D., Komppula, M., Lihavainen, H., de Leeuw, G., and Kerminen, V. M.: South African EUCAARI measurements: seasonal variation of trace gases and aerosol optical properties, Atmospheric Chemistry and Physics, 12, 1847-1864, doi:10.5194/acp-12-1847-2012, 2012.

Laban, T. L., van Zyl, P. G., Beukes, J. P., Vakkari, V., Jaars, K., Borduas-Dedekind, N., Josipovic, M., Thompson, A. M., Kulmala, M., and Laakso, L.: Seasonal influences on surface ozone variability in continental South Africa and implications for air quality, Atmospheric Chemistry and Physics Discussions, doi:https://doi.org/10.5194/acp-2017-1115, 2018.

Lin, Y., and Cobourn, W. G.: Fuzzy system models combined with nonlinear regression for daily ground-level ozone predictions, Atmospheric Environment, 41, 3502-3513, 2007.

Lourens, A. S., Beukes, J. P., Van Zyl, P. G., Fourie, G. D., Burger, J. W., Pienaar, J. J., Read, C. E., and Jordaan, J. H.: Spatial and temporal assessment of gaseous pollutants in the Highveld of South Africa, South African Journal of Science, 107, 1-8, 2011.

Lourens, A. S. M., Butler, T. M., Beukes, J. P., Van Zyl, P. G., Beirle, S., Wagner, T. K., Heue, K.-P., Pienaar, J. J., Fourie, G. D., and Lawrence, M. G.: Re-evaluating the $NO_2$ hotspot over the South African Highveld, doi:10.4102/sajs.v108i11/12.1146, 2012.

Melkonyan, A., and Kuttler, W.: Long-term analysis of NO, NO2 and O3 concentrations in North Rhine-Westphalia, Germany, Atmospheric Environment, 60, 316-326, 2012.

Mikkonen, S., Korhonen, H., Romakkaniemi, S., Smith, J. N., Joutsensaari, J., Lehtinen, K. E. J., Hamed, A., Breider, T. J., Birmili, W., Spindler, G., Plass-Duelmer, C., Facchini, M. C., and Laaksonen, A.: Meteorological and trace gas factors affecting the number concentration of atmospheric Aitken ($D_p$=50 nm) particles in the continental boundary layer: parameterization using a multivariate mixed effects model, Geoscientific Model Development, 4, 1-13, doi:10.5194/gmd-4-1-2011, 2011.

Milanchus, M. L., Rao, S. T., and Zurbenko, I. G.: Evaluating the effectiveness of ozone management efforts in the presence of meteorological variability, Journal of the Air & Waste Management Association, 48, 201-215, 1998.

Neter, J., Kutner, M., Nachtsheim, C., and Wasserman, W.: Applied linear statistical models. McGraw-Hill, New York, Applied linear statistical models. 4th ed. McGraw-Hill, New York., 283, 1996.

NRC: Rethinking the Ozone Problem in Urban and Regional Air Pollution, The National Academies Press, Washington, DC, 524 pp., 1991.

NRC: Estimating mortality risk reduction and economic benefits from controlling ozone air pollution, National Academies Press, 2008.

Ooka, R., Khiem, M., Hayami, H., Yoshikado, H., Huang, H., and Kawamoto, Y.: Influence of meteorological conditions on summer ozone levels in the central Kanto area of Japan, Procedia Environmental Sciences, 4, 138-150, 2011.

Ordonez, C., Mathis, H., Furger, M., Henne, S., Hüglin, C., Staehelin, J., and Prévôt, A.: Changes of daily surface ozone maxima in Switzerland in all seasons from 1992 to 2002 and discussion of summer 2003, Atmospheric Chemistry and Physics, 5, 1187-1203, 2005.

Otero, N., Sillmann, J., Schnell, J. L., Rust, H. W., and Butler, T.: Synoptic and meteorological drivers of extreme ozone concentrations over Europe, Environmental Research Letters, 11, 024005, 2016.

Pearce, J. L., Beringer, J., Nicholls, N., Hyndman, R. J., and Tapper, N. J.: Quantifying the influence of local meteorology on air quality using generalized additive models, Atmospheric Environment, 45, 1328-1336, 2011.

Porter, W. C., Heald, C. L., Cooley, D., and Russell, B.: Investigating the observed sensitivities of air-quality extremes to meteorological drivers via quantile regression, Atmospheric Chemistry and Physics, 15, 10349-10366, 2015.

R Development Core Team: R: A language and environment for statistical computing, Retrieved from http://www.R-project.org, 2009.

Rao, S. T., and Zurbenko, I. G.: Detecting and tracking changes in ozone air quality, Air & Waste, 44, 1089-1092, 1994.

Rasmussen, D., Fiore, A., Naik, V., Horowitz, L., McGinnis, S., and Schultz, M.: Surface ozone-temperature relationships in the eastern US: A monthly climatology for evaluating chemistry-climate models, Atmospheric Environment, 47, 142-153, 2012.

Ryan, W. F.: Forecasting severe ozone episodes in the Baltimore metropolitan area, Atmospheric Environment, 29, 2387-2398, 1995.

Schlink, U., Herbarth, O., Richter, M., Dorling, S., Nunnari, G., Cawley, G., and Pelikan, E.: Statistical models to assess the health effects and to forecast ground-level ozone, Environmental Modelling & Software, 21, 547-558, 2006.

Seinfeld, J. H., and Pandis, S. N.: Atmospheric chemistry and physics: from air pollution to climate change, 2nd ed., Wiley, New York, xxviii, 1202 p. pp., 2006.

Sillman, S., and Samson, P. J.: Impact of temperature on oxidant photochemistry in urban, polluted rural and remote environments, Journal of Geophysical Research: Atmospheres, 100, 11497-11508, doi:10.1029/94JD02146, 1995.

Sillman, S.: The relation between ozone, $NO_x$ and hydrocarbons in urban and polluted rural environments, Atmospheric Environment, 33, 1821-1845, doi:http://dx.doi.org/10.1016/S1352-2310(98)00345-8, 1999.

Stauffer, R. M., Thompson, A. M., Oltmans, S. J., and Johnson, B. J.: Tropospheric ozonesonde profiles at long-term US monitoring sites: 2. Links between Trinidad Head, CA, profile clusters and inland surface ozone measurements, Journal of Geophysical Research: Atmospheres, 122, 1261-1280, 2017.

Tawfik, A. B., and Steiner, A. L.: A proposed physical mechanism for ozone-meteorology correlations using land–atmosphere coupling regimes, Atmospheric Environment, 72, 50-59, doi:http://dx.doi.org/10.1016/j.atmosenv.2013.03.002, 2013.

Thompson, A. M., Balashov, N. V., Witte, J. C., Coetzee, J. G. R., Thouret, V., and Posny, F.: Tropospheric ozone increases over the southern Africa region: bellwether for rapid growth in Southern Hemisphere pollution?, Atmospheric Chemistry and Physics, 14, 9855-9869, doi:10.5194/acp-14-9855-2014, 2014.

Thompson, A. M., Stauffer, R. M., Miller, S. K., Martins, D. K., Joseph, E., Weinheimer, A. J., and Diskin, G. S.: Ozone profiles in the Baltimore-Washington region (2006–2011): satellite comparisons and DISCOVER-AQ observations, Journal of Atmospheric Chemistry, 72, 393-422, 2015.

Thompson, M. L., Reynolds, J., Cox, L. H., Guttorp, P., and Sampson, P. D.: A review of statistical methods for the meteorological adjustment of tropospheric ozone, Atmospheric Environment, 35, 617-630, 2001.

Tiitta, P., Vakkari, V., Croteau, P., Beukes, J. P., van Zyl, P. G., Josipovic, M., Venter, A. D., Jaars, K., Pienaar, J. J., Ng, N. L., Canagaratna, M. R., Jayne, J. T., Kerminen, V. M., Kokkola, H., Kulmala, M., Laaksonen, A., Worsnop, D. R., and Laakso, L.: Chemical composition, main sources and temporal variability of $PM_1$ aerosols in southern African grassland, Atmospheric Chemistry and Physics, 14, 1909-1927, doi:10.5194/acp-14-1909-2014, 2014.

Tsakiri, K. G., and Zurbenko, I. G.: Prediction of ozone concentrations using atmospheric variables, Air Quality, Atmosphere & Health, 4, 111-120, 2011.

Vakkari, V., Laakso, H., Kulmala, M., Laaksonen, A., Mabaso, D., Molefe, M., Kgabi, N., and Laakso, L.: New particle formation events in semi-clean South African savannah, Atmospheric Chemistry and Physics, 11, 3333-3346, doi:10.5194/acp-11-3333-2011, 2011.

Vakkari, V., Beukes, J. P., Laakso, H., Mabaso, D., Pienaar, J. J., Kulmala, M., and Laakso, L.: Long-term observations of aerosol size distributions in semi-clean and polluted savannah in South Africa, Atmospheric Chemistry and Physics, 13, 1751-1770, doi:10.5194/acp-13-1751-2013, 2013.

Venter, A. D., Vakkari, V., Beukes, J. P., Van Zyl, P. G., Laakso, H., Mabaso, D., Tiitta, P., Josipovic, M., Kulmala, M., Pienaar, J. J., and Laakso, L.: An air quality assessment in the industrialised western Bushveld Igneous Complex, South Africa, South African Journal of Science, doi:10.4102/sajs.v108i9/10.1059, 2012.

Venter, A. D., van Zyl, P. G., Beukes, J. P., Josipovic, M., Hendriks, J., Vakkari, V., and Laakso, L.: Atmospheric trace metals measured at a regional background site (Welgegund) in South Africa, Atmospheric Chemistry and Physics, 17, 4251-4263, doi:10.5194/acp-17-4251-2017, 2017.

Wild, O.: Modelling the global tropospheric ozone budget: exploring the variability in current models, Atmospheric Chemistry and Physics, 7, 2643-2660, 2007.

Wood, S. N.: Generalized additive models: an introduction with R, CRC press, 2017.

Zheng, J., Swall, J. L., Cox, W. M., and Davis, J. M.: Interannual variation in meteorologically adjusted ozone levels in the eastern United States: A comparison of two approaches, Atmospheric Environment, 41, 705-716, 2007.

Zou, H., Hastie, T., and Tibshirani, R.: Sparse principal component analysis, Journal of Computational and Graphical Statistics, 15, 265-286, 2006.

Zunckel, M., Venjonoka, K., Pienaar, J. J., Brunke, E. G., Pretorius, O., Koosialee, A., Raghunandan, A., and van Tienhoven, A. M.: Surface ozone over southern Africa: synthesis of monitoring results during the Cross Border Air Pollution Impact Assessment project, Atmospheric Environment, 38, 6139-6147, doi:https://doi.org/10.1016/j.atmosenv.2004.07.029, 2004.

Zunckel, M., Koosailee, A., Yarwood, G., Maure, G., Venjonoka, K., van Tienhoven, A. M., and Otter, L.: Modelled surface ozone over southern Africa during the Cross Border Air Pollution Impact Assessment project, Environmental Modelling & Software, 21, 911-924, doi:https://doi.org/10.1016/j.envsoft.2005.04.004, 2006.

## Appendix

**Table A1.** MLR models for prediction of daily max 8-h $O_3$ for each measurement site

| **WELGEGUND** | **Constant** | **$O_3$-1 (ppb)** | **T ($^oC$)** | **RH (%)** | **u (m/s)** | **v (m/s)** | **NO (ppb)** | **CO (ppb)** |
|---|---|---|---|---|---|---|---|---|
| Regression coefficient (β) | 9.10 | 0.59 | 0.28 | -0.10 | -0.21 | 0.08 | -1.44 | 0.07 |
| Standard error | 0.95 | 0.01 | 0.02 | 0.01 | 0.04 | 0.05 | 0.19 | 0.00 |
| t-statistic | 9.57 | 42.36 | 11.23 | -13.26 | -5.39 | 1.83 | -7.54 | 20.36 |
| P-value | 3.56E-21 | 1.16E-270 | 2.65E-28 | 2.57E-38 | 7.99E-08 | 0.06747224 | 7.77E-14 | 6.94E-83 |
| **$R^2$=0.768** | **Adjusted $R^2$=0.767** | | | **RMSE=4.75** | | **F-statistic=828** | | |
| **BOTSALANO** | **Constant** | **$O_3$-1 (ppb)** | **T ($^oC$)** | **Rad ($W/m^2$)** | **CO (ppb)** | | | |
| Regression coefficient (β) | -0.31 | 0.48 | 0.45 | 0.01 | 0.09 | | | |
| Standard error | 1.51 | 0.03 | 0.07 | 0.00 | 0.01 | | | |
| t-statistic | -0.20 | 16.23 | 6.78 | 2.09 | 11.94 | | | |
| P-value | 0.83958521 | 1.94E-47 | 3.65E-11 | 0.03712663 | 6.49E-29 | | | |
| **$R^2$=0.695** | **Adjusted $R^2$=0.693** | | | **RMSE=5.14** | | **F-statistic=271** | | |
| **MARIKANA** | **Constant** | **$O_3$-1 (ppb)** | **T ($^oC$)** | **Rad ($W/m^2$)** | **v (m/s)** | **NO (ppb)** | **CO (ppb)** | |
| Regression coefficient (β) | -18.19 | 0.73 | 0.48 | 0.01 | 0.70 | -0.24 | 0.07 | |
| Standard error | 1.91 | 0.02 | 0.09 | 0.00 | 0.21 | 0.08 | 0.00 | |
| t-statistic | -9.55 | 39.12 | 5.08 | 4.07 | 3.40 | -2.91 | 14.46 | |
| P-value | 3.16E-20 | 8.56E-169 | 4.96E-07 | 5.36E-05 | 0.00070864 | 0.00369032 | 5.48E-41 | |
| **$R^2$=0.830** | **Adjusted $R^2$=0.828** | | | **RMSE=6.93** | | **F-statistic=498** | | |
| **ELANDSFONTEIN** | **Constant** | **$O_3$-1 (ppb)** | **T ($^oC$)** | **RH (%)** | **v (m/s)** | **$NO_2$ (ppb)** | **NO (ppb)** | |
| Regression coefficient (β) | 18.45 | 0.69 | 0.32 | -0.19 | -0.30 | 0.15 | -0.50 | |
| Standard error | 3.16 | 0.03 | 0.09 | 0.02 | 0.16 | 0.05 | 0.09 | |
| t-statistic | 5.84 | 26.31 | 3.47 | -8.32 | -1.83 | 2.76 | -5.28 | |
| P-value | 8.63E-09 | 2.92E-100 | 0.00055166 | 6.48E-16 | 0.06774829 | 0.00593864 | 1.87E-07 | |
| **$R^2$=0.672** | **Adjusted $R^2$=0.669** | | | **RMSE=9.04** | | **F-statistic=193** | | |

**Table A2.** PCR models for prediction of daily max 8-h $O_3$ for each measurement site

| **Welgegund** | **Constant** | **PC1** | **PC2** | **PC3** | **PC4** |
|---|---|---|---|---|---|
| **Regression coefficient** | -0.13 | -0.42 | 5.96 | 0.86 | -0.71 |
| **$R^2$** | 0.62 | | | | |
| **F-statistic** | 444 | | | | |
| **P-value** | 1.63E-226 | | | | |
| **Estimate of error variance (MSE)** | 35.98 | | | | |
| **RMSE** | 6.00 | | | | |
| **Botsalano** | **Constant** | **PC1** | **PC2** | **PC3** | **PC4** |
| **Regression coefficient** | -0.25 | -4.88 | -0.09 | 0.07 | -2.18 |
| **$R^2$** | 0.64 | | | | |
| **F-statistic** | 191 | | | | |
| **P-value** | 2.75E-94 | | | | |
| **Estimate of error variance (MSE)** | 31.67 | | | | |
| **RMSE** | 5.63 | | | | |
| **Marikana** | **Constant** | **PC1** | **PC2** | **PC3** | **PC4** |
| **Regression coefficient** | 0.01 | 4.15 | -3.73 | 1.01 | -9.93 |
| **$R^2$** | 0.77 | | | | |
| **F-statistic** | 516 | | | | |
| **P-value** | 8.94E-195 | | | | |
| **Estimate of error variance (MSE)** | 64.69 | | | | |
| **RMSE** | 8.04 | | | | |
| **Elandsfontein** | **Constant** | **PC1** | **PC2** | **PC3** | **PC4** |
| **Regression coefficient** | -0.31 | -0.38 | -2.31 | -1.44 | 10.36 |
| **$R^2$** | 0.61 | | | | |
| **F-statistic** | 217 | | | | |
| **P-value** | 1.53E-112 | | | | |
| **Estimate of error variance (MSE)** | 97.66 | | | | |
| **RMSE** | 9.88 | | | | |

**Table A3.** GAMs for prediction of daily max 8-h $O_3$ for each measurement site: includes tests for each smooth, the degrees of freedom for each smooth, adjusted R-squared for the model and deviance for the model

**GAM (Welgegund)**

Family: Gaussian
Link function: identity

Formula:
$O_3$ ~ s($O_3$-1) + s(T) + s(RH) + s(u) + s(v) + s($NO_2$) + s(NO) + s(CO)

Parametric coefficients:

| term | Estimate | Std. Error | t value | Pr(> \| t \| ) |
|---|---|---|---|---|
| (Intercept) | 45.5907 | 0.1075 | 423.9 | <2e-16 |

Approximate significance of smooth terms:

| | term | edf | Ref.df | F | p-value |
|---|---|---|---|---|---|
| 1 | s($O_3$-1) | 6.782 | 7.943 | 220.022 | < 2e-16 |
| 2 | s(T) | 6.277 | 7.493 | 16.296 | < 2e-16 |
| 3 | s(RH) | 4.422 | 5.485 | 40.596 | < 2e-16 |
| 4 | s(u) | 2.933 | 3.77 | 3.683 | 7.76E-03 |
| 5 | s(v) | 2.204 | 2.86 | 3.395 | 2.68E-02 |
| 6 | s($NO_2$) | 4.006 | 4.993 | 9.407 | 7.52E-09 |
| 7 | s(NO) | 2.532 | 3.248 | 20.323 | 1.76E-13 |
| 8 | s(CO) | 8.323 | 8.877 | 36.994 | < 2e-16 |

R-sq. (adj) = 0.79 Deviance explained = 79.3%
GCV score = 20.85 Scale est. = 20.39 n = 1763
AIC score = 10349 RMSE = 4.47

5

**Table A3.** Continued

**GAM (Botsalano)**

Family: Gaussian
Link function: identity

Formula:
$O_3$ ~ s($O_3$-1) + s(T) + s(Rad) + s(u) + s(v) + s(CO)

Parametric coefficients:

| term | Estimate | Std. Error | t value | Pr(> I t I ) |
|---|---|---|---|---|
| (Intercept) | 46.7474 | 0.2187 | 213.7 | <2e-16 |

Approximate significance of smooth terms:

| | term | edf | Ref.df | F | p-value |
|---|---|---|---|---|---|
| 1 | s($O_3$-1) | 3.088 | 3.912 | 66.936 | < 2e-16 |
| 2 | s(T) | 1 | 1 | 26.666 | 3.56E-07 |
| 3 | s(Rad) | 2.07 | 2.641 | 5.668 | 1.89E-03 |
| 4 | s(u) | 4.829 | 5.965 | 2.677 | 1.49E-02 |
| 5 | s(v) | 3.733 | 4.743 | 2.443 | 3.60E-02 |
| 6 | s(CO) | 4.332 | 5.396 | 35.054 | < 2e-16 |

R-sq. (adj) = 0.73 Deviance explained = 74.3%
GCV score = 23.96 Scale est. = 22.96 n = 480
AIC score = 28888 RMSE = 4.69

**Table A3.** Continued

**GAM (Marikana)**

Family: Gaussian
Link function: identity

Formula:
$O_3 \sim s(O_3\text{-}1) + s(T) + s(Rad) + s(u) + s(NO_2) + s(NO) + s(CO)$

Parametric coefficients:

| term | Estimate | Std. Error | t value | Pr(> I t I ) |
|---|---|---|---|---|
| (Intercept) | 51.0886 | 0.2629 | 194.3 | <2e-16 |

Approximate significance of smooth terms:

| | term | edf | Ref.df | F | p-value |
|---|---|---|---|---|---|
| 1 | $s(O_3\text{-}1)$ | 4.12 | 5.137 | 305.399 | < 2e-16 |
| 2 | s(T) | 1 | 1 | 18.271 | 2.22E-05 |
| 3 | s(Rad) | 1 | 1 | 29.151 | 9.58E-08 |
| 4 | s(u) | 4.441 | 5.541 | 3.117 | 6.80E-03 |
| 5 | $s(NO_2)$ | 5.213 | 6.323 | 3.46 | 2.25E-03 |
| 6 | s(NO) | 7.72 | 8.536 | 4.481 | 2.10E-05 |
| 7 | s(CO) | 3.619 | 4.574 | 23.334 | < 2e-16 |

| | | |
|---|---|---|
| R-sq. (adj) = 0.85 | Deviance explained = 85.4% | |
| GCV score = 44.90 | Scale est. = 42.86 | n = 620 |
| AIC score = 4119 | RMSE = 6.39 | |

**Table A3.** Continued

**GAM (Elandsfontein)**

Family: Gaussian
Link function: identity

Formula:
$O_3 \sim s(O_3\text{-}1) + s(T) + s(RH) + s(u) + s(NO_2) + s(NO)$

Parametric coefficients:

| term | Estimate | Std. Error | t value | Pr(> \| t \| ) |
|---|---|---|---|---|
| (Intercept) | 48.8052 | 0.3657 | 133.5 | <2e-16 |

Approximate significance of smooth terms:

| | term | edf | Ref.df | F | p-value |
|---|---|---|---|---|---|
| 1 | $s(O_3\text{-}1)$ | 1.664 | 2.1 | 341.565 | < 2e-16 |
| 2 | s(T) | 2.298 | 2.923 | 4.403 | 5.54E-03 |
| 3 | s(RH) | 1 | 1 | 61.999 | 1.58E-14 |
| 4 | s(u) | 4.759 | 5.871 | 5.371 | 3.04E-05 |
| 5 | $s(NO_2)$ | 1 | 1 | 4.94 | 2.66E-02 |
| 6 | s(NO) | 2.41 | 3.026 | 10.294 | 1.20E-06 |

R-sq. (adj) = 0.69 Deviance explained = 69.6%
GCV score = 78.56 Scale est. = 76.62 n = 573
AIC score = 4128 RMSE = 8.64

# CHAPTER 6

# GROWTH AND PHYSIOLOGICAL RESPONSES OF TWO SUGARCANE VARIETIES EXPOSED TO ELEVATED OZONE: A CASE STUDY

## 6.1 AUTHOR LIST, CONTRIBUTIONS AND CONSENT

**Tracey Leah Laban[1], Pieter Gideon van Zyl[1], Johan Paul Beukes[1], Jacques Maynard Berner[1], Philippus Daniel Riekert Van Heerden[2]**

[1]Unit for Environmental Sciences and Management, North-West University, Private Bag X6001, Potchefstroom, 2520, South Africa

[2]South African Sugarcane Research Institute, Private Bag X02, Mount Edgecombe, 4300, South Africa

The bulk of the work was done by the first author, **T.L. Laban**, including field work from 1 October 2014 to 31 May 2015, data collection, analysis, interpretation and writing of the manuscript. Contributions of the various co-authors were as follows: PG van Zyl and JP Beukes were the promoters of this study and assisted with conceptual ideas and editing of the manuscript. JM Berner provided the facilities and equipment and made conceptual contributions to the study. PDR van Heerden provided the plant material and contributed in an advisory capacity on study conception and design.

All the co-authors on the article have been informed that the PhD will be submitted in article format and have given their consent.

## 6.2 FORMATTING AND CURRENT STATUS OF ARTICLE

The article was formatted in accordance with the journal specifications to which it will be submitted, i.e. *South African Journal of Science*. The article is presented in the style, format and length required by the journal. The author's guide that was followed in preparation of the article was available at https://www.sajs.co.za/navigationMenu/view/guidelines-authors (Date of access: 25 May 2018). At the time when this PhD was submitted for examination, this article had not yet been submitted for review, but the intention is to submit it soon thereafter.

# Growth and physiological responses of two sugarcane varieties exposed to elevated ozone: A case study

Running head: Influence of elevated ozone levels on sugarcane varieties

Keywords: AOT40, crop impacts, carbon dioxide ($CO_2$), chlorophyll *a* fluorescence, open-top chambers, South Africa

**Tracey Leah Laban[1], Pieter Gideon van Zyl[1]*, Johan Paul Beukes[1], Jacques Maynard Berner[1], Philippus Daniel Riekert Van Heerden[2]**

1 Unit for Environmental Sciences and Management, North-West University, Private Bag X6001, Potchefstroom, 2520, South Africa
2 South African Sugarcane Research Institute, Private Bag X02, Mount Edgecombe, 4300, South Africa

*Correspondence to: P.G. van Zyl (pieter.vanzyl@nwu.ac.za);

Postal address: Private Bag X6001, South Africa, Potchefstroom, 2520; Tel: +27 18 299 2395; Fax: +27 18 299 2350

## Abstract

Surface ozone ($O_3$) pollution is known to have a detrimental impact on agriculture, while rising $CO_2$ concentrations are often found to protect plants against $O_3$ effects. Considering the important role of sugarcane (*Saccharum* spp.) as a major food crop in South Africa, the tolerance of this $C_4$ crop to $O_3$ damage must be established. Open-top chamber experiments were conducted, whereby two local sugarcane varieties (NCo376 and N31) were enclosed and exposed to controlled $O_3$ levels during the summer growth season to investigate the impact of elevated $O_3$ alone or combined with elevated carbon dioxide ($CO_2$). The treatments consisted of charcoal-filtered air, $O_3$ at 80 ppb, and $O_3$ at 80 ppb with $CO_2$ at 750 ppm. Two indicators of stress were monitored, namely plant growth (leaf and stalk parameters, and number of tillers) and plant physiological responses affecting photosynthetic performance (chlorophyll *a* fluorescence, chlorophyll content and stomatal conductance). Plant growth results indicate that $O_3$ had no significant effect on the NCo376 variety growth, while N31 sugarcane initially showed a response by some growth parameters, but revealed recovery during the vegetative growth phase. Physiological responses indicated that the photosynthetic efficiency of the NCo376 sugarcane variety is more sensitive to $O_3$ exposure. The combined effects of elevated $O_3$ and elevated $CO_2$ improved photosynthetic efficiency and chlorophyll content to a certain extent, while the hypothesis that elevated $CO_2$ protects plants from $O_3$ damage by reducing the stomatal conductance could not be conclusively proven. Results indicate that N31 sugarcane is likely to be more tolerant towards high $O_3$ levels compared to the traditionally reliable NCo376 variety, which may be potentially more viable for productivity in $O_3$-impacted regions.

## Introduction

Elevated concentrations of $O_3$ are globally recognised as a possible threat to vegetation and agricultural crops. Typical $O_3$-related stress effects include foliar injuries[1,2], damage to physiological functions, e.g. reduced photosynthesis[3], as well as reductions in growth and subsequent yields of crops.[4-6] The extent of these effects varies for different plant species and -varieties/cultivars.[7] $O_3$-induced damage to crops is expected to offset a significant portion of the GDP growth rate for economies that largely rely on agriculture.[8] In addition, as economies continue to expand, especially in developing countries, air pollution and $O_3$ concentrations are expected to increase, which could threaten crop production resulting in economic losses and threatening food security in those countries.[8,9] In India, for instance, it was calculated that $O_3$ damage to wheat and rice resulted in a total yield loss that could have been sufficient food supply for 94 million people living below the poverty line in that country.[10]

The extent of the adverse effects of $O_3$ on crops and other vegetation depends on the magnitude and duration of $O_3$ exposure. Long and Naidu[11] indicate two types of $O_3$ exposure, i.e. acute- and chronic exposures that have different impacts on plants. Acute exposure refers to the exposure of plants to very high levels of $O_3$ (> 120 ppb) for shorter periods (typically hours), while chronic exposure refers to plants being exposed to high $O_3$ concentrations (40-120 ppb) over several days.[11] Acute exposure can destroy plant cells, which manifests as visible injury on plants, while chronic exposure generally induces non-visible symptoms, e.g. decreased photosynthetic capacity and accelerated senescence.[11,12] According to Köllner and Krause,[13] very high $O_3$ episodes are more important for yield losses than constant elevated $O_3$ exposure. The impact of $O_3$ on vegetation is also influenced by other factors, such as soil moisture, temperature, solar radiation and relative humidity, which have an influence on stomatal conductance and consequently on $O_3$ uptake by plants.[14,15] Low humidity, for instance, causes plants to close their stomata and reduces plant transpiration, which will therefore also not absorb $O_3$ from the atmosphere.[16] Atmospheric $CO_2$ levels can also influence the impacts of $O_3$ on vegetation with elevated $CO_2$ possibly offsetting the detrimental impacts of $O_3$, which include reducing stomatal conductance and subsequent $O_3$ uptake into leaves, as well as providing substrates for detoxification and repair processes.[14]

The most commonly known indicators applied to estimate the potential risk of damage by $O_3$ on vegetation are the seasonal cumulative exposure over a threshold of 60 ppb or 40 ppb, i.e. SUM06 and AOT40, respectively.[17] SUM06 is recommended in the United States and is defined

as the sum of hourly mean $O_3$ concentrations when the hourly $O_3$ equals or exceeds 60 ppb,[15] while AOT40 is the standard in Europe, which refers to the hourly mean $O_3$ concentration accumulated above a threshold concentration of 40 ppb during daylight hours of the growing season.[18] The AOT40 critical level is 3 000 ppb h for agricultural crops and 5 000 ppb h for forests. $O_3$ exposure-response functions have been developed for a wide range of crops in the United States, Europe and, more recently, Asia through numerous controlled environment-, greenhouse- and field experiments[14] in order to establish air quality guidelines and yield response functions for vegetation (e.g. critical levels).

Sugarcane (*Saccharum spp.*) is an important agricultural crop grown in tropical and subtropical regions, from which sucrose and ethanol are commonly produced. Being a $C_4$ plant, it is assumed that sugarcane will be more tolerant to $O_3$ compared to $C_3$ crop species that are considered more sensitive to $O_3$. Studies have shown that photosynthesis in $C_3$ plants is affected by a lower carboxylation efficiency induced by $O_3$, which implies that the Rubisco enzyme that fixes atmospheric $CO_2$ in the Calvin cycle in photosynthesis is affected. $C_4$ plants, however, have an evolved mechanism in dry conditions to enhance the efficiency of the Rubisco enzyme by concentrating $CO_2$ around it, which allows the stomata to open less frequently.[19] Published peer-reviewed evidence of the sensitivity and/or tolerance of sugarcane with regard to elevated $O_3$ concentrations at present does not exist.[20] In addition, no $O_3$ exposure-response data exist for sugarcane for which yield response functions can be derived.

The aim of this study was to assess the sensitivity of two South African sugarcane cultivars to chronic $O_3$ exposure, either alone or combined with elevated $CO_2$, during the growth season in order to assist in establishing yield response functions for these plant species. High levels of surface ozone ($O_3$) air pollution occur in southern Africa, which increase significantly during late winter and early spring (hourly maximum $O_3$ exceeding 50 ppb) due to increased open biomass burning and household combustion.[21-23] These high $O_3$ levels coincide with the beginning of the growth season, which is typically in October with the onset of the wet season in the southern African interior.[24] Agriculture also contributes significantly to the economy in southern Africa, with large sugarcane production occurring in the eastern parts of this region. The specific objectives of this study were to determine the effects on the growth and physiology of sugarcane, as well as to establish whether increased ambient $CO_2$ concentrations would ameliorate these negative $O_3$ effects.

## Materials and methods

### Site characteristics and plant material

An open-top chamber (OTC) research facility at the North-West University, Potchefstroom, South Africa (26°40'50" S, 27°05'48" E, altitude 1348 m a.s.l.) was utilised to conduct $O_3$ exposure trials. These OTCs are transparent plastic 5 $m^3$ ventilated cylinders in which plants can be enclosed and the concentrations of air pollutants controlled, while maintaining natural climatic field conditions.[25] Since each chamber could accommodate eight potted plants, four of each of the two sugarcane varieties investigated were placed in each chamber. In total, 64 plants were used in the study.

Two commercial South African sugarcane cultivars, i.e. NCo376 and N31, were obtained from the South African Sugar Research Institute (SASRI). The N31 variety has the ability to grow rapidly and produce very high yields after an 18- to 24-month cycle, but has a relatively low sucrose content.[26] The NCo376 cultivar is a traditional South African variety with a relatively high sucrose content that produces good yields (although not as high as N31). However, the growth of the NCo376 cultivar is weaker than the N31 variety during severe water stress occurences.[27] The growth season of sugarcane coincides with warmers months, since favourable temperatures for sugarcane growth range between 22°C and 32°C.[28]

### Treatments

Speedlings of the N31 and NCo376 varieties were transplanted into 30 cm pots, which were placed inside the OTCs on 9 October 2014. Four chambers served as the control chambers, which only received carbon-filtered (Purafil filter) ambient air from which $O_3$ (< 4 ppb $O_3$) and other contaminants were removed. Plants in two OTCs were exposed only to 80 ppb $O_3$, while plants in two other OTCs were exposed to a mixture of 80 ppb $O_3$ and 750 ppm $CO_2$. These concentrations were maintained in each of the chambers during daytime (08:00-17:00) for the duration of the growth period. An $O_3$ generator (UV-20 HO, Olgear) was used to provide a continuous supply of additional $O_3$ into the ambient air stream feeding the OTCs to bring the $O_3$ concentration to the required level. The $O_3$ concentration in each chamber was controlled by means of an overflow valve, which could be adjusted to control the $O_3$ concentration within 10% of the target concentration in the chambers. The $O_3$ concentration in the OTCs was periodically

verified with an $O_3$ monitor (Model 205, 2B Technologies Inc.). The 80 ppb $O_3$ exposure levels were chosen in order to relate results obtained in this study for sugarcane to $O_3$ exposure-response data available for other South African crops at this level.[29,30] The selection of the 750 ppm $CO_2$ level (twice ambient concentrations) was based on the two upper representative concentration pathways (RCP 6.0 and 8.5) future scenarios used in the latest IPCC assessment report.[31] $CO_2$ exposure commenced on 5 November 2014, while $O_3$ treatment started on 20 November 2014. The plants were grown for almost eight months and the above-ground biomass of the plants was harvested on 18 May 2015.

The soil in the pots consisted of silica sand, vermiculite and filter press in a 4:1:½ ratio, together with a 5 cm layer of gravel placed at the bottom of the pots. The pots were placed over buckets that served as water reservoirs, which were connected to a network of irrigation tubing that converges into a main water source. All pots contained four nylon suction wicks immersed in water reservoirs to draw up the water into the growth medium. Irrigation by the pot-reservoir system was carried out every morning and evening to grow the plants under well-watered conditions in order to exclude drought stress. A fertiliser solution containing macro- and micro-nutrients ideal for sugarcane growth was applied to all pots once every three weeks and dissolved by irrigation.[32] Analysis of the soil indicated that pH, elemental concentrations, acidity and organic matter were all within acceptable limits for sugarcane.[32] The plants were also treated with insecticide to prevent disease and insect attack.[32]

### Growth measurements

The growth measurements, which were conducted twice a month, included the number of green and dead leaves, top visible dewlap (TVD) leaf length and width, stalk height and number of tillers. The TVD leaf blade refers to the uppermost fully expanded leaf with a clearly visible dewlap or collar (a band of membranous tissue between the leaf sheath and leaf blade) (http://edis.ifas.ufl.edu/sc076) often used in sugarcane studies. Green and dead leaves were counted starting from the base of the stalk to the TVD leaf, while the stalk height was measured from the soil surface to the TVD leaf. The number of tillers present for each plant was counted, excluding the main tiller (primary shoot or stalk).

### Chlorophyll *a* fluorescence and chlorophyll content measurements

Chlorophyll (Chl) *a* fluorescence is used to monitor photosystem II (PSII) activity and the processes that affect it,[33] which can be very useful in studying the effects of various stressors on

the physiological state of plants.[34] Illumination of photosynthetic samples, kept in darkness for some length of time, causes a rapid rise in fluorescence from PSII (~1 s), followed by a slow (few minutes) decline. Analysis of the fluorescence O-J-I-P transient, which describes the fluorescence changes that occur in less than 1 s, allows for the evaluation of the physiological condition of PSII and photosynthetic electron transport chain components.[35] A portable fluorimeter Handy PEA (Plant Efficiency Analyzer, Hansatech Instrument Ltd, UK) was used to measure the chl *a* fluorescence kinetics *in situ* at a 10 µs time resolution for 1 s. Measurements were taken at night to ensure that the sample leaves have already been dark-adapted for at least one hour. The first step in the measurement process was to cover the fully expanded area of the TVD leaf blade with a small, lightweight leaf clip. A high intensity (3 500 µMol.$m^{-2}$.$s^{-1}$), short flash (1s) was applied to the leaf, which transiently closes all PSII reaction centres, reducing the overall photochemical efficiency so that fluorescence levels rise for 1 to 2 seconds, after which the fluorescence levels typically decrease again over a time-scale of a few minutes.[36] Three replicate measurements were taken per plant. The first chl *a* fluorescence measurements were performed eight weeks after planting, where after monthly measurements were conducted.

The original fluorescence transients are double normalised between steps O (0.03 ms) and P (300 ms) of the O-J-I-P curve by using the initial ($F_0$) and maximum ($F_P$) fluorescence intensity to calculate the relative (or normalised) variable fluorescence, $V_{OP}$, between $F_0$ and $F_P$:

$$V_{\mathrm{OP}} = {(F_t - F_{0.03})}\Big/{(F_{300} - F_{0.03})}$$

where $F_t$ is the fluorescence intensity at time t after the onset of illumination; $F_{0.03}$ is the fluorescence intensity at 0.03 µs ($F_0$); and $F_{300}$ is the fluorescence intensity at 300 µs ($F_M$ or $F_P$). $V_{OP}$ values were normalised again to obtain the difference ($\Delta V_{OP} = V_{treatment} - V_{control}$) between the treated and control plant samples.

Chlorophyll content measurements commenced 17 weeks after planting, where after it was measured once a month. Three replicate measurements were made for each plant using a hand-held meter (Model CCM 300, Opti-Sciences, USA) by placing the leaf clip on the fully expanded area of the TVD leaf.

### Stomatal conductance measurements

Stomatal closure by plants in response to $O_3$ stress can be a protective mechanism to prevent the damaging effects of $O_3$ uptake by the leaves. However, closing of the stomata can also limit $CO_2$ absorption, which leads to decreased photosynthetic activity.[37] To assess $O_3$ uptake, stomatal conductance was measured once a month using a hand-held porometer (Model AP4, Delta-T Devices, Cambridge, UK). Three measurements were taken per plant on the fully expanded area of the TVD leaf between 12:00 and 2:00 pm.

### Meteorological measurements

Local meteorological conditions were obtained from the Welgegund atmospheric research station (6.57$^o$ S, 26.94$^o$ E, 1480 m a.s.l.) (http://www.welgegund.org/) for the period of the trial. Welgegund is located approximately 30 km from Potchefstroom and could provide detailed continuous monitoring data for meteorological parameters.[38,39]

## Results and discussion

### Meteorology during trial period

In Table 1, meteorological measurements relevant to plant activity are presented. As expected, the highest temperatures and global radiation were recorded during summer (December-January-February), while October also had relatively high global radiation values. Relative humidity and rainfall were the highest from November to March, which coincides with the characteristic wet season from mid-October to mid-May in this region.[38] Comparison of ambient temperature and relative humidity measured at Welgegund with measurements conducted inside the OTCs indicated that the temperature and relative humidity were somewhat higher (by 2-5$^o$C and 10-20%, respectively) inside the chambers compared to ambient conditions.

**TABLE 1:** Ambient temperature, global radiation, relative humidity and monthly accumulated precipitation during the period of the OTC trial. Monthly averages are presented with the minimum and maximum values given in parenthesis.

| Month | Temperature ($^oC$) | Global radiation ($W/m^2$) | Relative humidity (%) | Accumulated precipitation (mm) |
|---|---|---|---|---|
| Oct-14 | 20 (4−32) | 291 (0−1086) | 40 (6−99) | 6 |
| Nov-14 | 19 (7−30) | 252 (0−1165) | 60 (13−100) | 25 |
| Dec-14 | 21 (13−32) | 270 (0−1207) | 62 (11−100) | 16 |
| Jan-15 | 21 (12−33) | 298 (0−1219) | 63 (11−100) | 55 |
| Feb-15 | 22 (11−34) | 303 (0−1143) | 52 (9−99) | 10 |
| Mar-15 | 19 (10−30) | 231 (0−1061) | 64 (10−100) | 21 |
| Apr-15 | 17 (4−26) | 212 (0−924) | 58 (9−100) | 8 |
| May-15 | 17 (5−28) | 192 (0−831) | 35 (7−99) | 0 |

## Visible foliar injuries

Visual inspection at regular intervals for any signs of injury on plants revealed yellow patches and brown rust specks/dots on the leaf surface, which could be signs of chlorosis and necrosis, as well as accelerated senescence.[2] However leaf injury was only found on some of the plants representing each cultivar, while the magnitude of these effects could not be distinguished between the two cultivars.

## Growth parameters

In Figure 1, the various growth parameters measured for the two sugarcane varieties in the control chamber, the $O_3$ exposed chamber, and the combined $O_3$ and $CO_2$ exposed chamber are presented. Comparison of the two sugarcane cultivars in the control chambers indicates that NCo376 generally has more green leaves than the N31 variety, while elevated $O_3$ levels had no significant effect on the number of green leaves for both varieties. However, combining elevated $O_3$ and $CO_2$ levels led to a slightly higher number of green leaves for N31. Both exposure conditions also do not seem to affect the number of dead leaves for NCo376, while the N31 cultivar had fewer dead leaves compared to its control. In general, it seems that $O_3$ exposure does not have a signifcant effect on leaf lifetime (accelerated leaf senescence). The N31 variety generally has a higher TVD leaf length and -width compared to the NCo376 cultivar.

Comparison of the exposed samples to the control indicated that TVD leaf length and -width for the N31 variety were higher (approximately 25 cm longer and 1 cm wider) in the control sample after five weeks, while a marginal difference is observed for the NCo376 cultivar after this period. However, after 13 to 15 weeks, no signifcant difference in TVD leaf length and -width was observed for N31, which is indicative of these plants adapting to the exposure. For the NCo376 cultivar, the combined exposure to $O_3$ and $CO_2$ increased its TVD length significantly (~10 cm) after 17 weeks, which indicates a positive response to additional $CO_2$. Exposure of the NCo376 sugarcane did not cause any difference in the stalk height in the plants. However, the stalk heights of the N31 variety were ~15% higher in the controlled samples, which could translate to a significant reduction in terms of yield and profitability of the crop. Comparison of the influence of exposure on the number of tillers of the two sugarcane cultivars indicates that the number of tillers of NCo376 were relatively lower for plants exposed to $O_3$ and $CO_2$, while the N31 variety had relatively signifcant less tillers when exposed to only $O_3$. An increased number of tillers is related to increased yield and millable harvest. These results indicate that elevated $O_3$ had no significant impact on most of the growth parameters of NCo376. The N31 cultivar showed some response from growth symptoms when exposed to elevated $O_3$. However, these results also indicate that the N31 variety has the ability to adapt to increased $O_3$ levels.

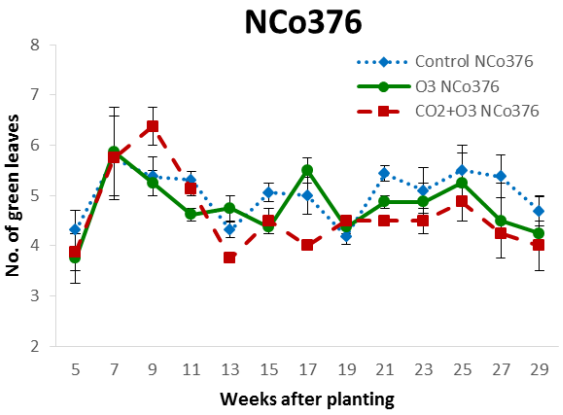


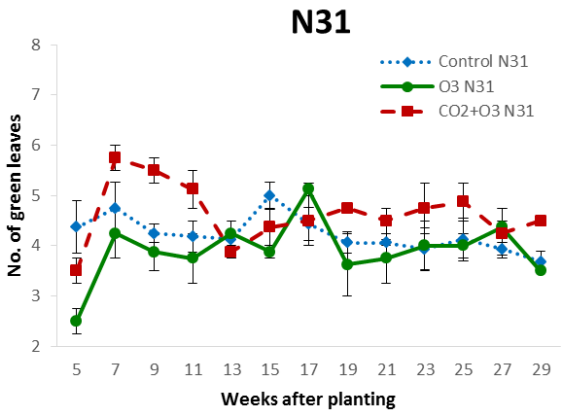

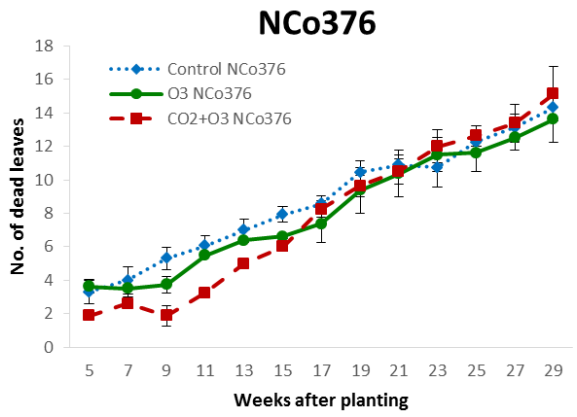
NCo376
Control NCo376
O3 NCo376
CO2+O3 NCo376
No. of dead leaves
Weeks after planting

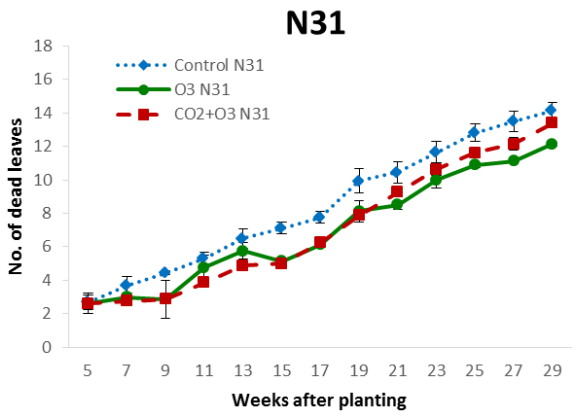
N31
Control N31
O3 N31
CO2+O3 N31
No. of dead leaves
Weeks after planting

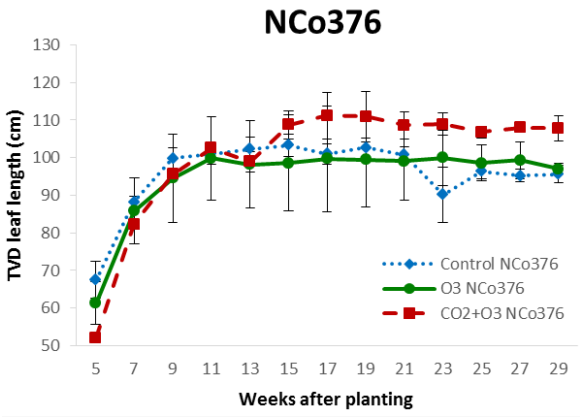
NCo376
Control NCo376
O3 NCo376
CO2+O3 NCo376
TVD leaf length (cm)
Weeks after planting

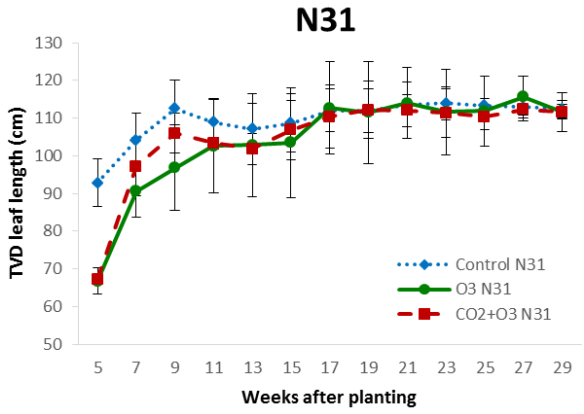
N31
Control N31
O3 N31
CO2+O3 N31
TVD leaf length (cm)
Weeks after planting

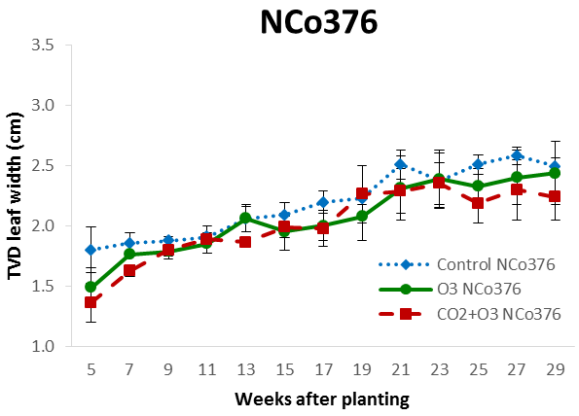
NCo376
Control NCo376
O3 NCo376
CO2+O3 NCo376
TVD leaf width (cm)
Weeks after planting

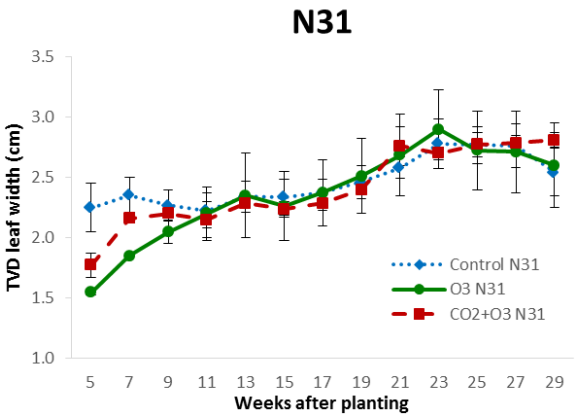
N31
Control N31
O3 N31
CO2+O3 N31
TVD leaf width (cm)
Weeks after planting

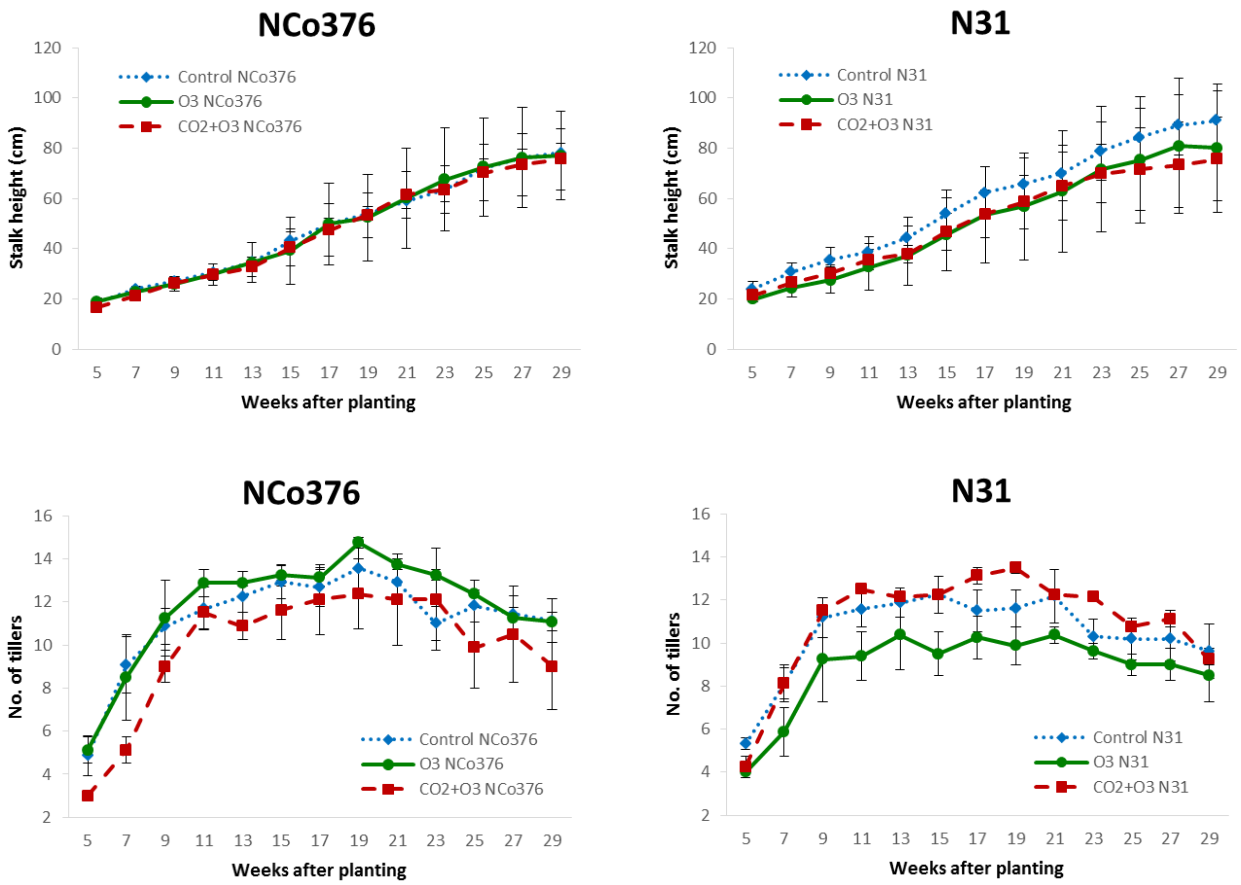


**FIGURE 1:** Mean values (± standard error) of growth parameters determined for NCo376 and N31 cultivars in different OTC experiments.

## Chl *a* fluorescence

In order to compare the difference in fluorescence transients between the $O_3$-treated and control plants, the difference in relative $\Delta V_{OP}$ from 0.03 to 300 ms was calculated, which is shown in Figure 2. The trial was divided into three periods, i.e. Dec 2014 to Jan 2014; Feb 2015 to March 2015 and Apr 2015 to May 2015, which represent different stages of growth. The average chlorophyll *a* fluorescence transient measured for each of these periods was used to calculate $\Delta V_{OP}$. The most affected components of the photosynthetic electron transport chain appear to be the ΔJ-band (at approximately 2 ms) and the ΔI-band (at approximately 30 ms).

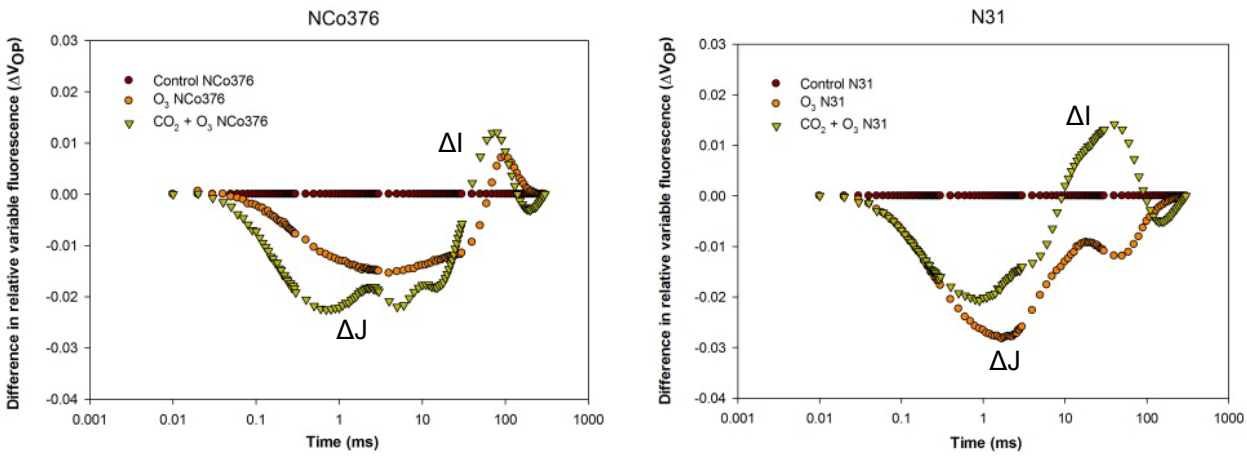


**(a) Dec 2014 to Jan 2015**

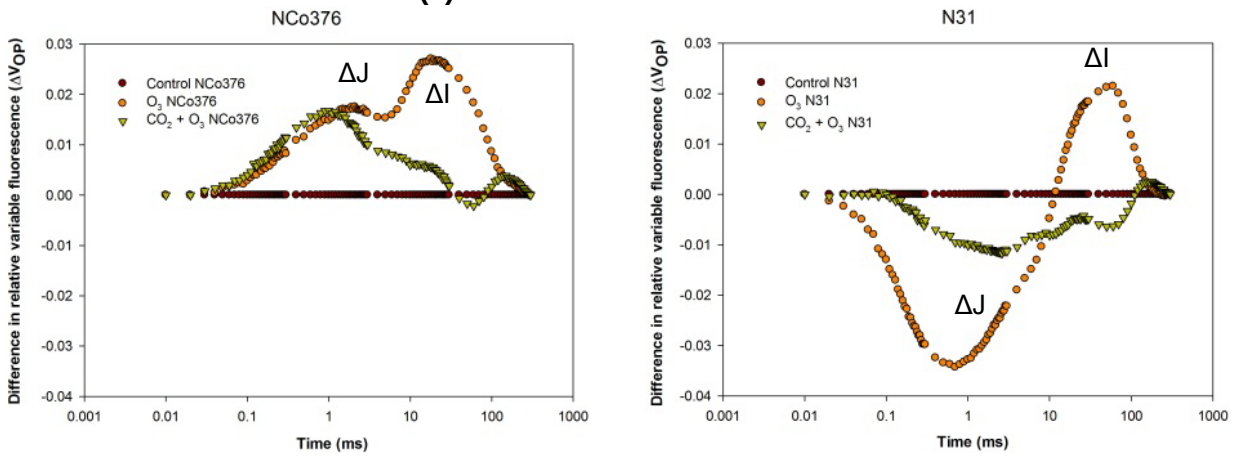


**(b) Feb 2015 to Mar 2015**

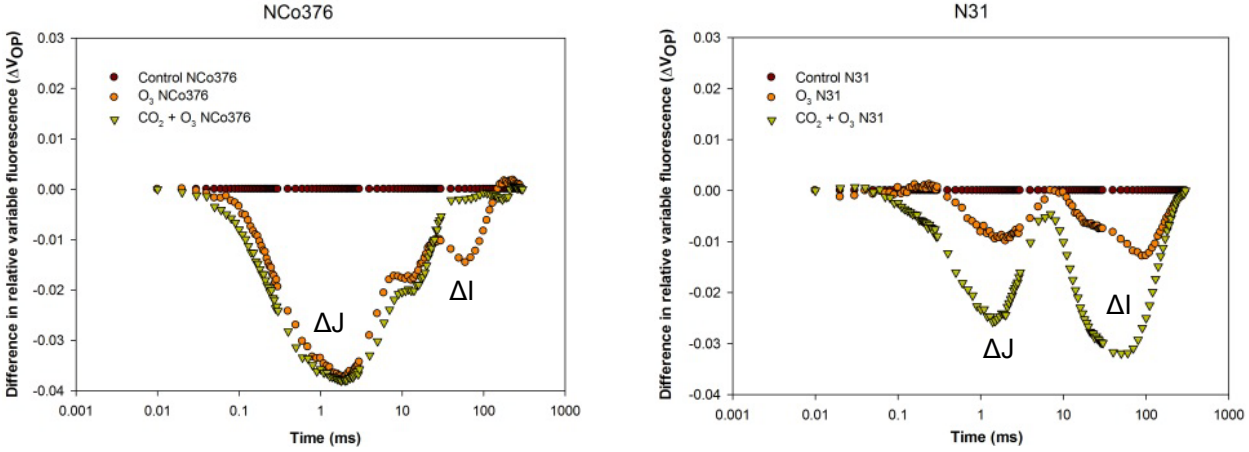


**(c) Apr 2015 to May 2015**

**FIGURE 2:** $\Delta V_{OP}$ (= $V_{treatment} - V_{control}$) determined for NCo376 and N31 leaves after exposure to elevated $O_3$, as well as elevated $O_3$ combined with $CO_2$ in OTCs during different stages of growth.

The ΔJ band of the fluorescence transients represents the redox state of the primary quinone acceptor of PSII, i.e. $Q_A$. A positive ΔJ-band indicates the accumulation of reduced $Q_A$ ($Q_A^-$), which cannot be reoxidised since electrons are blocked and cannot move beyond $Q_A^-$ to the secondary quinone acceptor, $Q_B^-$ of PSII.[40] A negative ΔJ-band indicates more efficient flow of electrons beyond $Q_A^-$. Both cultivars exposed to $O_3$ demonstrate a negative band early in the growth season as observed in Figure 2(a). In the middle of the growth season (Figure 2(b)), NCo376 displays a positive ΔJ-band, indicating an inability of the electron transport system to transfer electrons, which suggests a relatively more stressed environment. No positive ΔJ-band is evident for N31 during this stage of growth, which points to the resistant physiological properties of this cultivar. Towards the latter part of the growing season (Figure 2(c)), the presence of a negative ΔJ-band in both $O_3$-treated cultivars suggests plant recovery over a longer duration of stress. The ΔJ-band for the sugarcane varieties exposed to a combination of $O_3$ and $CO_2$ follows a similar pattern than that observed for only elevated $O_3$ exposure.

The ΔI-band represents the accumulation of electrons between PSII and PSI.[41] Exposure of both cultivars to $O_3$ indicated a positive ΔI band during the middle of the growth season (Figure 2(b)), which implies inhibition of the reduction of end electron acceptors at the PSI acceptor.[41] The ΔI-band determined for the combined exposure to $CO_2$ and $O_3$ during this middle of the growth season period, indicated less stressed conditions for the plants compared to only $O_3$ exposure. However, during the early part of the growth season (Figure 2(a)), a positive ΔI-band was also observed for cultivars exposed to $O_3$ and $CO_2$, suggesting hindrances to the photosynthetic electron transport chain near PSI and end electron acceptors. According to chl *a* fluorescence measurements, it seems that changes in the photosynthetic performance of the NCo376 cultivar are more sensitive to the stress associated with elevated $O_3$ exposure than the N31 variety.

## Chlorophyll content

Leaf chlorophyll content also provides valuable information on the physiological status of plants, since chlorophyll molecules absorb radiation that provides energy essential for photosynthesis. It can be observed from the controls in Figure 4 that NCo376 has a higher chlorophyll content than N31. From Figure 3, it seems that the chlorophyll content of the NCo376 cultivar is more sensitive to $O_3$ exposure, as indicated by the decrease in chlorophyll content of the samples exposed to $O_3$ from week 17 to week 21. The measurements also indicate that the chlorophyll content of the NCo376 cultivar recovers during continued exposure to $O_3$. However, at the end

of the trial period, the chlorophyll content of the NCo376 cultivar did decrease significantly. The decrease in the chlorophyll content of the NCo376 sample exposed to elevated $O_3$ and $CO_2$ was lower compared to the decrease observed for exposure only to elevated $O_3$. The chlorophyll content of the N31 variety shows no significant response to $O_3$ exposure, which emphasises the resistant properties of N31.

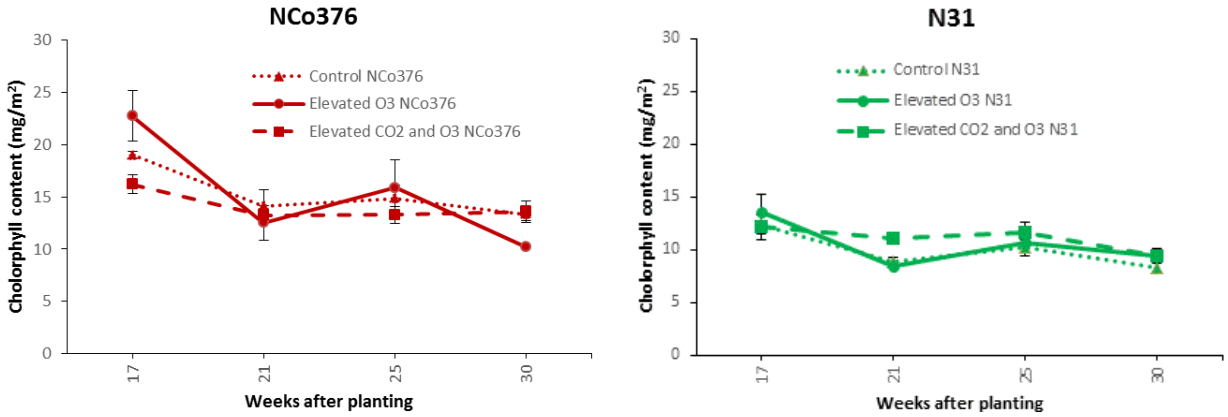


**FIGURE 3:** Mean values (± standard error) of chlorophyll content ($mg/m^2$) of NCo376 and N31 leaves after exposure to elevated $O_3$, and combined elevated $O_3$ and $CO_2$ in OTCs.

## Stomatal conductance

In Figure 4, the stomatal conductances measured for the sugarcane varieties are presented. Stomatal conductance is regulated by means of vapour pressure deficit (VPD), soil moisture deficit, phenology, global radiation and temperature.[42] While higher VPD increases the physical process of diffusion, enabling plants to transpire, plants may regulate water loss through stomatal closure. High VPDs resulting in stomatal closure often tend to occur concurrently with high $O_3$ concentrations. However, VPD is ultimately the limiting factor for $O_3$ uptake leading to a lower $O_3$ influx into the leaves. In general, the stomatal conductance was the highest during the rainy summer months (13-21 weeks after planting), and decreased as the growth season progressed into the drier autumn months (25-32 weeks after planting) (Table 1), pointing to the importance of VPD on stomatal conductance.

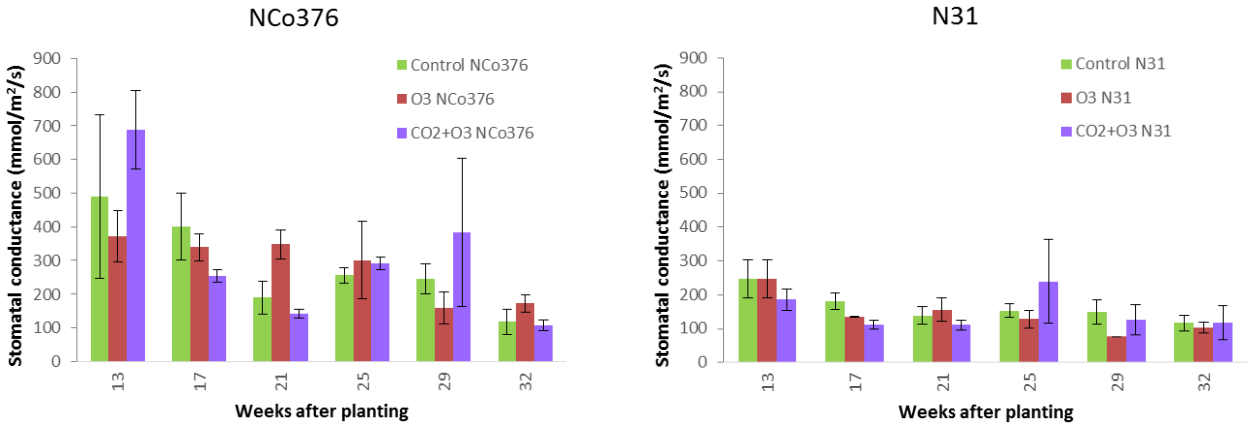


**FIGURE 4:** Mean values (± standard error) of stomatal conductance of NCo376 and N31 leaves after exposure to charcoal filtered air (control), elevated $O_3$ (80 ppb) and elevated $O_3$ and $CO_2$ (80 ppb and 750 ppm) in open-top chambers.

Higher stomatal conductances are associated with the NCo376 as indicated in Figure 3, which is indicative of faster-growing species that might be more sususcpetable to elevated $O_3$ levels. The stomatal conductance of the two sugercane cultivars was not significantly different for the control samples compared to samples exposed to elevated $O_3$ levels, which may result in more $O_3$ entering the plants causing possible damage, especially for the NCo376 variety. N31 plants showed a marginal decrease in stomatal conductance in response to elevated $O_3$ exposure, which suggests that N31 could be more resistant to the $O_3$ threat. Increased $CO_2$ levels in conjunction with elevated $O_3$ increased stomatal conductance in certain instances for the

NCo376 variety, while no conclusive contribution to stomatal conductance is observed for the N31 cultivar in the combined exposure to elevated $CO_2$ and $O_3$.

## AOT40 for field conditions

In an effort to obtain an approximate AOT40 for the region where the trials were performed, monthly AOT values were calculated for the sugarcane growth season, i.e. trial period in this study by utilising continuously measured $O_3$ data at Welgegund. Ambient $O_3$ concentrations measured at Welgegund during the trial period are presented in Figure 5(a), from which daytime levels (08:00-17:00) were used to calculate AOT40 values. In Europe, AOT40 is only calculated for three months (May to July), while the daylight period might also be shorter.[43] From Figure 5(b), it is evident that the European cumulative AOT40 critical level of 3 000 ppb h for agricultural crops is reached within the first three months at Welgegund, which indicates that there would be considerable exceedances of the European AOT40 standard for crop damage if it was applied in southern Africa. Although higher concentration thresholds have been suggested for southern Africa, the European OTC experiments demonstrated that the 40 ppb threshold provides a much better linear fit to the exposure-response data than the use of higher thresholds.[6] Nevertheless, linear exposure-response relationships at higher critical levels must be investigated for locally adapted crops. The necessity for an adapted threshold for southern Africa is emphasised in this study as the AOT40 calculated in ambient air at Welgegund was almost 10 000 ppb h for the growth period (October to May), while, inside the chamber, the AOT40 was much higher (80-40 ppb*9 hours*179 days = 64440 ppb h) due to daily chronic exposure to $O_3$ levels of 80 ppb from 08:00 to 17:00 during the fumigation period.

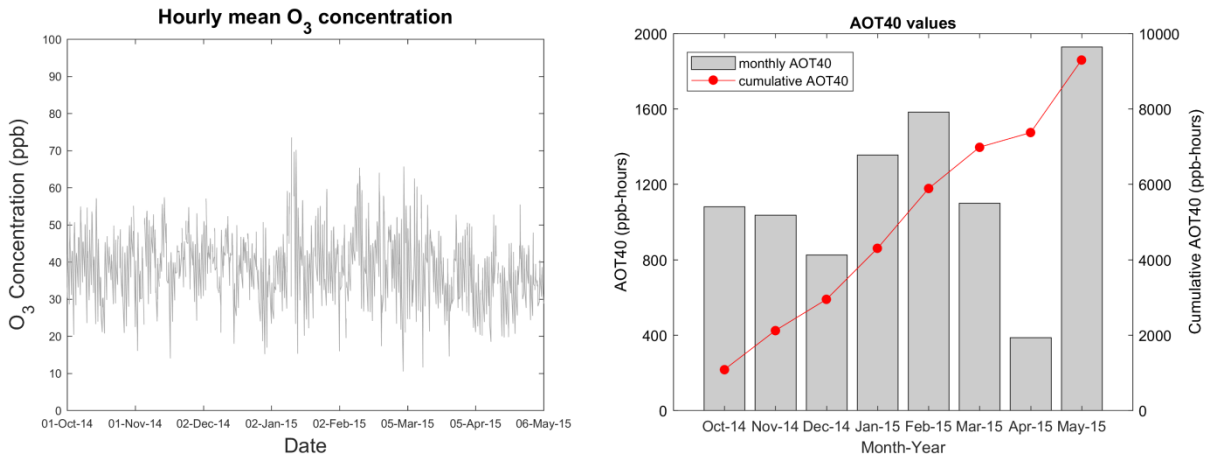


(a) (b)

**FIGURE 5:** (a) Average hourly $O_3$ concentration and (b) AOT40 (including cumulative values) at Welgegund, a background site near Potchefstroom during the trial period.

## Conclusions

This study provides an explorative assessment of the sensitivity of two local sugarcane cultivars in South Africa to elevated atmospheric $O_3$ levels, as well as combined elevated $O_3$ and $CO_2$ concentrations, which, as far as the authors can assess, is the first attempt to present quantitative exposure-response data on sugarcane under controlled conditions. Although visible injuries were observed on some of the plants, there was no consistency in the visible damage across all plants exposed to $O_3$. The growth parameters of the NCo376 cultivar showed no significant response to increased $O_3$, while the growth of the N31 variety indicated some response to increased $O_3$, but also the ability to adapt to increased $O_3$ levels. There were some indications that elevated $CO_2$ ameliorated the effects of elevated $O_3$ on growth, especially for the N31 cultivar. Chl *a* fluorescence, chlorophyll content and stomatal conductance measurements indicated that the physiological functions (photosynthesis) of the NCo376 sugarcane variety are more sensitive to $O_3$ exposure, while photosynthetic performance of the N31 cultivar did not show any significant response. The combined effects of elevated $O_3$ and elevated $CO_2$ improved photochemical efficiency and chlorophyll content relative to the $O_3$-treated plants to a certain extent, with the effects more pronounced for N31 than NCo376. The

hypothesis that elevated $CO_2$ protects plants from $O_3$ damage by reducing the stomatal conductance and reducing stomatal $O_3$ uptake[44] could not be conclusively proven in this study. In general, the results indicate that N31 is likely to be more tolerant towards high $O_3$ levels when compared to NCo376, and may potentially yield better crops in regions where high atmospheric $O_3$ concentrations are prevalent.

It has been argued that OTCs provide climatic conditions similar, but not identical to outside field conditions, which could result in an overestimation of the response of plants to the effects on increased atmospheric pollutants.[7,45] Therefore, our results, which can be considered an overestimation compared to field conditions, suggest that chronic exposure to $O_3$ levels of 80 ppb did not induce significant stress and adverse effects in the sugarcane. These results suggest the capability of plant species to evolve in order to tolerate and adapt to elevated $O_3$ levels as seen in some Mediterranean species.[46]

It is recommended that future studies should also determine the acute effects of exposure to very high $O_3$ concentrations (>120 ppb) for short periods of time. In addition, in this study, the influence of abiotic factors (e.g. soil water stress, heat stress) together with increased $O_3$ exposure was not investigated. In semi-arid conditions, drought is considered to be the stronger stress factor on vegetation. Therefore, the combination of $O_3$ and drought might produce plant responses that either reduce (mask) or exacerbate the damaging effects of $O_3$ on sugarcane, which must be investigated.

## Acknowledgements

This work is based on the research supported in part by the National Research Foundation of South Africa (Grant Numbers 97006 and 111287). Opinions expressed and conclusions arrived at are those of the authors and are not necessarily to be attributed to the NRF. The authors are grateful to SASRI for supplying the plant materials. Thanks and appreciation is conveyed to Prabhu Inbaraj, Charné Malan, Monja Gerber and Mmbulaheni Netshimbupfe for assistance with fieldwork and data processing.

## References


1. De Temmerman L, Karlsson GP, Donnelly A, Ojanperä K, Jäger H-J, Finnan J, et al. Factors influencing visible ozone injury on potato including the interaction with carbon dioxide. European Journal of Agronomy. 2002;17(4):291-302.
2. Benton J, Fuhrer J, Gimeno B, Skärby L, Palmer-Brown D, Ball G, et al. An international cooperative programme indicates the widespread occurrence of ozone injury on crops. Agriculture, Ecosystems & Environment. 2000;78(1):19-30.
3. Karnosky DF, Skelly JM, Percy KE, Chappelka AH. Perspectives regarding 50 years of research on effects of tropospheric ozone air pollution on US forests. Environmental Pollution. 2007;147(3):489-506.
4. Biswas D, Xu H, Li Y, Sun J, Wang X, Han X, et al. Genotypic differences in leaf biochemical, physiological and growth responses to ozone in 20 winter wheat cultivars released over the past 60 years. Global Change Biology. 2008;14(1):46-59.
5. Piikki K, Vorne V, Ojanperä K, Pleijel H. Potato tuber sugars, starch and organic acids in relation to ozone exposure. Potato Research. 2003;46(1-2):67-79.
6. Fuhrer J, Skärby L, Ashmore MR. Critical levels for ozone effects on vegetation in Europe. Environmental Pollution. 1997;97(1-2):91-106.
7. Feng Z, Kobayashi K. Assessing the impacts of current and future concentrations of surface ozone on crop yield with meta-analysis. Atmospheric Environment. 2009;43(8):1510-1519.
8. Van Dingenen R, Dentener FJ, Raes F, Krol MC, Emberson L, Cofala J. The global impact of ozone on agricultural crop yields under current and future air quality legislation. Atmospheric Environment. 2009;43(3):604-618.
9. Wang X, Mauzerall DL. Characterizing distributions of surface ozone and its impact on grain production in China, Japan and South Korea: 1990 and 2020. Atmospheric Environment. 2004;38(26):4383-4402.
10. Ghude SD, Jena C, Chate D, Beig G, Pfister G, Kumar R, et al. Reductions in India's crop yield due to ozone. Geophysical Research Letters. 2014;41(15):5685-5691.
11. Long S, Naidu S. Effects of oxidants at the biochemical, cell and physiological levels, with particular reference to ozone. Air Pollution and Plant Life. 2002;2:69-88.
12. Krupa S, Grünhage L, Jäger H-J, Nosal M, Manning W, Legge A, et al. Ambient ozone ($O_3$) and adverse crop response: a unified view of cause and effect. Environmental Pollution. 1995;87(1):119-126.

13. Köllner B, Krause G. Changes in carbohydrates, leaf pigments and yield in potatoes induced by different ozone exposure regimes. Agriculture, Ecosystems & Environment. 2000;78(2):149-158.
14. Fiscus EL, Booker FL, Burkey KO. Crop responses to ozone: uptake, modes of action, carbon assimilation and partitioning. Plant, Cell & Environment. 2005;28(8):997-1011.
15. Pochanart P, Akimoto H, Kinjo Y, Tanimoto H. Surface ozone at four remote island sites and the preliminary assessment of the exceedances of its critical level in Japan. Atmospheric Environment. 2002;36(26):4235-4250.
16. Kavassalis SC, Murphy JG. Understanding ozone-meteorology correlations: A role for dry deposition. Geophysical Research Letters. 2017;44(6):2922-2931.
17. Mauzerall DL, Wang X. Protecting agricultural crops from the effects of tropospheric ozone exposure: reconciling science and standard setting in the United States, Europe, and Asia. Annual Review of Energy and the Environment. 2001;26(1):237-268.
18. CLRTAP. Mapping critical levels for vegetation, Chapter III of Manual on methodologies and criteria for modelling and mapping critical loads and levels and air pollution effects, risks and trends. UNECE Convention on Long-Range Transboundary Air Pollution. 2014.
19. Lara MV, Andreo CS. $C_4$ plants adaptation to high levels of $CO_2$ and to drought environments. Abiotic Stress in Plants-Mechanisms and Adaptations: InTech; 2011.
20. Moura BB, Hoshika Y, Ribeiro RV, Paoletti E. Exposure-and flux-based assessment of ozone risk to sugarcane plants. Atmospheric Environment. 2017.
21. Laakso L, Beukes JP, Van Zyl PG, Pienaar JJ, Josipovic M, Venter AD, et al. Ozone concentrations and their potential impacts on vegetation in southern Africa. In: Matyssek R, Clarke N, Cudlin P, Mikkelsen TN, Tuovinen J-P, Wieser G, et al., editors. Climate change, air pollution and global challenges understanding and perspectives from forest research: Elsevier; 2013. p. 1 online resource (647 pages).
22. Zunckel M, Venjonoka K, Pienaar JJ, Brunke EG, Pretorius O, Koosialee A, et al. Surface ozone over southern Africa: synthesis of monitoring results during the Cross Border Air Pollution Impact Assessment project. Atmospheric Environment. 2004;38(36):6139-6147.
23. Laban TL, van Zyl PG, Beukes JP, Vakkari V, Jaars K, Borduas-Dedekind N, et al. Seasonal influences on surface ozone variability in continental South Africa and implications for air quality. Atmospheric Chemistry and Physics Discussions. 2018.

24. Wessels KJ, Prince S, Malherbe J, Small J, Frost P, Van Zyl D. Can human-induced land degradation be distinguished from the effects of rainfall variability? A case study in South Africa. Journal of Arid Environments. 2007;68(2):271-297.
25. Heyneke E, Smit P, Van Rensburg L, Kruger G. Open-top chambers to study air pollution impacts in South Africa. Part I: microclimate in open-top chambers. South African Journal of Plant and Soil. 2012;29(1):1-7.
26. South African Sugarcane Research Institute. Information Sheet Variety N31 2006 [cited 2018 3 April]. Available from: http://www.sasa.org.za/Libraries/Variety_Information/N31.sflb.ashx.
27. South African Sugarcane Research Institute. Information Sheet Variety NCo376 2006 [cited 2018 3 April]. Available from: www.sasa.org.za/Libraries/Variety_Information/NCo376.sflb.ashx.
28. Inman-Bamber N, Smith D. Water relations in sugarcane and response to water deficits. Field Crops Research. 2005;92(2-3):185-202.
29. Berner J, Maliba B, Inbaraj P. Impact of elevated levels of $CO_2$ and $O_3$ on the yield and photosynthetic capabilities of Brassica napus. Procedia Environmental Sciences. 2015;29:255.
30. Scheepers CCW. Physiological and biochemical constraints on photosynthesis of leguminous plants induced by elevated ozone in open–top chambers. MSc dissertation, Potchefstroom, North-West University; 2011.
31. IPCC. Climate change 2013: The physical science basis: contribution of Working Group I to the Fifth Assessment Report of the Intergovernmental Panel on Climate Change. Stocker TF, Qin D, Plattner G-K, Tignor M, Allen SK, Boschung J, et al., editors: Cambridge University Press; 2013.
32. Malan C. Influence of elevated $CO_2$ on the growth, yield and photosynthesis of sugarcane. MSc dissertation, Potchefstroom, North-West University; 2017.
33. Schansker G, Tóth SZ, Strasser RJ. Dark recovery of the Chl *a* fluorescence transient (OJIP) after light adaptation: the qT-component of non-photochemical quenching is related to an activated photosystem I acceptor side. Biochimica et Biophysica Acta (BBA)-Bioenergetics. 2006;1757(7):787-797.
34. Stirbet A. On the relation between the Kautsky effect (chlorophyll *a* fluorescence induction) and photosystem II: basics and applications of the OJIP fluorescence transient. Journal of Photochemistry and Photobiology B: Biology. 2011;104(1-2):236-257.

35. Kalaji HM, Jajoo A, Oukarroum A, Brestic M, Zivcak M, Samborska IA, et al. Chlorophyll *a* fluorescence as a tool to monitor physiological status of plants under abiotic stress conditions. Acta Physiologiae Plantarum. 2016;38(4):102.
36. Maxwell K, Johnson GN. Chlorophyll fluorescence—a practical guide. Journal of Experimental Botany. 2000;51(345):659-668.
37. Efeoğlu B, Ekmekci Y, Cicek N. Physiological responses of three maize cultivars to drought stress and recovery. South African Journal of Botany. 2009;75(1):34-42.
38. Tiitta P, Vakkari V, Croteau P, Beukes JP, van Zyl PG, Josipovic M, et al. Chemical composition, main sources and temporal variability of $PM_1$ aerosols in southern African grassland. Atmospheric Chemistry and Physics. 2014;14(4):1909-1927.
39. Beukes JP, Van Zyl PG, Venteric AD, Josipov M, Jaars K, Tiitta P, et al. Source region plume characterisation of the interior of South Africa as observed at Welgegund. Clean Air Journal/Tydskrif vir Skoon Lug. 2013;23(1):7-10.
40. Strasser RJ, Tsimilli-Michael M, Srivastava A. Analysis of the chlorophyll a fluorescence transient. Chlorophyll a fluorescence: Springer; 2004. p. 321-362.
41. Strasser RJ, Tsimilli-Michael M, Dangre D, Rai M. Biophysical phenomics reveals functional building blocks of plants systems biology: a case study for the evaluation of the impact of mycorrhization with Piriformospora indica. Advanced Techniques in Soil Microbiology: Springer; 2007. p. 319-341.
42. Emberson L, Ashmore M, Cambridge H, Simpson D, Tuovinen J-P. Modelling stomatal ozone flux across Europe. Environmental Pollution. 2000;109(3):403-413.
43. Van Tienhoven AM, Otter L, Lenkopane M, Venjonoka K, Zunckel M. Assessment of ozone impacts on vegetation in southern Africa and directions for future research: commentary. South African Journal of Science. 2005;101(3-4):143-148.
44. Harmens H, Mills G, Emberson LD, Ashmore MR. Implications of climate change for the stomatal flux of ozone: a case study for winter wheat. Environmental Pollution. 2007;146(3):763-770.
45. Feng Z, Kobayashi K, Ainsworth EA. Impact of elevated ozone concentration on growth, physiology, and yield of wheat (Triticum aestivum L.): a meta-analysis. Global Change Biology. 2008;14(11):2696-2708.
46. Paoletti E. Impact of ozone on Mediterranean forests: a review. Environmental Pollution. 2006;144(2):463-474.

# CHAPTER 7

## PROJECT EVALUATION AND FUTURE RESEARCH

*In this chapter, the successes and shortcomings of the project are evaluated against the specific objectives defined in Chapter 1. Research efforts presented in Chapters 4, 5 and 6 are contributing to the advancement of knowledge on regional $O_3$ in southern Africa but gaps in the knowledge remain. Therefore this chapter concludes with recommendations for future research.*

## 7.1 PROJECT EVALUATION

The project presented in this thesis was an atmospheric measurement-based study, using continuous, long-term $O_3$ measurements, which are crucial to gain insights into atmospheric processes and for the validation of atmospheric models. As there are few reported observations of $O_3$ in the southern African environment, this project tries to build a regional picture of $O_3$ in four different environments, i.e. clean savannah at Botsalano, polluted savannah at Marikana, semi-clean grassland at Welgegund and polluted grassland at Elandsfontein. The research described here makes a contribution to three main areas: (1) understanding the regional and seasonal $O_3$ pollution variability over continental South Africa, and the most important sources contributing to elevated $O_3$ concentrations in this region; (2) quantifying the influence of chemical and meteorological factors on surface $O_3$ levels over continental South Africa through statistical analysis; and (3) investigating the impact of elevated $O_3$ on sugarcane, which is an important, regional agricultural crop. Understanding these key areas is crucial to air quality policy and atmospheric science. However, despite the research efforts to advance the knowledge on surface $O_3$ in southern Africa, gaps in the knowledge still remain. The five specific objectives listed in Chapter 1 are each evaluated in terms of the successes and limitations, while some insights into future directions relevant to the research topic are later recommended.

### 7.1.1 Determine the spatial and temporal variation of $O_3$ at background and source locations in the north-eastern interior of South Africa

High quality continuous $O_3$ ground observational data together with other gas species data relevant to surface $O_3$ were obtained for a number of years at four sites in the north-eastern interior of South Africa, representative of regional background and anthropogenically polluted regions in continental South Africa. From these measurements, spatio-temporal variations of $O_3$ in continental South Africa could be derived. In general, the monthly $O_3$ concentrations showed a well-defined seasonal variation at all four sites, with $O_3$ concentrations peaking in late winter and spring (August to November) and minimum concentrations occurring in autumn (March to May). A typical diurnal pattern was observed, with $O_3$ peaking between 12:00 and 15:00, with a maximum at approximately 15:00, when the atmospheric boundary layer is well mixed in response to maximum photochemical production. In addition, a spatial $O_3$ map for the north-eastern interior of South Africa could be produced by utilising the $O_3$ measurements from the four sites investigated in this study in conjunction with data obtained from the Tropospheric Ozone Assessment Report (TOAR) database, as well as from passive sampling conducted at 36 other sites located in the north-eastern interior of South Africa. The spatial distribution indicated that $O_3$ can be considered a regional problem in continental South Africa with $O_3$ concentrations being higher than 40 ppb across continental South Africa during spring.

### 7.1.2 Identify the probable sources and assess the contribution of individual sources to the problem of $O_3$ pollution in South Africa

The observed seasonal patterns at the four sites, i.e. late winter and early spring peaks, were indicative of sources of $O_3$ precursor species and meteorological conditions conducive to $O_3$ formation. The increase in $O_3$ levels at Welgegund, Marikana and Elandsfontein could be attributed to more pronounced inversion layers trapping low-level pollutants in conjunction with increased household combustion for space heating. Diurnal patterns of precursor species ($NO_x$ and CO) at the industrial Marikana site signified the influence of low-level emissions of precursors, while the influence of tall stack emissions of $NO_x$ was evident at Elandsfontein. The observed $O_3$ peaks at all the sites in spring were ascribed to increased open biomass burning endemic to this region. Back trajectory analysis was performed from which source maps were compiled at the two regional background sites, which indicated that higher $O_3$ concentrations corresponded with increased CO concentrations in air masses passing over a region in southern Africa, where a large number of open biomass fires occurred from June to September.

The regional transport of CO associated with open biomass burning in southern Africa was, therefore, considered a significant source of surface $O_3$ in continental South Africa. However, a limitation in this study was that no continuous VOC measurements were conducted at any of the sites and the contribution of VOC emissions to increased $O_3$ could therefore not be determined. Jaars *et al.* (2014) and Jaars *et al.* (2016) presented results for aromatic- and biogenic VOCs obtained from grab samples during a two-year sampling period at Welgegund, which indicated that VOC concentrations measured at Welgegund were relatively low, with biogenic VOCs being an order of magnitude lower compared to aromatic VOCs measured at Welgegund. In addition, biogenic VOC concentrations were significantly lower compared to biogenic VOC concentrations measured in other ecosystems in the world.

### 7.1.3 Statistically examine the influence of chemistry and meteorology on surface ozone concentrations in continental South Africa

The high quality data obtained from the four sites in the north-eastern interior of South African were subjected to statistical analysis. Three multivariate statistical models, i.e. multiple linear regression (MLR), principal component analysis (PCA) and a generalised additive model (GAM) were successfully employed to identify and quantify the influence of the chemical and meteorological factors driving $O_3$ variability over continental South Africa. A separate model was built for each measurement site to determine the importance of these factors at background and polluted areas in continental South Africa. Temperature, global radiation, relative humidity, wind speed and -direction, as well as NO, $NO_2$ and CO concentrations were included as input parameters in these models.

The common finding with these statistical models was that the most important parameters explaining daily maximum $O_3$ variation in continental South Africa were relative humidity, temperature and CO concentrations, with PCA indicating that these factors are not collinear. The influence of temperature on $O_3$ variability is expected, while the significance of CO emissions associated with biomass burning on surface $O_3$ levels was indicated through Objective 1.1.2. However, it was surprising that relative humidity has emerged as one of the most important variables influencing $O_3$ levels in semi-arid South Africa, with increases in $O_3$ associated with decreases in relative humidity. Reasons for the strong, negative $O_3$-relative humidity correlation could not be explained by the statistical models. Possible causes for the relationship were obtained from literature, which indicated a number of factors, mainly involving loss of $O_3$ or precursor species in the atmosphere in the aqueous phase or lower relative humidity being associated with meteorological conditions not conducive to $O_3$ formation. The

statistical models confirmed that regional-scale $O_3$ precursors coupled with meteorological conditions play a critical role in daily variation of $O_3$ levels in continental South Africa.

As also indicated in Objective 1.1.2, a limitation in the statistical analyses was that no continuous long-term VOC measurements were conducted at any of the sites, which could therefore not be included in the statistical models. The VOC data collected by Jaars *et al.* (2014) and Jaars *et al.* (2016) were not from a statistical perspective considered sufficient to be included in the statistical models utilised in this study. In addition, the influence of synoptic-scale meteorology was also not included in these models.

### 7.1.4 Determine the implications of these chemical and meteorological influences on air quality management in South Africa

The $O_3$ concentrations measured at the four sites in this study indicate that the South African National Ambient Air Quality Standard (NAAQS) for $O_3$ was regularly exceeded. Therefore, this study also attempted to provide information on factors that must be considered in implementing $O_3$ mitigation strategies for this region. In order to successfully deploy $O_3$ mitigation strategies, it is important to establish whether a region is $NO_x$- or VOC-limited. Therefore, in the absence of any continuous long-term VOC measurements for these sites, the correlations between $NO_x$, CO and $O_3$ were successfully utilised to indicate that the north-eastern interior of South Africa is predominantly VOC-limited if CO was considered a proxy for VOCs. Increased $O_3$ levels were strongly correlated with increased CO, while increased $O_3$ concentrations did not correspond with increased $NO_x$ levels (or even decreased). Furthermore, the limited VOC dataset that was available for Welgegund (Jaars *et al.*, 2016, Jaars *et al.*, 2014) was also successfully utilised to calculate the instantaneous $O_3$ production rate, $P(O_3)$, which indicated that at least 40% of $O_3$ production occurred in the VOC-limited regime. In addition to the limited VOC dataset available for the calculation of $P(O_3)$, OH radicals were also estimated in the calculation, since no OH radical measurement exists for this region.

Some new aspects on $O_3$ for continental South Africa have been indicated in this study, which must be taken into consideration when $O_3$ mitigation strategies are deployed. Emissions of $O_3$ precursor species (e.g. aromatic VOCs) associated with the concentrated location of industries in this area could be regulated, while it was indicated that CO and VOC emissions associated with household combustion and regional open biomass burning should also be targeted. However, emissions of $O_3$ precursor species associated with poor socio-economic circumstances and long-range transport provide a bigger challenge for regulators.

### 7.1.5 Investigate the impact of elevated levels of $O_3$ on agricultural crops with a special focus on sugarcane

An eight-month trial was successfully conducted to assess the sensitivity of two sugarcane cultivars (*Saccharum* spp.) commonly farmed in South Africa to chronic exposure to elevated $O_3$ levels, as well as combined elevated $O_3$ and $CO_2$ concentrations in open-top chambers (OTC) during the growth season. As far as the candidate can assess, this was the first attempt to present quantitative exposure-response data on sugarcane under controlled conditions. Two indicators of stress could be monitored, namely plant growth (leaf and stalk parameters and number of tillers), as well as plant physiology that affects photosynthetic performance (chlorophyll a fluorescence, stomatal conductance and chlorophyll content). It was indicated that the growth parameters of the NCo376 cultivar showed no significant response to increased $O_3$. Although the growth of the N31 variety indicated some response to increased $O_3$, it also showed the ability to adapt to increased $O_3$ levels. Some evidence of elevated $CO_2$ countering the effects of elevated $O_3$ on growth, especially for the N31 cultivar, was observed. The physiological functions, i.e. photosynthesis of the NCo376 sugarcane variety, were more susceptible to $O_3$ exposure compared to the N31 cultivar. The combined effects of elevated $O_3$ and elevated $CO_2$ improved photosynthetic efficiency and chlorophyll content relative to the $O_3$-treated plants to a certain extent, with the effects more pronounced for N31 than for NCo376. It was indicated that the N31 variety is probably more tolerant towards high $O_3$ levels compared to NCo376. In general, this study indicated that the effects of chronic $O_3$ exposure were not as severe as expected in the sugarcane, while it was also indicated that these plant species are capable of evolving in order to tolerate and adapt to elevated $O_3$ levels.

A limitation in this study was that the influence of abiotic factors (e.g. soil water stress, heat stress) together with increased $O_3$ exposure was not investigated. In semi-arid conditions, such as South Africa, drought is considered to be a stronger stress factor on vegetation. In addition, above-ground biomass was not measured at final harvest, which would have aided in determining the reduction in yield that results from exposure to $O_3$.

## 7.2 RECOMMENDATIONS FOR FUTURE RESEARCH

Continued research on surface $O_3$ concentrations in southern Africa is required, which includes determining their projected increase, acquiring an improved understanding of underlying mechanisms affecting $O_3$ variability, as well as establishing the sensitivities of local crop variants to $O_3$ in this region. Together with the shortcomings and limitations of the project identified in the previous section, this section outlines a number of possible areas for future work that would advance the knowledge of regional surface $O_3$ and its subsequent impacts on the southern African environment.

### 7.2.1 Continuous monitoring of VOCs

As indicated above, an important limitation in the determination of the $O_3$ production regime was the deficiency of VOC data for South Africa, with the exception of the grab sample dataset for Welgegund. VOC data will provide more conclusive evidence on whether continental South Africa can be considered VOC-limited. In addition, more research is required to speciate VOCs in South Africa in order to access reliable $O_3$ production information. Continuous, long-term measurements of VOCs with instruments such as proton transfer reaction mass spectrometer, which enable on-line sampling of individual VOCs, will be particularly valuable and will enrich the regional VOC observation database.

### 7.2.2 Measurement of total $^{\bullet}$OH reactivity

The abundance of peroxy radicals ($HO_2^{\bullet}$ and $RO_2^{\bullet}$) in the atmosphere, which are produced from the reaction of $^{\bullet}$OH with VOCs, was calculated in order to determine $P(O_3)$ in this study. The total $^{\bullet}$OH reactivity can also be measured in order to calculate the concentration of peroxy radicals, while a deeper understanding of the $^{\bullet}$OH budget can also be obtained. Some research groups have developed instruments to measure $^{\bullet}$OH reactivity (e.g. Stone *et al.*, 2012 and references therein), which is a challenging task that should be the focus of future work.

### 7.2.3 Calculation of other ratios

In addition to VOC-to-$NO_x$ ratios, several other 'indicator' ratios have been proposed as possible indicators of $NO_x$ or VOC sensitivity, such as $O_3/NO_y$ (where $NO_y$ represents total reactive nitrogen), $O_3/NO_z$ (where $NO_z$ represents the sum of oxidised products of $NO_x$ or $NO_y$-$NO_x$), $O_3/HNO_3$ and $H_2O_2/HNO_3$ (Sillman and Samson, 1995), but will require specialised studies to measure these species.

### 7.2.4 Photochemical modelling of $O_3$-formation regimes

The measured CO, $NO_x$ and $O_3$ concentrations together with the limited VOCs dataset can be used to initialise a photochemical model (chemical transport or box model) to further examine $O_3$ formation regimes and determine more detailed relationships between these $O_3$ precursor species. The detailed chemistry schemes included in these models can better quantify the contribution of VOCs, as well as further reactions of VOC oxidation intermediates and products involved in $O_3$ formation.

### 7.2.5 Box models to understand $O_3$-meteorology correlations

A box model of $O_3$ production and loss might also provide another method to evaluate the impact of meteorology on the chemical mechanisms (e.g. Kavassalis and Murphy, 2017). For example, a box model can simulate the formation of $O_3$ using simple meteorological input and detailed reaction schemes, which could shed more light on the initial and boundary conditions that cause the negative $O_3$-relative humidity correlation.

### 7.2.6 Validation of regional air quality models

The statistical relationships found between daily maximum 8-h $O_3$ concentrations, and meteorological and chemical parameters in this study, based on continuous ground-level $O_3$ measurements, should be compared with the statistical analyses of modelled $O_3$ levels determined with regional air quality models typically used in South Africa (e.g. US EPA's CMAQ). If there is a systematic difference in the response of modelled $O_3$ to these parameters, then it can serve as a useful diagnostic evaluation to identify elements of the model code or input that need further investigation, such as the relationship between $O_3$ and relative humidity indicated in this study.

### 7.2.7 $O_3$ impacts on sugarcane

It is recommended that more trials be carried out on sugarcane varieties to provide an improved mechanistic understanding of the impacts. Further investigations could study spatial and temporal variability in concentration-response relationships, as well as inter-annual differences. In addition, the experimental data can be utilised in the $DO_3SE$ (Deposition of $O_3$ for Stomatal Exchange) model (Emberson *et al.*, 2000), which parameterises the effect of temperature, soil water deficit and vapour pressure deficit on stomatal conductance, thereby offering a better understanding of how multiple stressors affect $O_3$ damage. At present, local crop modelling capabilities for sugarcane do not extend to include $O_3$ damage.

### 7.2.8 Health impacts of $O_3$

There is a need for South Africa-specific studies to quantify the burden of $O_3$ on health. These impacts on health effects can be quantified by using the US EPA approach, which involves a software package (BenMAP) that contains a library of $PM_{2.5}$ and $O_3$ mortality and morbidity concentration-response functions based on epidemiological studies conducted in the US (Fann *et al.*, 2012). Since there is currently a deficiency in local concentration-response functions, international dose and response metrics can be used until South Africa-specific epidemiological studies become available.

## 7.3 CLOSING REMARKS

This thesis strongly links CO to $O_3$ production and contributes towards understanding $O_3$ impact on food security. A significant feature in this part of the world during the dry season is biomass burning, known to emit significant quantities of CO, VOCs and $NO_x$ into the atmosphere, which in combination leads to increased $O_3$ production. The background stations in this study highlighted the strong influence of biomass burning on the annual $O_3$ peak. It is also important to be aware that biomass burning fires in the southern African region are both of anthropogenic and natural origin. Therefore, policy expectations might be overly optimistic on the levels to which $O_3$ can be lowered simply by implementing emission reduction strategies, while biomass burning remains a 'natural' feature in the region responsible for enhancing surface $O_3$ concentrations. However, those fires caused by anthropogenic practices (e.g. crop residue, pasture maintenance fires, opening burning of garbage, domestic burning) can be targeted for intervention and solutions sought to reduce the injection of higher $O_3$ precursor loads on the regional atmosphere. This study also highlighted the contribution of household combustion to ambient $O_3$ air pollution which is a symptom of socio-economic circumstances in this region that can only be improved by increased economic growth in southern Africa.

Certainly control of CO, whether from biomass burning or domestic burning or internal combustion engines would improve air quality. However the emphasis should not be on CO alone, but a policy of reducing both CO and VOCs as local industrial activities are presumably the source of aromatic VOCs that were measured. Furthermore, even if large areas of South Africa are VOC-limited, it is never good policy to keep $NO_x$ emissions high to keep $O_3$ low because more $NO_x$ eventually leads to more $O_3$ somewhere. There are times and places when it is cost effective to allocate resources to VOC controls to help abate $O_3$ but in the long term it would be preferable to reduce both $NO_x$ and VOC emissions appreciably to secure worthwhile reductions in $O_3$.

# APPENDICES

# Appendix A

In this appendix, some results that were not included in any of the research papers are presented here for completeness and additional information.

## A.1 Interannual variation in $O_3$

Sufficiently long records (typical 10 years or longer) are useful to investigate interannual variation and provide estimates of long-term trends of surface $O_3$. From all the sites, Welgegund has the longest dataset, spanning a period of almost 6 years and was used to ascertain if $O_3$ has been decreasing or increasing during the period May 2010 to December 2015 (Figure A-1). A cyclical pattern can be observed in the monthly $O_3$ data which is due to seasonal fluctuations of $O_3$ from year to year. If a straight line is fitted to the monthly medians, there is a slight upward trend over the entire period although the goodness of the fit ($R^2$) of the linear equation is not high. Including the 2015 data reveals a positive trend in surface $O_3$ concentrations. The highest monthly-averaged $O_3$ recorded at Welgegund was observed in October 2015 which was also the one of the the hottest and driest years on record due to a very strong El Niño weather cycle. During the rainy season (October 2015 to March 2016), southern Africa experienced an El Niño-induced drought which persisted into the first half of 2016. The next rainy season (October 2016 to March 2017) coincided with the development of the La Niña phase which tends to be associated with above-average rainfall in southern Africa.

Trend analysis of the South African Highveld from 1990 to 2007 showed little change in surface $O_3$ (Balashov *et al.*, 2014) whilst a 15-20% surface $O_3$ increase was observed at Cape Point from 1990-2010, although most of it occurred in the 1990s (Oltmans *et al.*, 2013). Furthermore, after re-examination of free-tropospheric ozonesonde records from 1990 to 2007 over southern Africa, no statistically significant trends were found in near-surface $O_3$ in September and October when biomass burning impacts were most pronounced (Thompson *et al.*, 2014). In summary, results of surface $O_3$ trends over southern Africa show no trend or are inconclusive, emphasizing the need for more long-term measurements to enable one to distinguish between short-term variability (seasonal or diurnal trends) and long-term trends.

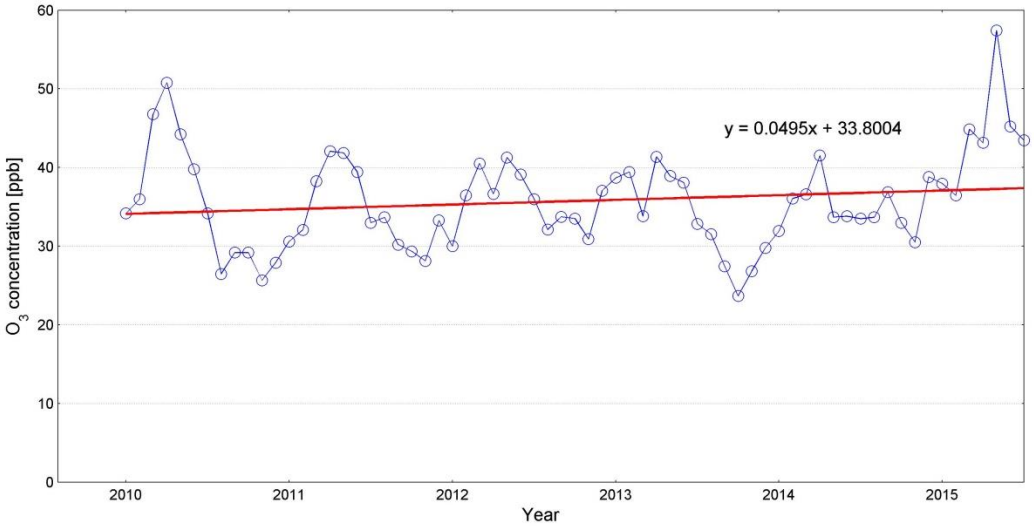


Figure A-1: Interannual variation in $O_3$ (monthly median values) at Welgegund from May 2010 to December 2015.

## A.2 Dependence of $O_3$ on regional transport

To assess the influence of transport into a given location on surface $O_3$ exceedances, back trajectory analysis was performed. In Figure A-2 the overlay back trajectories compiled for each of the sites are presented. Hourly back trajectories were calculated for air masses arriving at the measurement sites between 1400-1600 h (local time) on days on which the daily max 8-h $O_3$ exceeded the NAAQS limit of 61 ppbv. The daily max 8-h $O_3$ occurred between 1400-1600 h and was considered to be the most representative $O_3$ level associated with the combined contribution of regional and local influences on ambient $O_3$ levels.

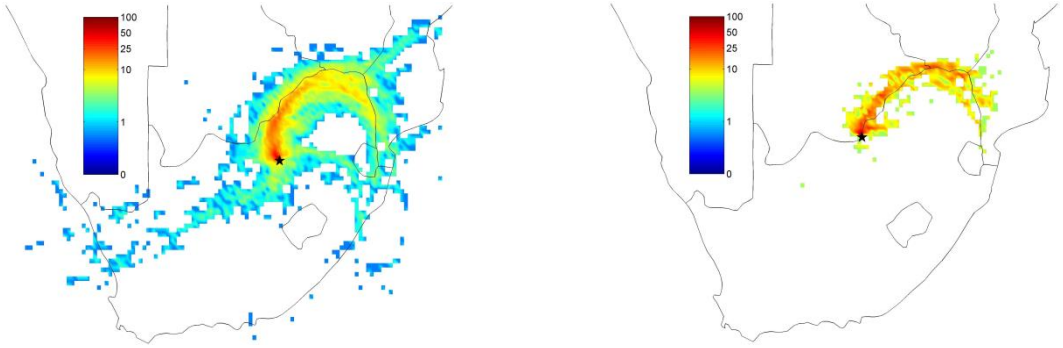


(a) Welgegund (b) Botsalano

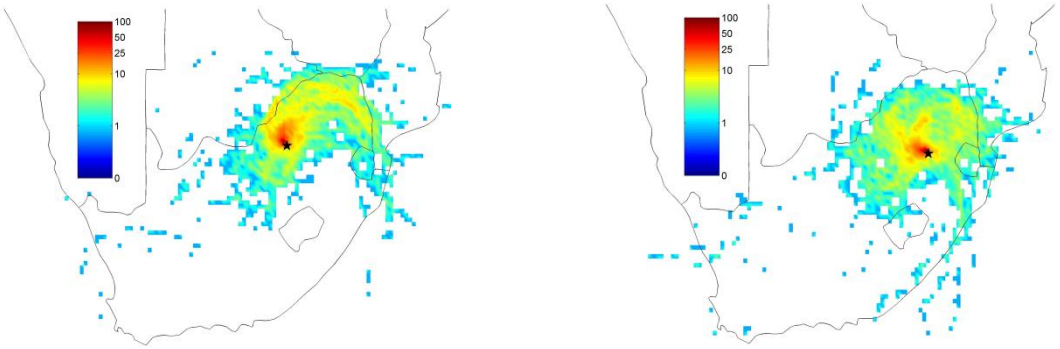


(c) Marikana (d) Elandsfontein

Figure A-2: Four day overlay back trajectories with a 100 m arrival height arriving hourly at the measurement sites between 1400-1600 h (local time, UTC+2) on days on which $O_3$ exceeded the NAAQS of 61 ppbv. The black star denotes the measurement site. The areas indicated in red have the highest percentage of air mass movement towards the measurement site.

The back trajectories for the two regional background stations, i.e. Welgegund and Botsalano indicate that $O_3$ exceedances were predominantly associated with anticyclonic recirculation of air masses, which is especially true for Botsalano. As a rural background station, Botsalano has limited $NO_x$ sources available but if the air mass encountered more anthropogenic sources of $NO_x$ emissions as it is being advected and before it reaches the station, this leads to increased $O_3$ productivity. Back trajectories for Welgegund also indicate the impact of emissions from the Johannesburg-Pretoria megacity source region to the east, as well as the lesser influence of the relatively clean background region to the west on $O_3$ exceedances measured at the site. Back trajectory analysis at Marikana indicates the combined influence from regional transport and local sources to $O_3$ exceedances. The back trajectories compiled for Elandsfontein indicate the predominant influence of local sources (coal-fired power plants and a petrochemical coal plant) on $O_3$ exceedances compared to a smaller contribution from the regional transport of air masses.

## A.3 Dependence of $O_3$ on local sources

It would be useful to check from which directions the highest $O_3$ and $O_3$ precursors are coming to the measurement sites in order to assess the dependence of $O_3$ on local sources. Figure A-3 depicts the pollution roses over twelve wind sectors for $O_3$, $NO_x$ and CO on days when the daily max 8-h $O_3$ exceeded the South African National Air Quality Standard (NAAQS) limit of 61 ppbv at the four sites. The net wind vectors for each day were calculated for the period 7:00-18:00

(local time) for each site. This was done by first calculating the hourly u and v components of wind, then calculating the daily mean of these wind components, then transforming the daily mean wind components to a daily mean wind direction in degrees by trigonometry. The result is a single value that estimates the magnitude of the wind and net direction of air transport for each day during daytime (Geddes *et al.*, 2009). Average $NO_x$ and CO concentrations were also calculated for the period 7:00-18:00 (local time) for days when the daily maximum 8-h moving average of $O_3$ was exceeded.

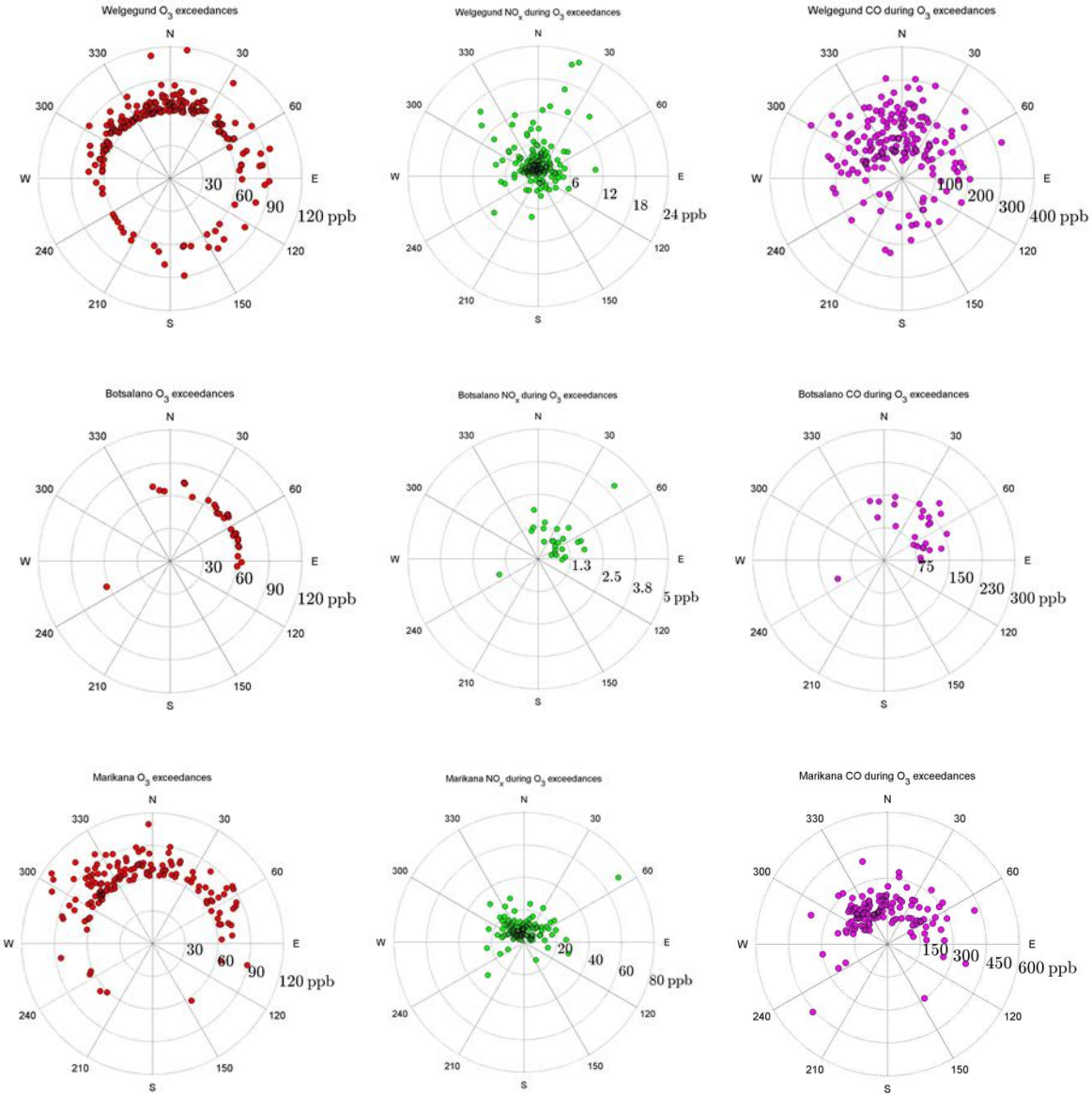

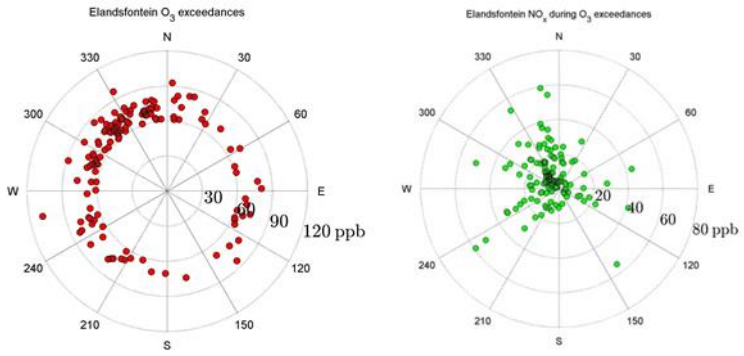


Figure A-3: Pollution roses of daily max 8-h $O_3$, daily average $NO_x$ and daily average CO as a function of the net daily wind vector on days when the daily max 8-h $O_3$ value exceeded the 61 ppb air quality standard. The concentric rings represent gas concentration (in ppb).

It is evident from Figure A-3 that $O_3$ exceedances at Welgegund were associated with all the wind directions, with relatively more $O_3$ exceedances related to the west to north to east sectors. The average $NO_x$ and CO concentrations were also relatively higher in these sectors and this can be attributed to air masses moving over the western Bushveld Igneous Complex, as well as anticyclonic recirculation of air masses impacting Welgegund (Jaars *et al.*, 2014). At Botsalano, $O_3$ exceedances were related to winds almost entirely in the quadrant north to east, while average $NO_x$ and CO concentrations were very low within this quadrant. This is indicative of the significant influence of the regional transport of $O_3$ at this rural background site. For Marikana, winds originating from the west to north to east sectors coincided predominantly with $O_3$ exceedances and relatively high $NO_x$ and CO concentrations, whilst a narrow clean sector to the mountains is seen south of the site. The polluted sector is as a result of the influence of local sources e.g. household combustion that is mainly responsible for the $O_3$ exceedances measured at Marikana (Venter *et al.*, 2012). $O_3$ exceedances at Elandsfontein were associated predominantly with the sectors west to north, pointing to nearby power stations within a 50 km radius to the west and north of the monitoring site (Laakso *et al.*, 2012).

## A.4 Estimated $^{\bullet}$OH concentrations at Welgegund

As discussed in Chapter 3, the production rate of $HO_x$ ($P(HO_x)$) was used to calculate the $^{\bullet}$OH radical concentration. The $P(HO_x)$ was estimated to be estimated to be $6.09 \times 10^6$ molec $cm^{-3}$ $s^{-1}$ or 0.89 ppbv $h^{-1}$ (calculated for a campaign $O_3$ average of 41 ppbv and a campaign RH average of 42 % at 11:00 LT each day) at at standard pressure and temperature. Estimated $^{\bullet}$OH concentrations in Figure A-4 are somewhat higher than theoretical estimates given in literature (e.g. Martinez *et al.*, 2010).

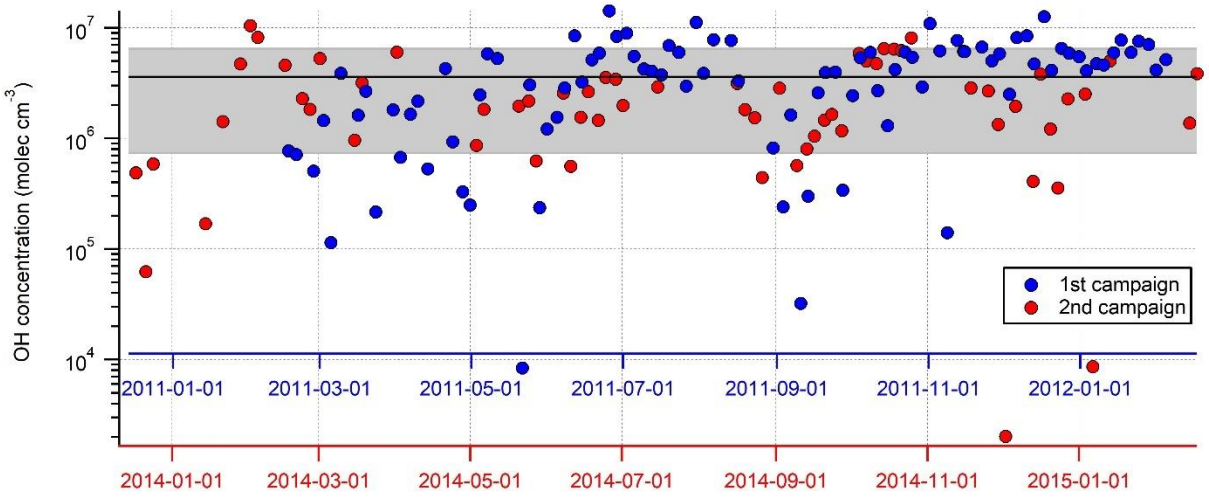


Figure A-4: Estimated concentrations of OH radicals using the VOC and $NO_x$ measurements. Production of $HO_x^{\bullet}$ was estimated using 41 ppbv of $O_3$ and 42 % relative humidity (both campaign averages for 11:00 LT data) as well as $J(O_3) = 3 \times 10^{-5}$ $s^{-1}$. The black line represents the campaign daytime average, 3.60 (± 2.86) × $10^6$ molec/$cm^3$.

# Commentary
# Measurement of surface ozone in South Africa with reference to impacts on human health

**Tracey L. Laban, Johan P. Beukes, Pieter G. van Zyl**

Unit for Environmental Sciences and Management, North-West University, Potchefstroom

At the bottom of the troposphere, the boundary layer (below the free troposphere) where we live and breathe, ground-level ozone ($O_3$) (also called surface $O_3$ because it forms just above the earth's surface) pollution has direct impacts on human health, agriculture and vegetation. Surface $O_3$ is a secondary atmospheric pollutant formed by reactions between oxides of nitrogen ($NO_x$) and volatile organic compounds (VOCs) or carbon monoxide (CO) in the presence of sunlight. The sources of these $O_3$ precursors originate from a range of anthropogenic and natural processes (Oltmans et al., 2013). Stratospheric intrusions of $O_3$-rich air to the free troposphere that contribute to surface $O_3$ may also occur (Lin et al., 2012).

The distribution of $O_3$ throughout the troposphere is not homogenous since it extends in vertical (altitude) and horizontal (spatial) directions, as well as over different periods of time (temporal). In order to study $O_3$ phenomena on these different time and space scales requires that three characteristics of tropospheric $O_3$ are routinely measured viz.: (i) surface $O_3$ by ground-based monitoring stations; (ii) total column $O_3$ from satellites and (iii) the vertical profile of $O_3$ with balloon ozonesondes and aircraft monitoring.

Meteorological conditions play a significant role in chemical production and transport of surface $O_3$. The synoptic scale meteorology of southern Africa is largely characterised by semi-permanent anticyclonic high pressure systems (Tyson and Preston-Whyte, 2000). Stable atmospheric layers associated with anticyclonic circulation traps pollutants near the surface and transport these species over the region (Tyson and Preston-Whyte, 2000; Abiodun et al., 2014). The interaction between meteorological parameters (e.g. temperature, precipitation, clouds) and $O_3$ precursors determines the amount of surface $O_3$ produced (Balashov et al., 2014). In fact, temperature can be used as a simple proxy for meteorological influences as it was found that the correlation with temperature can account for most of the influence of meteorological variables on $O_3$ (Jacob et al., 1993).

Spatial and temporal surface $O_3$ variability have been studied in southern Africa (Zunckel et al., 2004; Martins et al., 2007; Josipovic et al., 2010; Lourens et al., 2011; Laakso et al., 2012). Two major field campaigns (SAFARI-92 and SAFARI 2000) were conducted to understand the effects of biomass burning emissions on $O_3$ over southern Africa, which provided important insights on the regional $O_3$ seasonal cycle (Diab et al. 1996). An analysis of surface $O_3$ measurements during 1999-2001, albeit limited to a few sites outside urban areas, showed that the highest $O_3$ concentrations occur over Botswana and the Mpumalanga Highveld where the springtime maximum concentrations range between 40 and 55 parts per billion by volume (ppb) but exceeded 90 ppb at times (Zunckel et al., 2004). Due to limited measured data for the southern African region, regional-scale photochemical modelling was conducted (Zunckel et al., 2006). Interestingly, the modelling study concluded that the formation of surface $O_3$ over the region is due to the combined contribution of precursors from both anthropogenic and biogenic origin.

Currently, measurements of surface $O_3$ in South Africa are conducted at a number of government- and industry-owned ambient air quality monitoring stations. The longest ongoing $O_3$ measurements are conducted at the South African Weather Service (SAWS) Cape Point Global Atmosphere Watch (GAW) station with measurements from 1983 up until present (Brunke and Scheel, 1998). This site is representative of background-maritime air with $O_3$ concentrations of 15 ppb in summer and 30 ppb in winter with an annual average of approximately 22 ppb. In addition to state- and industry-run stations, surface $O_3$ monitoring has been ongoing for almost five years at the Welgegund air quality research station (30 km north of Potchefstroom), which is considered a regional background site impacted by anthropogenic activities (Beukes et al., 2015). Long-term measurement data of $O_3$ spanning several years are beneficial as they account for the influence of inter-annual meteorological variability on the results.

Tropospheric $O_3$ profiles over South Africa indicate annual and decadal increases in $O_3$ levels in certain regions (Diab et al., 2003; Clain et al., 2009; Thompson et al., 2012). Oltmans et al. (2013) reported that the Cape Point station displayed a 15–20% $O_3$ increase from 1990 to 2000, followed by a period of zero-to-low growth. Most recently, $O_3$ sounding measurements at Irene from 1990-2007 showed a 30% increase per decade in $O_3$ concentration during the early winter period (Thompson et al., 2014). The cause for this winter time free troposphere increase was linked to long-range transport of emissions from South American megacities. The lifetime of $O_3$ in the troposphere is sufficiently long, i.e. in the order of days to months depending on the altitude (Jonson et al., 2010), to cause pollution on a global scale. However, the large increase in free tropospheric $O_3$ reported by Thompson et al. (2014) is not observed for surface $O_3$ in the South African Highveld (north-eastern South Africa) where it was reported that there was no change in surface $O_3$ on the Highveld for the period 1990–2007 (Balashov et al.,

2014). The Highveld is an industrialised region containing the majority of the coal-fired power plants in South Africa that emit large quantities of nitrogen oxides (NO + $NO_2$ = $NO_x$) that affects surface $O_3$ levels through their inter-related chemistry. Satellite images indicate the South African Highveld as a well-known $NO_2$ 'hotspot'. This prompts the authors to ask, "Is tropospheric $O_3$ over southern Africa really increasing?" At present interannual variability and trends over southern Africa remain inconclusive, or at least complex and require further investigation.

Mean surface $O_3$ concentrations over southern Africa exhibit a pronounced seasonal and diurnal cycle. In general the seasonal maximum occurs in spring and the minimum occurs in autumn. At Welgegund the data show a late winter-spring (August to October) maximum for $O_3$. The observed late winter-spring $O_3$ maximum coincides with the biomass burning period in southern Africa, which occurs almost exclusively during winter and early spring, from July to October (Silva et al., 2003). Aghedo et al. (2007) reported that the largest contributor to surface $O_3$ pollution over Africa is biomass burning, while biogenic (isoprene) emissions makes a larger contribution to global $O_3$. The diurnal patterns of $O_3$ measurements are similar for all four seasons, increasing from a minimum at sunrise to maximum values in the early afternoon and then decreasing rapidly during sunset with $O_3$ continuing to decrease at night to a minimum again at sunrise. The increase during the day is due to photochemical formation of $O_3$. The decrease during the night and early morning is because of (i) the absence of sunlight that prevents the formation of $O_3$; (ii) $O_3$ removal due to titration of remaining $O_3$ by nitric oxide (NO) and (iii) $O_3$ loss due to dry deposition. Local $O_3$ titration ($O_3$ removal) was observed on several nights in October 2014 at the Welgegund station and is currently being investigated. Ambient $O_3$ is expected to be low at night (<30 ppb) but more surprising is the sharp drop in $O_3$ concentrations to (almost) 0 ppb recorded at the station. A major increase in $NO_x$ concentration could be observed, peaking at the exact time when $O_3$ drops to almost zero.

The South African National Ambient Air Quality Standard (NAAQS) for $O_3$ is an 8-h running average of 61 parts per billion (ppb) not to be exceeded more than 11 times in a year. All stations in the South African Highveld and Vaal Triangle designated priority areas exceeded the NAAQS for $O_3$ in 2014, with the highest number of exceedances occurring in August-September-October. As mentioned above, this is the southern African burning season and points to biomass burning as the source of the $O_3$ precursors that may be responsible for the exceedances. Monitoring stations closely influenced by NO emissions demonstrate noticeable titration of $O_3$ by NO. The titration effect of $O_3$ by NO can assist in explaining why sometimes it is observed that the $O_3$ levels in a rural area are higher than those in urban and industrial areas. The monitoring station in the rural town Hendrina recorded 234 exceedances of the NAAQS in 2014, which may be attributed to a lack of NO emission sources in the area to titrate the $O_3$ formed.

The chemical interdependence between $O_3$, $NO_x$ and VOCs is widely known, however this relationship is complex and non-linear. The production of $O_3$ requires $NO_x$ and VOCs to exist in the correct ratios, and sunlight for the photochemical reaction to take place. When the VOC to $NO_x$ ratio is high, $O_3$ formation is limited by the availability of $NO_x$ ($NO_x$-limited), while when the VOC to $NO_x$ ratio is low, $O_3$ production is limited by the availability of VOCs (VOC-limited). In general, increasing VOC concentrations mean more $O_3$, but increasing $NO_x$ may lead to either more or less $O_3$ depending on the prevailing VOC-to-$NO_x$ ratio (Seinfeld and Pandis, 2006). The industrialised Highveld is a good example where the large-scale variability of surface $O_3$ point to other factors (e.g. biogenic VOCs), which lead to some areas in the Highveld being $NO_x$-limited whilst others are VOC-limited.

The non-linear relationship between $NO_x$ and $O_3$ is also illustrated by the "weekend effect". Since the early 1970s, researchers have reported the difference between weekday and weekend $O_3$ concentrations with higher $O_3$ concentrations occurring on weekends, particularly in urban areas. Traffic emissions should be higher during weekdays thereby providing more precursors ($NO_x$ and VOCs) for $O_3$ formation. However contrary to this thinking, at weekends when emissions are reduced, the $NO_x$ falls and the $O_3$ concentration rises. An explanation for the weekend effect is that due to the low level of $NO_x$ emissions during the weekend, the reaction whereby NO removes $O_3$ by titration to form $NO_2$ is suppressed. Dumont (1996) also reported significantly higher $O_3$ levels in Belgian conurbations in the weekend compared to weekdays. However, the sum of $O_3$ and $NO_2$ (total oxidant), often called Ox, was similar no matter what day was taken. Total oxidant Ox is in fact a better measure of the real photochemical production of $O_3$ than $O_3$ itself, as $O_x$ production and loss are independent of the rapid photochemical reactions that convert $O_3$ to $NO_2$ and vice versa in the urban and suburban atmosphere. By comparing day-of-week patterns in $O_x$ to those in $O_3$, it was shown that titration by NO is the main source of a weekend effect in ozone. The weekend phenomenon has also been reported for Johannesburg (Padayachi et al., 2013).

The reduction of $O_3$ concentrations in South Africa requires control of either $NO_x$ or VOC emissions, or both, depending on the limiting mechanism for $O_3$ production, since limiting solar radiation is not an option. An effective reduction policy for $O_3$ can only be achieved when the dependence of photochemical $O_3$ on the precursors of $O_3$ is determined definitively. The $O_3$-$NO_x$-VOC sensitivity needs to be investigated individually for different regions since there is no geographically uniform response to $NO_x$ and VOCs (Hidy, 2000). In East Asia, for instance, all the megacities were found to be VOC-limited ($NO_x$-saturated) (Liu, 2008). Lourens et al. (2015) also found that $O_3$ formation in the Johannesburg-Pretoria megacity is VOC-limited. A VOC-only control strategy would be effective in these large urban areas but may be less beneficial downwind. In other areas with appreciable natural VOC concentrations leading to a $NO_x$-limited regime, measures to limit VOC emissions in these areas produced little or no effect on $O_3$ pollution. Therefore, a

combined VOC-$NO_x$ strategy should be more effective than a VOC- or $NO_x$-only strategy in reducing $O_3$ over a large geographic area. The United States were partly misdirected in the first two decades of $O_3$ mitigation attempts, where models concluded $O_3$ production was VOC-limited, which led to a strong regulatory effort to target VOC emission reductions. However, there was mixed success in this control strategy. Later measurements and model calculations showed that $O_3$ production over most of the United States is primarily $NO_x$-limited, not VOC-limited. Early models underestimated emissions of VOCs from mobile sources (Pierson et al., 1990) and failed to account for biogenic VOCs (Chameides et al., 1988). In the long term it would be preferable to reduce both $NO_x$ and VOC emissions appreciably to secure worthwhile reductions in $O_3$. In the short term it may be necessary to identify regions as $NO_x$- or VOC-limited in order to maximise the cost effectiveness of strategies.

Review of scientific evidence links ozone exposure to adverse health effects. Epidemiological studies have shown that atmospheric $O_3$ and fine particulate matter ($PM_{2.5}$) have the most significant influences on human health, including premature mortality. Most of the impacts of $O_3$ on human health relate to the respiratory system, which include reduced lung function, lung irritation and increased risk of mortality from long-term exposure (Jerrett et al., 2009). Atmospheric modelling studies have provided an estimate of the global burden of anthropogenic $O_3$ and $PM_{2.5}$ on premature human mortality. Mortality estimates vary with different models, but most recently, Lelieveld et al. (2013) estimated a global respiratory mortality of 773 000/year and found that the highest premature mortality rates are found in Southeast Asia and Western Pacific regions where more than a dozen of the most highly polluted megacities are located. This study did not include Africa.

An assessment of the health effects and economic valuation of $O_3$ pollution based on the impact pathway approach involves first, assessing population exposure associated with ambient concentrations, second, estimating the health impacts associated with population exposure, and third, valuation of the health impacts in monetary terms. A key challenge is the lack of specific data for South Africa. Firstly, reliable pollutant concentration data is needed for South Africa (especially for secondary pollutants such as $O_3$). Secondly, to quantify the health effects requires exposed population data, baseline incidence rates and concentration-response functions from epidemiological studies for the South African population, which is unfortunately not available. Thirdly, valuation of the health impacts in monetary terms requires costs for morbidity (illnesses) e.g. costs of hospitalisation, costs of treatment in the South African context and costs for mortality.

Recent evidence suggests that the health related impacts of $O_3$ could be significant (Jerrett et al., 2009). However, health risk quantification in South Africa generally does not consider $O_3$ as a key pollutant of concern. Since there is more evidence for particulate matter (PM) and concentration-response factors are more widely available, several studies use only PM as the indicator of ambient air pollution. However, selecting only one ambient air pollutant may underestimate the magnitude of the health effects. Adding the health effect estimates of another air pollutant uncorrelated with particulate matter (for example, $O_3$) can minimise the extent of this underestimation.

The issue of formation, effects and abatement of $O_3$ is complex due to its non-linear relationship with precursor species and its zone of impact extending to local and regional scales, which calls for spatially differentiated abatement strategies. Quantification of the health risks attributed to air pollution (including $O_3$) will determine the level of effort needed. Monetisation of health impacts might be viewed as contentious. However, in South Africa where economic growth, job creation and poverty alleviation are pressing issues, environmental priorities have to be compared in similar terms as economic priorities that are often deemed more valuable. In addition, the transboundary nature of $O_3$ requires international effort in developing effective policies to cope with the problem. For these reasons $O_3$ will continue to be a subject of intense research and collaboration.

## Acknowledgements

The financial assistance of the National Research Foundation (NRF) towards this research is hereby acknowledged. Opinions expressed and conclusions arrived at, are those of the author and are not necessarily to be attributed to the NRF.

## References

Abiodun, B.J., Ojumu, A.M., Jenner, S., Ojumu, T.V., 2014. The transport of atmospheric $NO_x$ and $HNO_3$ over Cape Town. Atmos. Chem. Phys., 14, 559-575.

Aghedo, A.M., Schultz, M.G., Rast, S., 2007. The influence of African air pollution on regional and global tropospheric ozone. Atmos. Chem. Phys. 7, 1193-1212. www.atmos-chem-phys.net/7/1193 /2007/acp-7-1193-2007.pdf.

Balashov, N. V., Thompson, A. M., Piketh, S. J., and Langerman, K. E., 2014. Surface ozone variability and trends over the South African Highveld from 1990 to 2007. J. Geophys. Res.-Atmos., 119, 4323–4342, doi:10.1002/2013JD020555.

Beukes, J. P. et al., 2015. Source region plume characterisation of the interior of South Africa, as measured at Welgegund. Atmos. Chem. Phys., in preparation.

Brunke, E-G., Scheel, H.E., 1998. Surface ozone measurements at Cape Point (34oS, 18oE). In: Bojkov, R.D., Visconti, G. (Eds.). Atmospheric Ozone. Proceedings of the XVIII Quadrennial Ozone Symposium, L'Aquila, Italy, 12–21 September 1996, pp. 331–334.

Chameides, W.L., Lindsay, R.W., Richardson, J., Kiang, C.S., 1988. The role of biogenic hydrocarbons in urban photochemical smog: Atlanta as a case study. Sci., 241, 1473-1475.

Clain, G., Baray, J.L., Delmas, R., Diab, R., Leclair de Bellevue, J., Keckhut, P., Posny, F., Metzger, J.M., Cammas, J.P., 2009. Tropospheric ozone climatology at two Southern Hemisphere tropical/subtropical

sites, (Reunion Island and Irene, South Africa) from ozonesondes, LIDAR, and in situ aircraft measurements. Atmos. Chem. Phys., 9, 1723–1734, doi:10.5194/acp-9-1723-2009.

Diab, R.D., Raghunandan, A., Thompson, A.M., Thouret, V., 2003. Classification of tropospheric ozone profiles over Johannesburg based on mozaic aircraft data. Atmos. Chem. Phys., 3, 713–723.

Diab, R.D. et al., 1996. Vertical ozone distribution over southern Africa and adjacent oceans during SAFARI-92. J. Geophys. Res.-Atmos., 101, 23823– 23833, doi:10.1029/96jd01267.

Dumont, G., 1996. Effects of short term measures to reduce ambient ozone concentrations in Brussels and in Belgium. Paper presented at the Ministerial Conference on Tropospheric Ozone in Northwest Europe, London, UK, May 1996.

Hidy, G.M., 2000. Ozone process insights from field experiments. Part I: Overview, Atmos. Environ., 34, 2001– 2022, doi:10.1016/S1352-2310 (99)00456-2.

Jacob, D.J., Logan, J.A., Gardner, G.M., Yevich, R.M., Spivakovsky, C.M., Wofsy, S.C., Sillman, S., Prather, M.J., 1993. Factors regulating ozone over the United States and its export to the global atmosphere. J. Geophys. Res., 98(D8), 14, 817-14,826.

Jerrett, M., Burnett, R.T., Arden Pope III, C., Ito, K., Thurston, G., Krewski, D., Shi, Y., Calle, E., Thun, M., 2009. Long-term ozone exposure and mortality. New Engl. J. Med., 360, 11, 1085-95, doi:10.1056/NEJMoa0803894.

Jonson, J.E. et al., 2010. A multi-model analysis of vertical ozone profiles. Atmos. Chem. Phys., 10, 5759–5783, doi:10.5194/acp-10-5759-2010.

Josipovic, M., Annegarn, H. J., Kneen, M.A., Pienaar, J.J., Piketh, S.J., 2010. Concentrations, distributions and critical levels exceedance assessment of $SO_2$, $NO_2$ and $O_3$ in South Africa. Environ. Monit. Assess., 171(1), 181–196.

Lelieveld, J., Barlas, C., Giannadaki, D., Pozzer, A., 2013. Model calculated global, regional and megacity premature mortality due to air pollution. Atmos. Chem. Phys., 13, 7023-7037, doi:10.5194/acp-13-7023-2013.

Laakso, L. et al., 2012. South African EUCAARI measurements: Seasonal variation of trace gases and aerosol optical properties, Atmos. Chem. Phys., 12(4), 1847–1864.

Lin, J., Fiore, A.M., Cooper, O.R., Horowitz, L.W., Langford, A.O., Levy II, H., Johnson, B.J., Naik, V., Oltmans, S.J., Senff, C.J., 2012. Springtime high surface ozone events over the western United States: Quantifying the role of stratospheric intrusions. Geophys. Res.-Atmos., 117(D00V22), doi:10.1029/2012JD018151.

Liu, S.C., 2008. A review of ozone formation in megacities of east Asia and its potential impact on the ozone trends. Recent Progress in Atmospheric Sciences, pp. 438-457. doi: 10.1142/ 9789812818911 _0021.

Lourens, A. S., Beukes, J. P., Van Zyl, P. G., Fourie, G. D., Burger, J. W., Pienaar, J. J., Read, C. E., Jordaan, J. H., 2011. Spatial and temporal assessment of gaseous pollutants in the Highveld of South Africa. S. Afr. J. Sci., 107, 8 pp., doi:10.4102/sajs.v107i1/2.269.

Lourens, A.S.M., Butler, T.M., Beukes, J.P., Van Zyl, P.G., Pienaar, J.J., 2014. Investigating photochemical processes in the Johannesburg-Pretoria megacity using a box model. S. Afr. J. Sci., in preparation.

Martins, J.J., Dhammapala, R.S., Lachmanna, G., Galy-Lacauxb, C. and Pienaar, J.J., 2007. Long-term measurements of sulphur dioxide, nitrogen dioxide, ammonia, nitric acid and ozone in southern Africa using passive samplers. S. Afr. J. Sci., 103, 336-342, 2007.

Pierson, W.R., 1990. Memorandum to CRC-APRAC vehicle emissions modeling workshop attendees. 30-31 October 1990, Newport Beach, California, United States.

Oltmans, S., Lefohn, A., Shadwick, D., Harris, J., Scheel, H., Galbally, I., Tarasick, D., Johnson, B., Brunke, E.-G., Claude, H., 2013. Recent tropospheric ozone changes – a pattern dominated by slow or no growth. Atmos. Environ., 67, 331–351, doi:10.1016/j.atmosenv.2012.10.057, 2013.

Padayachi et al., 2014. An investigation of high ozone episodes in the city of Johannesburg. NACA conference, 8-10 October 2014, Umhlanga, South Africa.

Seinfeld, J.H. and Pandis, S.N., 2006. In: Atmospheric chemistry and physics: From air pollution to climate change. 2nd edition. John Wiley, New York, US, pp. 235-238.

Silva, J.M.N, Pereira, J.M.C, Cabral, A.I., Sá, A.C.L, Vasconcelos, M.J.P., Mota, B., Grégoire, J.-M., 2003. An estimate of the area burned in southern Africa during the 2000 dry season using SPOT-VEGETATION satellite data. J. Geophys. Res.-Atmos., 108(D13), 8498, doi:10.1029/2002JD002320.

Thompson, A.M., Balashov, N.V., Witte, J.C., Coetzee, J.G.R., Thouret, V., Posny, F., 2014. Tropospheric ozone increases over the southern Africa region: bellwether for rapid growth in Southern Hemisphere pollution? Atmos. Chem. Phys., 14, 9855-9869, doi:10.5194/acp-14-9855-2014.

Thompson, A. M. et al., 2012. Southern hemisphere additional ozonesondes (SHADOZ) ozone climatology (2005–2009): Tropospheric and tropical tropopause layer (TTL) profiles with comparisons to OMI-based ozone products, J. Geophys. Res.-Atmos., 117(D23301), doi:10.1029/2011JD016911.

Tyson, P. D., and Preston-Whyte, R.A., 2000. The Weather and Climate of Southern Africa, Oxford Univ. Press, Cape Town, SA, 396 pp.

Zunckel, M., Venjonoka, K., Pienaar, J.J., Brunke, E.-G., Pretorius, O., Koosialee, A., Raghunandan, A., van Tienhoven, A.M., 2004. Surface ozone over southern Africa: synthesis of monitoring results during the Cross Border Air Pollution Impact Assessment project. Atmos. Environ., 38, 6139–6147.

Zunckel, M., Koosailee, A., Yarwood, G., Maure, G., Venjonoka, K., Tienhoven, A.M., Otter, L., 2006. Modelled surface ozone over southern Africa during the Cross Border Air Pollution Impact Assessment Project. Environ. Model. Softw., 21, 911–924.

http://www.rsc.org/chemistryworld/Issues/2003/May/weekend.asp

# Commentary
# Impacts of ozone on agricultural crops in southern Africa

**Tracey L. Laban, Johan P. Beukes, Pieter G. van Zyl, Jacques M. Berner**
Unit for Environmental Sciences and Management, North-West University, Potchefstroom

The potential for ozone ($O_3$) damage to agricultural crops, trees and native plants is well documented in literature. $O_3$ has been shown to cause a wide variety of effects to important agricultural crops including visible leaf injury, growth and yield reductions, as well as deteriorating nutritional quality in certain crops. $O_3$-induced damage is especially an issue of concern if it threatens food supply and the economies of countries that are based strongly on agricultural production. With the availability of global chemistry transport models, global and regional estimates of crop losses can be obtained (Van Dingenen, 2009; Avnery et al., 2011; Wang and Mauzerall, 2004). Present day global relative yield losses due to $O_3$ damage are estimated to range between 7% and 12% for wheat, 6% and 16% for soybean, 3% and 4% for rice and 3% and 5% for maize (Van Dingenen, 2009). In India it was calculated that $O_3$ damage to wheat and rice resulted in a nationally aggregated yield loss of 9.2%, that is sufficient to feed 94 million people living below the poverty line in that country (Ghude et al., 2014).

Agricultural crops contribute significantly to the economy in southern African countries. Staple crops in South Africa that meet the food needs for local consumption are maize and wheat, whilst economically important crops include sunflowers and sugarcane. These crops must be assessed for $O_3$-induced effects. The potential for elevated concentrations of $O_3$ is particularly high in many regions of South Africa because of the combination of intense and extended solar radiation, and the relatively high emission of precursor species, such as nitrogen oxides and volatile organic compounds, from human and natural sources. Rural and agricultural areas in southern Africa, subject to regional air pollution events could have even higher $O_3$ concentrations than industrialised areas (sources of $O_3$ precursors) if polluted air masses are transported to these areas.

An assessment of surface $O_3$ measurements over southern Africa indicated that maximum $O_3$ concentrations are between 40 and 60 ppb, but can reach more than 90 ppb during the springtime (Zunckel et al., 2004). Furthermore, modelled $O_3$ as part of the Cross Border Impact Assessment Project, indicated large areas on the sub-continent where surface $O_3$ concentrations exceed 40 ppb for up to 10 h per day (Zunckel et al., 2006). The implications are that at these levels of exposure southern African vegetation may be at risk to damage by $O_3$. Josipovic et al. (2010) did an assessment of critical level exceedance for $O_3$, utilising passive samplers and found $O_3$ levels below the critical levels. However, the methodology applied did not consider cumulative $O_3$ exposure over time, which really determines the long-term effects on crops. The seasonal pattern of $O_3$ in southern Africa reveals the highest concentrations during spring and winter, with lower concentrations during summer (Laakso et al., 2013). The diurnal cycle of $O_3$ is characterised by an increase from a minimum near sunrise to maximum values in the early afternoon, and decreasing to the early morning minimum (Zunckel et al., 2004). Therefore plant uptake of $O_3$ should be highest during midday and early afternoon when high rates of leaf gas-exchange coincide with rising $O_3$ concentrations.

$O_3$ enters the plant mainly through its open stomata (leaf pores) when plants take up carbon dioxide ($CO_2$) for photosynthesis. $O_3$ is a highly reactive molecule; inside the plant it produces several reactive oxygen species such as superoxides, peroxides and hydroxyl radicals. Among other negative effects, the oxidative action of $O_3$ destroys key enzymes and proteins, including the photosynthetic enzyme Rubisco, which will result in a much reduced photosynthetic efficiency. $O_3$ also causes damage to the stomatal apparatus resulting in the inability of the plant to control the opening and closing of the stomata. Reduced Rubisco and impaired stomatal function will cause less $CO_2$ being taken up by the plant leading to a reduced photosynthetic efficiency, and will ultimately lead to reduced growth rates and yield. At short periods of high concentrations of $O_3$, visible injury symptoms associated with $O_3$ damage include small flecks or stipples on leaf tissues. Visible injuries usually appears early in the growing season and continues to develop during the season. Continuous exposure over long periods to relatively low concentrations of $O_3$ may induce some of the same visible symptoms, including chlorosis (loss of chlorophyll), necrosis (premature death of cells and living tissue) and accelerated senescence (ageing) in leaves (De Temmerman et al., 2002). Injuries not visible to the naked eye result from pollutant impacts on plant physiological or biochemical processes. Some of these changes increase the resistance of the leaf to subsequent $O_3$ exposure whilst others decrease photosynthetic function.

$O_3$ damage to crops can be evaluated based on the AOT40, an index used in Europe that serves as the standard for protection of vegetation against $O_3$ pollution. AOT40 is defined as the accumulated $O_3$ exposure above a threshold concentration of 40 ppb during daylight hours of the growing season (UNECE, 2010). The AOT40 exposure index is cumulative, i.e. it integrates

$$AOT40\ (ppb\ h) = \sum_{i=1}^{n}([O_3]_i - 40), \qquad \text{for } O_3 \geq 40 \text{ ppb}$$

exposure over time in order to detect long-term effects. Experimental data has shown that the impacts of $O_3$ on plants are often better related to accumulated exposure above a threshold concentration rather than the mean concentration over the growing season. The European AOT40 critical level is 3000 ppb h for agricultural crops (over a growing season of 3 months) and 5000 ppb h for forests. However the AOT40 approach has limitations since it does not directly reflect the $O_3$ absorbed by plant surfaces, with damage being calculated solely on the basis of ambient $O_3$ concentrations. $O_3$ flux, which is the rate at which $O_3$ is absorbed by plant surfaces, is a better measure of biological response. The use of an impact assessment method approach based on the actual flux of $O_3$ through the plant stomata is recommended, but requires additional information such as $O_3$ flux data and dose-response relationships of different plant species.

Experiments to determine dose-response functions for plants have used controlled-environment greenhouses, field chambers and free-air systems (U.S. EPA, 2006). Research studies have derived relationships between "$O_3$ dose" or "$O_3$ exposure" and the yield of the major crop species through controlled $O_3$ fumigation experiments under near-field conditions using open-top chambers. An open-top chamber research facility exists at North-West University where $O_3$ assessments have been performed on maize, snap beans, garden peas and canola plants, and have demonstrated adverse physiological and growth effects due to elevated $O_3$ levels. Most recently, a sugarcane trial is underway on two local cultivars to determine the effects of elevated $CO_2$ concentrations, elevated $O_3$ concentrations, and also the combined effects of elevated $CO_2$ with elevated $O_3$ in the absence of drought stress. To our knowledge, there is no quantitative data on $O_3$ exposure-plant response (E-R functions) for sugarcane currently available.

Compared to the control plants (exposed to charcoal-filtered air), sugarcane plants exposed to concentrations of 80 ppb $O_3$ for 9 hours a day (photoperiod) showed chlorotic and necrotic lesions on their leaves, leaf senescence, as well as stunted growth. Evidence from visual changes also suggests that sugarcane crops are more sensitive to the elevated $O_3$ early in the growth season, while later showing signs of recovery to sustained $O_3$ stress. In this trial, seedlings of sugarcane were used in the open-top chambers and $O_3$ fumigation only commenced after a few weeks, once the plants had reached some level of maturity. Plant response to $O_3$ may vary with physiological age and young plants are considered more sensitive to $O_3$ exposure in the early stages of development (Reiling and Davison, 1994 and references therein). Developmental stage plays a major role in determining plant sensitivity to $O_3$.

It is important to note that $O_3$ stress does not act independently, but is one of many stresses that will affect growth and productivity of crops. $O_3$ can also cause altered sensitivity to biotic (e.g. pest and pathogen attack) and abiotic stresses (e.g. drought, floods). In some regions of southern Africa, drought stress is more common than $O_3$ stress and the combination of

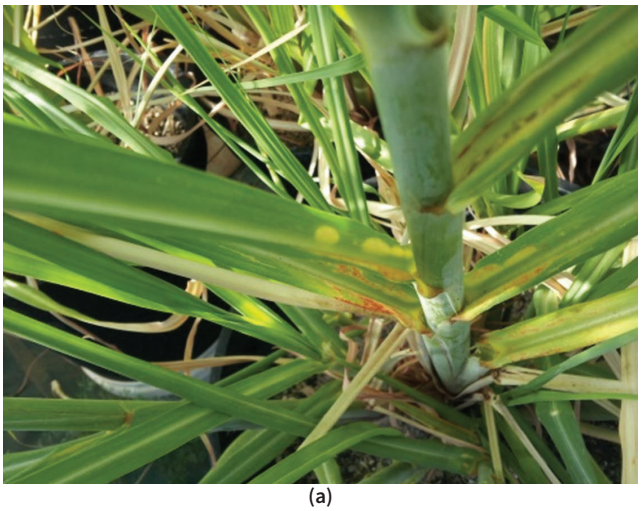

**(a)**

*Sugarcane leaves exhibiting visible injury from $O_3$ exposure: tiny, brown spots (stipples) and yellow patches early on – yellowing is a sign of chlorosis.*

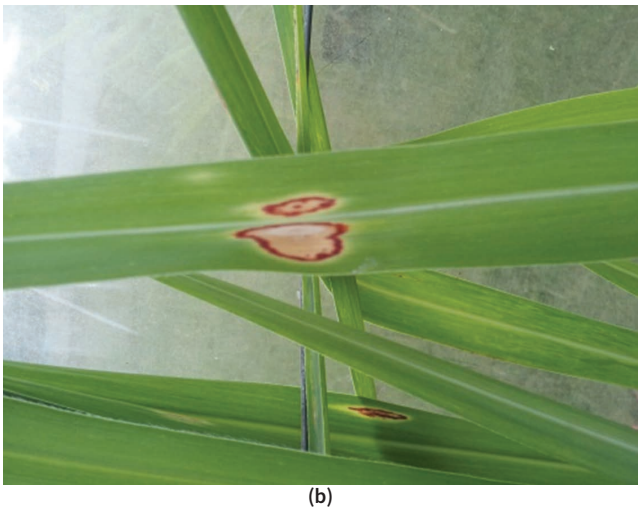

**(b)**

*Sugarcane leaves exhibiting visible injury from $O_3$ exposure: reddish-brown lesions later on – a sign of necrosis.*

$O_3$ stress and drought will often produce plant responses that are due primarily to the effect of drought (van Tienhoven, 2005). The more frequent occurrence of drought stress make plants in the southern African region more tolerant to $O_3$ stress compared to plants in Europe. Drought stress reduces the stomatal opening, and hence reduces $O_3$ uptake by the plant. There are also interactions between $O_3$ stress and other atmospheric gases that can modify the impact of $O_3$. For example, rising levels of atmospheric $CO_2$ are thought to ameliorate the influence of increasing ground-level $O_3$ concentrations i.e. plant stress caused by $O_3$ is offset by $CO_2$. $O_3$ stress on its own leads to foliar injury, suppressed growth and yield in plants, whereas elevated $CO_2$ generally enhances growth and yield; the combination of elevated $O_3$ and $CO_2$ can affect plant response differently compared to each stress occurring separately (Heagle et al., 1999). Also, the presence of other pollutants such as sulphur dioxide may act synergistically with $O_3$, increasing growth reductions (WHO, 2000).

There are two types of $O_3$ exposure, i.e. acute exposure where concentrations are high and range from 120 – 500 ppb for hours (as is the case at polluted sites), or chronic exposure where there is an elevated background concentration with daily peak concentrations of 40 – 120 ppb over several days in the growing season (Long and Naidu, 2002). But what is more damaging to plants, short-term exposure to very high $O_3$ concentrations or long-term exposure to moderate $O_3$ concentrations? In South Africa, chronic exposure in the range that can affect plants interspersed with short duration pollution episodes of peak concentrations often occurs. It has been stated that intermediate concentrations of $O_3$ may have the largest impact on crop yields (Krupa et al., 1995). On the other hand, Köllner and Krause (2000) pointed out that $O_3$ peaks are more important for yield losses than constant elevated $O_3$ exposure. Opinions therefore differ as to the extent of yield reductions resulting from periodic exposure to high concentrations (well above any supposed threshold) or chronic exposure to concentrations near the threshold. Nevertheless, more studies link chronic exposure to consequences of reduced growth and yield, adding that the severity varies for different crop species and also for different cultivars within a crop species.

Southern African impact studies to date have adopted the European AOT40 for assessing $O_3$ damage to crops (Avnery et al., 2011; van Tienhoven et al., 2006). However, despite the AOT40 for the southern African environment exceeding the European AOT40 level for crop damages (3000 ppb h), no vegetation damages have been reported. Van Tienhoven et al. (2005) explained that the reasons for this could be either that there is a lack of knowledge to distinguish between actual $O_3$-induced effects and effects from other stresses, or that the local vegetation may have had hundreds of years to adapt to elevated $O_3$ levels, as some Mediterranean species. The adaption aspect was also discussed by Scholes and Scholes (1998), who argued that local indigenous species, especially on the savannah, may be less sensitive to $O_3$ exposure compared to planted alien species such as pine and eucalyptus. The applicability of the AOT40 to tolerant southern African crops should be revisited. Note that while a value of 40 ppb (AOT40) has been employed in impact assessment research in Europe, a higher value of 60 ppb (AOT60) has been used in the U.S. The open-top chamber trials at North-West University have historically used 80 ppb $O_3$ treatments on maize, snap beans and canola, and found adverse physiological and biochemical effects on these species. Therefore these effects might be better related to the use of a higher threshold concentration than 40 ppb. However, the suitability of a higher threshold for South African species must still be established.

Most of the actions taken to control ground-level $O_3$ pollution are aimed at reducing human exposure to this pollutant. Given the concentration thresholds for effects, these measures may therefore be expected to have the greatest beneficial impact in terms of health, with somewhat less of an impact in relation to plants. The South African National Ambient Air Quality Standard for $O_3$ (8-h running average of 61 ppb) is based on World Health Organisation (WHO) guidelines that are primarily concerned with the protection of human health. Air quality guidelines based on the United Nations Economic Commission for Europe (UNECE) critical levels (UNECE, 1998) provide the best available scientific basis for the protection of natural ecosystems against $O_3$. However, country-specific research on exposure-response relationships is needed to provide sufficient data on the critical levels for South African vegetation (WHO, 2000). Information on critical levels is a means to update the existing air quality standards for ground-level $O_3$ which take into account not just the adverse effect on human health, but also on vegetative health, in order to protect the ecosystem as a whole.

$O_3$ impact studies focusing on local crop variants should be advanced using either the concentration-based AOT40 approach (good identification tool for crop damage, but not accounting for interacting stresses) or the flux-based approach (good yield loss assessment tool, but large data requirements). For the AOT40 approach, continuous ambient $O_3$ measurements are needed. For the flux-based approach, measurements of local environmental variables such as humidity and soil moisture (lower during droughts), temperature, radiation, vapour pressure deficit and wind speed are important parameters influencing $O_3$ uptake. Both these approaches will require exposure-response functions (concentration-response or dose-response) for local cultivars. The application of European crop exposure-response functions add to uncertainties in agricultural impact assessments. Therefore, local exposure-response relationships under ambient conditions, and in a changing climate, should be derived through routes such as open-top chamber experiments.

## Acknowledgements

The financial assistance of the National Research Foundation (NRF) towards this research is hereby acknowledged. Opinions expressed and conclusions arrived at, are those of the author and are not necessarily to be attributed to the NRF.

## References

Avnery, S., Mauzerall, D.L., Liu, J., Horowitz, Larry W., 2011. Global crop yield reductions due to surface ozone exposure: 1. Year 2000 crop production losses and economic damage. Atmos. Environ. 45, 2284–2296.

De Temmerman, L., Karlsson, G.P., Donnelly, A., Ojanperä, K., Jäger, H.-J., Finnan, J., Ball G., 2002. Factors influencing visible ozone injury on potato including the interaction with carbon dioxide. Europ. J. Agronomy 17, 291-302.

Ghude, S.D., Jena, C., Chate, D.M., Beig, G., Pfister, G.G., Kumar, R., Ramanathan, V., 2014. Reductions in India's crop yield due to ozone. Geophys. Res. Lett. 41, 5685-5691, doi:10.1002/2014GL060930.

Heagle, A.S., Miller, J.E., Booker, F.L., Pursley, W.A., 1999. Ozone stress, carbon dioxide enrichment, and nitrogen fertility interactions in cotton. Crop Sci., 39, 731-741.

Köllner, B., Krause, G.H.M., 2000. Changes in carbohydrates

leaf pigments and yield in potatoes induced by different ozone exposure regimes. Agric. Ecosyst. Environ. 78, 149-158.

Krupa, S.V., Grunhage, L., Jager, H.-J., Nosal, M., Manning, W.J., Legge, A.H., Hanewald, K., 1995. Ambient ozone ($O_3$) and adverse crop response: A unified view of cause and effect. Environ. Pollut., 87, 119-126.

Josipovic, M., Annegarn, H. J., Kneen, M.A., Pienaar, J.J., Piketh, S.J., 2010. Concentrations, distributions and critical levels exceedance assessment of $SO_2$, $NO_2$ and $O_3$ in South Africa. Environ. Monit. Assess., 171(1), 181–196.

Laakso, L. et al., 2013. Ozone concentrations and their potential impacts on vegetation in southern Africa. In: Matyssek, R., Clarke, N., Cudlin, P., Mikkelsen, T.N., Tuovinen, J-P., Wieser, G., Paoletti E. (Eds.), Climate Change, Air Pollution and Global Challenges: Understanding and Perspectives from Forest Research. Newnes, Boston, US, pp. 429-450.

Long, S.P., Naidu, S.L., 2002. Effects of oxidants at the biochemical, cell and physiological levels. In: Treshow, M. (Ed.), Air Pollution and Plant Life. John Wiley, London, UK, pp. 69–88.
Reiling, K., Davison A.W., 1994. Effect of exposure to ozone at different stages in the development of plantago major L. on chlorophyll fluorescence and gas exchange. New Phytol., 128, 509-514.

Scholes, R.J., Scholes, M.C., 1998. Natural and human-related sources of ozone-forming trace gases in southern Africa. S. Afr. J. Sci., 94, 422–425.

UNECE, 1998. Convention on Long-Range Transboundary Air Pollution, Internet web site (http://www.unece.org/env/lrtap_h.htm), UNECE, Geneva.

UNECE, 2010. Mapping critical levels for vegetation. Manual on Methodologies and Criteria for Modelling and Mapping Critical Loads & Levels and Air Pollution Effects, Risks and Trends. United Nations Economic Commission for Europe (UNECE) Convention on Long-range Transboundary Air Pollution, Geneva, Switzerland. http://icpvegetation.ceh.ac.uk/manuals/mapping_manual.html.

U.S. EPA, 2006. Air Quality Criteria for Ozone and Related Photochemical Oxidants EPA/600/R-05/004aF-cF. U.S. Environmental Protection Agency, Washington, D.C.

van Dingenen, R., Dentener, F.J., Raes, F., Krol, M.C., Emberson, L., Cofala J., 2009. The global impact of ozone on agricultural crop yields under current and future air quality legislation. Atmos. Environ., 43, 604-618.

van Tienhoven, A., Otter, L., Lenkopane, M., Venjonoka, K., Zunckel, M., 2005. Assessment of ozone impacts on vegetation in southern Africa and directions for future research. S. Afr. J. Sci., 101, 143–148.

van Tienhoven, A., Zunckel, M., Emberson, L., Koosailee, A., Otter, L., 2006. Preliminary assessment of risk of ozone impacts to maize (zea mays) in southern Africa. Environ. Pollut., 140, 220–230.

Wang, X., Mauzerall, D.L., 2004. Characterizing distributions of surface ozone and its impact on grain production in China, Japan and South Korea: 1990 and 2020. Atmos. Environ., 38, 4383-4402.

WHO Regional Office for Europe, 2000. Effects of ozone on vegetation. In: WHO (Ed.) Air quality guidelines for Europe. 2nd edition. WHO Regional Publications, European Series, No. 91.

Zunckel, M., Venjonoka, K., Pienaar, J.J., Brunke, E.-G., Pretorius, O., Koosialee, A., Raghunandan, A., van Tienhoven, A.M., 2004. Surface ozone over southern Africa: synthesis of monitoring results during the Cross Border Air Pollution Impact Assessment project. Atmos. Environ., 38, 6139–6147.

Zunckel, M., Koosailee, A., Yarwood, G., Maure, G., Venjonoka, K., Tienhoven, A.M., Otter, L., 2006. Modelled surface ozone over southern Africa during the Cross Border Air Pollution Impact Assessment Project. Environ. Model. Softw., 21, 911–924.

# BIBLIOGRAPHY


ABDUL-WAHAB, S. A., BAKHEIT, C. S. & AL-ALAWI, S. M. 2005. Principal component and multiple regression analysis in modelling of ground-level ozone and factors affecting its concentrations. *Environmental Modelling & Software,* 20**,** 1263-1271.

AGHEDO, A. M., SCHULTZ, M. G. & RAST, S. 2007. The influence of African air pollution on regional and global tropospheric ozone. *Atmospheric Chemistry and Physics,* 7**,** 1193-1212.

AINSWORTH, E. A. 2008. Rice production in a changing climate: a meta-analysis of responses to elevated carbon dioxide and elevated ozone concentration. *Global Change Biology,* 14**,** 1642-1650.

AIR RESOURCES LABORATORY 2017. Gridded Meteorological Data Archives.

ANDREAE, M., ATLAS, E., HARRIS, G., HELAS, G., KOCK, A. D., KOPPMANN, R., MAENHAUT, W., MANÖ, S., POLLOCK, W. & RUDOLPH, J. 1996. Methyl halide emissions from savanna fires in southern Africa. *Journal of Geophysical Research: Atmospheres,* 101**,** 23603-23613.

ANDREAE, M. O. 1991. Biomass burning: its history, use, and distribution and its impact. *In:* LEVINE, J. S. (ed.) *Global Biomass Burning: Atmospheric, Climatic, and Biospheric Implications* Cambridge, MA: MIT Press.

ANENBERG, S. C., HOROWITZ, L. W., TONG, D. Q. & WEST, J. J. 2010. An estimate of the global burden of anthropogenic ozone and fine particulate matter on premature human mortality using atmospheric modeling. *Environmental Health Perspectives,* 118**,** 1189.

ATKINSON, R. 2000. Atmospheric chemistry of VOCs and $NO_x$. *Atmospheric Environment,* 34**,** 2063-2101.

AVNERY, S., MAUZERALL, D. L., LIU, J. & HOROWITZ, L. W. 2011. Global crop yield reductions due to surface ozone exposure: 1. Year 2000 crop production losses and economic damage. *Atmospheric Environment,* 45**,** 2284-2296.

AWANG, N. R., RAMLI, N. A., YAHAYA, A. S. & ELBAYOUMI, M. 2015. Multivariate methods to predict ground level ozone during daytime, nighttime, and critical conversion time in urban areas. *Atmospheric Pollution Research,* 6**,** 726-734.

BAKER, A. K., SAUVAGE, C., THORENZ, U. R., VAN VELTHOVEN, P., ORAM, D. E., ZAHN, A., BRENNINKMEIJER, C. A. M. & WILLIAMS, J. 2016. Evidence for strong, widespread chlorine radical chemistry associated with pollution outflow from continental Asia. *Scientific Reports,* 6**,** 36821.

BALASHOV, N. V., THOMPSON, A. M., PIKETH, S. J. & LANGERMAN, K. E. 2014. Surface ozone variability and trends over the South African Highveld from 1990 to 2007. *Journal of Geophysical Research: Atmospheres,* 119**,** 4323-4342.

BARBOSA, P. M., STROPPIANA, D., GRÉGOIRE, J. M. & CARDOSO PEREIRA, J. M. 1999. An assessment of vegetation fire in Africa (1981–1991): Burned areas, burned biomass, and atmospheric emissions. *Global Biogeochemical Cycles,* 13**,** 933-950.

BARRIE, L., BOTTENHEIM, J., SCHNELL, R., CRUTZEN, P. & RASMUSSEN, R. 1988. Ozone destruction and photochemical reactions at polar sunrise in the lower Arctic atmosphere. *Nature,* 334**,** 138.

BERNER, J., MALIBA, B. & INBARAJ, P. 2015. Impact of elevated levels of $CO_2$ and $O_3$ on the yield and photosynthetic capabilities of Brassica napus. *Procedia Environmental Sciences,* 29**,** 255.

BIESENTHAL, T., BOTTENHEIM, J., SHEPSON, P., LI, S. M. & BRICKELL, P. 1998. The chemistry of biogenic hydrocarbons at a rural site in eastern Canada. *Journal of Geophysical Research: Atmospheres,* 103**,** 25487-25498.

BLOOMFIELD, P., ROYLE, J. A., STEINBERG, L. J. & YANG, Q. 1996. Accounting for meteorological effects in measuring urban ozone levels and trends. *Atmospheric Environment,* 30**,** 3067-3077.

BOERSMA, K., ESKES, H., MEIJER, E. & KELDER, H. 2005. Estimates of lightning $NO_x$ production from GOME satellite observations. *Atmospheric Chemistry and Physics,* 5**,** 2311-2331.

BOND, D. W., STEIGER, S., ZHANG, R., TIE, X. & ORVILLE, R. E. 2002. The importance of $NO_x$ production by lightning in the tropics. *Atmospheric Environment,* 36**,** 1509-1519.

BORRELL, P., BUILTJES, P., GRENNFELT, P. & HOV, O. 1997. *Photo-oxidants, acidification and tools: policy applications of EUROTRAC results: the report of the EUROTRAC application project*, Springer Science & Business Media.

CARPENTER, L. J., MACDONALD, S. M., SHAW, M. D., KUMAR, R., SAUNDERS, R. W., PARTHIPAN, R., WILSON, J. & PLANE, J. M. 2013. Atmospheric iodine levels influenced by sea surface emissions of inorganic iodine. *Nature Geoscience,* 6**,** 108.

CAZORLA, M. & BRUNE, W. H. 2010. Measurement of Ozone Production Sensor. *Atmospheric Measurement Techniques,* 3**,** 545-555.

CHRISTIAN, H. J., BLAKESLEE, R. J., BOCCIPPIO, D. J., BOECK, W. L., BUECHLER, D. E., DRISCOLL, K. T., GOODMAN, S. J., HALL, J. M., KOSHAK, W. J. & MACH, D. M. 2003. Global frequency and distribution of lightning as observed from space by the Optical Transient Detector. *Journal of Geophysical Research: Atmospheres,* 108**,** ACL 4-1-ACL 4-15.

CLRTAP 2014. Mapping critical levels for vegetation, Chapter III of Manual on methodologies and criteria for modelling and mapping critical loads and levels and air pollution effects, risks and trends. UNECE Convention on Long-Range Transboundary Air Pollution.

COMBRINK, J., DIAB, R., SOKOLIC, F. & BRUNKE, E. 1995. Relationship between surface, free tropospheric and total column ozone in two contrasting areas in South Africa. *Atmospheric Environment,* 29**,** 685-691.

COOPER, O. R., GAO, R. S., TARASICK, D., LEBLANC, T. & SWEENEY, C. 2012. Long-term ozone trends at rural ozone monitoring sites across the United States, 1990–2010. *Journal of Geophysical Research: Atmospheres,* 117.

COOPER, O. R., PARRISH, D., ZIEMKE, J., BALASHOV, N., CUPEIRO, M., GALBALLY, I., GILGE, S., HOROWITZ, L., JENSEN, N. & LAMARQUE, J.-F. 2014. Global distribution and trends of tropospheric ozone: An observation-based review. *Elem Sci Anth,* 2.

CRUTZEN, P. 1973. A discussion of the chemistry of some minor constituents in the stratosphere and troposphere. *Pure and Applied Geophysics,* 106**,** 1385-1399.

CRUTZEN, P. J. & ANDREAE, M. O. 1990. Biomass Burning in the Tropics: Impact on Atmospheric Chemistry and Biogeochemical Cycles. *Science,* 250**,** 1669-1678.

DAVIS, J., COX, W., REFF, A. & DOLWICK, P. 2011. A comparison of CMAQ-based and observation-based statistical models relating ozone to meteorological parameters. *Atmospheric Environment,* 45**,** 3481-3487.

DE TEMMERMAN, L., KARLSSON, G. P., DONNELLY, A., OJANPERÄ, K., JÄGER, H.-J., FINNAN, J. & BALL, G. 2002. Factors influencing visible ozone injury on potato including the interaction with carbon dioxide. *European Journal of Agronomy,* 17**,** 291-302.

DERWENT, R. G., MANNING, A. J., SIMMONDS, P. G., SPAIN, T. G. & O'DOHERTY, S. 2013. Analysis and interpretation of 25 years of ozone observations at the Mace Head Atmospheric Research Station on the Atlantic Ocean coast of Ireland from 1987 to 2012. *Atmospheric Environment,* 80**,** 361-368.

DIAB, R., THOMPSON, A., MARI, K., RAMSAY, L. & COETZEE, G. 2004. Tropospheric ozone climatology over Irene, South Africa, from 1990 to 1994 and 1998 to 2002. *Journal of Geophysical Research: Atmospheres,* 109.

DICKERSON, R. R., RHOADS, K. P., CARSEY, T. P., OLTMANS, S. J., BURROWS, J. P. & CRUTZEN, P. J. 1999. Ozone in the remote marine boundary layer: A possible role for halogens. *Journal of Geophysical Research: Atmospheres,* 104**,** 21385-21395.

DOMINICK, D., JUAHIR, H., LATIF, M. T., ZAIN, S. M. & ARIS, A. Z. 2012. Spatial assessment of air quality patterns in Malaysia using multivariate analysis. *Atmospheric Environment,* 60**,** 172-181.

DRAXLER, R. R. & HESS, G. D. 1998. An overview of the HYSPLIT_4 modeling system of trajectories, dispersion, and deposition. *Australian Meteorological Magazine,* 47**,** 295-308.

DUNLEA, E., HERNDON, S., NELSON, D., VOLKAMER, R., SAN MARTINI, F., SHEEHY, P., ZAHNISER, M., SHORTER, J., WORMHOUDT, J. & LAMB, B. 2007. Evaluation of nitrogen dioxide chemiluminescence monitors in a polluted urban environment. *Atmospheric Chemistry and Physics,* 7**,** 2691-2704.

DWYER, E., PEREIRA, J., GRÉGOIRE, J. M. & DACAMARA, C. C. 1999. Characterization of the spatio-temporal patterns of global fire activity using satellite imagery for the period April 1992 to March 1993. *Journal of Biogeography,* 27**,** 57-69.

DWYER, E., PINNOCK, S., GRÉGOIRE, J.-M. & PEREIRA, J. 2000. Global spatial and temporal distribution of vegetation fire as determined from satellite observations. *International Journal of Remote Sensing,* 21**,** 1289-1302.

EFEOĞLU, B., EKMEKCI, Y. & CICEK, N. 2009. Physiological responses of three maize cultivars to drought stress and recovery. *South African Journal of Botany,* 75**,** 34-42.

EMBERSON, L. D., ASHMORE, M. R., CAMBRIDGE, H. M., SIMPSON, D. & TUOVINEN, J. P. 2000. Modelling stomatal ozone flux across Europe. *Environmental Pollution,* 109**,** 403-413.

FANN, N., LAMSON, A. D., ANENBERG, S. C., WESSON, K., RISLEY, D. & HUBBELL, B. J. 2012. Estimating the national public health burden associated with exposure to ambient $PM_{2.5}$ and ozone. *Risk Analysis,* 32**,** 81-95.

FARMER, D., PERRING, A., WOOLDRIDGE, P., BLAKE, D., BAKER, A., MEINARDI, S., HUEY, L., TANNER, D., VARGAS, O. & COHEN, R. 2011. Impact of organic nitrates on urban ozone production. *Atmospheric Chemistry and Physics,* 11**,** 4085-4094.

FEHSENFELD, F., DICKERSON, R., HÜBLER, G., LUKE, W., NUNNERMACKER, L., WILLIAMS, E., ROBERTS, J., CALVERT, J., CURRAN, C. & DELANY, A. 1987. A ground-based intercomparison of NO, $NO_x$, and $NO_y$ measurement techniques. *Journal of Geophysical Research: Atmospheres,* 92**,** 14710-14722.

FELZER, B. S., CRONIN, T., REILLY, J. M., MELILLO, J. M. & WANG, X. 2007. Impacts of ozone on trees and crops. *Comptes Rendus Geoscience,* 339**,** 784-798.

FENG, Z., SUN, J., WAN, W., HU, E. & CALATAYUD, V. 2014. Evidence of widespread ozone-induced visible injury on plants in Beijing, China. *Environmental Pollution,* 193**,** 296-301.

FINLAYSON-PITTS, B. J. & PITTS, J. N. 1986. *Atmospheric Chemistry : Fundamentals and Experimental Techniques,* New York, Wiley.

FINLAYSON-PITTS, B. J. & PITTS JR, J. N. 2000. *Chemistry of the Upper and Lower Atmosphere: Theory, Experiments, and Applications,* San Diego, Academic Press.

FIORE, A. M., JACOB, D. J., BEY, I., YANTOSCA, R. M., FIELD, B. D., FUSCO, A. C. & WILKINSON, J. G. 2002. Background ozone over the United States in summer: Origin, trend, and contribution to pollution episodes. *Journal of Geophysical Research: Atmospheres,* 107**,** ACH 11-1-ACH 11-25.

FIORE, A. M., JACOB, D. J., LOGAN, J. A. & YIN, J. H. 1998. Long-term trends in ground level ozone over the contiguous United States, 1980–1995. *Journal of Geophysical Research: Atmospheres,* 103**,** 1471-1480.

FISCHER, E., JACOB, D. J., YANTOSCA, R. M., SULPRIZIO, M. P., MILLET, D., MAO, J., PAULOT, F., SINGH, H., ROIGER, A. & RIES, L. 2014. Atmospheric peroxyacetyl nitrate (PAN): a global budget and source attribution. *Atmospheric Chemistry and Physics,* 14**,** 2679-2698.

FISCUS, E. L., BOOKER, F. L. & BURKEY, K. O. 2005. Crop responses to ozone: uptake, modes of action, carbon assimilation and partitioning. *Plant, Cell & Environment,* 28**,** 997-1011.

FISHMAN, J., WATSON, C. E., LARSEN, J. C. & LOGAN, J. A. 1990. Distribution of tropospheric ozone determined from satellite data. *Journal of Geophysical Research: Atmospheres,* 95**,** 3599-3617.
FUSCO, A. C. & LOGAN, J. A. 2003. Analysis of 1970–1995 trends in tropospheric ozone at Northern Hemisphere midlatitudes with the GEOS-CHEM model. *Journal of Geophysical Research: Atmospheres,* 108.
GARDNER, M. & DORLING, S. 2000. Meteorologically adjusted trends in UK daily maximum surface ozone concentrations. *Atmospheric Environment,* 34**,** 171-176.
GARSTANG, M., TYSON, P. D., SWAP, R., EDWARDS, M., KÅLLBERG, P. & LINDESAY, J. A. 1996. Horizontal and vertical transport of air over southern Africa. *Journal of Geophysical Research: Atmospheres,* 101**,** 23721-23736.
GEDDES, J. A., MURPHY, J. G. & WANG, D. K. 2009. Long term changes in nitrogen oxides and volatile organic compounds in Toronto and the challenges facing local ozone control. *Atmospheric Environment,* 43**,** 3407-3415.
GHUDE, S. D., JENA, C., CHATE, D., BEIG, G., PFISTER, G., KUMAR, R. & RAMANATHAN, V. 2014. Reductions in India's crop yield due to ozone. *Geophysical Research Letters,* 41**,** 5685-5691.
GIGLIO, L., CSISZAR, I. & JUSTICE, C. O. 2006. Global distribution and seasonality of active fires as observed with the Terra and Aqua Moderate Resolution Imaging Spectroradiometer (MODIS) sensors. *Journal of Geophysical Research: Biogeosciences,* 111.
GORAI, A., TULURI, F., TCHOUNWOU, P. & AMBINAKUDIGE, S. 2015. Influence of local meteorology and $NO_2$ conditions on ground-level ozone concentrations in the eastern part of Texas, USA. *Air Quality, Atmosphere and Health,* 8**,** 81-96.
GOVERNMENT GAZETTE REPUBLIC OF SOUTH AFRICA 2009. National Environmental Management: Air Quality Act, 2004 (Act No. 39 of 2004) National Ambient Air Quality Standards. *In:* ENVIRONMENTAL AFFAIRS (ed.).
GRANGE, S. K. 2014. Averaging wind speeds and directions.
GREENSLADE, J. W., ALEXANDER, S. P., SCHOFIELD, R., FISHER, J. A. & KLEKOCIUK, A. K. 2017. Stratospheric ozone intrusion events and their impacts on tropospheric ozone in the Southern Hemisphere. *Atmospheric Chemistry and Physics,* 17**,** 10269-10290.
HAO, W. M. & LIU, M. H. 1994. Spatial and temporal distribution of tropical biomass burning. *Global Biogeochemical Cycles,* 8**,** 495-503.
HARDACRE, C., WILD, O. & EMBERSON, L. 2015. An evaluation of ozone dry deposition in global scale chemistry climate models. *Atmospheric Chemistry and Physics,* 15**,** 6419-6436.
HASTIE, T. & TIBSHIRANI, R. 1990. *Generalized additive models*, Wiley Online Library.
HAYN, M., BEIRLE, S., HAMPRECHT, F. A., PLATT, U., MENZE, B. H. & WAGNER, T. 2009. Analysing spatio-temporal patterns of the global $NO_2$-distribution retrieved from GOME satellite observations using a generalized additive model. *Atmospheric Chemistry and Physics,* 9**,** 6459-6477.
HEWITT, C. N. 1998. *Reactive hydrocarbons in the atmosphere*, Elsevier.
HEYNEKE, E., SMIT, P., VAN RENSBURG, L. & KRUGER, G. 2012. Open-top chambers to study air pollution impacts in South Africa. Part I: microclimate in open-top chambers. *South African Journal of Plant and Soil,* 29**,** 1-7.
HIDY, G. M. & BLANCHARD, C. L. 2015. Precursor reductions and ground-level ozone in the Continental United States. *Journal of the Air & Waste Management Association,* 65**,** 1261-1282.
HIRSIKKO, A., VAKKARI, V., TIITTA, P., HATAKKA, J., KERMINEN, V. M., SUNDSTRÖM, A. M., BEUKES, J. P., MANNINEN, H. E., KULMALA, M. & LAAKSO, L. 2013. Multiple daytime nucleation events in semi-clean savannah and industrial environments in South Africa: analysis based on observations. *Atmospheric Chemistry and Physics,* 13**,** 5523-5532.
HIRSIKKO, A., VAKKARI, V., TIITTA, P., MANNINEN, H. E., GAGNÉ, S., LAAKSO, H., KULMALA, M., MIRME, A., MIRME, S., MABASO, D., BEUKES, J. P. & LAAKSO, L.

2012. Characterisation of sub-micron particle number concentrations and formation events in the western Bushveld Igneous Complex, South Africa. *Atmospheric Chemistry and Physics,* 12**,** 3951-3967.
HOLLAND, M., KINGHORN, S., EMBERSON, L., CINDERBY, S., ASHMORE, M., MILLS, G. & HARMENS, H. 2006. Development of a framework for probabilistic assessment of the economic losses caused by ozone damage to crops in Europe. *CEH Rep. C02309NEW* Bangor, U.K.: NERC/Centre for Ecology and Hydrology.
HOLLOWAY, A. M. & WAYNE, R. P. 2010. *Atmospheric chemistry,* Cambridge, Royal Society of Chemistry.
HOV, Ø. 1997. *Tropospheric ozone research : tropospheric ozone in the regional and sub-regional context,* Berlin ; New York, Springer.
HU, L., JACOB, D. J., LIU, X., ZHANG, Y., ZHANG, L., KIM, P. S., SULPRIZIO, M. P. & YANTOSCA, R. M. 2017. Global budget of tropospheric ozone: evaluating recent model advances with satellite (OMI), aircraft (IAGOS), and ozonesonde observations. *Atmospheric Environment,* 167**,** 323-334.
INMAN-BAMBER, N. & SMITH, D. 2005. Water relations in sugarcane and response to water deficits. *Field Crops Research,* 92**,** 185-202.
IPCC 2007. *Climate change 2007: The physical science basis: contribution of Working Group I to the Fourth Assessment Report of the Intergovernmental Panel on Climate Change,* Cambridge ; New York, Cambridge University Press.
IPCC 2013. *Climate change 2013: The physical science basis: contribution of Working Group I to the Fifth Assessment Report of the Intergovernmental Panel on Climate Change*, Cambridge University Press.
ITO, A., ITO, A. & AKIMOTO, H. 2007. Seasonal and interannual variations in CO and BC emissions from open biomass burning in Southern Africa during 1998–2005. *Global Biogeochemical Cycles,* 21.
JAARS, K., BEUKES, J. P., VAN ZYL, P. G., VENTER, A. D., JOSIPOVIC, M., PIENAAR, J. J., VAKKARI, V., AALTONEN, H., LAAKSO, H., KULMALA, M., TIITTA, P., GUENTHER, A., HELLÉN, H., LAAKSO, L. & HAKOLA, H. 2014. Ambient aromatic hydrocarbon measurements at Welgegund, South Africa. *Atmospheric Chemistry and Physics,* 14**,** 7075-7089.
JAARS, K., VAN ZYL, P. G., BEUKES, J. P., HELLÉN, H., VAKKARI, V., JOSIPOVIC, M., VENTER, A. D., RÄSÄNEN, M., KNOETZE, L., CILLIERS, D. P., SIEBERT, S. J., KULMALA, M., RINNE, J., GUENTHER, A., LAAKSO, L. & HAKOLA, H. 2016. Measurements of biogenic volatile organic compounds at a grazed savannah grassland agricultural landscape in South Africa. *Atmospheric Chemistry and Physics,* 16**,** 15665-15688.
JACOB, D. J. 2000. Heterogeneous chemistry and tropospheric ozone. *Atmospheric Environment,* 34**,** 2131-2159.
JAFFE, D. & RAY, J. 2007. Increase in surface ozone at rural sites in the western US. *Atmospheric Environment,* 41**,** 5452-5463.
JAMMALAMADAKA, S. R. & LUND, U. J. 2006. The effect of wind direction on ozone levels: a case study. *Environmental and Ecological Statistics,* 13**,** 287-298.
JERRETT, M., BURNETT, R. T., POPE III, C. A., ITO, K., THURSTON, G., KREWSKI, D., SHI, Y., CALLE, E. & THUN, M. 2009. Long-term ozone exposure and mortality. *New England Journal of Medicine,* 360**,** 1085-1095.
JONNALAGADDA, S., BWILA, J. & KOSMUS, W. 2001. Surface ozone concentrations in Eastern Highlands of Zimbabwe. *Atmospheric Environment,* 35**,** 4341-4346.
JOSIPOVIC, M. 2009. *Acidic deposition emanating from the South African Highveld: a critical levels and critical loads assessment.* PhD thesis, University of Johannesburg.
JOSIPOVIC, M., ANNEGARN, H. J., KNEEN, M. A., PIENAAR, J. J. & PIKETH, S. J. 2010. Concentrations, distributions and critical level exceedance assessment of $SO_2$, $NO_2$ and $O_3$ in South Africa. *Environmental Monitoring and Assessment,* 171**,** 181-196.
KALAJI, H. M., JAJOO, A., OUKARROUM, A., BRESTIC, M., ZIVCAK, M., SAMBORSKA, I. A., CETNER, M. D., ŁUKASIK, I., GOLTSEV, V. & LADLE, R. J. 2016. Chlorophyll *a*

fluorescence as a tool to monitor physiological status of plants under abiotic stress conditions. *Acta Physiologiae Plantarum,* 38**,** 102.
KAVASSALIS, S. C. & MURPHY, J. G. 2017. Understanding ozone-meteorology correlations: A role for dry deposition. *Geophysical Research Letters,* 44**,** 2922-2931.
KIRKMAN, G. A., PIKETH, S. J., ANDREAE, M. O., ANNEGARN, H. J. & HELAS, G. 2000. Distribution of aerosols, ozone and carbon monoxide over southern Africa. *South African Journal of Science,* 96**,** 423.
KOPPMANN, R., CZAPIEWSKI, K. V. & REID, J. 2005. A review of biomass burning emissions, part I: gaseous emissions of carbon monoxide, methane, volatile organic compounds, and nitrogen containing compounds. *Atmospheric Chemistry and Physics Discussions***,** 10455-10516.
KREHER, K., JOHNSTON, P., WOOD, S., NARDI, B. & PLATT, U. 1997. Ground-based measurements of tropospheric and stratospheric BrO at Arrival Heights, Antarctica. *Geophysical Research Letters,* 24**,** 3021-3024.
KREHER, K., KEYS, J., JOHNSTON, P., PLATT, U. & LIU, X. 1996. Ground-based measurements of OClO and HCl in austral spring 1993 at Arrival Heights, Antarctica. *Geophysical Research Letters,* 23**,** 1545-1548.
KRUPA, S., MCGRATH, M. T., ANDERSEN, C. P., BOOKER, F. L., BURKEY, K. O., CHAPPELKA, A. H., CHEVONE, B. I., PELL, E. J. & ZILINSKAS, B. A. 2001. Ambient ozone and plant health. *Plant Disease,* 85**,** 4-12.
LAAKSO, L., BEUKES, J. P., VAN ZYL, P. G., PIENAAR, J. J., JOSIPOVIC, M., VENTER, A. D., JAARS, K., VAKKARI, V., LABUSCHAGNE, C., CHILOANE, K. & TUOVINEN, J.-P. 2013. Ozone concentrations and their potential impacts on vegetation in southern Africa. *In:* MATYSSEK, R., CLARKE, N., CUDLIN, P., MIKKELSEN, T. N., TUOVINEN, J.-P., WIESER, G. & PAOLETTI, E. (eds.) *Climate change, air pollution and global challenges understanding and perspectives from forest research.* Elsevier.
LAAKSO, L., LAAKSO, H., AALTO, P. P., KERONEN, P., PETÄJÄ, T., NIEMINEN, T., POHJA, T., SIIVOLA, E., KULMALA, M., KGABI, N., MOLEFE, M., MABASO, D., PHALATSE, D., PIENAAR, K. & KERMINEN, V. M. 2008. Basic characteristics of atmospheric particles, trace gases and meteorology in a relatively clean Southern African Savannah environment. *Atmospheric Chemistry and Physics,* 8**,** 4823-4839.
LAAKSO, L., VAKKARI, V., VIRKKULA, A., LAAKSO, H., BACKMAN, J., KULMALA, M., BEUKES, J. P., VAN ZYL, P. G., TIITTA, P., JOSIPOVIC, M., PIENAAR, J. J., CHILOANE, K., GILARDONI, S., VIGNATI, E., WIEDENSOHLER, A., TUCH, T., BIRMILI, W., PIKETH, S., COLLETT, K., FOURIE, G. D., KOMPPULA, M., LIHAVAINEN, H., DE LEEUW, G. & KERMINEN, V. M. 2012. South African EUCAARI measurements: seasonal variation of trace gases and aerosol optical properties. *Atmospheric Chemistry and Physics,* 12**,** 1847-1864.
LABAN, T. L., BEUKES, J. P. & VAN ZYL, P. G. 2015. Measurement of surface ozone in South Africa with reference to impacts on human health: commentary. *Clean Air Journal/Tydskrif vir Skoon Lug,* 25**,** 9-12.
LAMARQUE, J.-F., BOND, T. C., EYRING, V., GRANIER, C., HEIL, A., KLIMONT, Z., LEE, D., LIOUSSE, C., MIEVILLE, A. & OWEN, B. 2010. Historical (1850–2000) gridded anthropogenic and biomass burning emissions of reactive gases and aerosols: methodology and application. *Atmospheric Chemistry and Physics,* 10**,** 7017-7039.
LAURILA, T., HAKOLA, H., LINDFORS, V., MEINANDER, O., PUHTO, K. & JOKELA, V. 1999. Ozone, VOC and nitrogen species concentrations in ambient air in the boreal region of Europe. *Biogenic VOC emissions and photochemistry in the boreal regions of Europe, air pollution research report*.
LEE, B.-S. & WANG, J.-L. 2006. Concentration variation of isoprene and its implications for peak ozone concentration. *Atmospheric Environment,* 40**,** 5486-5495.
LEFOHN, A. S., SHADWICK, D. S. & ZIMAN, S. D. 1998. The difficult challenge of attaining EPA's new ozone standard. *Environmental Science & Technology,* 32**,** 276A-282A.

LELIEVELD, J., BARLAS, C., GIANNADAKI, D. & POZZER, A. 2013. Model calculated global, regional and megacity premature mortality due to air pollution. *Atmospheric Chemistry & Physics* 13**,** 7023-7037.
LELIEVELD, J. & DENTENER, F. J. 2000. What controls tropospheric ozone? *Journal of Geophysical Research: Atmospheres,* 105**,** 3531-3551.
LESER, H., HÖNNINGER, G. & PLATT, U. 2003. MAX-DOAS measurements of BrO and $NO_2$ in the marine boundary layer. *Geophysical Research Letters,* 30.
LEVINE, J. 2003. Biomass burning: the cycling of gases and particulates from the biosphere to the atmosphere. *Treatise on Geochemistry,* 4**,** 347.
LI, L., CHEN, C., HUANG, C., HUANG, H., ZHANG, G., WANG, Y., CHEN, M., WANG, H., CHEN, Y. & STREETS, D. 2011. Ozone sensitivity analysis with the MM5-CMAQ modeling system for Shanghai. *Journal of Environmental Sciences,* 23**,** 1150-1157.
LIM, S. S., VOS, T., FLAXMAN, A. D., DANAEI, G., SHIBUYA, K., ADAIR-ROHANI, H., ALMAZROA, M. A., AMANN, M., ANDERSON, H. R. & ANDREWS, K. G. 2012. A comparative risk assessment of burden of disease and injury attributable to 67 risk factors and risk factor clusters in 21 regions, 1990–2010: a systematic analysis for the Global Burden of Disease Study 2010. *The Lancet,* 380**,** 2224-2260.
LIOUSSE, C., ASSAMOI, E., CRIQUI, P., GRANIER, C. & ROSSET, R. 2014. Explosive growth in African combustion emissions from 2005 to 2030. *Environmental Research Letters,* 9**,** 035003.
LIU, S. C. 1977. Possible effects on tropospheric $O_3$ and OH due to NO emissions. *Geophysical Research Letters,* 4**,** 325-328.
LIU, Y., LI, L., AN, J., HUANG, L., YAN, R., HUANG, C., WANG, H., WANG, Q., WANG, M. & ZHANG, W. 2018. Estimation of biogenic VOC emissions and its impact on ozone formation over the Yangtze River Delta region, China. *Atmospheric Environment*.
LONG, S. & NAIDU, S. 2002. Effects of oxidants at the biochemical, cell and physiological levels, with particular reference to ozone. *Air Pollution and Plant Life,* 2**,** 69-88.
LOURENS, A. S., BEUKES, J. P., VAN ZYL, P. G., FOURIE, G. D., BURGER, J. W., PIENAAR, J. J., READ, C. E. & JORDAAN, J. H. 2011. Spatial and temporal assessment of gaseous pollutants in the Highveld of South Africa. *South African Journal of Science,* 107**,** 1-8.
LOURENS, A. S., BUTLER, T. M., BEUKES, J. P., VAN ZYL, P. G., FOURIE, G. D. & LAWRENCE, M. G. 2016. Investigating atmospheric photochemistry in the Johannesburg-Pretoria megacity using a box model. *South African Journal of Science,* 112**,** 01-11.
LÖVBLAD, G., TARRASÓN, L., TØRSETH, K. & DUTCHAK, S. 2004. EMEP Assessment Part I: European perspective. *Norwegian Meteorological Institute,* 43.
LUDWIG, J., MARUFU, L., HUBER, B., ANDREAE, M. & HELAS, G. 2003. Domestic combustion of biomass fuels in developing countries: a major source of atmospheric pollutants. *Journal of Atmospheric Chemistry,* 44**,** 23-37.
LUKE, W. T., KELLEY, P., LEFER, B. L., FLYNN, J., RAPPENGLÜCK, B., LEUCHNER, M., DIBB, J. E., ZIEMBA, L. D., ANDERSON, C. H. & BUHR, M. 2010. Measurements of primary trace gases and $NO_y$ composition in Houston, Texas. *Atmospheric Environment,* 44**,** 4068-4080.
MAFUSIRE, G., ANNEGARN, H. J., VAKKARI, V., BEUKES, J. P., JOSIPOVIC, M., VAN ZYL, P. G. & LAAKSO, L. 2016. Submicrometer aerosols and excess CO as tracers for biomass burning air mass transport over southern Africa. *Journal of Geophysical Research: Atmospheres,* 121**,** 10262-10282.
MALAN, C. 2017. *Influence of elevated $CO_2$ on the growth, yield and photosynthesis of sugarcane.* MSc dissertation, North-West University.
MARENCO, A., MEDALE, J. & PRIEUR, S. 1990. Study of tropospheric ozone in the tropical belt (Africa, America) from STRATOZ and TROPOZ campaigns. *Atmospheric Environment. Part A. General Topics,* 24**,** 2823-2834.
MARTINEZ, M., HARDER, H., KUBISTIN, D., RUDOLF, M., BOZEM, H., EERDEKENS, G., FISCHER, H., KLÜPFEL, T., GURK, C. & KÖNIGSTEDT, R. 2010. Hydroxyl radicals in

the tropical troposphere over the Suriname rainforest: airborne measurements. *Atmospheric Chemistry and Physics,* 10**,** 3759-3773.
MARTINS, J., DHAMMAPALA, R., LACHMANN, G., GALY-LACAUX, C. & PIENAAR, J. 2007. Long-term measurements of sulphur dioxide, nitrogen dioxide, ammonia, nitric acid and ozone in southern Africa using passive samplers. *South African Journal of Science,* 103**,** 336-342.
MARUFU, L., DENTENER, F., LELIEVELD, J., ANDREAE, M. & HELAS, G. 2000. Photochemistry of the African troposphere: Influence of biomass-burning emissions. *Journal of Geophysical Research: Atmospheres,* 105**,** 14513-14530.
MAXWELL, K. & JOHNSON, G. N. 2000. Chlorophyll fluorescence—a practical guide. *Journal of Experimental Botany,* 51**,** 659-668.
MCCARTHY, J. & LATTANZIO, R. 2016. Ozone air quality standards: EPA's 2015 revision *Congressional Research Service Report.*
MILLS, G., BUSE, A., GIMENO, B., BERMEJO, V., HOLLAND, M., EMBERSON, L. & PLEIJEL, H. 2007. A synthesis of AOT40-based response functions and critical levels of ozone for agricultural and horticultural crops. *Atmospheric Environment,* 41**,** 2630-2643.
MOKGATHLE, B. B. 2006. *Seasonal and diurnal variations of surface ozone on the Mpumalanga Highveld.* MSc dissertation, North-West University.
MONKS, P. S. 2000. A review of the observations and origins of the spring ozone maximum. *Atmospheric Environment,* 34**,** 3545-3561.
MONKS, P. S. 2005. Gas-phase radical chemistry in the troposphere. *Chemical Society Reviews,* 34**,** 376-395.
MONKS, P. S., ARCHIBALD, A. T., COLETTE, A., COOPER, O., COYLE, M., DERWENT, R., FOWLER, D., GRANIER, C., LAW, K. S., MILLS, G. E., STEVENSON, D. S., TARASOVA, O., THOURET, V., VON SCHNEIDEMESSER, E., SOMMARIVA, R., WILD, O. & WILLIAMS, M. L. 2015. Tropospheric ozone and its precursors from the urban to the global scale from air quality to short-lived climate forcer. *Atmospheric Chemistry and Physics,* 15**,** 8889-8973.
MURPHY, J. G., DAY, D. A., CLEARY, P. A., WOOLDRIDGE, P. J., MILLET, D. B., GOLDSTEIN, A. H. & COHEN, R. C. 2006. The weekend effect within and downwind of Sacramento: Part 2. Observational evidence for chemical and dynamical contributions. *Atmospheric Chemistry and Physics Discussions,* 2006**,** 11971-12019.
MURPHY, J. G., DAY, D. A., CLEARY, P. A., WOOLDRIDGE, P. J., MILLET, D. B., GOLDSTEIN, A. H. & COHEN, R. C. 2007. The weekend effect within and downwind of Sacramento - Part 1: Observations of ozone, nitrogen oxides, and VOC reactivity. *Atmospheric Chemistry and Physics,* 7**,** 5327-5339.
MURRAY, L. T. 2016. Lightning $NO_x$ and impacts on air quality. *Current Pollution Reports,* 2**,** 115-133.
MYHRE, G., SHINDELL, D., BRÉON, F., COLLINS, W., FUGLESTVEDT, J., HUANG, J., KOCH, D., LAMARQUE, J., LEE, D. & MENDOZA, B. 2013. Anthropogenic and natural radiative forcing. . *In:* STOCKER, T., QIN, D., PLATTNER, G.-K., TIGNOR, M., ALLEN, S., BOSCHUNG, J., NAUELS, A., XIA, Y., BEX, V. & MIDGLEY, P. (eds.) *Climate change 2013: The physical science basis: contribution of Working Group I to the Fifth Assessment Report of the Intergovernmental Panel on Climate Change.* Cambridge, United Kingdom and New York, NY, USA: Cambridge University Press.
NRC 1991. *Rethinking the Ozone Problem in Urban and Regional Air Pollution,* Washington, DC, The National Academies Press.
NRC 2008. *Estimating mortality risk reduction and economic benefits from controlling ozone air pollution*, National Academies Press.
OJELEDE, M. E., ANNEGARN, H. J., PRICE, C., KNEEN, M. A. & GOYNS, P. 2008. Lightning-produced $NO_x$ budget over the Highveld region of South Africa. *Atmospheric Environment,* 42**,** 5706-5714.
OLTMANS, S. J., LEFOHN, A. S., SHADWICK, D., HARRIS, J. M., SCHEEL, H. E., GALBALLY, I., TARASICK, D. W., JOHNSON, B. J., BRUNKE, E. G., CLAUDE, H., ZENG, G., NICHOL, S., SCHMIDLIN, F., DAVIES, J., CUEVAS, E., REDONDAS, A.,

NAOE, H., NAKANO, T. & KAWASATO, T. 2013. Recent tropospheric ozone changes – A pattern dominated by slow or no growth. *Atmospheric Environment,* 67**,** 331-351.
ORDONEZ, C., MATHIS, H., FURGER, M., HENNE, S., HÜGLIN, C., STAEHELIN, J. & PRÉVÔT, A. 2005. Changes of daily surface ozone maxima in Switzerland in all seasons from 1992 to 2002 and discussion of summer 2003. *Atmospheric Chemistry and Physics,* 5**,** 1187-1203.
OTERO, N., SILLMANN, J., SCHNELL, J. L., RUST, H. W. & BUTLER, T. 2016. Synoptic and meteorological drivers of extreme ozone concentrations over Europe. *Environmental Research Letters,* 11**,** 024005.
OTT, L. E., PICKERING, K. E., STENCHIKOV, G. L., ALLEN, D. J., DECARIA, A. J., RIDLEY, B., LIN, R. F., LANG, S. & TAO, W. K. 2010. Production of lightning $NO_x$ and its vertical distribution calculated from three-dimensional cloud-scale chemical transport model simulations. *Journal of Geophysical Research: Atmospheres,* 115.
OTTER, L. B., YANG, W. X., SCHOLES, M. C. & MEIXNER, F. X. 1999. Nitric oxide emissions from a southern African savanna. *Journal of Geophysical Research: Atmospheres,* 104**,** 18471-18485.
PAOLETTI, E. & MANNING, W. J. 2007. Toward a biologically significant and usable standard for ozone that will also protect plants. *Environmental Pollution,* 150**,** 85-95.
PARRA, R. & FRANCO, E. 2016. Identifying the Ozone Weekend Effect in the air quality of the northern Andean region of Ecuador. *In:* LONGHURST, J. W. S., BREBBIA, C. A. & BARNES, J. (eds.) *Air Pollution XXIV.* Southampton: WIT Press.
PEARCE, J. L., BERINGER, J., NICHOLLS, N., HYNDMAN, R. J. & TAPPER, N. J. 2011. Quantifying the influence of local meteorology on air quality using generalized additive models. *Atmospheric Environment,* 45**,** 1328-1336.
PETÄJÄ, T., VAKKARI, V., POHJA, T., NIEMINEN, T., LAAKSO, H., AALTO, P. P., KERONEN, P., SIIVOLA, E., KERMINEN, V.-M., KULMALA, M. & LAAKSO, L. 2013. Transportable aerosol characterization trailer with trace gas chemistry: design, instruments and verification. *Aerosol and Air Quality Research,* 13, No. 2**,** 421-435.
PITKÄNEN, M. R., MIKKONEN, S., LEHTINEN, K. E., LIPPONEN, A. & AROLA, A. 2016. Artificial bias typically neglected in comparisons of uncertain atmospheric data. *Geophysical Research Letters,* 43.
PLEIJEL, H. 2011. Reduced ozone by air filtration consistently improved grain yield in wheat. *Environmental Pollution,* 159**,** 897-902.
PLEIJEL, H., DANIELSSON, H., OJANPERÄ, K., TEMMERMAN, L. D., HÖGY, P., BADIANI, M. & KARLSSON, P. E. 2004. Relationships between ozone exposure and yield loss in European wheat and potato—a comparison of concentration- and flux-based exposure indices. *Atmospheric Environment,* 38**,** 2259-2269.
POCHANART, P., AKIMOTO, H., KINJO, Y. & TANIMOTO, H. 2002. Surface ozone at four remote island sites and the preliminary assessment of the exceedances of its critical level in Japan. *Atmospheric Environment,* 36**,** 4235-4250.
POLLACK, I. B., RYERSON, T. B., TRAINER, M., PARRISH, D. D., ANDREWS, A. E., ATLAS, E. L., BLAKE, D. R., BROWN, S. S., COMMANE, R., DAUBE, B. C., DE GOUW, J. A., DUBÉ, W. P., FLYNN, J., FROST, G. J., GILMAN, J. B., GROSSBERG, N., HOLLOWAY, J. S., KOFLER, J., KORT, E. A., KUSTER, W. C., LANG, P. M., LEFER, B., LUEB, R. A., NEUMAN, J. A., NOWAK, J. B., NOVELLI, P. C., PEISCHL, J., PERRING, A. E., ROBERTS, J. M., SANTONI, G., SCHWARZ, J. P., SPACKMAN, J. R., WAGNER, N. L., WARNEKE, C., WASHENFELDER, R. A., WOFSY, S. C. & XIANG, B. 2012. Airborne and ground-based observations of a weekend effect in ozone, precursors, and oxidation products in the California South Coast Air Basin. *Journal of Geophysical Research: Atmospheres,* 117.
PORTER, W. C., KHALIL, M. A., BUTENHOFF, C. L., ALMAZROUI, M., AL-KHALAF, A. K. & AL-SAHAFI, M. S. 2014. Annual and weekly patterns of ozone and particulate matter in Jeddah, Saudi Arabia. *Journal of the Air & Waste Management Association,* 64**,** 817-26.
PRATHER, M. J., EHHALT, D., DENTENER, F., DERWENT, R., DLUGOKENCKY, E., HOLLAND, E., ISAKSEN, I., KATIMA, J., KIRCHHOFF, V. & MATSON, P. 2001.

Chapter 4: Atmospheric chemistry and greenhouse gases. *In:* HOUGHTON, J. T., DING, Y., GRIGGS, D. J., NOGUER, M., VAN DER LINDEN, P. J., DAI, X., MASKELL, K. & JOHNSON, C. A. (eds.) *Climate change 2001: the scientific basis: contribution of Working Group I to the Third Assessment Report of the Intergovernmental Panel on Climate Change.* New York: Cambridge University Press.

PUGLIESE, S., MURPHY, J., GEDDES, J. & WANG, J. 2014. The impacts of precursor reduction and meteorology on ground-level ozone in the Greater Toronto Area. *Atmospheric Chemistry and Physics,* 14**,** 8197-8207.

PUSEDE, S. & COHEN, R. 2012. On the observed response of ozone to $NO_x$ and VOC reactivity reductions in San Joaquin Valley California 1995–present. *Atmospheric Chemistry and Physics,* 12**,** 8323-8339.

REBBECK, J. & SCHERZER, A. 2002. Growth responses of yellow-poplar (Liriodendron tulipifera L.) exposed to 5 years of $O_3$ alone or combined with elevated $CO_2$. *Plant, Cell & Environment,* 25**,** 1527-1537.

SCHANSKER, G., TÓTH, S. Z. & STRASSER, R. J. 2006. Dark recovery of the Chl *a* fluorescence transient (OJIP) after light adaptation: the qT-component of non-photochemical quenching is related to an activated photosystem I acceptor side. *Biochimica et Biophysica Acta (BBA)-Bioenergetics,* 1757**,** 787-797.

SCHEEPERS, C. C. W. 2011. *Physiological and biochemical constraints on photosynthesis of leguminous plants induced by elevated ozone in open–top chambers.* MSc dissertation, North-West University.

SCHLINK, U., HERBARTH, O., RICHTER, M., DORLING, S., NUNNARI, G., CAWLEY, G. & PELIKAN, E. 2006. Statistical models to assess the health effects and to forecast ground-level ozone. *Environmental Modelling & Software,* 21**,** 547-558.

SCHOLES, M. & ANDREAE, M. O. 2000. Biogenic and pyrogenic emissions from Africa and their impact on the global atmosphere. *AMBIO: A Journal of the Human Environment,* 29**,** 23-29.

SCHUMANN, U. & HUNTRIESER, H. 2007. The global lightning-induced nitrogen oxides source. *Atmospheric Chemistry and Physics,* 7**,** 3823-3907.

SEILER, W. & CRUTZEN, P. J. 1980. Estimates of gross and net fluxes of carbon between the biosphere and the atmosphere from biomass burning. *Climatic Change,* 2**,** 207-247.

SEINFELD, J. H. & PANDIS, S. N. 2006. *Atmospheric chemistry and physics: from air pollution to climate change,* New York, Wiley.

SILLMAN, S. 1999. The relation between ozone, $NO_x$ and hydrocarbons in urban and polluted rural environments. *Atmospheric Environment,* 33**,** 1821-1845.

SILLMAN, S. 2003. Tropospheric ozone and photochemical smog. *Environmental Geochemistry,* 9**,** 407-31.

SILLMAN, S. & SAMSON, P. J. 1995. Impact of temperature on oxidant photochemistry in urban, polluted rural and remote environments. *Journal of Geophysical Research: Atmospheres,* 100**,** 11497-11508.

SILVA, J. M. N., PEREIRA, J. M. C., CABRAL, A. I., SÁ, A. C. L., VASCONCELOS, M. J. P., MOTA, B. & GRÉGOIRE, J.-M. 2003. An estimate of the area burned in southern Africa during the 2000 dry season using SPOT-VEGETATION satellite data. *Journal of Geophysical Research: Atmospheres,* 108.

SILVA, R. A., WEST, J. J., ZHANG, Y., ANENBERG, S. C., LAMARQUE, J.-F., SHINDELL, D. T., COLLINS, W. J., DALSOREN, S., FALUVEGI, G. & FOLBERTH, G. 2013. Global premature mortality due to anthropogenic outdoor air pollution and the contribution of past climate change. *Environmental Research Letters,* 8**,** 034005.

SIMPSON, D. 1992. Long-period modelling of photochemical oxidants in Europe. Model calculations for July 1985. *Atmospheric Environment. Part A. General Topics,* 26**,** 1609-1634.

SOUTH AFRICAN SUGARCANE RESEARCH INSTITUTE. 2006a. *Information Sheet Variety N31* [Online]. Available: http://www.sasa.org.za/Libraries/Variety_Information/N31.sflb.ashx [Accessed 3 April 2018].

SOUTH AFRICAN SUGARCANE RESEARCH INSTITUTE. 2006b. *Information Sheet Variety NCo376* [Online]. Available: www.sasa.org.za/Libraries/Variety_Information/NCo376.sflb.ashx [Accessed 3 April 2018].

STEIN, A. F., DRAXLER, R. R., ROLPH, G. D., STUNDER, B. J. B., COHEN, M. D. & NGAN, F. 2015. NOAA's HYSPLIT atmospheric transport and dispersion modeling system. *Bulletin of the American Meteorological Society,* 96**,** 2059-2077.

STEPHENS, S., MADRONICH, S., WU, F., OLSON, J. B., RAMOS, R., RETAMA, A. & MUÑOZ, R. 2008. Weekly patterns of México City's surface concentrations of CO, $NO_x$, $PM_{10}$ and $O_3$ during 1986–2007. *Atmospheric Chemistry and Physics,* 8**,** 5313-5325.

STEVENSON, D., DENTENER, F., SCHULTZ, M., ELLINGSEN, K., VAN NOIJE, T., WILD, O., ZENG, G., AMANN, M., ATHERTON, C. & BELL, N. 2006. Multimodel ensemble simulations of present-day and near-future tropospheric ozone. *Journal of Geophysical Research: Atmospheres,* 111.

STIRBET, A. 2011. On the relation between the Kautsky effect (chlorophyll *a* fluorescence induction) and photosystem II: basics and applications of the OJIP fluorescence transient. *Journal of Photochemistry and Photobiology B: Biology,* 104**,** 236-257.

STOHL, A. 1998. Computation, accuracy and applications of trajectories - a review and bibliography. *Atmospheric Environment,* 32**,** 947-966.

STONE, D., WHALLEY, L. K. & HEARD, D. E. 2012. Tropospheric OH and $HO_2$ radicals: field measurements and model comparisons. *Chemical Society Reviews,* 41**,** 6348-6404.

SWAP, R. J., ANNEGARN, H. J., SUTTLES, J. T., KING, M. D., PLATNICK, S., PRIVETTE, J. L. & SCHOLES, R. J. 2003. Africa burning: A thematic analysis of the Southern African Regional Science Initiative (SAFARI 2000). *Journal of Geophysical Research: Atmospheres,* 108.

TAI, A. P., MARTIN, M. V. & HEALD, C. L. 2014. Threat to future global food security from climate change and ozone air pollution. *Nature Climate Change,* 4**,** 817-821.

TANG, G., LI, X., WANG, Y., XIN, J. & REN, X. 2009. Surface ozone trend details and interpretations in Beijing, 2001–2006. *Atmospheric Chemistry and Physics,* 9**,** 8813-8823.

THE ROYAL SOCIETY 2008. Ground-level ozone in the 21st century: future trends, impacts and policy implications. *Royal Society Science Policy Report,* 15.

THOMPSON, A. M. 1992. The oxidizing capacity of the Earth's atmosphere: Probable past and future changes. *Science,* 256**,** 1157-1165.

THOMPSON, A. M., BALASHOV, N. V., WITTE, J. C., COETZEE, J. G. R., THOURET, V. & POSNY, F. 2014. Tropospheric ozone increases over the southern Africa region: bellwether for rapid growth in Southern Hemisphere pollution? *Atmospheric Chemistry and Physics,* 14**,** 9855-9869.

THOMPSON, A. M., PICKERING, K. E., MCNAMARA, D. P., SCHOEBERL, M. R., HUDSON, R. D., KIM, J. H., BROWELL, E. V., KIRCHHOFF, V. W. J. H. & NGANGA, D. 1996. Where did tropospheric ozone over southern Africa and the tropical Atlantic come from in October 1992? Insights from TOMS, GTE TRACE A, and SAFARI 1992. *Journal of Geophysical Research: Atmospheres,* 101**,** 24251-24278.

THOMPSON, M. L., REYNOLDS, J., COX, L. H., GUTTORP, P. & SAMPSON, P. D. 2001. A review of statistical methods for the meteorological adjustment of tropospheric ozone. *Atmospheric Environment,* 35**,** 617-630.

THORNTON, J. A., KERCHER, J. P., RIEDEL, T. P., WAGNER, N. L., COZIC, J., HOLLOWAY, J. S., DUBÉ, W. P., WOLFE, G. M., QUINN, P. K. & MIDDLEBROOK, A. M. 2010. A large atomic chlorine source inferred from mid-continental reactive nitrogen chemistry. *Nature,* 464**,** 271.

TIITTA, P., VAKKARI, V., CROTEAU, P., BEUKES, J. P., VAN ZYL, P. G., JOSIPOVIC, M., VENTER, A. D., JAARS, K., PIENAAR, J. J., NG, N. L., CANAGARATNA, M. R., JAYNE, J. T., KERMINEN, V. M., KOKKOLA, H., KULMALA, M., LAAKSONEN, A., WORSNOP, D. R. & LAAKSO, L. 2014. Chemical composition, main sources and

temporal variability of $PM_1$ aerosols in southern African grassland. *Atmospheric Chemistry and Physics,* 14**,** 1909-1927.
TONG, D. Q., MATHUR, R., KANG, D., YU, S., SCHERE, K. L. & POULIOT, G. 2009. Vegetation exposure to ozone over the continental United States: Assessment of exposure indices by the Eta-CMAQ air quality forecast model. *Atmospheric Environment,* 43**,** 724-733.
TRAINER, M., WILLIAMS, E. J., PARRISH, D. D., BUHR, M. P., ALLWINE, E. J., WESTBERG, H. H., FEHSENFELD, F. C. & LIU, S. C. 1987. Models and observations of the impact of natural hydrocarbons on rural ozone. *Nature,* 329**,** 705-707.
TSAKIRI, K. G. & ZURBENKO, I. G. 2011. Prediction of ozone concentrations using atmospheric variables. *Air Quality, Atmosphere & Health,* 4**,** 111-120.
TYSON, P., GARSTANG, M. & SWAP, R. 1996. Large-scale recirculation of air over southern Africa. *Journal of Applied Meteorology,* 35**,** 2218-2236.
TYSON, P. D., GARSTANG, M., THOMPSON, A. M., D'ABRETON, P., DIAB, R. D. & BROWELL, E. V. 1997. Atmospheric transport and photochemistry of ozone over central Southern Africa during the Southern Africa Fire-Atmosphere Research Initiative. *Journal of Geophysical Research: Atmospheres,* 102**,** 10623-10635.
TYSON, P. D. & PRESTON-WHYTE, R. A. 2000. *The weather and climate of southern Africa*.
UNEP 2006. Report on Atmosphere and Air Pollution *African regional implementation review for the 14th Session of the Commission on Sustainable Development (CSD-14).*
VAKKARI, V., BEUKES, J. P., LAAKSO, H., MABASO, D., PIENAAR, J. J., KULMALA, M. & LAAKSO, L. 2013. Long-term observations of aerosol size distributions in semi-clean and polluted savannah in South Africa. *Atmospheric Chemistry and Physics,* 13**,** 1751-1770.
VAKKARI, V., KERMINEN, V.-M., BEUKES, J. P., TIITTA, P., VAN ZYL, P. G., JOSIPOVIC, M., VENTER, A. D., JAARS, K., WORSNOP, D. R., KULMALA, M. & LAAKSO, L. 2014. Rapid changes in biomass burning aerosols by atmospheric oxidation. *Geophysical Research Letters,* 41**,** 2644-2651.
VAKKARI, V., LAAKSO, H., KULMALA, M., LAAKSONEN, A., MABASO, D., MOLEFE, M., KGABI, N. & LAAKSO, L. 2011. New particle formation events in semi-clean South African savannah. *Atmospheric Chemistry and Physics,* 11**,** 3333-3346.
VAN DINGENEN, R., DENTENER, F. J., RAES, F., KROL, M. C., EMBERSON, L. & COFALA, J. 2009. The global impact of ozone on agricultural crop yields under current and future air quality legislation. *Atmospheric Environment,* 43**,** 604-618.
VAN TIENHOVEN, A. M., OTTER, L., LENKOPANE, M., VENJONOKA, K. & ZUNCKEL, M. 2005. Assessment of ozone impacts on vegetation in southern Africa and directions for future research: commentary. *South African Journal of Science,* 101**,** 143-148.
VENTER, A., BEUKES, J., VAN ZYL, P., BRUNKE, E.-G., LABUSCHAGNE, C., SLEMR, F., EBINGHAUS, R. & KOCK, H. 2015. Statistical exploration of gaseous elemental mercury (GEM) measured at Cape Point from 2007 to 2011. *Atmospheric Chemistry and Physics,* 15**,** 10271-10280.
VENTER, A. D., VAKKARI, V., BEUKES, J. P., VAN ZYL, P. G., LAAKSO, H., MABASO, D., TIITTA, P., JOSIPOVIC, M., KULMALA, M., PIENAAR, J. J. & LAAKSO, L. 2012. An air quality assessment in the industrialised western Bushveld Igneous Complex, South Africa. *South African Journal of Science*.
VENTER, A. D., VAN ZYL, P. G., BEUKES, J. P., JOSIPOVIC, M., HENDRIKS, J., VAKKARI, V. & LAAKSO, L. 2017. Atmospheric trace metals measured at a regional background site (Welgegund) in South Africa. *Atmospheric Chemistry and Physics,* 17**,** 4251-4263.
VINGARZAN, R. 2004. A review of surface ozone background levels and trends. *Atmospheric Environment,* 38**,** 3431-3442.
WAGNER, P. & KUTTLER, W. 2014. Biogenic and anthropogenic isoprene in the near-surface urban atmosphere — A case study in Essen, Germany. *Science of The Total Environment,* 475**,** 104-115.
WAKAMATSU, S., MORIKAWA, T. & ITO, A. 2013. *Air pollution trends in Japan between 1970 and 2012 and impact of urban air pollution countermeasures*.

WALLINGTON, T., KAISER, E. & FARRELL, J. 2006. Automotive fuels and internal combustion engines: a chemical perspective. *Chemical Society Reviews,* 35**,** 335-347.
WANG, X. & MAUZERALL, D. L. 2004. Characterizing distributions of surface ozone and its impact on grain production in China, Japan and South Korea: 1990 and 2020. *Atmospheric Environment,* 38**,** 4383-4402.
WANG, Y., HU, B., TANG, G., JI, D., ZHANG, H., BAI, J., WANG, X. & WANG, Y. 2013. Characteristics of ozone and its precursors in Northern China: A comparative study of three sites. *Atmospheric Research,* 132**,** 450-459.
WANG, Y., JACOB, D. J. & LOGAN, J. A. 1998a. Global simulation of tropospheric $O_3$-$NO_x$-hydrocarbon chemistry, 1. Model formulation. *Journal of Geophysical Research,* 103**,** 726.
WANG, Y., LOGAN, J. A. & JACOB, D. J. 1998b. Global simulation of tropospheric $O_3$-$NO_x$-hydrocarbon chemistry: 2. Model evaluation and global ozone budget. *Journal of Geophysical Research: Atmospheres,* 103**,** 10727-10755.
WAYNE, R. P. 1991. *Chemistry of atmospheres,* Oxford (UK), Clarendon Press.
WHO 2006. *Air quality guidelines: Global update 2005. Particulate matter, ozone, nitrogen dioxide and sulfur dioxide*, World Health Organization.
WHO 2016. WHO global urban ambient air pollution database (update 2016).
WICHMANN, J. & VOYI, K. V. V. 2006. Impact of cooking and heating fuel use on acute respiratory health of preschool children in South Africa. *Southern African Journal of Epidemiology and Infection,* 21**,** 48-54.
WILKINSON, S., MILLS, G., ILLIDGE, R. & DAVIES, W. J. 2012. How is ozone pollution reducing our food supply? *Journal of Experimental Botany,* 63**,** 527-536.
WOOD, S. N. 2017. *Generalized additive models: an introduction with R*, CRC press.
WU, S., MICKLEY, L. J., JACOB, D. J., LOGAN, J. A., YANTOSCA, R. M. & RIND, D. 2007. Why are there large differences between models in global budgets of tropospheric ozone? *Journal of Geophysical Research: Atmospheres,* 112.
YOUNG, P., ARCHIBALD, A., BOWMAN, K., LAMARQUE, J.-F., NAIK, V., STEVENSON, D., TILMES, S., VOULGARAKIS, A., WILD, O. & BERGMANN, D. 2013. Pre-industrial to end 21st century projections of tropospheric ozone from the Atmospheric Chemistry and Climate Model Intercomparison Project (ACCMIP). *Atmospheric Chemistry and Physics,* 13**,** 2063-2090.
YOUNG, P. J., NAIK, V., FIORE, A. M., GAUDEL, A., GUO, J., LIN, M., NEU, J., PARRISH, D., RIEDER, H. & SCHNELL, J. 2018. Tropospheric Ozone Assessment Report: Assessment of global-scale model performance for global and regional ozone distributions, variability, and trends. *Elementa: Science of the Anthropocene,* 6.
ZENG, G., PYLE, J. & YOUNG, P. 2008. Impact of climate change on tropospheric ozone and its global budgets. *Atmospheric Chemistry and Physics,* 8**,** 369-387.
ZHANG, Y., COOPER, O. R., GAUDEL, A., THOMPSON, A. M., NÉDÉLEC, P., OGINO, S.-Y. & WEST, J. J. 2016. Tropospheric ozone change from 1980 to 2010 dominated by equatorward redistribution of emissions. *Nature Geoscience,* 9**,** 875.
ZHAO, B., SU, Y., HE, S., ZHONG, M. & CUI, G. 2016. Evolution and comparative assessment of ambient air quality standards in China. *Journal of Integrative Environmental Sciences,* 13**,** 85-102.
ZUNCKEL, M., KOOSAILEE, A., YARWOOD, G., MAURE, G., VENJONOKA, K., VAN TIENHOVEN, A. M. & OTTER, L. 2006. Modelled surface ozone over southern Africa during the Cross Border Air Pollution Impact Assessment project. *Environmental Modelling & Software,* 21**,** 911-924.
ZUNCKEL, M., PIKETH, S. & FREIMAN, T. 1999. Dry deposition of sulphur at a high-altitude background station in South Africa. *Water, Air, and Soil Pollution,* 115**,** 445-463.
ZUNCKEL, M., VENJONOKA, K., PIENAAR, J., BRUNKE, E., PRETORIUS, O., KOOSIALEE, A., RAGHUNANDAN, A. & VAN TIENHOVEN, A. 2004. Surface ozone over southern Africa: synthesis of monitoring results during the Cross Border Air Pollution Impact Assessment project. *Atmospheric Environment,* 38**,** 6139-6147.